SUPPLEMENTO
AL VOLUME IV, SERIE X, DEL
NUOVO CIMENTO
A CURA DELLA SOCIETÀ ITALIANA DI FISICA

1956 1° Semestre N. 4

ARTICOLI
SCRITTI DA FISICI RUSSI

ARTICLES
DE PHYSICIENS RUSSES

PAPERS
BY RUSSIAN PHYSICISTS

Gli articoli di rassegna raccolti in questo fascicolo hanno il medesimo carattere e il medesimo scopo di quelli pubblicati nel fascicolo n. 1 del *Supplemento* al Volume III, Serie X, del *Nuovo Cimento*, 1° Semestre 1956; e, come quelli, anche questi sono scritti da fisici russi. Si potrebbero pertanto ripetere qui testualmente le parole di presentazione pubblicate in testa a quel fascicolo, ma sarebbe superfluo e ad esse rimandiamo il lettore.

Non vogliamo però perdere l'occasione per rinnovare i ringraziamenti più vivi sia verso l'Accademia delle Scienze di Mosca, che così cortesemente volle interessarsi presso i fisici russi per la compilazione delle rassegne, sia verso questi stessi. La collaborazione loro e dell'Accademia ha un significato che stimiamo superi lo stretto campo dell'episodio. E quindi siamo ben lieti che il nostro giornale, che attraverso il proficuo suggerimento del Presidente dell'Unione Internazionale di Fisica, prof. N. F. MOTT, ha atteso alla pubblicazione di rassegne circa l'attività degli scienziati sovietici in Fisica, abbia raggiunto una meta più alta e più vasta di quella inizialmente sperata.

A chiusura di queste brevi parole di presentazione, ci è gradito aggiungere anche questa volta i ringraziamenti più vivi alla signorina dott. LUISA BASILICO per l'aiuto datoci nella preparazione di questo fascicolo.

La Direzione del « Nuovo Cimento »

INDICE DEGLI SCRITTI

A. Ahiezer – On the Interaction of Electromagnetic Waves with Charged Particles and on the Oscillations of the Electronic Plasma . . . . . pag. 591

S. Al'tšuler and B. M. Kozyrev – Some Problems of Paramagnetic Resonance . . . . . » 614

D. I. Blohincev – The Non-linear Field Theory and the Theory of Relativity . . . . . » 629

N. A. Dobrotin, G. T. Zacepin, S. I. Nikol'skij and G. B. Hristiansen – Interaction of Ultra High Energy Particles with Nucleons and Atomic Nuclei . . . . . » 635

E. L. Feinberg and I. Pomerančuk – High Energy Inelastic Diffraction Phenomena . . . . . » 652

E. F. Gross – Optical Spectrum of Excitons in the Crystal Lattice . . . » 672

A. F. Ioffe – On Thermal Conduction in Semiconductors . . . . . » 702

M. Lifšic – Some Problems of the Dynamic Theory of Non-Ideal Crystal Lattices . . . . . » 716

E. M. Lifšic and I. M. Halatnikov – Hydrodynamics of Liquid Helium » 735

A. Sokolov – On the Relativistic Motion of Electrons in Magnetic Fields when Quantum Effects are Taken into Account . . . . . » 743

M. Markov – On Dynamically Deformable Form Factors in the Theory of Elementary Particles . . . . . » 760

B. K. Vajnštein – Structure Analysis by Electron Diffraction . . . . . » 773

Nella traslitterazione delle parole russe, sono state seguite le norme fissate dalla I.S.O. con la « Recommendation n. 9 » del Settembre 1954, riportate a pag. 133 del *Supplemento* al Vol. III, Serie X, del *Nuovo Cimento*, 1° Semestre 1956.

SUPPLEMENTO AL VOLUME III, SERIE X
DEL NUOVO CIMENTO

N. 4, 1956
1° Semestre

On the Interaction of Electromagnetic Waves with Charged Particles and on the Oscillations of the Electronic Plasma.

A. AHIEZER

Academy of Sciences of the USSR - Moscow

CONTENTS. — **1.** Polarization energy loss and Čerenkov radiation in dielectrics and magnetics. – **2.** The penetration of a charged particle through electronic plasma. – **3.** The Čerenkov and the Doppler effects in composite systems. – **4.** The interactions of a beam of charged particles with slow electromagnetic waves. – **5.** The propagation of a beam of charged particles through electronic plasma. – **6.** The longitudinal plasma oscillators in external fields. – **7.** The scattering of the electromagnetic waves by the plasma oscillations. – **8.** The non-linear wave motions in plasma.

The aim of the present article is to give a short survey of the results of several works on the theory of the interaction of charged particles with electromagnetic waves in dielectrics, magnetics, composite waveguides and electronic plasma, as well as on the theory of oscillations of free electronic plasma and of plasma in external fields.

We begin with considering the general question about the polarization energy loss and the Čerenkov radiation in homogeneous dielectrics and magnetics.

1. – Polarization Energy Loss and Čerenkov Radiation in Dielectrics and Magnetics.

The energy loss of a charged particle moving in a dielectric and in a magnetic due to « far » collisions, consists as shown by FERMI [2], of the polarization loss and the loss due to Čerenkov radiation, the theory of which

was given by TAMM and FRANK [1] (*). The simplest way to determine these losses is to compute, according to LANDAU (+), the work (per unit path) of the force, which the field of the moving charge exerts on the charge itself.

Let us consider, at first, a uniform motion of a charge q in an isotropic medium characterized by a dielectric constant $\varepsilon(\omega)$ and a magnetic permeability $\mu(\omega)$. Using Maxwell's equations in which the current density and the charge density are equal to $\boldsymbol{j} = q\boldsymbol{v}\,\delta(\boldsymbol{r} - \boldsymbol{v}t)$, $\varrho = q\,\delta(\boldsymbol{r} - \boldsymbol{v}t)$ ($\boldsymbol{v}$ is the velocity of the charge) and developing the field in Fourier integral, it is easy to show that the energy loss at the « far » collisions is equal to

$$(1) \qquad -\left(\frac{\mathrm{d}\varepsilon}{\mathrm{d}z}\right)_{\text{far}} = -\frac{q}{v}\,(\boldsymbol{vE})_{\boldsymbol{r}=\boldsymbol{v}t} = -\frac{iq^2}{\pi c^2}\int_0^{x_m} x\,\mathrm{d}x \int_{-\infty}^{\infty} \frac{[\mu(\omega) - (1/\beta^2\varepsilon(\omega))]\omega\,\mathrm{d}\omega}{x^2 + (\omega^2/v^2)[1 - \beta^2\varepsilon(\omega)\mu(\omega)]}$$

where $\beta = v/c$. This expression diverges, if $x \to \infty$, this fact being connected with the unapplicability at short distances of the macroscopical approach. Therefore, one must integrate here up to a certain maximum value x_m. It is necessary to add to (1) the energy loss due to pair collisions. Consequently, we obtain the formula (1), in which x_m has the value [4]

$$(2) \qquad x_m = \begin{cases} 1.123\,\dfrac{mv^2}{qe}, & \text{if} \quad v < \dfrac{eq}{\hbar}\,. \\ 1.123\,\dfrac{mv}{\hbar}, & \text{if} \quad v > \dfrac{eq}{\hbar}\,, \end{cases}$$

As $\varepsilon(-\omega) = \varepsilon^*(\omega)$ and $\mu(-\omega) = \mu^*(\omega)$, the integration over x gives:

$$(3) \qquad -\frac{\mathrm{d}\varepsilon}{\mathrm{d}z} = -\frac{q^2}{\pi c^2}\,\mathrm{Re}\,i\int_0^{\infty}\left(\mu - \frac{1}{\beta^2\varepsilon}\right)\ln\left[1 + \frac{x_m^2 v^2}{\omega^2(1 - \beta^2\varepsilon\mu)}\right]\omega\,\mathrm{d}\omega\,.$$

In the case of an optically transparent medium, i.e. at infinitely small attenuation, this formula is reduced to [6]

$$(4) \qquad -\frac{\mathrm{d}\varepsilon}{\mathrm{d}z} = \frac{q^2}{v^2}\sum_i \mathrm{Res}\left\{\frac{2\omega}{\varepsilon(\omega)}\ln 1.123\,\frac{mv^3}{qe\omega}\right\}_{\omega_i} + \frac{q^2}{c^2}\int_{\beta^2 n^2 > 1}\mu(\omega)\left[1 - \frac{1}{\beta^2 n^2}\right]\omega\,\mathrm{d}\omega\,,$$

where $n(\omega) = \sqrt{\varepsilon(\omega)\mu(\omega)}$ is the index of refraction, and ω_i are the positive real roots of the equation $\varepsilon(\omega) = 0$.

The second term is here the loss due to Čerenkov radiation. Indeed,

---

(*) The quantum mechanical theory of the Čerenkov effect is given by V. GINZBURG [5].

(+) See appendix to the Russian translation of N. BOHR's book [3].

substituting in the dispersion equation of the medium $(\omega^2/c^2)n^2(\omega) = k^2$ ($\boldsymbol{k}$ is the wave vector), $x^2+(\omega^2/v^2)$ for k^2 (x is the component of $\boldsymbol{k}$ perpendicular to the velocity), we obtain $\beta^2n^2 - 1 = (x^2v^2/\omega^2)$ i.e. the propagating waves satisfy the condition $\beta^2n^2 > 1$ fulfilled in the second term. Hence we conclude that the first term in (4) is the polarisation loss and the loss due to pair collisions. Notice that this term does not include $\mu(\omega)$.

Let us determine now the energy loss at the « far » collisions of a particle moving in an anisotropic dielectric (*).

Supposing for simplicity that $\mu = 1$, and that the medium possesses axial symmetry, we obtain the following expression for the energy loss of a particle moving along the axis of symmetry [10]:

$$-\frac{\mathrm{d}\varepsilon}{\mathrm{d}z} = -\frac{iq^2}{\pi c^2}\int_0^{x_m} x\,\mathrm{d}x \int_{-\infty}^{\infty} \frac{\{1-(1/\beta^2\varepsilon_r)\}\omega\,\mathrm{d}\omega}{x^2+(\omega^2/v^2)(\varepsilon_z/\varepsilon_r)(1-\beta^2\varepsilon_r)} \tag{5}$$

where ε_r and ε_z are the principal values of the tensor of dielectric constants. If $\varepsilon_r(\omega)$ and $\varepsilon_z(\omega)$ have no common zeroes, we obtain after integration

$$-\frac{\mathrm{d}\varepsilon}{\mathrm{d}z} = \frac{q^2}{c^2}\int \left|1-\frac{1}{\beta^2\varepsilon_r}\right| \omega\,\mathrm{d}\omega \tag{6}$$

where one must integrate over the region

$$\frac{x_m^2v^2}{\omega^2} > \frac{\varepsilon_z(\omega)}{\varepsilon_r(\omega)}\,[\beta^2\varepsilon_r(\omega)-1] > 0\,. \tag{7}$$

For the investigation of the character of the energy loss in an anisotropic dielectric, let us consider the dispersion equation of this medium

$$\frac{x^2}{\varepsilon_z(\omega)} + \frac{k_z^2}{\varepsilon_r(\omega)} = \frac{\omega^2}{c^2}\,,$$

where k_z is the component of the wave vector parallel to the direction of motion, obviously equal to $k_z = \omega/v$. The condition of the possibility of wave propagation, being simultaneously the condition of Čerenkov radiation, has the form $(\varepsilon_z/\varepsilon_r)(\beta^2\varepsilon_r - 1) > 0$. Thus, in a transparent (with infinitely small attenuation) anisotropic dielectric the total energy loss is completely reduced to the loss due to the Čerenkov radiation [10].

(*) The works [7-9] are dedicated to the theory of Čerenkov radiation in anisotropic media.

Let us consider the limit transition from an anisotropic to an isotropic dielectric. The region of frequencies, in which ε_z and ε_r have different signs, tends to a point at the transition to the isotropic case. The frequency, for which $\varepsilon = 0$, does not satisfy the condition of propagation, and, therefore, the corresponding term determines the polarization energy loss [8].

The boundary of the bands of Čerenkov radiation does not depend on the indefinite magnitude x_m, though the condition of Čerenkov radiation includes it. Indeed, one must take into consideration the left part of the inequality (7) only for those frequencies, for which ε_r is small enough. But then the imaginary part of ε_r, i.e. the wave attenuation, must be taken into account. This attenuation cuts off the spectrum of the radiated frequencies, and, therefore, the boundaries of the bands of Čerenkov radiation are approximately determined from the condition $\operatorname{Im} \varepsilon_r(\omega) \approx \operatorname{Re} \varepsilon_r(\omega)$ [10].

Notice that in the case of an anisotropic dielectric the value of the velocity of the particle may tend to zero, while in the isotropic case this is impossible. If $\beta \to 0$, the Čerenkov energy loss is determined by the formula [10]

$$-\frac{\mathrm{d}\varepsilon}{\mathrm{d}z} = \frac{q^2}{v^2}\int \frac{\omega\,\mathrm{d}\omega}{|\varepsilon_r|}, \quad \frac{x_m^2 v^2}{\omega^2} > -\frac{\varepsilon_z}{\varepsilon_r} > 0\,. \tag{8}$$

The energy loss of a particle moving in an optically active anisotropic medium with the dielectric constant tensor

$$\varepsilon_{ik} = \begin{pmatrix} \varepsilon_1\,, & -i\varepsilon_2, & 0 \\ i\varepsilon_2\,, & \varepsilon_1, & 0 \\ 0\,, & 0\,, & \varepsilon_3 \end{pmatrix}$$

is determined by the following formula [11] (*)

$$-\frac{\mathrm{d}\varepsilon}{\mathrm{d}z} = \frac{q^2}{v^2}\left\{\int \frac{(1-\varepsilon_1\beta^2)(n_1^2-\varepsilon_1)-\beta^2\varepsilon_2^2}{\varepsilon_1(n_2^2-n_1^2)}\,\omega\,\mathrm{d}\omega + \right. \tag{9}$$

$$\left. + \int \frac{(1-\varepsilon_1\beta^2)(n_2^2-\varepsilon_1)-\beta^2\varepsilon_2^2}{\varepsilon_1(n_1^2-n_2^2)}\,\omega\,\mathrm{d}\omega \right\} + \frac{q^2}{v^2}\sum_i \frac{\omega_i}{(\mathrm{d}\varepsilon_1/\mathrm{d}\omega)_i} \ln\left[1 + \frac{x_m^2}{\omega_i^2} v^2 \left(\frac{\varepsilon_1}{\varepsilon_3}\right)_i\right],$$

where

$$n_{1,2}^2 = \frac{1}{2\varepsilon_1\beta^2}\{(\varepsilon_1^2-\varepsilon_2^2+\varepsilon_1\varepsilon_3)\beta^2+\varepsilon_1-\varepsilon_3 \pm \sqrt{(\varepsilon_1^2-\varepsilon_2^2-\varepsilon_1\varepsilon_3)^2\beta^4 - 2\varepsilon_1(\varepsilon_1^2-\varepsilon_2^2+\varepsilon_3^2)\beta^2 + }$$

$$+ 2\varepsilon_3(2\varepsilon_1^2+\varepsilon_2^2)\beta^2+(\varepsilon_3-\varepsilon_1)^2\}$$

(*) See also [12].

are the values of the refraction indexes in the directions corresponding to the maxima of Čerenkov radiation. In the first two terms the integration is performed over the region defined by the inequalities $x_m^2 e^2/\omega^2 > n_{1,2}^2 \beta^2 > 1$ and in the third term the summation is performed over the frequencies ω_i for which ε_1, ε_2 and ε_3 become zero simultaneously.

2. – The Penetration of a Charged Particle Through Electronic Plasma.

Let us consider now the interaction of a charged particle with electronic plasma. Let a charge q move uniformly with the velocity $\boldsymbol{v}$ through the plasma, the state of which is described by the distribution function $F(\boldsymbol{r}, \boldsymbol{u}, t)$ ($\boldsymbol{u}$ is the velocity of electrons of the plasma). In the case of the high frequency oscillations of the plasma, the collisions of electrons with ions and with one another may not be taken into account, and we may base upon the following kinetic equation [13, 14].

$$\frac{\partial F}{\partial t} + \boldsymbol{u}\frac{\partial F}{\partial \boldsymbol{r}} + \frac{e}{m}\left(\boldsymbol{E} + \frac{1}{c}[\boldsymbol{u}\boldsymbol{H}]\right)\frac{\partial F}{\partial \boldsymbol{u}} = 0 \tag{10}$$

where $\boldsymbol{E}$ and $\boldsymbol{H}$ are the selfconsistent electric and magnetic fields acting in the plasma. Supposing that the distribution function differs little from Maxwell's function $f_0 = n_0(m/2\pi T)^{\frac{3}{2}} \exp[-\varepsilon/T]$ (n_0 is the equilibrium density of electrons, T is the temperature in ergs, ε is the energy of one electron), we obtain the following linearized system of equations for the field $\boldsymbol{E}$ and the deviation f of the distribution function from Maxwell's function (it is supposed that rot $\boldsymbol{E} = 0$)

$$\begin{cases} \dfrac{\partial f}{\partial t} + \boldsymbol{u}\dfrac{\partial f}{\partial \boldsymbol{r}} + \dfrac{e}{m}\boldsymbol{E}\dfrac{\partial f_0}{\partial \boldsymbol{u}} = 0 \\ \operatorname{div}\boldsymbol{E} = 4\pi e\int f\,\mathrm{d}\boldsymbol{u} + 4\pi q\,\delta(\boldsymbol{r} - \boldsymbol{v}t)\,. \end{cases} \tag{11}$$

One can show that the Fourier component of the electric field $\boldsymbol{E}_k$ is equal

$$\boldsymbol{E}_k = -i\frac{q}{2\pi^2}\boldsymbol{k}\left(k^2 - \frac{w(z)}{a^2}\right)^{-1} \tag{11'}$$

where $\omega = \boldsymbol{k}\boldsymbol{v}$, $a = \sqrt{T/4\pi n_0 e^2}$ (Debye's radius), $z = \sqrt{(3/2)}(\omega/ks)$, $s = \sqrt{3T/m}$ (the mean thermal velocity of the electrons of the plasma), and

$$w(z) = \frac{1}{\sqrt{\pi}}\,\text{V.p.}\int_{-\infty}^{\infty}\frac{y\exp[-y^2]}{z-y}\,\mathrm{d}y - i\sqrt{\pi}z\exp[-z^2] \tag{12}$$

The energy loss due to «far» collisions is equal [15]

$$(13)\qquad -\left(\frac{d\varepsilon}{dz}\right)_{far} = 2i\frac{q^2\Omega^2}{\pi v^2}\int_0^{x_m} k\,dk \int_{-\sqrt{\frac{2}{3}}(v/s)}^{\sqrt{\frac{2}{3}}(v/s)} \frac{w(z)\,z\,dz}{k^2-(w(z)/a^2)} =$$

$$= \frac{2q^2\Omega^2}{\pi v^2}\,\mathrm{Re}\, i\int_0^{\sqrt{\frac{2}{3}}(v/s)} \ln\left[1-\frac{x_m^2 a^2}{w(z)}\right] z w(z)\,dz\,,$$

where $\Omega = \sqrt{4\pi n_0 e^2/m}$. The energy loss due to pair collisions must be added to this expression. Such addition is equivalent to the choice of x_m according to (2).

In the limiting case $v \gg s$ we obtain a formula similar to Bohr's one:

$$(14)\qquad -\frac{d\varepsilon}{dz} = \frac{q^2\Omega^2}{v^2}\left(\ln 1.123\,\frac{mv^3}{eq\Omega} - \frac{1}{2}\,\frac{s^2}{v^2}\right)$$

(it is supposed that $v < eq/\hbar$).

Notice that the first term in (14) may be obtained from the general formula for polarization energy loss in a dielectric if we assume that $\varepsilon = 1 - (\Omega/\omega)^2$. Thus, at sufficiently low temperatures ($s \ll v$) it is possible to consider a plasma as a dielectric.

If $v \ll s$

$$(14')\qquad -\left(\frac{d\varepsilon}{dz}\right)_{far} = \sqrt{\frac{6}{\pi}}\,\frac{q^2\Omega^2}{s^3}\,v\ln\frac{x_m s}{\Omega}\,.$$

Notice that in the limiting cases $v \gg s$ and $v \ll s$ the interaction of a particle with a transversal field is essentially less than with a longitudinal field.

Let us quote now some more formulae for the energy loss of a particle moving through plasma in an external magnetic field $\boldsymbol{H}_0(\boldsymbol{H}_0 \| \boldsymbol{v})$ (*).

If $\omega_H = eH_0/mc \ll \Omega$ and $v \gg s$

$$(15)\qquad -\left(\frac{d\varepsilon}{dz}\right)_{far} = \frac{q^2\Omega^2}{2v^2}\left\{\ln\frac{x_m^2 v^2}{\Omega^2} - (1-\beta^2)\,\frac{\omega_H^2}{\Omega^2}\right\}.$$

If $\omega_H \gg \Omega(1-\beta^2)^{-\frac{1}{2}}$ and $v \gg s$

$$(15')\qquad -\left(\frac{d\varepsilon}{dz}\right)_{far} = \frac{q^2\Omega^2}{2v^2}\left\{\ln\frac{x_m^2 v^2}{\omega_H^2(1-\beta^2)} - 1\right\}.$$

Thus, an external magnetic field lessens the energy loss of a particle.

(*) These formulae are obtained by I. Fainberg, A. Sitenko, C. Stepanov and the author.

3. – The Čerenkov and the Doppler Effects in Composite Systems.

The Čerenkov radiation may take place, as pointed out by L. MANDELSTAMM, not only in the case of a particle moving in a continuous dielectric, but also in the case of a particle moving close by its boundary. The theory of the Čerenkov radiation of a charge moving in a canal through a dielectric was given by V. GINZBURG and I. FRANCK.

It is worth noticing that for the Čerenkov radiation the dielectric constant of the surrounding medium must not necessarily be greater than unit [17]. If a canal is made, for example, in plasma, radiation takes place, too. It is due to the fact that slow electromagnetic waves, with phase velocity less than c and with frequency corresponding to the negative values of the dielectric constant of the plasma, can propagate along that canal. The full energy loss, reduced in this case to Čerenkov's one, is equal [17]

$$-\frac{\mathrm{d}\varepsilon}{\mathrm{d}z}=\frac{2q^2\omega^2}{v^2\Omega^2}(1-\beta^2)\frac{x_2a}{(x_1a)^2}\frac{1-\beta^2\varepsilon(\omega)}{2-\beta^2\varepsilon(\omega)}\frac{K_0(x_2a)}{I_0^2(x_1a)K_1(x_2a)}\,, \tag{16}$$

where I_0, K_0, K_1 are the modified Bessel functions, a is the radius of the canal, $x_1=(\omega/v)\sqrt{1-\beta^2}$, $x_2=(\omega/v)\sqrt{1-\beta^2\varepsilon(\omega)}$, ω is the frequency of the wave, the phase velocity of which equals v.

The presence of a dielectric is not necessary for the existence of radiation at a uniform motion of a charge; a particle can also radiate moving through a composite system containing no dielectric (for example, through a system of connected resonators), if only waves with phase velocity less than c can propagate in that system (*). In this case it is convenient to use the method of normal oscillations for the investigation of the radiation, developing the transversal part of the vector potential $\boldsymbol{A}(\boldsymbol{r}, t)$ in series of eigenoscillations of the corresponding problem. If $\boldsymbol{A}_\lambda(\boldsymbol{r})\exp[i\omega_\lambda t]$ designate different eigenwaves able to propagate in the considered system (λ is a set of the indices characterizing the wave, ω_λ is its frequency), this development has the form

$$\boldsymbol{A}(\boldsymbol{r}, t)=\sum_\lambda q_\lambda(t)\boldsymbol{A}_\lambda(\boldsymbol{r})\,,$$

where q_λ satisfy the equations

$$\ddot{q}_\lambda+\omega_\lambda^2 q_\lambda=f_\lambda(t)\,,\quad f_\lambda(t)=\frac{1}{c}\int\boldsymbol{j}\boldsymbol{A}_\lambda^*\,\mathrm{d}V\,, \tag{17}$$

(*) The results cited below belong to G. LUBARSKIJ, I. FAINBERG and the author [18].

($\boldsymbol{j}$ is the current due to the moving particle; $\boldsymbol{A}_\lambda$ are normalized according to the condition $\int \boldsymbol{A}_\lambda \boldsymbol{A}_\lambda^* \, \mathrm{d}V = 4\pi c^2 \delta_{\lambda\lambda'}$).

This equation is the one describing the forced oscillations of an oscillator subjected to the action of the force $f_\lambda(t)$. The possibility of radiation is equivalent to the existence of resonance between the eigenoscillations and the force $f_\lambda(t)$. If this force is characterized by a frequency spectrum $\Omega_{\lambda n}$, the condition of the resonance has such a form (*)

$$\omega_\lambda = \Omega_{\lambda n} . \tag{18}$$

Let us consider the radiation of a charge moving uniformly through a chain of resonators connected with one another. We shall consider the linear periodic structure consisting of a set of identical resonators connected with one another with apertures situated along the x-axis. The particle moves through these apertures with the velocity $\boldsymbol{v}$. In this case

$$\boldsymbol{A}_\lambda(\boldsymbol{r}) = \exp [ikx] \boldsymbol{a}_{kp}(\boldsymbol{r}) , \tag{19}$$

where $\boldsymbol{a}_{kp}$ is a function periodical with respect to x with the period l (l is the length of the resonators along the x-axis), k is a continuous parameter in the interval $(-\pi/l, \pi/l)$ and p one or several discrete parameters characterizing separate waves. The frequency spectrum of the force $f_\lambda(t)$ is in this case $\Omega_{kn} = (k + (2\pi n/l))v$ ($n = 0, \pm 1, \pm 2, \ldots$) and the condition of resonance takes the following form

$$\omega_{kp} = \left(k + \frac{2\pi n}{l} \right) v . \tag{20}$$

For determining the intensity of radiation, it is necessary to know the Fourier components of the function $(\boldsymbol{v}/v)\boldsymbol{a}_\lambda(x, 0, 0)$. One may show that the intensity of radiation equals

$$I = \frac{q^2 v^2 l}{4c^2} \sum_{n, \lambda_j} \frac{|b_\lambda^{(n)}|^2}{|(\mathrm{d}\omega_\lambda/\mathrm{d}k) - v|_{\lambda = \lambda_j}} , \quad b_\lambda^{(n)} = \frac{1}{l} \int_0^l \frac{\boldsymbol{v}}{v} \boldsymbol{a}_\lambda(x, 0, 0) \exp \left[-\frac{2\pi i n x}{l} \right] \mathrm{d}x , \tag{21}$$

where λ_j are the values of λ satisfying the equation $\omega_\lambda - \Omega_{kn} = 0$. Thus, the intensity of radiation is determined by the character of the dispersional dependance $\omega_\lambda \equiv \omega_p(k)$ and by the Fourier components $b_\lambda^{(n)}$.

(*) In an unlimited dielectric $\Omega_{\lambda n} = \boldsymbol{k}\boldsymbol{v}$ ($\boldsymbol{k}$ is the wave vector, $\boldsymbol{v}$ is the velocity of the particle) the condition of resonance also brings us directly to the condition of the Čerenkov radiation: $\cos\theta = 1/(\beta\sqrt{\varepsilon})$ (where θ is the angle between $\boldsymbol{v}$ and $\boldsymbol{k}$).

The frequency spectrum of a linear chain of identical cylindrical resonators, connected with one another by small apertures situated along the common axis of the resonators, consists of discrete bands. In the lower band the frequency ω is connected with k by the relation [19]

$$\omega = \omega_0[1 + \alpha(1 - \cos kl)], \qquad \alpha = \frac{2}{3\pi J_1^2(\mu_1)} \frac{a^3}{R^2 l}, \tag{22}$$

where ω_0 is the lower frequency of the resonator (a is the radius of the aperture, R is the radius of the resonator, l is its length, J_1 is the Bessel function, μ_1 is the first root of J_0).

If a particle moves through the apertures with a velocity exceeding $l\omega_0/\pi$, it will radiate. Using (21) it is possible to show that the intensity of radiation in the lower band of frequencies is determined by the formula

$$I = \frac{16q^2v^3}{R^2l^2\omega_0^2 J_1^2(\mu_1)} \frac{\sin^2(\omega_0 l/2v)}{1 - (\alpha\omega_0 l/v)\sin(\omega_0 l/v)}. \tag{23}$$

An essential difference between the character of the Čerenkov radiation in an unlimited dielectric and the radiation in periodic structures consists of the following: in the first case a particle with a given velocity radiates a continuous spectrum, a particular frequency corresponding to each direction, and in the second case the particle radiates a discrete spectrum.

A discrete spectrum is also radiated by a particle moving along the axis of a homogeneous waveguide filled with a dielectric. In this case $\omega_\lambda = \sqrt{\omega_g^2 + k^2 s^2}$, where ω_g is the boundary frequency and $s = c/\sqrt{\varepsilon(\omega)}$. The condition of resonance leads to the relation $\sqrt{\omega_g^2 + k^2 s^2} = vk$ or

$$\omega = \frac{\omega_g}{\sqrt{1 - (s/v)^2}}. \tag{24}$$

whence it is clear that ω can assume only discrete values.

Using (21), one can show that the intensity of radiation of a particle moving along the axis of a cylindrical waveguide filled with a dielectric is equal to

$$I = \frac{2q^2v^2}{c^2R^4} \sum \frac{\mu_p^2 s^4}{J_1^2(\mu_p)\omega^2} \frac{1}{|(\mathrm{d}\omega/\mathrm{d}k) - v|}, \tag{25}$$

where ω as a function of k is defined from the equation $\omega = s(\omega)\sqrt{k^2 + (\mu_p^2/R^2)}$ (R is the radius of the waveguide, μ_p are the roots of Bessel function J_0). The radiated frequencies ω in (25) satisfy the condition of resonance

$$\omega = s(\omega)\sqrt{k^2 + \frac{\mu_p^2}{R^2}} = kv. \tag{25'}$$

We consider now the question about the radiation of an oscillator moving uniformly along the axis of a periodic structure [18]. In this case, as well as in the case of motion of an oscillator in a medium or in a channel made in a dielectric, a peculiar Doppler effect takes place. Here the current is $j_x = \Omega d \cos \Omega t\, \delta(x - vt)$, $j_y = j_z = 0$, where $d = d_0\sqrt{1-(v/c)^2}$, $\Omega = \Omega_0\sqrt{1-(v/c)^2}$, d_0 is the dipole moment and Ω_0 is the frequency of the oscillator in the coordinate system connected with it.

The condition of resonance is the condition of radiation and has the following form in the considered case [18]

$$\omega_\lambda = \left| v\left(k + \frac{2\pi n}{l}\right) \pm \Omega \right| . \tag{26}$$

In particular, the condition (26) for an oscillator moving in an unlimited homogeneous dielectric has the form

$$\omega = \frac{\Omega}{|1 - (\sqrt{\varepsilon}/c)\, v \cos\theta|} , \tag{26'}$$

where θ is the angle between the direction of the propagation of waves and the velocity of the oscillator.

The intensity of the radiation of a moving oscillator is determined by a formula similar to (21); only the coefficient before the sum is $\Omega_0^2 l d^2/16c^2$ instead of $q^2v^2l/4c^2$ [18].

4. – The Interaction of a Beam of Charged Particles with Slow Electromagnetic Waves.

Let us consider the question about the propagation of a beam of charged particles through a medium or a system in which slow electromagnetic waves can propagate. For definity we shall speak at first about a medium with the dielectric constant ε, though, as we shall see later, we can consider as well a chain of connected resonators.

Thus, we consider an unlimited dielectric in which an infinite beam moves in the direction of the x-axis. The unperturbed state of the beam is determined by the velocity v_0 and the charge density ϱ_0, which are considered to be constant and independent from the coordinates. To make the existence of such a state possible, one must suppose either that there is an ion beam parallel to the electron beam with the same value of the velocity and the density, or that there exists a strong enough focusing magnetic field.

Let us suppose that the deviations of the velocity v and the density ϱ from

the unperturbed values are small in comparison with v_0 and ϱ_0 and that v is directed along the x-axis. Then we may base upon Maxwell's equations in which the current density is $j = \varrho v_0 + v\varrho_0$ and upon linearized equations of motion and of continuity

$$\frac{\partial v}{\partial t} + v_0 \frac{\partial v}{\partial x} = \frac{e}{m} E , \qquad \frac{\partial \varrho}{\partial t} + \frac{\partial}{\partial x}(\varrho_0 v + v_0 \varrho) = 0 .$$

The solution of the equations in the form of plane waves $\exp[i(\omega t - \boldsymbol{kr})]$ leads to the following dispersion equation [21] (*)

$$\frac{\omega_0}{\omega^2 - s^2 k_x^2} + \frac{\Omega_b^2}{(\omega - v_0 k_x)^2} = 1 , \tag{27}$$

where $\omega_0 = \varkappa s$, $\varkappa = \sqrt{k^2 - k_x^2}$, $s = c/\sqrt{\varepsilon}$, $\Omega_b^2 = 4\pi e \varrho_0 / m$.

It is possible to show that, ε being real and k_x being given, the equation (27) leads to complex ω, if $v_0 \gg s$ [21, 23]. In other words, the state of the beam becomes unstable if its unperturbed velocity exceeds the critical velocity on the Čerenkov effect.

In the case of small density of the beam ($\Omega_b \ll \omega_0$) the frequency corresponding to $k_x = \omega_0 / \sqrt{v_0^2 - s^2}$ has the maximal imaginary part. The frequency of oscillations and the negative attenuation are then equal

$$\begin{cases} \omega = \omega_0 \dfrac{1}{(1 - (s^2/v_0^2))^{\frac{1}{2}}} - \dfrac{\omega_0}{2^{\frac{4}{3}}} \left(1 - \dfrac{s^2}{v_0^2}\right)^{\frac{1}{3}} \left(\dfrac{\Omega_b}{\omega_0}\right)^{\frac{2}{3}} \\ \gamma = -3^{\frac{1}{2}} 2^{-\frac{5}{3}} \left(1 - \dfrac{s^2}{v_0^2}\right)^{\frac{1}{2}} \omega_0 \left(\dfrac{\Omega_b}{\omega_0}\right)^{\frac{2}{3}} . \end{cases} \tag{28}$$

Considering (27) as an equation for k_x, ω being given, the maximal unstability, i.e. the maximal negative imaginary part k_x, corresponds to the frequency $\omega = \omega_0 (1 - (s^2/v_0^2))^{-\frac{1}{2}}$. This imaginary part is equal

$$\xi = 3^{\frac{1}{2}} 2^{-\frac{4}{3}} \frac{\omega_0}{v_0} \left(\frac{v_0}{s}\right)^{\frac{1}{3}} \left(1 - \frac{s^2}{v_0^2}\right)^{\frac{1}{3}} \left(\frac{\Omega_b}{\omega_0}\right)^{\frac{2}{3}} . \tag{28'}$$

The maximum of ξ as a function of v_0 is equal to $\xi_{\max} = (3^{\frac{1}{2}}/4)(\omega_0/s)(\Omega_b/\omega_0)^{\frac{2}{3}}$ and corresponds to the frequency $\sqrt{2}\,\omega_0$ to be the most amplified [21].

(*) A similar equation for a beam moving in a waveguide with no dielectric is obtained in [22].

Let us consider now the propagation of a beam of particles through a linear chain of connected identical cylindrical resonators (*). (The resonators are connected by means of round apertures in the bases of the cylinders, through which passes the beam focussed by a sufficiently strong magnetic field). The connection between the resonators being supposed small, a strong perturbance of the field takes place only near the apertures. Almost in the entire value of the « n-th » resonator the field has, therefore, the form $E_n = q_n E_0$ where E_0 is the field in the isolated resonator, corresponding to the lower frequency ω_0.

In the absence of a beam the values q_n satisfy, as shown by V. Vladimirskij [19], the following finite difference equation

$$(\omega^2 - \omega_0^2) q_n - \alpha(2q_n - q_{n-1} - q_{n+1})\,\omega_0^2 = 0\,, \tag{29}$$

where ω is the frequency of the coupled oscillations of the resonators. From (29) it follows that [19]

$$q_n = q_0 \exp[in\psi]\,, \qquad \omega = \omega_0[1 + \alpha(1 - \cos\psi)]\,. \tag{29'}$$

If a beam of charged particles moves through a chain of resonators, the presence of space charges is equivalent to the introduction of a dielectric constant

$$\varepsilon = 1 - \frac{\Omega_b^2 l^2}{c^2(2\beta \operatorname{tg}(\psi/2) - (\omega l/c))} \tag{30}$$

(l is the length of the resonator, β v_0/c). In this case the following equation must be substituted for (29)

$$(\omega^2 - \omega_0^2) q_n + 4\pi i\omega \int (\varrho_0 v_n + v_0 \varrho_n) E_0^*\, \mathrm{d}V - \alpha\varepsilon(2q_n - q_{n-1} - q_{n+1})\omega_0^2 = 0 \tag{31}$$

where ϱ_n and v_n are the deviations of the charge density and the velocity of the beam from the equilibrium values in the « n-th » resonator (Integration is performed over the volume of the « n-th » resonator (+)).

The quantities ϱ_n and v_n are connected with the field by the equations of

(*) This question has been investigated by J. Fainberg and the author.

(+) The field E_0 is normalized according to the condition $\int |E_0|^2 \mathrm{d}V = 1$.

motion and of continuity:

$$(31') \qquad \begin{cases} -i\omega\frac{l}{2}(v_n + v_{n-1}) + v_0(v_n - v_{n-1}) = \frac{el}{2m}(E_n + E_{n-1}) \\ -i\omega\frac{l}{2}(\varrho_n + \varrho_{n-1}) + r_0(\varrho_n - \varrho_{n-1}) - \varrho_0(v_n - v_{n-1}) = 0 . \end{cases}$$

The following dispersion equation can be obtained from (31) and (31')

$$(32) \qquad \left[\frac{\omega^2}{\omega_0^2} - 2\alpha(1 - \cos\psi)\right]\left[1 - \frac{\Omega_b^2 l^2}{c^2(2\beta\,\mathrm{tg}\,(\psi/2) - (\omega l/c))^2}\right] = 1 .$$

For small ψ it degenerates into the equation (27) with the propagation velocity $s = \sqrt{\alpha}\omega_0 l$.

Thus, a chain of resonators is, in the case of small connection, equivalent to a dielectric with the phase velocity of the wave propagation $s = \sqrt{\alpha}\omega_0 l$. Therefore, in the case of $v_0 > \sqrt{\alpha}\omega_0 l$, the state of a beam passing through the resonators becomes unstable, and the density fluctuations existing in it propagate in the form of waves with a growing amplitude.

The discussed unstability of the beam and the increasing oscillations are analogous to the increasing oscillations, found by PIERCE [24] and HAEFF [25] during the investigation of different methods of amplification and generation of microwaves.

These discussions stress the close connection between these processes and the Čerenkov radiation of a single particle.

Let us still consider the question of the stability of an infinite beam moving in a dielectric medium situated in constant homogeneous electric and magnetic fields.

Let the electric and the magnetic fields $\boldsymbol{E}$ and $\boldsymbol{H}$ be directed correspondingly along the X- and Z-axes. Then, as it is known, a stationary motion of charges along the Y-axis with the velocity $v_0 = c(E/H)$ is possible. It is interesting to see under what conditions this state of the beam is unstable.

An unstability arises if $v_0 > s$ [26]. In the case of small velocities of the beam the generated frequency is equal

$$(33) \qquad \omega = \omega_H \frac{1}{(v_0/s) - 1} ,$$

where $\omega_H = (eH/mc)$. The imaginary part of frequency is equal

$$(33') \qquad \gamma = \frac{\Omega_b}{2}\left(\frac{v_0}{s} - 1\right)^{\frac{1}{2}} .$$

5. – The Propagation of a Beam of Charged Particles Through Electronic Plasma.

The propagation of a beam of charged particles through electronic plasma needs a special consideration because one may consider the plasma as a dielectric only at low temperatures [21]. For the investigation of this question it is reasonable to base upon the kinetic equation (11), using moreover the linearized equations

$$\operatorname{div} \boldsymbol{E} = 4\pi e \int f \, \mathrm{d}\boldsymbol{u} + 4\pi\varrho \,,$$

$$\frac{\partial \boldsymbol{v}}{\partial t} + (\boldsymbol{v}_0 \nabla)\boldsymbol{v} = \frac{e}{m}\boldsymbol{E} \,,$$

$$\frac{\partial \varrho}{\partial t} + \varrho_0 \operatorname{div} \boldsymbol{v} + v_0 \operatorname{grad} \varrho = 0 \,,$$

for the deviations of the density of the beam ϱ and the velocity $\boldsymbol{v}$ from the equilibrium values ϱ_0 and $\boldsymbol{v}_0$. Supposing $\boldsymbol{v}_0$ and $\boldsymbol{v}$ to be directed along the X-axis, and considering the solutions of the form $\exp[i(\omega t - kx)]$ it is possible to show that the dispersion equation has in this case the form [21]

$$-\frac{4\pi e^2}{mk}\int_{-\infty}^{\infty}\frac{f_0'(u)}{\omega - uk}\,\mathrm{d}u + \frac{\Omega_b^2}{(\omega - kv_0)^2} = 1 \,, \tag{34}$$

where $f_0 = n_0\sqrt{m/2\pi T}\exp[-(mu^2/2T)]$.

For sufficiently small Ω_b the equation (34), considered as an equation relatively to ω, has the root $\omega = kv_0 + \eta$, where $|\eta| \ll kv_0$ and is determined by the expression:

$$\frac{\Omega_b^2}{\eta^2} = 1 - \frac{1}{a^2k^2}\left\{\frac{3}{2}\left(\frac{v_0}{s}\right)^2 \exp\left[-\frac{3}{2}\left(\frac{r_0}{s}\right)^2\right]\int_0^1 \exp\left[\frac{3}{2}\left(\frac{r_0}{s}\right)^2 y\right]\frac{\mathrm{d}y}{\sqrt{y}} + \right.$$
$$\left. + i\sqrt{\frac{3\pi}{2}}\frac{v_0}{s}\exp\left[-\frac{3}{2}\left(\frac{v_0}{s}\right)^2\right] - 1\right\}, \tag{35}$$

where $s = \sqrt{3T/m}$. As (35) includes the square of η there always exists a root with $\operatorname{Im}\omega < 0$, corresponding to a wave with a growing amplitude. Thus, the state of a beam propagating through the plasma is unstable for all values of its velocity [21, 27].

Notice that, if $v_0 > s$, the dispersion equation acquires the form

$$\frac{\Omega^2}{\omega^2 - s^2k^2} + \frac{\Omega_b^2}{(\omega - kv_0)^2} + i\sqrt{\frac{3\pi}{2}}\exp\left[-\frac{3}{2}\left(\frac{\omega}{ks}\right)^2\right] = 1 \,, \tag{34'}$$

which differs only by a small term from the dispersion equation for the dielectric, in which the phase velocity is equal to the thermal velocity of electrons in plasma.

6. – The Longitudinal Plasma Oscillators in External Fields.

We proceed to the theory of plasma oscillations. We begin with small oscillations of plasma in a magnetic field $\boldsymbol{H}_0$ and an electric field $\boldsymbol{E}_0$ both constant and homogeneous.

The linearized kinetic plasma equation has in this case the form

$$\frac{\partial f}{\partial t} + \boldsymbol{u}\frac{\partial f}{\partial \boldsymbol{r}} + \frac{e\boldsymbol{E}_0}{m}\frac{\partial f}{\partial \boldsymbol{u}} + \frac{e\boldsymbol{E}}{m}\frac{\partial F_0}{\partial \boldsymbol{u}} + \frac{e}{mc}[\boldsymbol{u}\boldsymbol{H}_0]\frac{\partial f}{\partial \boldsymbol{u}} + \frac{1}{\tau}f = 0\,, \tag{36}$$

where $f(\boldsymbol{r}, \boldsymbol{u}, t)$ is the deviation of the electron distribution function from the equilibrium one $F_0(\boldsymbol{u})$, and $\boldsymbol{E}$ is the electric field due to plasma oscillations. The last term describes phenomenologically the pair collisions (τ is the mean time between the collisions of electrons with ions and with one another). Considering the high frequency oscillations of a free plasma, as well as of the plasma in a magnetic field, this term may be neglected, but we cannot neglect it in the case of electric field.

The influence of the thermal factors is negligible in the case of the propagation of transverse electromagnetic waves (*). Therefore, we shall consider here only the longitudinal plasma oscillations, for which the eletric field is potential (the longitudinal plasma oscillations in a magnetic field may be considered separately from the transversal oscillations under the condition $ck \gg \omega$ [30]).

We consider firstly the case of plasma in a magnetic field. In this case the dispersion equation has the form

$$\int f_0(u^2)\exp\left[i(\eta\sin\vartheta + \zeta\vartheta)\right]\left\{\frac{\int_0^{2\pi}\exp\left[-i(\eta\sin\psi + \zeta\psi)\right]\boldsymbol{k}\boldsymbol{u}\,\mathrm{d}\psi}{1-\exp\left[2\pi i\zeta\right]} + \right.$$

$$\left. + \int_0^{\vartheta}\exp\left[-i(\eta\sin\psi + \zeta\psi)\right]\boldsymbol{k}\boldsymbol{u}\mathrm{d}\psi\right\}\mathrm{d}\boldsymbol{u} = -in_0\omega_B(ka)^2$$

or

$$1 + k^2a^2 - \exp\left[-\mu\right]\sum_{n=-\infty}^{\infty} I_{|n|}(\mu)\frac{z_0}{\sqrt{\pi}}\cdot \tag{37}$$

$$\cdot\left(\text{V.p.}\int_{-\infty}^{\infty}\frac{\exp\left[-y^2\right]}{z_n - y}\,\mathrm{d}y - \pi i\exp\left[-z_n^2\right]\right) = 0\,,$$

(*) The theory of the propagation of transversal waves in plasma is exposed in the monograph [28]. See also [29].

where $I_n(\mu)$ is the modified Bessel function,

$$\eta = \frac{k_x u_x}{\omega_H}, \quad \zeta = \frac{k_z u_z - \omega}{\omega_H}, \quad z_n = \sqrt{\frac{3}{2}}\frac{\omega - n\omega_H}{k_z s}, \quad \mu = 3\left(\frac{k_x s}{\omega_H}\right)^2$$

(the Z-axis is directed along the magnetic field, the vector $\boldsymbol{k}$ lies in the XZ-plane, ϑ is the angle between the X-axis and the projection of $\boldsymbol{u}$ on the XY-plane).

In the case of weak magnetic field, when $\omega_H \ll \Omega$, the equation (37) is reduced to the form

$$(37') \qquad (ka)^2 - w(z) + \frac{3}{2}\left(\frac{\omega_H}{\Omega}\right)^2 \sin^2\theta z^2 w'''(z) = 0,$$

where θ is the angle between $\boldsymbol{H}_0$ and $\boldsymbol{k}$, and $w(z)$ is defined by (12). The frequency and the attenuation of the oscillations are equal to [31, 32]

$$(38) \qquad \begin{cases} \omega = \Omega + \dfrac{1}{2\Omega}(\omega_H^2 \sin^2\theta + k^2 s^2), \\ \gamma = \sqrt{\dfrac{\pi}{8}}\dfrac{\Omega}{(ka)^3}\left(1 + \dfrac{1}{4!}\dfrac{\omega_H^2 \sin^2\theta}{\Omega^2 k^6 a^6}\right)\exp\left[-\dfrac{\omega^2}{2k^2a^2\Omega^2}\right]. \end{cases}$$

(If $\omega_H \to 0$ the formula for γ coincides with the expression for the attenuation of the free plasma oscillations found by LANDAU [14]).

In the limiting case of low temperatures, when $sk \ll \omega_H$, the dispersion equation (37) has two solutions [31, 32]

$$(39) \qquad \omega_1 = \omega_+(1 + \varepsilon_+), \qquad \omega_2 = \omega_-(1 + \varepsilon_-)$$

where

$$\omega_\pm^2 = \frac{1}{2}\Omega^2\left(1 + \nu \pm \sqrt{(1+\nu)^2 - 4\nu\cos^2\theta}\right)$$

$$\varepsilon_\pm = \frac{1}{2}(ka)^2 \frac{(\xi_\pm - \nu)^2}{(\xi_\pm - \nu)^2 + \nu\sin^2\theta}\left\{\frac{3\cos^4\theta}{\xi_\pm^2} - \left[\frac{\xi_\pm^2 + 3\xi_\pm\nu}{\nu(\xi_\pm - \nu)^3} - \frac{1}{\xi_\pm - \nu}\right]\cdot\sin^2\theta\cos^2\theta + \right.$$
$$\left. + \frac{3\sin^4\theta}{(\xi_\pm - 4\nu)(\xi_\pm - \nu)}\right\},$$

$$\nu = \left(\frac{\omega_H}{\Omega}\right)^2, \quad \xi_\pm = \left(\frac{\omega_\pm}{\Omega}\right)^2.$$

The attenuations corresponding to these frequencies are equal [31]

$$(39') \qquad \gamma_{1,2} = \sqrt{\frac{\pi}{8}}\frac{\Omega\xi_\pm(\xi_\pm - \nu)^2}{(ka)^3\cos\theta[(\xi_\pm - \nu)^2 + \nu\sin^2\theta]}\left\{\exp\left[-\frac{\omega_{1,2}^2}{2k^2a^2\Omega^2\cos\theta}\right] + \right.$$
$$\left. + \frac{1}{2\nu}(ka\sin\theta)^2\exp\left[-\frac{(\omega_{1,2} - \omega_H)^2}{2k^2a^2\Omega^2\cos^2\theta}\right]\right\}.$$

Here it is supposed that $\gamma_{1,2} \ll \varepsilon_{\pm} < \omega_{\pm}$, $|z_n| \gg 1$. If $\Omega > \omega_H$, these inequalities are no longer fulfilled for the frequencies $\omega_1 = n\omega_H$ ($n = 2, 3, \ldots$). For the discussion of this case we shall consider at first the angles θ not near to $\pi/2$. Then we can show, that if $\omega_1 = n\omega_H$ a strong attenuation determined by the following expression takes place [31]:

$$(40) \qquad \gamma_1 = \frac{\sqrt{\pi}}{(n-1)!}\, 2^{-(n+\frac{3}{2})} \frac{\sin^{2n}\theta}{\cos\theta} \frac{n^3\omega_H}{\cos^2\theta + [n^2 \sin\theta/(n^2-1)]^2} \left(\frac{ka\Omega}{\omega_H}\right)^{2n-3}, \quad (n \geqslant 2)$$

(it is supposed that $\gamma_1 \ll ks\cos\theta$).

If $\theta \approx \pi/2$, the formula (40) is not valid. In this case it is found that [31]

$$(40') \qquad \omega_1 = n\omega_H \pm \varepsilon_n, \qquad \varepsilon_n = \omega_H \frac{n^2-1}{\sqrt{2^{n+1}n!}} \left(\frac{ka\Omega}{\omega_H}\right)^{n-1}, \quad \varepsilon_n \gg sk\cos\theta, \quad (n \geqslant 2).$$

Thus, in the case of $\theta \sim \pi/2$ and a given magnetic field, longitudinal waves in the intervals of the frequencies $n\omega_H - \varepsilon_n < \omega < n\omega_H + \varepsilon_n$ ($n = 2, 3, \ldots$) cannot propagate in plasma (the existence of «gaps» of such a kind was pointed out by GROSS [30] who has found ε_2).

Let us consider now the plasma oscillations in an external electric field. In this case

$$F_0 = f_0(u^2) - \boldsymbol{u}\boldsymbol{E}_0 f_1(u^2), \qquad f_0 = C\exp\left[-w + \int_0^w \left(1 + \frac{w}{\xi}\right)^{-1} \mathrm{d}w\right], \quad f_1 = -\frac{el}{m}\frac{\partial f_0}{\partial u},$$

where $w = mu^2/2T$, $\xi = \frac{1}{6}(M/m)(eE_0 l/T)^2$, M is the mass of an ion and l is the mean free path of an electron. If l does not depend upon the velocity [33]

$$f_0 = C\exp[-w + \xi\ln(w+\xi)].$$

With the condition $m\Omega u/eE_0 \gg 1$ ($\bar{u}$ is the mean velocity of electrons), we shall get the following dispersion equation [34]

$$(41) \qquad k^2 - k^2\frac{\Omega^2}{\omega'^2} - k^2\bar{u}^2\frac{\Omega^2}{\omega'^4} - 2\Omega^2\frac{k^2}{\omega'^3}(\boldsymbol{k}\bar{\boldsymbol{u}}) - 3i\Omega^2\frac{e\boldsymbol{E}_0\boldsymbol{k}}{m}\frac{k^2}{\omega'^4} = 0,$$

where

$$\bar{u}^2 = \frac{1}{n_0}\int u^2 f_0(u^2)\,\mathrm{d}\boldsymbol{u}, \quad \bar{\boldsymbol{u}} = \frac{1}{3n_0}\boldsymbol{E}_0\int u^2 f_1(u^2)\,\mathrm{d}\boldsymbol{u}$$

and ω' is the complex frequency including also the term i/τ.

If $k^2\bar{u}^2 \ll \Omega^2$, $k\bar{u} \ll \Omega$, the real and imaginary parts of ω', i.e. the frequency

and the attenuation of the oscillations are equal to [34]

$$\omega = \Omega + \boldsymbol{k}\bar{\boldsymbol{u}} + \frac{1}{2}\frac{k^2\bar{u}^2}{\Omega}, \qquad \gamma = \frac{1}{\tau} - \frac{3}{2}\frac{e\boldsymbol{E}_0\boldsymbol{k}}{m\Omega}. \tag{42}$$

Thus, an electric field lowers the attenuation if the angle between the wave vector $\boldsymbol{k}$ and the electric field $\boldsymbol{E}_0$ is less than $\pi/2$. Even in the case of strong field, however, we have the inequality $eE_0k/m\Omega \ll 1/\tau$.

In the limiting cases of the weak and the strong fields the frequency is equal

$$\begin{cases} \omega = \Omega + \dfrac{1}{2}\dfrac{k^2s^2}{\Omega^2} + \sqrt{\dfrac{8}{3\pi}}\dfrac{el\cdot\boldsymbol{kE}_0}{ms}, & \dfrac{1}{6}\dfrac{M}{m}\left(\dfrac{eE_0l}{T}\right)^2 \ll 1 \\ \omega = \Omega + \dfrac{1}{2}\dfrac{\Gamma(5/4)}{\Gamma(3/2)}\dfrac{k^2\sigma^2}{\Omega} + \dfrac{4}{3}\dfrac{\Gamma(3/2)}{\Gamma(3/4)}\dfrac{el\cdot\boldsymbol{kE}_0}{m\sigma}, & \dfrac{1}{6}\dfrac{M}{m}\left(\dfrac{eE_0l}{T}\right)^2 \gg 1, \end{cases} \tag{42'}$$

where $s^2 = 3T/m$, $\sigma^2 = \sqrt{(4/3)(M/m)}(eE_0l/m)$.

7. – The Scattering of the Electromagnetic Waves by the Plasma Oscillations.

By the propagation of the electromagnetic waves in plasma there may appear combinational scattering of these waves by the density oscillations of the plasma. The electric and the magnetic fields of the scattered waves with the frequencies $\omega = |\omega_0 \pm \Omega|$ (ω_0 is the frequency of the incident wave) are determined by the Maxwell equations, in which the current and the charge densities have the form

$$\boldsymbol{j} = \frac{1}{4\pi}\frac{\partial}{\partial t}(\varepsilon'\boldsymbol{E}_0), \qquad \varrho = -\frac{1}{4\pi}\operatorname{div}(\varepsilon'\boldsymbol{E}_0),$$

where $\boldsymbol{E}_0$ is the electric field of the incident wave, and ε' is the fluctuation of the dielectric constant of the plasma, equal to $\varepsilon' = (\Omega^2/\omega^2)(n(\boldsymbol{r}, t)/n_0)$ (n is the deviation of the density of electrons from the equilibrium value n_0).

The differential scattering cross-section per unit volume is determined by the following formula

$$\mathrm{d}\sigma_\omega = \frac{1}{4}\left(\frac{e^2}{mc^2}\right)^2\left(\frac{\omega}{\omega_0}\right)^4\sqrt{\frac{\varepsilon(\omega)}{\varepsilon(\omega_0)}}\,|n_{\boldsymbol{k}-\boldsymbol{k}_0}|^2\,\frac{1+\cos^2\vartheta}{2}\,2\pi\sin\vartheta\,\mathrm{d}\vartheta,$$

where $n_q(t)$ is the space Fourier component of the density fluctuation $n(\boldsymbol{r}, t)$, ϑ is the angle between the wave vectors of the incident and the scattered

waves $\boldsymbol{k}_0$, $\boldsymbol{k}$; the line over n^2 means the time average. The value of $\overline{n_{\boldsymbol{q}}^2}$ can be found by using the expression for the energy of the plasma

$$\varepsilon = \int\left(\frac{1}{2}\, n_0 m u^2 + \frac{1}{8\pi} E^2\right) \mathrm{d}V = \sum_{\boldsymbol{q}} \frac{m}{2 n_0 q^2} \left(|\dot{n}_{\boldsymbol{q}}|^2 + \Omega^2 |n_{\boldsymbol{q}}|^2\right).$$

Supposing the law of the equal distribution of energy to be valid, we shall find that

$$\overline{|n_{\boldsymbol{q}}|^2} = \frac{q^2 T}{2\pi e^2}$$

and therefore

$$\mathrm{d}\sigma_\omega = \frac{1}{16\pi} \frac{e^2 T}{m^2 c^6} \left(\frac{\omega}{\omega_0}\right)^4 \sqrt{\frac{\varepsilon(\omega)}{\varepsilon(\omega_0)}} \{\omega^2 \varepsilon(\omega) + \omega_0^2 \varepsilon(\omega_0) - \\ - 2\omega\omega_0 \sqrt{\varepsilon(\omega)\varepsilon(\omega_0)} \cos\vartheta\}(1 + \cos^2\vartheta)\, 2\pi \sin\vartheta \,\mathrm{d}\vartheta . \tag{43}$$

The integral scattering cross-section is equal (*)

$$\sigma_\omega = \frac{1}{3} \frac{e^2 T}{m^2 c^6} \left(\frac{\omega}{\omega_0}\right)^4 \sqrt{\frac{\varepsilon(\omega)}{\varepsilon(\omega_0)}} [\omega^2 \varepsilon(\omega) + \omega_0^2 \varepsilon(\omega_0)] . \tag{43'}$$

8. – The Non-Linear Wave Motions in Plasma.

Finally, we shall consider the general theory of the wave motions in plasma. Such a theory, not based on the usually performed linearization of equations, can be developed without taking the temperature effects into account, i.e. supposing the temperature of plasma equal to zero (+). The state of plasma may be characterized here not by the distribution function, but by the density of electrons $n(\boldsymbol{r}, t)$. In the case of the wave motion we shall consider the density, and the velocity of the electrons, and the fields depend only upon one variable $\xi = \boldsymbol{i}\boldsymbol{r} - Vt$, where V is the velocity of the wave, and $\boldsymbol{i}$ is the unit vector in the direction of its propagation. Maxwell's equations and the motion equations

(*) These formulae are obtained by A. Sitenko, I. Prohoda.

(+) The results cited below belong to R. Polovin and the author.

acquire the form

$$[\boldsymbol{iE}'] = \beta \boldsymbol{H}', \qquad [\boldsymbol{iH}'] = -\beta \boldsymbol{E}' + \frac{4\pi}{c} e n \boldsymbol{v},$$

$$\boldsymbol{iE}' = 4\pi e(n - n_0), \qquad \boldsymbol{iH}' = 0,$$

$$(\boldsymbol{iv} - V)\boldsymbol{p}' = e\boldsymbol{E} + \frac{e}{c}[\boldsymbol{vH}]$$

where $\beta = V/c$ and $\boldsymbol{p} = m\boldsymbol{v}/\sqrt{1-(v^2/c^2)}$ is the electron momentum. Hence, the dimensionless momentum $\boldsymbol{\rho} = \boldsymbol{p}/mc$ satisfies the equations

$$(44) \qquad \begin{cases} \dfrac{\mathrm{d}^2 \varrho_{x,y}}{\mathrm{d}\tau^2} + \Omega^2 \dfrac{\beta^2}{\beta^2 - 1} \dfrac{\beta}{\beta - u_z} u_{x,y} = 0 \\ \dfrac{\mathrm{d}}{\mathrm{d}\tau}\left\{ (u_z - \beta) \dfrac{\mathrm{d}\varrho_z}{\mathrm{d}\tau} + u_x \dfrac{\mathrm{d}\varrho_x}{\mathrm{d}\tau} + u_y \dfrac{\mathrm{d}\varrho_y}{\mathrm{d}\tau} \right\} = \Omega^2 \dfrac{\beta^2 u_z}{\beta - u_z}, \end{cases}$$

where $\boldsymbol{u} = \boldsymbol{v}/c$, $\tau = t - (z/V)$ (the Z-axis directed along $\boldsymbol{i}$).

The limited solutions are possible only in the case of $V > c$, i.e. $\beta > 1$ (*).

The equations (44) can be obtained from the Lagrangian

$$(44') \qquad \mathcal{L} = \frac{1}{2}\left[\left(\frac{\mathrm{d}\xi}{\mathrm{d}\tau}\right)^2 + \left(\frac{\mathrm{d}\eta}{\mathrm{d}\tau}\right)^2 + \left(\frac{\mathrm{d}\zeta}{\mathrm{d}\tau}\right)^2\right] - \Omega^2 \frac{\beta^2}{\beta^2 - 1}\left[\beta\sqrt{\beta^2 - 1 + \xi^2 + \eta^2 + \zeta^2} + \zeta\right],$$

where

$$\xi = \sqrt{\beta^2 - 1}\,\varrho_x, \qquad \eta = \sqrt{\beta^2 - 1}\,\varrho_y, \qquad \zeta = \beta\varrho_z - \sqrt{1 + \varrho^2}.$$

Thus, the problem of the wave motions of plasma is equivalent to the problem of nonrelativistic motion of a particle in the field

$$U = \Omega^2 \frac{\beta^2}{\beta^2 - 1}\left[\beta\sqrt{\beta^2 - 1 + \xi^2 + \eta^2 + \zeta^2} + \zeta\right].$$

The general conservation laws follow from the expression for $\mathcal{L}$:

$$(45) \qquad \begin{cases} \dfrac{\beta}{2\pi}(E^2 + H^2) + \beta n_0 \dfrac{mc^2}{\sqrt{1-(v^2/c^2)}} - \dfrac{\boldsymbol{i}}{4\pi}[\boldsymbol{EH}] = \text{Const.} \\ \boldsymbol{pH} = \text{Const.} \end{cases}$$

(*) This conclusion is obvious for the transversal components of the velocity. The third equation (44) for u_z admits limited solutions for every value of β, if $u_x = u_y = 0$. However, such purely longitudinal motions are unstable, if $\beta < 1$.

Let us consider the longitudinal plasma oscillations. Putting

$$(46)\qquad \begin{cases} u = \dfrac{2k\,\mathrm{sn}\,(x,k)}{1+k^2\,\mathrm{sn}^2\,(x,k)}\,, \\ k = \sqrt{\dfrac{1-\sqrt{1-u_m^2}}{1+\sqrt{1-u_m^2}}}\,, \qquad k' = \sqrt{1-k^2}\,, \end{cases}$$

we obtain the following relation between x and τ

$$(47)\qquad \frac{k}{\beta k'}\frac{\mathrm{cn}\,(x,k)}{\mathrm{dn}(x,k)} - k'x + \frac{1}{k'K}\left[2Ex + \frac{\vartheta_3'(x/2k,\,q)}{\vartheta_3(x/2k,\,q)}\right] = \Omega\tau\,,$$

where u_m is the maximum value of u, and

$$K = \int_0^1 \frac{\mathrm{d}x}{\sqrt{(1-x^2)(1-k^2x^2)}}\,, \qquad E = \int_0^1 \sqrt{\frac{1-k^2x^2}{1-x^2}}\,\mathrm{d}x\,,$$

$$K' = \int_0^1 \frac{\mathrm{d}x}{\sqrt{(1-x^2)(1-k'^2x^2)}}\,, \qquad q = \exp\left[-\pi\frac{K'}{K}\right].$$

The frequency of the longitudinal oscillations depends upon their amplitude u_m and is determined by the following formula

$$(48)\qquad \omega = \Omega\frac{k'}{2E - k'^2K}\,.$$

In the limiting cases of small and great u_m the following expressions are valid

$$(49)\qquad \begin{cases} \omega = \Omega\left(1-\dfrac{3}{16}u_m^2\right), & u_m \ll 1 \\ \omega = \dfrac{\pi}{2\sqrt{2}}\,\Omega(1-u_m^2)^{\frac{1}{2}}\,, & 1-u_m \ll 1\,. \end{cases}$$

If $u_m \to 0$, ω degenerates into Langmuir's frequency Ω, and if $u_m \to 1$, ω tends to zero.

The electric field $E(\tau)$ and the density $n(\tau)$ are connected with $u(\tau)$ by means of the expressions

$$(50)\qquad eE = \pm\sqrt{2}\,mc\Omega\sqrt{\frac{1}{\sqrt{1-u_m^2}} - \frac{1}{\sqrt{1-u^2}}}\,, \quad n = \frac{n_0\beta}{\beta - u}\,.$$

The maximum value of E at $1 - u_m \ll 1$ is equal to

$$eE_{\max} = \sqrt{2}\, mc\Omega(1 - u_m^2)^{-\frac{1}{4}}.$$

Let us consider now the transversal oscillations. In the case of purely transversal oscillations $\varrho^2 = \text{const}$, and the electrons have circular orbits with the frequency

$$\omega = \Omega \frac{\beta}{\sqrt{\beta^2 - 1}} (1 + \varrho^2)^{-\frac{1}{4}}. \tag{51}$$

It is possible to consider the oscillations near to the transversal ones, for which ϱ differs little from a certain value ϱ_0. The frequencies of these oscillations are equal

$$\omega_{1,2} = \frac{\beta\Omega}{\sqrt{\beta^2 - 1}} \frac{1}{\sqrt{1 + \varrho_0^2}} \cdot \tag{52}$$

$$\cdot \sqrt{\frac{4\beta^2\varrho_0^2 + 5\beta^2 - 1}{2\beta^2\sqrt{1 + \varrho_0^2}} \pm \sqrt{\left(\frac{4\beta^2\varrho_0^2 + 5\beta^2 - 1}{2\beta^2\sqrt{1 + \varrho_0^2}}\right)^2 - \frac{1}{\beta^2}(\beta^2 - 1)(4 + 3\varrho_0^2)}}.$$

Let us notice at last that in the cases of $\beta \gg 1$ and $\beta \sim 1$ coupled longitudinal-transversal oscillations may be investigated, since in these cases the equations (44) may be exactly integrated.

REFERENCES

[1] I. Tamm and I. Franck: *Dokl. Akad. Nauk SSSR*, **14**, 107 (1937).
[2] E. Fermi: *Phys. Rev.*, **57**, 485 (1940).
[3] N. Bohr: *The Penetration of Atomic Particles through Matter* (appendix), (Moscow, 1950).
[4] E. Fermi: *Nuclear Physics* (Chicago, 1950).
[5] V. Ginzburg: *J. of Phys. USSR*, **2**, 441 (1940).
[6] A. Sitenko: *Dokl. Akad. Nauk SSSR*, **98**, 377 (1954).
[7] V. Ginzburg: *J. of Phys. USSR*, **3**, 101 (1940).
[8] A. Kolomenskij: *Dokl. Akad. Nauk SSSR*, **86**, 1097 (1952).
[9] M. Kaganov: *Žu. Tehn. Fiz.*, **23**, 507 (1953).
[10] A. Sitenko and M. Kaganov: *Dokl. Akad. Nauk SSSR*, **100**, 681 (1955).
[11] A. Sitenko: *Žu. Éksper. Teor. Fiz.*, in press.
[12] A. Kolomenskij: *Žu. Éksper. Teor. Fiz.*, **24**, 167 (1953).
[13] A. Vlassov: *Žu. Éksper. Teor. Fiz.*, **8**, 291 (1938).
[14] L. Landau: *Žu. Éksper. Teor. Fiz.*, **16**, 574 (1946).
[15] A. Ahiezer and A. Sitenko: *Žu. Éksper. Teor. Fiz.*, **23**, 161 (1952).
[16] V. Ginzburg and I. Frank: *Dokl. Akad. Nauk SSSR*, **56**, 699 (1949).

[17] L. Pjatigorskij: *Učenye Zapiski Harkov. Gosud. Univ.*, 1954.
[18] A. Ahiezer, G. Lubarskij and J. Fainberg: *Dokl. Akad. Nauk SSSR*, **73**, 55 (1950).
[19] V. Vladimirskij: *Žu. Tehn. Fiz.*, **17**, 1277 (1947).
[20] I. Frank: *Izv. Akad. Nauk SSSR, Ser. Fiz.*, **6**, 2 (1942).
[21] A. Ahiezer and J. Fainberg: *Žu. Éksper. Teor. Fiz.*, **21**, 1262 (1951).
[22] S. Ramo: *Phys. Rev.*, **56**, 276 (1939).
[23] M. Kaganov: *Žu. Tehn. Fiz.*, **23**, 514, 523 (1953).
[24] I. Pierce: *Proc. Inst. Radio Engrs.*, **35**, 111 (1947).
[25] A. Haeff: *Proc. Inst. Radio Engrs.*, **37**, 4 (1949).
[26] A. Ahiezer and R. Polovin: *Žu. Tehn. Fiz.*, **22**, 1794 (1952).
[27] D. Bohm and E. Cross: *Phys. Rev.*, **75**, 1851, 1864 (1949).
[28] J. Alpert, V. Ginzburg and E. Feinberg: *The Propagation of Radio Waves*. (Moscow, 1953).
[29] B. Geršman: *Žu. Éksper. Teor. Fiz.*, **24**, 559 (1953).
[30] E. P. Gross: *Phys. Rev.*, **82**, 232 (1951).
[31] A. Sitenko and C. Stepanov: *Žu. Éksper. Teor. Fiz.*, in press.
[32] A. Ahiezer and L. Pargamanik: *Učenye Zapiski Harkov. Gosud. Univ.*, 1948.
[33] B. Davydov: *Žu. Éksper. Teor. Fiz.*, **7**, 1069 (1937).
[34] A. Ahiezer and A. Sitenko: *Žu. Éksper. Teor. Fiz.*, **30**, 217 (1956).

SUPPLEMENTO AL VOLUME III, SERIE X
DEL NUOVO CIMENTO

N. 4, 1956
1° Semestre

Some Problems of Paramagnetic Resonance.

S. A. Al'tšuler

V. I. Lenin-Uljanov State University - Kazan, USSR

B. M. Kozyrev

Kazan Section of the Academy of Sciences of the USSR

Contents. — **1.** Introduction. – **2.** Brief survey. – **3.** Acoustic paramagnetic resonance. – **4.** Paramagnetic resonance in iron group salt solutions

1. – Introduction.

Paramagnetic resonance (PR), discovered in 1944 by Zavojskij [1] (Kazan, USSR) consists in the transmission of energy of a radiofrequency field of frequency ν to a paramagnetic substance, as a result of magnetic dipole transitions between energy sublevels created by the static magnetic field H. Resonance absorption occurs when the energy quantum of the variable field equals the difference of energy between the magnetic sublevels. In the simplest case, the resonance condition has the form

$$g\beta H = h\nu\,, \tag{1}$$

where g is the spectroscopic splitting factor, and β is the Bohr magneton. In a first approximation, the rate of magnetic dipole transitions is, in the overwhelming majority of cases, different from zero only when the variable and constant magnetic field sare mutually perpendicular.

Zavojskij thoroughly investigated PR in salts of the iron group elements. He also began the study of PR in solutions of paramagnetic salts and in metals [1, 2]. A natural continuation of investigations of electronic PR is the discovery in 1946 of nuclear magnetic resonance by Purcell [3] and Bloch [4] and their co-workers. Directly linked to PR research is the dis-

covery of ferromagnetic resonance, independently, by GRIFFITHS [5] and ZAVOJSKIJ [6], and theoretically examined as far back as 1935 by LANDAU and LIFŠIC [7]. It should be noted that the selective absorption of the energy of a variable electromagnetic field by ferromagnetics, discovered by ARKADEV [8], DORFMAN [9], suggested the idea of magnetic resonance as early as 1923.

The Zavojskij effect makes it possible to determine the position of the energy levels of magnetic particles. Hence, the study of PR is a necessary part of radiospectroscopy. The effect is also intimately connected with the magnetic cooling method and with paramagnetic relaxation, as both these phenomena have to do with kinetic processes of magnetization.

While in the study of paramagnetism in constant fields the basic quantity is the static susceptibility χ_0, in variable fields the susceptibility becomes a complex magnitude: $\chi = \chi' - \chi''$. The purpose of the theory of paramagnetic dispersion and absorption is to investigate the dependence of the coefficients χ' and χ'' on the frequency ν and field intensity H. It is well known that the magnetic properties of solid and liquid paramagnetic substances depend on internal electric fields and on the magnetic and exchange interactions of the paramagnetic ions. These internal forces are also most essential for the PR phenomenon.

Firstly, thanks to these forces the paramagnetic substance as a whole absorbs the energy of the radio-frequency field which stimulates both induced radiation and energy absorption with equal probability. For processes of the second type to predominate there must be a mechanism ensuring the restoration of thermodynamic equilibrium by continuous transmission of energy to the thermal motion of the atomic particles. It is the dependence of the internal forces (which act on the paramagnetic particles) upon the thermal motion that creates the so-called « spin-lattice » interaction.

Secondly, these forces determine the shape of the paramagnetic resonance lines. The natural width of the lines in the radio-frequency range is quite negligible. Therefore, the form of the lines can depend only on the thermal motion and interaction of the magnetic particles between themselves and with the diamagnetic particles.

Thirdly, these forces considerably influence the form of the PR spectrum, and the number and position of the absorption lines.

From the above it follows that experimental and theoretical investigation of PR phenomena may proceed in three directions: 1) determination of PR spectra in different substances; 2) ascertainment of the form of the PR lines, and 3) determination of the magnitude of the spin-lattice interaction.

PR enables one to measure the mechanical and magnetic moments of atoms and atomic nuclei with greater precision than by other methods. PR underlies also the more effective methods of producing nuclear alignment. Moreover

the Zavojskij effect makes it possible to draw conclusions regarding the fine structure of crystals and liquids, and, lastly, to solve certain chemical problems.

In this article we give a brief survey of PR research carried out in Kazan (Sect. 1), and dwell in somewhat greater detail on two problems we have been working on lately: resonance absorption of ultrasound by paramagnetics (Sect. 2), and PR in liquid solutions (Sect. 3).

2. – Brief Survey.

2·1. *PR spectra.* – ZAVOJSKIJ made his PR discovery in polycrystals of the iron group salts. In all cases there was a sharp absorption peak the position of which (in agreement with the theory and the static susceptibility of substances) corresponded to pure spin magnetism. For organic free radicals, PR was first observed by KOZYREV and SALIHOV [10]. Continuing his research on organic substances, KOZYREV [11] demonstrated that latent paramagnetism could be detected by the PR method.

If the electronic spin of an atom is greater than $\frac{1}{2}$, then, firstly, there must be lines of weak intensity, corresponding to transitions $\Delta M > 1$, where M is the magnetic quantum number. In 1947, ZAVOJSKIJ [12] succeeded in detecting this phenomenon in certain salts.

Secondly, the fine structure of PR lines due to a weak splitting of the energy ground level may appear even in the absence of an external magnetic field H. This structure was experimentally detected by ZAVOJSKIJ [13] in chromium alum powders, and theoretically interpreted by WEISS [14]. For detailed study of the fine structure monocrystals of solid solutions of paramagnetic salts are used. In this way GARIF'JANOV [15] investigated the fine structure in gadolinium nitrate, and ZARIPOV and ŠAMONIN [16] in synthetic ruby (Al_2O_3 with and admixture of Cr_2O_3).

Hyperfine structure of PR lines may be observed in the cases when the nucleus of the paramagnetic atom has a spin different from zero. The influence of the nuclear spin on the shape of the PR spectrum was first established by AL'TŠULER, KOZYREV and SALIHOV [17] in 1948, in solutions of Mn^{++} salts.

ZARIPOV [18] has lately proposed a theory of the hyperfine structure of singular electron levels. Calculations show that this effect should be observable in a number of salts in which the paramagnetic ions have an even number of electrons. This phenomenon may be regarded as intermediary between purely electronic and purely nuclear PR.

2·2. *The form of PR lines.* – The first theoretical interpretation of PR experiments of ZAVOJSKIJ was advanced by FRENKEL [19]. He obtained formulae describing the form of PR lines, assuming that their broadening is con-

ditioned by the interaction of the spins with the thermal oscillations of the lattice. In 1947, Al'tšuler, Zavojskij and Kozyrev [20] established certain empirical laws from which it followed that the usual spin-lattice interaction does not determine the form of the PR line and that the width of the line depends primarily upon the mutual interaction of the magnetic particles. They also found that purely magnetic interaction cannot explain the observed width. It was therefore assumed that serious influence on the width should be exerted by the exchange interactions and the internal electrical fields in the substance.

Developing Van Vleck's [21] theory, Glebašev [22] carried out exceptionally laborious calculations to determine the 6th moment of the absorption line. A comparison of these calculations with experiment confirmed Gorter's and Van Vleck's [23] idea regarding the exchange narrowing of the absorption line.

By means of PR measurements in solid paramagnetic solutions, Kašaev [24] studied experimentally the dependence of the line width upon exchange interactions.

As stated above, paramagnetic absorption is accompanied by a dispersion of the susceptibility. PR dispersion was first investigated by Zavojskij [25] on manganese sulphate at $\nu = 10^9$ Hz. Dispersion measurements at still lower frequencies were carried out by Romanov [25]. Dispersion in the centimeter band was also studied by Kozyrev, Salihov and Šamonin [27], and, lastly, on a large number of substances, by Neprimerov [28].

The integral relations between χ' and χ'' were found by Kramers [29] for the case when the variable quantity is the frequency ν of the external field. Al'tšuler [30] obtained analogous relations for a practically more important case when the variable is the intensity of the static field, H. These relations have the form:

$$(2)\qquad \begin{cases} \chi_0 - \chi'(H) = \dfrac{1}{\pi}\displaystyle\int_0^\infty \frac{F(H+H_1) - F(H-H_1)}{H_1}\,\mathrm{d}H_1\,, \\ F(H) = \dfrac{1}{\pi}\displaystyle\int_0^\infty \frac{\chi'(H+H_1) - \chi'(H-H_1)}{H_1}\,\mathrm{d}H_1\,. \end{cases}$$

Here $F = \chi''_{\mathrm{res}} - \chi''_{\mathrm{nonr}}$, where χ''_{res} is the absorption coefficient for the rotating field, whose direction of rotation coincides with the direction of the Larmor spin precession, and χ''_{nonr} is the coefficient for the field rotating in the opposite direction.

The relations (2) were used in a number of experimental works.

PR may be detected not only by measurement of χ' and χ'', but also by

observing the rotation of the polarization plane of microwaves about the field H in the paramagnetic substances. A detailed study of PR rotation bas been carried out by NEPRIMEROV [31] in a number of salts.

2·3. *Spin-lattice interaction.* – Let us first consider the spin-lattice relaxation time theory. AL'TSULER [32] carried out calculations for hydrated salts of rare-earth elements (Cl^{+++}), and obtained the following formula for the Raman scattering of phonons:

$$\tau \simeq \frac{\varrho^2 \Delta^4 v^{10} J(J+1)}{h^2 (e\mu/R)^4 I_8}, \tag{3}$$

where τ is the relaxation time, ϱ the crystal density, Δ the energy splitting due to the crystal electric field, v the velocity of sound, μ the effective dipole moment of the water molecule, R the equilibrium distance of this molecule from the paramagnetic ion, I_8 the integral determining the dependence of τ on the temperature [33]. From formula (3) it follows that at room temperature τ should be of the order of $10^{-10} \div 10^{-12}$ s, which agrees with experiment.

Besides this, AL'TŠULER [34] calculated the relaxation time for ions in the S-state and also generalized the Waller [35] spin-lattice relaxation theory. The experimental study of spin-lattice and spin-spin interaction was carried out, mainly in parallel static and oscillating magnetic fields.

2·4. *Investigations in parallel fields.* – The extensive studies in this field by GORTER and his collaborators [36] are well known. ZAVOJSKIJ introduced some highly sensitive methods for measuring paramagnetic losses and these enables him [37], KOZYREV [38] and others to obtain a number of new results. Particularly noteworthy is the possibility that the methods of Zavojskij have opened up for measuring and detecting relaxation effects in liquid solutions of paramagnetic salts at room temperature. Of great importance for the theory of paramagnetic relaxation is the work of ŠAPOŠNIKOV [39]. The initial theory of CASIMIR and DU PRÉ [40] took into account only spin-lattice relaxation. Using the methods worked out by LEONTOVIČ and MANDELŠTAM [41] for acoustic relaxation phenomena, ŠAPOŠNIKOV evolved a general phenomenological theory taking into account also spin-spin relaxation. His formula has the following form:

$$\begin{cases} \dfrac{\chi'}{\chi_0} = \dfrac{1 + (1-F)\tau^2\nu^2}{[1-(1-F)\tau\tau'\nu^2]^2 + (\tau+\tau')^2\nu^2}, \\ \dfrac{\chi''}{\chi_0} = \dfrac{(F\tau+\tau')\nu + (1-F)^2\tau^2\tau'\nu^3}{[1-(1-F)\tau\tau'\nu^2]^2 + (\tau+\tau')^2\nu^2}. \end{cases} \tag{4}$$

Here $F = H^2/((b/C) + H^2)$, b is the magnetic specific heat, C the Curie constant, τ' is the spin-spin relaxation time. Šapošnikov's formulae have been repeatedly used by experimenters. RIVKIND [42] carried out absolute measurements of χ'' at low frequencies in perpendicular fields and determined the spin-spin relaxation time for a whole series of substances. These measurements confirmed the correctness of Šapošnikov's theory for weak magnetic fields. By measurements in parallel fields, GARIF'JANOV [43] and SITNIKOV [44] confirmed Šapošnikov's theory for higher frequencies at which the predominant role is played by spin-spin relaxation. These experiments have made it possible to determine the magnetic heat capacity of many salts.

3. – Acoustic PR.

The possibility of supersonic resonance absorption by paramagnetics was suggested by ZAVOJSKIJ. AL'TŠULER [45] developed the theory of this phenomenon. Acoustic PR consists in the transmission of supersonic energy to a system of magnetic particles when the energy quantum of elastic oscillations equals the difference between the energies of the magnetic levels. Thus, as in the case of ordinary PR, the acoustic effect will take place when condition (1) is observed (ν in this case being the supersonic frequency).

The nature of the mechanism by which the sonic energy is transmitted to paramagnetic particles is the same as that of paramagnetic lattice relaxation in which one-phonon processes are involved. Ultrasound resonance absorption can, therefore, be regarded as inverted paramagnetic relaxation. Under the influence of sonic oscillations, the forces acting on the magnetic particles will change periodically, and transitions from one magnetic energy sublevel to the other will arise. Due to the great population of the lower sublevels the number of transitions associated with energy absorption will exceed the number of inverse transitions. Equilibrium will be restored by the transmission of the excess energy of the paramagnetic particles to the lattice thermal oscillations.

The ultrasound absorption by paramagnetics is calculated by a method similar to the one used for calculating the time of paramagnetic lattice relaxation due to processes of the first order. This yields the following formula for evaluating the effect in solids:

$$\sigma = \frac{h^2}{8\pi\tau} \frac{Nv^2}{kT \cdot kT_0 \cdot \nu_{\frac{1}{2}}}. \tag{5}$$

Here σ is the absorption coefficient of sound, i.e., the ratio of the energy absorbed per second in 1 cm^3 to the energy incident per 1 cm^2; N is the number

of magnetic atoms per 1 cm^3; $\nu_{\frac{1}{2}}$ is the half-width of the absorption line; T the temperature of the substance; T_0 the temperature at which relaxation time τ is determined. The experimental results yield for the coefficient σ values of the order of 0.1 cm^{-1}. Hence, the effect in question is sufficiently large to be observable. Calculations of σ were subsequently undertaken for different types of paramagnetics, assuming various mechanisms of spin-lattice bond.

At first, resonance absorption of ultrasound was investigated in paramagnetic salts in which the spin-lattice bond is due to modulation of the crystal's internal electric field by elastic oscillations of the lattice. The coefficient σ was calculated for some typical salts of the iron group (titanium and chromium alums), for rare-earth element salts (cerium nitrate, praseodymium ethylsulphate) and, lastly, for salts whose magnetic ions are in the S-state (iron alums). The following coefficient was obtained for titanium alums:

$$\sigma \simeq \hbar^2 P \left(\frac{\lambda}{\delta^2}\right)^2 \left(\frac{e\mu}{R^2}\right)^2 \nu^4 , \tag{6}$$

where $P = \pi^2 N/\varrho K T v^3 \nu_{\frac{1}{2}}$, λ is the spin-orbit interaction constant, and δ the energy splitting caused by the trigonal field. At $T = 20°$ numerical evaluation yields $\sigma \sim 2 \cdot 10^{-38}$ cm^{-1}. For chromium alums, with Δ signifying complete energy splitting by a cubic symmetry field, we have:

$$\sigma \sim \left(\frac{e\mu}{R^2}\right)^2 \left(\frac{\lambda}{\Delta}\right)^4 P \nu^2 . \tag{7}$$

The numerical evaluation yields $\sigma \sim 10^{-21} \nu^2$ cm^{-1} at room temperature. A different dependence of the absorption on the ultrasound frequency was obtained for titanium and chromium salts. This is explained by the fact that in the case of chromium alums the spin degeneracy is partially removed even in the absence of the external magnetic field.

If the cristal field produces only Kramers degeneracy of the magnetic ions energy levels (which is not removed by changes in the electric field due to lattice oscillations) then, as computations show, resonance absorption of ultrasound should be very small in the rare-earth salts.

Thus, for cerium nitrate at $T = 20$ °K, $\sigma \sim 3 \cdot 10^{-44}$ cm^{-1}. In rare-earth ethyl-sulphates the crystal field is hexagonally symmetrical. If the rare-earth ion contains an even number of electrons, the energy levels retain the non-Kramers' degeneracy, and the sound absorption effect should therefore be high. Thus, for praseodymium ethylsulphate

$$\sigma \sim P \left(\frac{e\mu}{R^2}\right)^2 \left(\frac{\bar{r}^2}{R^2}\right)^2 \nu^2 . \tag{8}$$

Hence at $T = 20\,^{\circ}\mathrm{K}$ we have $\sigma \sim 10^{-15}\,\mathrm{cm}^{-1}$. The effect is so great that this salt is evidently most suitable for experimental investigation.

For iron alums in which the ion Fe^{+++} is in the S-state, the absorption coefficient is relatively small, and is of the order of $\sim 10^{-24}\,\nu^2\,\mathrm{cm}^{-1}$ at room temperature.

In gadolinium salts for which, as is well known, splitting of the paramagnetic ion energy ground level by the crystal's electric field is much greater than in the iron ion, it may be expected that the acoustic effect will be approximately 10^4 times higher.

Ultrasound resonance absorption has also been treated on the assumption that the spin-lattice bond is due to variation of magnetic interaction between the particles caused by elastic oscillations of the lattice (the Waller mechanism). In this case the absorption coefficient is:

$$\sigma = \frac{253}{21} PZ \left(\frac{g^2\beta^2}{a^3}\right)^2 S(S+1)^2(2S+1)\nu^2 , \tag{9}$$

where Z is the number of the atom's closest neighbours in the crystal lattice, a the shortest distance between the magnetic atoms, S the electron spin. In substances with higher magnetic atom density of the MnF_2 type this mechanism can make the coefficient σ to be $\sim 10^{-19}\nu^2\,\mathrm{cm}^{-1}$ at room temperature.

After paramagnetic salts, the effect in question was investigated for all rare-earth metals. In other metals sound resonance absorption should be small as conduction electrons also participate in the exchange of energy between the lattice oscillations and electron spins in the external magnetic field.

The highest sound absorption is to be observed in rare-earth metals having a cubic lattice, and in metals with a hexagonal lattice, whose ions contain an even number of electrons. If e' signifies the ion's effective charge, then the absorption coefficient for such metals may be estimated by the formula:

$$\sigma \sim P \left(\frac{ee'}{a}\right)^2 \left(\frac{\bar{r}^2}{R^2}\right) \nu^2 , \tag{10}$$

which at room temperature yields $\sigma \sim 10^{-16}\nu^2\,\mathrm{cm}^{-1}$.

Ultrasound resonance absorption will evidently take place not only in electron paramagnetics but also in substances possessing nuclear paramagnetism. Favourable conditions for the nuclear effect are the small width of the paramagnetic absorption lines and the high density of magnetic particles. The small values of the nuclear magnetic and quadrupole moments are the reason for the relatively weak spin-lattice bond, which, naturally, will reduce the effect.

In solid dielectrics, in which the spin-lattice bond is conditioned by the

magnetic interaction of the nuclei, the absorption coefficient may be calculated by formula (9), where now β signifies the nuclear magneton. For NaBr crystals, for example, at $T = 300$ °K, the coefficient $\sigma \sim 10^{-25}\nu^2$ cm^{-1}. For substances in which the spin-lattice bond is due to nuclei quadrupole interaction, the coefficient σ may be much smaller (of the order of $10^{-20}\nu^2$ cm^{-1}). A still greater effect may be expected in metals in which the interaction between the nuclear spin and lattice oscillations is enhanced by interaction of the nuclei with the conduction electrons. A substantial effect may also be obtained in liquids whose spin-lattice bond may be strengthened by the addition of paramagnetic salts.

It is interesting to compare ultrasound resonance absorption with paramagnetic resonance in variable magnetic fields.

a) Comparison of the magnitudes of both effects is easy if we take into account that the electromagnetic field energy absorption coefficient is:

$$\sigma_e = \frac{8\pi^2}{c}\nu\chi'' \simeq \frac{8\pi^2}{c\nu_{\frac{1}{2}}}\chi_0\nu^2 . \tag{11}$$

Usually, for « electron » paramagnetics $\nu_{\frac{1}{2}} \sim 10^9$ Hz, $\chi_0 \sim 10^{-5}$ and therefore $\sigma \sim 10^{-22}\nu^2$ cm^{-1}. For the ultrasound absorption coefficient we have likewise obtained in many cases an expression proportional to ν^2, with the proportionality factor greatly depending on the magnitude of the matrix element of the spin-lattice interaction operator. If this matrix element is different from zero in the first approximation, then for the coefficient σ we obtain values greatly exceeding σ_e. If, however, higher approximations are needed, then σ and σ_e are usually of the same order of magnitude.

It should be noted that the absorption coefficients for the longitudinal and transverse waves will, generally speaking, vary. For solids we have everywhere given the average values of the coefficient σ.

b) Ordinarily, PR greatly depends on the angle between the static and variable magnetic fields. The acoustic effect is not very sensitive to changes in the direction of propagation of the sound waves relative to the field H.

c) Ultrasound absorption frequently results from the transitions between such sublevels for which magnetic dipole transitions are forbidden.

d) The absorption lines may have entirely different shapes in the acoustic and the usual effects. This is explained by the fact that in both phenomena we deal with the same bands of energy levels created by magnetic and other interactions, but the laws governing the rates of transition between these levels due to ultrasound and the action of the external variable magnetic field are entirely different in their nature.

In spite of the fact that in many cases the ultrasound absorption coefficient greatly exceeds the radio-frequency field energy absorption coefficient, the low sensitivity of the ultrasound investigation method calls for the use of indirect ways of detecting acoustic PR. The « saturation » of the nuclear magnetic sublevels, which occurs at high sonic intensities enables one to observe acoustic PR. Another method may be based on the variation of magnetization under ultrasound influence. Further experiments in resonance paramagnetic absorption of ultrasound should essentially supplement the data obtained by investigation of ordinary resonance and paramagnetic relaxation. They should facilitate a deeper insight in the nature of the spin-lattice interaction, and the determination of its characteristic constants; they should also help to establish the structure of the energy levels of rare-earth metals, the study of which by the ordinary methods is difficult; finally they should reveal new absorption lines the appearence of which under the influence of the radio-frequency field is impossible due to the absence of magnetic dipole transitions.

In conclusion it should be noted that ultrasound resonance absorption should exist not only in paramagnetic but also in ferromagnetic and antiferromagnetic substances. The absence of a satisfactory spin-lattice interaction theory for ferro- and antiferromagnetics handicaps a quantitative evaluation of this acoustic effect. As we know, the ordinary ferro and antiferromagnetic resonance effects are of no smaller magnitude than resonance absorption by paramagnetics. It therefore may be expected that ultrasound resonance absorption will likewise be substantial in ferro- and antiferromagnetic substances.

4. – PR in Iron Group Salt Solutions.

The study of PR in solutions has a twofold purpose: firstly, it furnishes new data on the magnetic properties of substances and, secondly, makes it possible to clarify certain details of the microstructure of solutions.

PR measurements were made [46, 47] in solutions of the iron group salts, VO^{++}, Cr^{+++}, Mn^{++}, Fe^{+++}, Co^{++}, Ni^{++} and Cu^{++}, at room temperature in water and in certain organic solvents (ethyl alcohol, glycerine, acetone). Besides that, N. S. Garif'janov [48] has measured PR in highly supercooled solutions of salts of the above named ions in organic solvents.

The measurements were made mainly at frequencies of $\nu \sim 10\,000$ MHz by the wave transmission method with maximum modulation of the magnetic field H. The position of the absorption peaks was determined by proton resonance. At lower frequencies (from 10 to $\sim 1\,000$ MHz) the Zavojskij [1] grid-current method was used, modulation of the field H also being applied.

An observable effect at room temperature was found in the solutions of the salts of VO^{++}, Cr^{+++}, Mn^{++} and Cu^{++}. At very high concentrations, a

single peak was observed in all of the salts used. When diluted below several mole per liter, the effect in the pure organic solvents at room temperature could no longer be observed (with the exception of Cu^{++} salt solutions) owing to a very great broadening of the absorption lines.

Diluted solutions of Mn^{++} salts in aqueous as well as in mixed aqueous-organic solvents have a hyperfine structure (h.f.s.). For frequencies of $\nu \simeq 10\,000$ MHz the h.f.s. can be satisfactorily described by the following formula from the general theory of ABRAHAM and PRICE [49] for the case of isotropic media and for transitions $(M, m) \longleftrightarrow (M-1, m)$:

$$H^* = H_0 - Am - \frac{A^2}{2H_0}[I(I+1) - m^2] - \frac{A^2 m}{2H_0}(2M-1)\,. \tag{12}$$

Here H^* is the resonant value of field H, A the h.f.s. constant, I the spin of the paramagnetic ion nucleus, and m and M are respectively the magnetic quantum numbers of the nucleus and of the electron shell of the ion.

For aqueous and mixed solutions of Mn^{++} salts the best agreement with experiment is obtained when we put $A = 96.5$ Oe, $g = 2.000 \pm 0.002$, which practically coincides with the results of the measurements by TINKAM, WEINSTEIN and KIP [50]. The impossibility of observing the h.f.s. effect in diluted solutions of Mn^{++} salts in organic solvents at room temperature is explained by the short relaxation time. Deep cooling of these solutions (down to the temperature of liquid oxygen) has made it possible to observe [48] the h.f.s. of the absorption line and, as expected, the A and g constants proved to be practically the same as for water solutions: $A = 97$ Oe and $g = 2.000 \pm 0.002$ for any solvent.

At low frequencies ($\nu \geqslant 200$ MHz) and small concentrations of manganese salts, i.e., under conditions corresponding to the Zeeman effect of the resultant spin F of the nucleus and the electron shell of Mn^{++} in weak fields, the h.f.s. can be described by the formula:

$$H^* = h\nu/g_F\beta\,.$$

Here

$$g_F = g\,\frac{F(F+1) - I(I+1) \quad J(J+1)}{2F(F+1)}\,.$$

where J is the electron shell spin. For manganese salts $I = J = \frac{5}{2}$ and therefore formula (13) yields a single peak with $g_F = 1$, which was found in 1948 by AL'TŠULER, KOZYREV and SALIHOV [17].

At room temperature and high frequencies, h.f.s. in diluted water solutions of VO^{++} salts is characterized by the constants $A = 116$ Oe and $g = 1.962 \pm 0.002$. In mixed solvents the magnitude of A is somewhat different.

In supercooled solutions of VO^{++} salts in organic solvents [48] a complex spectrum is observed, which, presumably, is the result of the superposition of two h.f.s. spectra, of which one, characterized by the constants $A = 76$ Oe and $g = 1.960 \pm 0.003$, consists of narrower and more intense lines, and the other, with $A = 200$ Oe and $g = 1.92$, contains broader and weaker lines. The presence of this complex spectrum, and the variability of the constant A, are evidently associated with changes in the molecular structure of the VO^{++} ion due to variation of the medium and temperature.

In Cr^{+++} salt solutions not enriched with isotope ^{53}Cr, h.f.s. has not been observed. It is interesting to note that aqueous solutions of salts of the violet modification containing $[Cr(H_2O)_6]^{+++}$ ions yield a relatively narrower and more easily measurable absorption line at $g = 1.972 \pm 0.006$ than solutions of the green modification containing $[Cr(H_2O)_4X_2]^{+}$ ions. The line of the latter is very broad and difficult to measure.

Fe^{+++} salt solutions do not yield a measurable effect at room temperature, owing to very great width of the lines. In supercooled $FeCl_3$ alcohol solutions, however, GARIF'JANOV [48] succeded in detecting a weak resonance maximum corresponding to $g \approx 2$. Partially hydrolized $FeCl_3$ salt produces, besides this maximum, a second one corresponding to $g = 4.33 \pm 0.03$. The latter is also obtained if the $FeCl_3$ alcohol solution is heated until the colour changes. Thus, colloidal products of hydrolized $FeCl_3$ possess unusual magnetic properties, and it is possible that we have a ferromagnetic substance.

As was previously mentioned, high concentrations of VO^{++} and Mn^{++} salt solution yield a single and relatively narrow absorption peak. This was observed earlier with regard to Mn^{++} by GARSTENS and LIEBSON [51], who explained it by assuming exchange interactions between the Mn^{++} ions at very high concentration. Exchange narrowing of absorption line in ions, which is accompanied by removal of h.f.s., takes place at the concentration of ~ 5.8 mole/l. No exchange narrowing was observed in Cr^{+++} salt solutions.

Exchange interactions are most intense in Cu^{++} salt solution, as was to be expected from experiments with solid salts.

In $Cu(NO_3)_2$ solutions the following PR properties were observed at room temperature:

1) PR is observable beginning from the highest concentration to those of several thents mole/l;

2) In this whole range of concentrations a single resonance peak without h.f.s. is observed.

3) The width of the line does not depend on Cu^{++} concentration and equals ~ 140 Oe; the intensity rapidly drops with dilution.

These PR properties in $Cu(NO_3)_2$ solutions have been confirmed by measu-

rements at lower frequencies. Previous observations at low frequencies [17] which showed very weak absorption maximums, attributed to the influence of the Cu nuclear spin, have not been confirmed by more thorough investigations.

H.f.s. of Cu^{++} ions is not observed in organic solvents. However the witdh of the line and the precise value of g greatly depend on the immediate environment of the Cu^{++} ion and this has made it possible to apply the PR method for the investigation of complex formation in salt solutions.

The only possible explanation of the effect observed in Cu^{++} salt solution is the following one: it is entirely due to those Cu^{++} ions which exhibit strong exchange interaction. This in turn indicates the existence of a sort of quasi-crystal structure in not too much diluted Cu^{++} salt solutions: the lifetime of the microscopic formations containing at least two Cu^{++} ions should not be shorter than 10^{-7} s at room temperature. Cu^{++} ions between which there are no strong exchange interactions do not produce measurable effects at room temperature, evidently because the relaxation time is too short. This is confirmed by experiments [48] with supercooled Cu^{++} salt solution in organic solvents. At 90 °K and for concentrations of Cu^{++} ions of 1 mole/l or lower, these solutions have revealed, besides an « exchange » peak corresponding to $g = 2.091 \pm 0.002$, four h.f.s. peaks described by formula (12), if we put $A = 130$ Oe and $g = 2.369 \pm 0.003$.

Rising temperature rapidly reduces the intensity of the Cu^{++} exchange peak both in water and other solvents; and at temperatures close to the boiling point it disappears altogether. This apparently signifies the decay of the microcrystal formations which are responsible for the exchange interactions.

On the whole, the experimental results show a fairly close analogy between diluted liquid solutions and the polycrystal solids of the respective ions. In particular the relaxation time in liquid solutions, as a rule, increases with rising temperature in the same manner as in solids. The presence of exchange effects in concentrated (and in the case of copper even in fairly diluted) solutions of certain ions likens them to pure solid paramagnetics. All this indicates that there is a close order in the position of particles in solutions at temperatures sufficiently remote from the boiling point. Particles situated near the paramagnetic ion should undoubtedly have much less freedom of motion than pure liquid molecules. Precisely because of this, the principal role in the PR effect in solutions should be played not by the mean correlation time τ_c but by the nature of the immediate environment of the paramagnetic ion and by the local electric fields (acting on the ion) determined by this environment. This is well illustrated, for example, by experiments in which the viscosity of solutions is varied: changing by 50 times the viscosity of a 0.1 mole/l $MnCl_2$ aqueous solution by partial substitution of water by saccharose, the Mn^{++} h.f.s. structure still remains clearly distinguishable, whereas a corresponding

change of viscosity by glycerine makes the effect utterly unobservable. This may be explained only by the fact that there are glycerine molecules, but no saccharose molecules, in the immediate neighbourhood of the Mn^{++} ion.

In conclusion it will be noted that, as RIVKIND [52] has recently found, the close order in the position of particles should be taken into account also in studying proton resonance phenomena in paramagnetic ion solutions. We are not discussing here his findings as they are beyond the scope of the present article.

Further investigation both of electron and proton resonance promises to become a highly effective method of research in the structure of solutions.

REFERENCES

[1] E. K. ZAVOJSKIJ: *Thesis for Doctor's Degree* (Lebedev Institute of Physics, Academy of Sciences of the USSR, 1944).
[2] E. K. ZAVOJSKIJ: *J. of Phys. USSR*, **9**, 211 (1945).
[3] E. M. PURCELL, R. V. POUND and N. S. TORREY: *Phys. Rev.*, **69**, 37 (1946).
[4] F. BLOCH, W. W. HANSEN and M. PACCARD: *Phys. Rev.*, **69**, 127 (1946).
[5] J. GRIFFITHS: *Nature*, **158**, 670 (1946) ,
[6] E. K. ZAVOJSKIJ: *Žu. Éksper. Teor. Fiz.*, **17**, 883 (1947).
[7] L. D. LANDAU and E. M. LIFŠIC: *J. of Phys. USSR*, **8**, 153 (1935).
[8] V. K. ARKADEV: *Žu. Russ. Fiz.-Him. Obšč., Fiz. Otdel.*, **45**, 103 (1913).
[9] Y. G. DORFMAN: *Zeits. f. Phys.*, **17**, 98 (1923).
[10] B. M. KOZYREV and S. G. SALIHOV: *Dokl. Akad. Nauk USSR*, **58**, 1023 (1947).
[11] B. M. KOZYREV: *Dokl. Akad. Nauk SSSR*, **81**, 427 (1951).
[12] E. K. ZAVOJSKIJ: *Dokl. Akad. Nauk SSSR*, **57**, 887 (1947).
[13] E. K. ZAVOJSKIJ: *J. of Phys. USSR*, **10**, 170, 197 (1946).
[14] P. R. WEISS: *Phys. Rev.*, **79**, 470 (1948).
[15] N. S. GARIF'JANOV: *Dokl. Akad. Nauk SSSR*, **84**, 931 (1952).
[16] M. M. ZARIPOV and JU. JA. ŠAMONIN: *Žu. Éksper. Teor. Fiz.*, **30**, 291 (1956).
[17] S. A. AL'TŠULER, B. M. KOZYREV and S. G. SALIHOV: *Dokl. Akad. Nauk SSSR*, **71**, 755 (1950).
[18] M. M. ZARIPOV: *Thesis* (Kazan State University, 1955).
[19] J. I. FRENKEL: *Žu. Éksper, Teor. Fiz.*, **15**, 409 (1945).
[20] S. A. AL'TŠULER, E. K. ZAVOJSKIJ and B. M. KOZYREV: *Žu. Éksper. Teor. Fiz.*, **7**, 1121 (1947).
[21] J. H. VAN VLECK; *Phys. Rev.*, **74**, 1168 (1948).
[22] G. Y. GLEBAŠEV: *Žu. Éksper. Teor. Fiz.* (in print).
[23] C. J. GORTER and J. H. VAN VLECK: *Phys. Rev.*, **72**, 1128 (1947).
[24] S. H. G. KAŠAEV: *Dokl. Akad. Nauk SSSR* (in print).
[25] E. K. ZAVOJSKIJ: *Žu. Éksper. Teor. Fiz.*, **17**, 155 (1947).
[26] I. M. ROMANOV: *Uč. Zap. Kazansk. Univ.*, **113**, 187 (1953).
[27] B. M. KOZYREV, S. G. SALIHOV and JU. JA. ŠAMONIN: *Žu. Éksper. Teor. Fiz.*, **22**, 56 (1953).
[28] N. NEPRIMEROV: *Izv. Akad. Nauk SSSR, Ser. Fiz.*, **18**, 360 (1954).

[29] N. A. KRAMERS: *Atti del Congresso Internazionale dei Fisici*, vol. II, p. 545 (Como, 1927).
[30] S. A. AL'TŠULER: *Žu. Éksper. Teor. Fiz.*, **20**, 1047 (1950).
[31] N. N. NEPRIMEROV: *Izv. Akad. Nauk SSSR, Ser. Fiz.*, **18**, 368 (1954).
[32] S. A. AL'TŠULER: *Žu. Éksper. Teor. Fiz.*, **24**, 681 (1953).
[33] J. H. VAN VLECK: *Phys. Rev.*, **57**, 426 (1940).
[34] S. A. AL'TŠULER: *Thesis for Doctor's Degree* (Lebedev' Institute of Physics, Academy of Sciences of the USSR, 1955).
[35] I. WALLER: *Zeits. f. Phys.*, **79**, 370 (1932).
[36] C. J. GORTER: *Paramagnetic Relaxation* (Amsterdam, 1947).
[37] E. K. ZAVOJSKIJ: *J. of Phys. USSR*, **8**, 377 (1944).
[38] B. M. KOZYREV: *Thesis* (Kazan Institute of Chemical Technology, 1945).
[39] I. G. ŠAPOŠNIKOV: *Žu. Éksper. Teor. Fiz.*, **18**, 533 (1948).
[40] H. B. G. CASIMIR and F. K. DU PRÉ: *Physica*, **5**, 507 (1938).
[41] L. I. MANDELŠTAM and M. A. LEONTOVIČ: *Žu. Éksper. Teor. Fiz.*, **17**, 438 (1937).
[42] A. I. RIVKIND: *Izv. Akad. Nauk SSSR, Ser. Fiz.*, **16**, 541 (1952).
[43] N. S. GARIF'JANOV: *Žu. Éksper. Teor. Fiz.*, **25**, 359 (1953).
[44] K. P. SITNOKOV: *Thesis* (Kazan State University, 1954).
[45] S. A. AL'TŠULER: *Dokl. Akad. Nauk SSSR*, **85**, 1225 (1952); *Žu. Éksper. Teor. Fiz.*, **28**, 38, 49 (1955).
[46] N. S. GARIF'JANOV and B. M. KOZYREV: *Dokl. Akad. Nauk SSSR*, **98**, 929 (1954).
[47] B. M. KOZYREV: *Dokl. Akad. Nauk SSSR*, **103**, 53 (1955).
[48] N. S. GARIF'JANOV: *Dokl. Akad. Nauk SSSR*, **101**, 503 (1955); **103**, 41 (1955).
[49] B. BLEANEY and D. J. E. INGRAM: *Proc. Roy. Soc.* (*London*), A **205**, 336 (1951).
[50] M. TINKAM, R. WEINSTEIN and A. F. KIP: *Phys. Rev.*, **84**, 848 (1951).
[51] M. A. GARSTENS and S. H. LIEBSON: *J. Chem. Phys.*, **20**, 1677 (1952).
[52] A. I. RIVKIND: *Dokl. Akad. Nauk SSSR*, **100**, 933 (1955); **102**, 1197 (1955).

SUPPLEMENTO AL VOLUME III, SERIE X
DEL NUOVO CIMENTO

N. 4, 1956
1° Semestre

The Non-linear Field Theory and the Theory of Relativity.

D. I. BLOHINCEV

Academy of Sciences of the USSR - Moscow

CONTENTS. — **1.** Introduction. – **2.** A classification of non-linear theories. **3.** – Equations of class A. – **4.** Equations of class B.

1. – Introduction.

In recent years, the development of the quantum field theory has been marked by successful application of the method of renormalizing the mass of the particles. However, this method is only a mathematical procedure that makes it possible to circumvent phenomena and processes relating to very high frequencies and to very small scales. In addition, this method is not always applicable.

For this reason, along with the development of methods of renormalization, various theories were developed in which the divergence of the self-energy of the particles is excluded not by additional methods but on the basis of the initial physical content of the theory.

The following two trends are represented by an especially large number of works: 1) the non-local field theory, and 2) the non-linear field theory.

In this report we shall consider the main peculiarities of the second trend, the non-linear field theory.

The introduction of a certain field scale φ_0 is characteristic of this theory; thus, indirectly, there is introduced a certain length $s_0 = \sqrt{g}/\varphi_0$ (where g is the charge of the particle), length which may conditionally be regarded as « the size of the particle ».

The following main problem is then discussed: to what extent is the non-linear field theory capable of eliminating, in principle, the above-mentioned difficulties of the quantum theory?

It is not necessary to analyze the concrete form of the theory in order to investigate this aspect of the problem.

It is sufficient to examine its general features.

2. – A Classification of Non-linear Theories.

Non-linear equations of any physical field (for example, of a meson, electromagnetic, and any other such field) may be obtained from the variational principle which is invariant with respect to Lorentz transformation

$$\delta \int L(K, I, \ldots) \mathrm{d}x \, \mathrm{d}t = 0 \,, \tag{1}$$

where L is the Lagrange function, and K, I, ... are field invariants. We shall limit ourselves to equations not above the second order, and therefore K, I, ... are assumed to be composed of components of the field and its first derivatives. Then the fields arising from equation (1) have the following form (*):

$$A \frac{\partial^2 \varphi}{\partial t^2} + 2B \frac{\partial^2 \varphi}{\partial t \, \partial x} + C \frac{\partial^2 \varphi}{\partial x^2} + D = 0 \,. \tag{2}$$

With the aim of correspondence to non-linear theory, the Lagrangian should be selected in such a way that in the region where $|\varphi| \ll \varphi_0$, $|\partial\varphi/x$, $|\partial\varphi/\partial t| \ll \varphi_0/s_0$, the equations become linear. This is a very slight limitation on the selection of the value L.

Let us now consider the velocity of signal propagation in non-linear theory, that is the velocity of the front of a wave bounded by a weak discontinuity. The value of this velocity ξ is equal to the slope of the characteristics and is determined from the equation:

$$A\xi^2 - 2B\xi + C = 0 \,. \tag{3}$$

It is obvious that this velocity will be a function of the field φ and of its derivatives.

With respect to the velocity of signal propagation, all the Lawrence-invariant equations may be divided into two classes: *A*) equations, the characteristics of which do not differ from the characteristics of linear equations $|\xi| = 1$; *B*) those where $|\xi|$ is in general not equal to 1.

To the first class belongs for example an equation of the following type:

$$-\frac{\partial^2 \varphi}{\partial t^2} + \frac{\partial^2 \varphi}{\partial x^2} + D(\varphi) = 0 \,, \tag{4}$$

(*) We limit ourselves to the one dimensional case, which is entirely sufficient for our purposes.

considered by SCHIFF in a number of his works [1, 4]. To the second class belong the equations of the electromagnetic field, equations which were suggested long ago by M. BORN [2]. These equations follow from the variational principle (1) when $K = \frac{1}{2}(\varepsilon^2 - H^2)$ and $I = (\varepsilon H)^2$.

For the one dimensional case these equations are:

$$(1 + \alpha\varepsilon^2)\frac{\partial\varepsilon}{\partial t} + \alpha\varepsilon H\frac{\partial\varepsilon}{\partial x} - \alpha\varepsilon H\frac{\partial H}{\partial t} + (1 - \alpha H^2)\frac{\partial H}{\partial x} = 0\,, \tag{5}$$

$$\frac{\partial\varepsilon}{\partial x} + \frac{\partial H}{\partial t} = 0\,, \tag{5'}$$

$c = 1$ is the velocity of light in the vacuum, and $\alpha = (\partial^2 L/\partial K^2)/(\partial L/\partial K)$. HEISENBERG [3] recently considered a similar equation for the meson field q. It should be noted that the signal velocity ξ of these equations is obtained in the following form:

$$\xi = \frac{\pm\sqrt{1 + 2\alpha K} - \alpha pq}{(1 + \alpha p^2)}\,. \tag{6}$$

In the case of an electromagnetic field $K = \frac{1}{2}(\varepsilon^2 - H^2)$, $p = \varepsilon$, $q = H$. In the case of a meson field $K = \frac{1}{2}(p^2 - q^2)$, $p = \partial\varphi/\partial t$, $q = \partial\varphi/\partial x$ and ξ may be either less than the velocity of light in the vacuum or it may be greater.

3. – Equations of Class A.

Non-linear equations having characteristics $\xi = \pm 1$ naturally represent a theory entirely compatible with the theory of relativity. There may also be found variants (the selection of the function L) which give the limited self-energy of the particles. Therefore, such equations may serve as a basis for a classical non-linear field theory. These equations are also compatible with the usual rules of quantization:

$$[\dot{\varphi}(x, t), \varphi(x', t)] = i\delta(x - x')\,. \tag{7}$$

Nevertheless, they do not lead to a consistent quantum field theory that does not contain divergencies. The fact of the matter is that the zero energy E_0 of the field, in the case of non-linear theory, is not only infinite (as is the case also in linear theory), but is also non-additive to the energy of the excited states.

In other words, the energy of a non-linear field cannot be represented as the sum of the energy of excitation ε and the energy of the vacuum E_0.

For this reason SCHIFF introduced a method of quantization of a non-linear field, the essence of which consists in substituting the continuous functions $\varphi(x)$ by the assembly of values φ_s in the nodes of a certain spatial lattice with a period l [4].

In the linear theory, this method would not be of any fundamental importance, since all the results of the theory would be retained.

In the non-linear theory, the self-values of the energy of a field tend to ∞ as $\exp[-3(n-2)/(n+2)]$ for $D = \alpha\varphi^n$.

Whereas when $l \neq 0$, from the equations of the field

$$\varphi_s'' + \frac{\partial U}{\partial \varphi_s} = \sum_{r \neq s} A_{sr}\varphi_r \tag{8}$$

where

$$A_{sr} = \frac{1}{N}\sum_k k^2 \exp[ik(x_s - x_r)], \qquad |k| < \frac{\pi}{e}, \tag{9}$$

it follows that, if $\varphi = a_r \cdot \delta(t)$, then

$$\dot{\varphi}_s(+0) - \dot{\varphi}_s(-0) = A_{sr}a_r \neq 0\,, \tag{10}$$

which signifies that the signal propagates through the lattice with an infinitely large velocity (though its intensity diminishes as the distance becomes larger than $l|s-r|$).

Hence it follows that: either the self-values of the field diverge ($\varepsilon \to \infty$) or the theory becomes incompatible with the theory of relativity (the velocity of the signal $|\xi| > 1$). That is, the theory acquires features of the non-local field theory. This, however, does not discredit the non-linear equations in themselves, since we may still count on the application of renormalization. For example, the Hamiltonian:

$$H = \int \mathrm{d}x \{\tfrac{1}{2}\pi^2 + \tfrac{1}{2}\nabla\varphi^2 + \tfrac{1}{2}x^2\varphi^2 + \tfrac{1}{2}\alpha x^2\varphi^4\}\,, \tag{11}$$

may be substituted by

$$H^* = \int \mathrm{d}x \{\tfrac{1}{2}\pi^2 + \tfrac{1}{2}\nabla\varphi^2 + \tfrac{1}{2}x^2\varphi^2 + \tfrac{1}{2}\alpha x^2(\varphi^2 - A)^2\} - E_0\,, \tag{11'}$$

where A and E_0 are renormalizing constants. Following this course, we may obtain approximate self-values H^*, if we borrow the value φ^2 from linear theory;

we obtain:

$$H^* = \sum_k h\omega_k n_k + \sum_k \frac{h\omega_k}{2} - E_0 , \tag{12}$$

$$\omega_k^2 = c^2 k^2 + c^2 x^2 \left[1 + \tfrac{1}{2}\alpha h \sum_k (n_k^0/\omega_k^0)\right], \quad \omega_k^0 = \sqrt{c^2 k^2 + c^2 x^2} . \tag{13}$$

It follows from the above that non-linear field theory does not of itself eliminate quantum divergencies, and requires additional procedures of the renormalization type.

4. – Equations of Class B.

The propagation of the field in this case is similar in several respects to hydrodynamics on the one hand, and to crystal optics on the other. The possible equations in this class may be divided into two groups: 1) $|\xi| \leqslant 1$; and 2) $|\xi|$ may also be greater than 1 (*).

The equations of the first group do not contradict the theory of relativity, but of course lead to the same difficulties as the equations of class A do. For example, the M. Born (+) equations belong to this class. It should be noted that the application of these equations to an electromagnetic field is objected to because it is proved that the velocity of propagation of electromagnetic signals close to the charges is not equal to the velocity of light.

Therefore, the Einstein determination of time near the particles becomes invalid. One might expect that it would be possible to construct such a metrics that would preserve the relativistic requirement of the velocity of light being constant.

However, such a metrics actually proves non-unique, since (as is the case in crystal optics) there is not one but several velocities of propagation of luminous signals.

In a general case, there are also directions of propagation for which the characteristics are imaginary [6].

The second group of equations, in which the velocity of signal propagation may be greater than the velocity of light in the vacuum, has some features of the non-local theory and is incompatible with that form of causality on which the physical interpretation of the theory of relativity is essentially based.

Thus, a very curious situation arises: the Lorentz invariancy of the varia-

---

(*) A curious case is possible where the equation may become elliptic [5].

(+) V. V. Orlov showed [6] that the Lagrangian given by M. Born is the only one which does not lead to the formation of field shock waves.

tional principle proves insufficient by itself for the compatibility of the field theory with the theory of relativity.

It is still necessary to require that the propagation velocity of weak discontinuities should always be less than the velocity of light in the vacum.

Thus we see that non-linear field theories of the class B contain fundamental difficulties prior to quantization, and that not any formally invariant non-linear field theory is compatible with the theory of relativity.

Even in his first work dealing with the theory of relativity, A. EINSTEIN left the question of simultaneousness «in a point» for future investigators.

It is hard to say whether the time has come for a critical revision of the conceptions of space, time and causality in the region of small scales. At any rate, if we take non-linear field theories seriously, they bring us right up to these problems.

REFERENCES

[1] L. SCHIFF: *Phys. Rev.*, **84**, 1 (1951).
[2] M. BORN: *Proc. Roy. Soc.*, A **143**, 410 (1934).
[3] W. HEISENBERG: *Zeits. f. Phys.*, **133**, 65 (1952).
[4] L. SCHIFF: *Phys. Rev.*, **92**, 766 (1952).
[5] D. BLOHINCEV: *Dokl. Akad. Nauk SSSR*, **32**, 553 (1951).
[6] D. BLOHINCEV and V. ORLOV: *Žu. Èksper. Teor. Fiz.*, **25**, 503 (1953).

SUPPLEMENTO AL VOLUME III, SERIE X
DEL NUOVO CIMENTO

N. 4, 1956
1° Semestre

Interaction of Ultra High Energy Particles with Nucleons and Atomic Nuclei.

N. A. DOBROTIN, G. T. ZACEPIN, S. I. NIKOL'SKIJ and G. B. HRISTIANSEN

Institute of Physics of the Academy of Sciences of the USSR - Moscow
State University - Moscow

CONTENTS. — **1.** Introduction. – **2.** Extensive air showers. The cascade theory. – **3.** The nuclear-cascade hypothesis. – **4.** The method of correlated hodoscopes. – **5.** Results. – **6.** Conclusions.

1. – Introduction.

A number of specific phenomena arise when particles of high or ultra high energy interact with nucleons or atomic nuclei. As an example of phenomena of this type one might mention the multiple particle creation, the nuclear cascade process, the peculiar energy distribution of secondary particles, the creation of particles of different masses etc. At these energies the parameters describing the intrinsic properties of nucleons and other elementary particles should be especially manifest, and the investigation of these properties is therefore undoubtedly one of the most acute problems of modern physics.

It is just for these reasons that physicists are investigating most carefully high and ultra high energy phenomena and in particular extensive air showhers.

In this paper we present a short review of some of the experiments of Soviet physicists on extensive air showers carried out with the purpose of determining the main features of the interaction of ultra high energy particles with nucleons and atomic nuclei.

The work was carried out by the Cosmic ray group of the P. N. Lebedev Institute of Physics of the Academy of Sciences of the USSR and of the Moscow State University, under the general supervision of the Academician D. V. SKOBEL'CYN.

Starting from 1945 the experiments were conducted at the Pamir mountains in the Central Asia at a height of 3860 meters above sea level. and in Moscow at sea level.

2. – Extensive Air Showers. The Cascade Theory.

As is well known, extensive air showers were discovered independently by AUGER and KOLHÖRSTER almost simultaneously with the appearance of the so-called cascade theory.

As the overwhelming majority of shower particles was found to consist of electrons, positrons and photons, it was natural to assume that extensive showers are giant electron-photon cascades produced in the atmosphere by ultra high energy electrons or positrons. This viewpoint was supported, in particular, by EULER.

However, a detailed study of the phenomenon showed that one cannot even approximately explain the properties of extensive air showers by considering only the electromagnetic processes of pair production and bremsstrahlung.

Experiments performed in our and other laboratories (in particular in that of Prof. COCCONI) established the existence of three classes of phenomena which the electromagnetic cascade theory is unable to explain.

The first group of phenomena is related to the spatial distribution of shower particles.

As early as 1942, D. V. SKOBEL'CYN noted [1] that AUGER's experimental data corresponding to a counter separation of 300 meters do not agree well with what one would expect for pure electron-photon showers. Later on, in 1946, at the Pamir station, showers were recorded at counter separation up to 1 km [2]. The shower rate could not be reconciled with the theoretical predictions of MOLIÈRE for the spatial distribution of electrons in electron-photon cascades [3]. These discrepancies prompted us to carry out further investigations on the structure of the showers. As a result of these investigations, which we describe below, it has become possible to explain some of the shower peculiarities.

The second group of phenomena which the electromagnetic cascade theory is unable to explain is connected with the altitude dependence of the showers. It is well known that the distribution of showers with respect to the particle density can be expressed by the relation

$$C(\varrho) \sim \varrho^{\varkappa+1} \mathrm{d}\varrho \,.$$

According to cascade theory, $\varkappa = \gamma/S$, where γ is the exponent in the primary

particle energy spectrum and S is the well known parameter of cascade theory associated with the degree of shower development.

It follows that the density distribution of showers or, as it is called, the shower density spectrum, should vary with altitude. This means that the shower altitude curve should depend on the density of the primary energy spectrum selected by the experimental arrangement. Thus, according to cascade theory, the change of shower frequency between 3 860 m and sea level should be three times greater for showers with a density of 3 particles/m² than for showers of 300 particles/m². This is a reliable theoretical conclusion and it cannot be modified even by a refinement of the theory, in particular, by changing the magnitude of radiation unit.

The experiments, however, do not reveal practically any relation between the altitude dependence of showers and the particle density. This can be seen from our data obtained by varying the counter area [1] at two different altitudes, the other conditions being identical.

Shower density spectra derived from these experimental data are shown in Fig. 1. The logarithm of the number $C(>\varrho)$ of showers per hour possessing a density exceeding a given value is plotted against the logarithm of the shower particle density ϱ, expressed in particles/m². The upper curve refers to the altitude of 3 680 m, the lower (full) curve to sea level. As it can be seen from the Fig. 1, both curves are practically parallel over a broad density region.

The dashed curve gives the relation between $C(>\varrho)$ and ϱ computed from cascade theory on the basis of data obtained at 3860 m. It can be seen from the figure that the discrepancy between the theoretical and experimental results is far beyond the experimental errors.

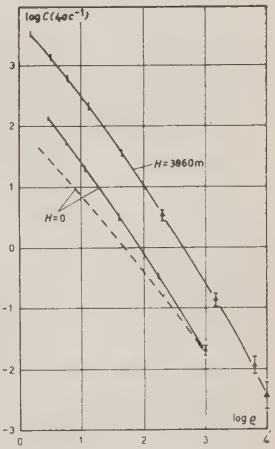

Fig. 1.

This signifies that, contrary to the predictions of cascade theory the increase of the shower intensity with altitude is independent of the particle density.

The data on the composition of extensive showers also sharply contradict the cascade theory. Already DAUDIN and other pioneer investigators of showers [5] were able to demonstrate the presence of a small portion of penetrating particles which could not be identified with the electron-photon component.

In order to obtain more quantitative information on the number of these penetrating particles it seemed desirable to use counters surrounded by lead shields sufficiently thick to stop all shower electrons. Accordingly in 1946

and 1947 absorption experiments with lead and aluminium filters [6] were carried out at the Pamir station. The results are shown in Fig. 2. The logarithm of the triple counting rate in three counter sets arranged at the corners of a triangle of 1.6 m side is plotted against the thickness of the lead shields over the counter trays.

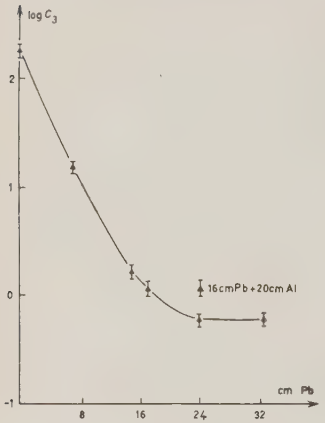

Fig. 2.

As can be seen from the figure, the absorption of shower particles is rapid up to 20 cm Pb and only after 24 cm Pb it becomes small.

In order to check that the particles penetrating 16 cm Pb but absorbed in thicker filters are electrons and photons and not low energy mesons, an aluminium filter, equivalent to 8 cm Pb with respect to ionization losses, was placed over the 16 cm Pb absorber. This aluminium layer was found to absorb the shower particles just in accordance with the value of its thickness measured in radiation units (the corresponding point is designated by a triangle in Fig. 2). Therefore the absorption is not due to ionization losses.

These experiments also show that a small amount of weakly absorbed particles which can penetrate through 24 cm Pb are present in the shower. Similar experiments were carried out by Cocconi and co-workers: they arrived at the same conclusions [7].

Penetrating shower particles were usually considered as playing an insignificant role in the showers and as being only a small admixture in the electron-photon part of the shower.

Moreover some authors even assumed that no penetrating particles are present in air showers and that the particles recorded by shielded counters are generated in the shielder [8].

The first experiments which proved the fallacy of these assumptions were carried out at the Pamir station in 1947 [9]. These experiments and also those that followed them [10] showed that the fraction of penetrating particles increases with the distance from the shower core and this is inconsistent with the assumption of the local creation of penetrating particles. Moreover, the experiments showed that the remote periphery of the shower consists mainly of μ-mesons and of equilibrium electrons. A summary of the results of the investigation of this problem during the last few years at the Pamir station is presented in Fig. 3. The results were obtained by the method of « correlated hodoscopes » described below. The logarithm of the fraction of pene-

trating particles (expressed in %) is plotted against the distance from the shower axis (in meters). Triangles and crosses refer to different series of experiments. The squares are COCCONI's data [11]. The slow decrease of the μ-meson density with the distance from the shower axis leads to the result that the overwhelming majority of mesons is present in the remote periphery of the shower and therefore is not recorded by closely spaced counter systems. As a whole, penetrating particles represent over 10% of the total amount of shower particles at sea level. As the average energy of the shower particles exceeds by at least one order of magnitude that of the electrons and photons, this signifies that the total energy carried by the penetrating particles is higher than that of the electron-photon component. Thus the penetrating particles are of major importance in showers.

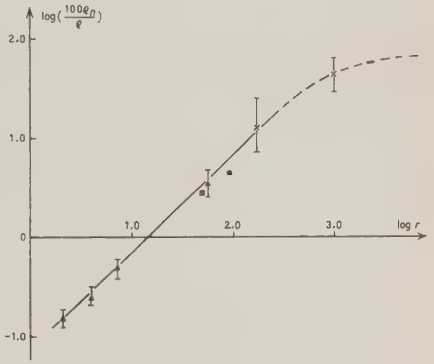

Fig. 3.

3. – The " Nuclear Cascade „ Hypothesis.

An analysis of these discrepancies between the experimental results and the predictions of cascade theory and also of the data on electron-nuclear showers [12] obtained at the Pamir station, led in 1948 one of the authors to propose the nuclear-cascade hypothesis of shower development [13]; this hypothesis has now received general recognition.

COCCONI independently arrived at a similar picture of the shower development [14].

As is well known, the essence of this scheme is the following: primary protons of ultra high energy collide with the nuclei of air and create an electron-nuclear shower; the latter consists of secondary nucleons (also of ultra-high or high energy) and of charged and neutral π-mesons. Finally there is also present a small amount of other types of mesons which at sufficiently high energies apparently interact with nuclei with a geometrical cross-section. At lower energies these particles decay into π- or μ-mesons.

The secondary nucleons and other nuclear-active particles passing through the atmosphere form new electron-nuclear showers of the same type etc.

Decaying neutral π-mesons give rise to the electron-photon component; charged π-mesons may either decay and thus form the nuclear-inactive particles of the extensive showers, or else create new electron-nuclear showers.

Thus, in accordance with this nuclear-cascade scheme, the extensive atmospheric showers may be considered as consisting of two parts: a cascade of nuclear-active particles forming the skeleton of the shower, and the electron-photon cascade which over the full path of the shower in the atmosphere derives its energy (through π^0-mesons) from the nuclear-active particles.

The role of the nuclear cascade process at various stages of development of the shower could be different depending on the nature of the elementary act of this process and also on the effective « threshold » of formation of the electron-nuclear shower. However, direct experimental investigation of the composition of the penetrating component of atmospheric showers performed by us at sea-level (see below) indicate that even in late stages of shower development the fraction of nuclear-active particles (i.e. of penetrating particles, generating electron-nuclear showers) does not decrease; this means that the nuclear cascade process is decisive at all the studied stages of development of the showers.

Without dwelling to compare this scheme with experiment (*) we may note that it yields a natural and simple explanation of the peculiarities of the spatial distribution of the shower particles, of the altitude dependence and of the particle composition of the showers (+).

However, in order to turn from this qualitative picture to a quantitative examination of the phenomenon or, what is most important, to a study of the properties of the elementary interaction act at ultra high energies on the basis of shower data, it was necessary to obtain detailed information on the properties of the showers themselves. This in turn led to the necessity of substantial improvement of the experimental methods.

4. – The Method of " Correlated Hodoscopes ".

The experiments carried out in the early stages of investigation of showers yielded only quantities which represented the average for a number of showers. As an example one may mention the « decoherence curve » i.e. the dependence of the coincidence rate on the distance between the counters. However, this approach is unsatisfactory if one wishes to obtain detailed data on the showers created by primary particles of given energy. In this con-

---

(*) Experiments carried out at the Pamir station in 1947-1948 [15] confirmed the main feature of this scheme, i. e. the existence of high energy nuclear-active particles in extensive air showers.

(+) For details see our survey in *Uspehi Fizičeskih Nauk*, **49**, 185 (1953).

nection a new method permitting the investigation of separate showers has been applied by us of late. We call this method the method of « correlated hodoscopes ». In its first variant it was used by us at the Pamir station in 1950 [16].

The essence of the method is the following. Shower particles are detected by a large number of counter sets located at a certain distance from each other. Each counter is connected to a corresponding hodoscope cell containing a neon lamp. When the master counters discharge, the neon lamps connected to counters discharging simultaneously with the master counters give a short flash which is photographed on a moving film. If the number of counter sets and the number of counters in each set is sufficiently high, the method of correlated hodoscopes will permit one to obtain a true picture of the shower density almost over a continuous and comparatively large region.

It is easy to see that compared to the « core-selector » method described in the literature [11], the method of «correlated hodoscopes » has some distinct advantages. Thus the position of the shower axis can be determined with much higher accuracy (by placing the counter trays at small distances from each other) and this facilitates the study of the shower structure near the axis. On the other hand, the investigation of remote parts of the showers can be carried out with widely separated counter trays and this considerably increases the « aperture ratio » of the method. Thus the time necessary to obtain a given statistical accuracy is by tens of times smaller in the method of « correlated hodoscopes » than in the «core-selector» method.

However, in order to get a detailed picture of the shower, the number of hodoscope counters must be very large. Therefore, if hundreds or even thousands of counters are used, it is very essential that each hodoscope system be as simple as possible, reliable, compact and cheap. The experiments performed in our laboratory (and described below) were possible in consequence of the development of a very simple hodoscope system. These hodoscopes, designed by L. N. Korablev [17], contain in each cell only one neon lamp with three-electrodes, five small condensers and three resistances. No conventional radio tubes are used. A photograph of a hodoscope cell containing 12 counters is shown in Fig. 4. A hodoscope photograph of an extensive shower is shown in the same figure. Approximately 1000 counters were photographed simultaneously.

The method of correlated hodoscopes permits one to identify each shower with a high degree of accuracy, i.e. to determine the position of the shower axis and the total number of shower particles. Knowing the total number of particles one can then determine the energy of the primary particle.

It should be noted that with the help of correlated hodoscopes the structure of showers with very different number of particles (from 10^4 to 10^9 particles) can be investigated; moreover, the distance from the axis can be varied from

$\sim$ 10 cm up to several kilometers. Using the method described above a detailed study of the structure of extensive air showers was carried out during 1950-1954 at the Pamir station (3 860 m) and in Moscow (sea level), by measuring the spatial distribution of the particle density.

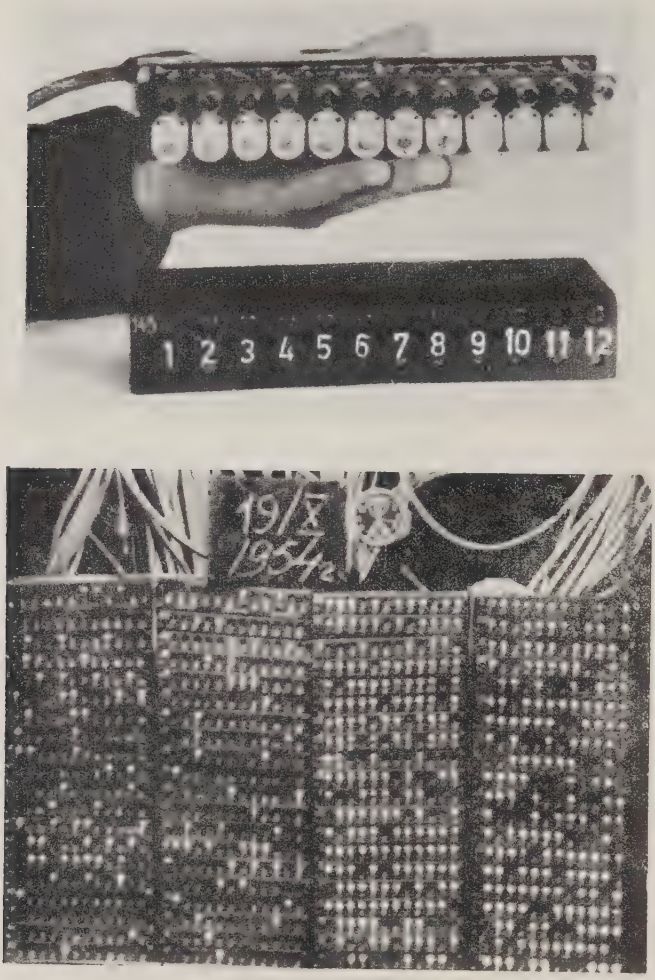

Fig. 4.

The counter arrangement used in the 1952 experiments at the Pamir station is shown in Fig. 5. Altogether 1500 hodoscope counters were used,

these being divided into 22 sets. The majority of sets contained 48 counters of various areas. The shower particle density of any given point could be determined with an accuracy of 30% from the number of counters trigge-

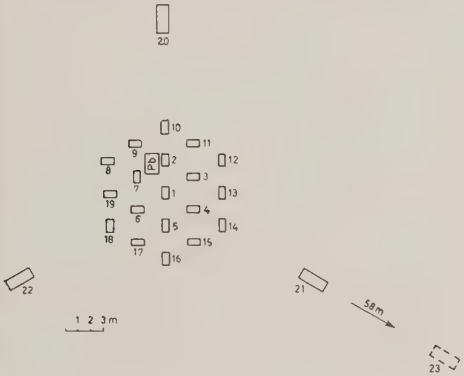

Fig. 5.

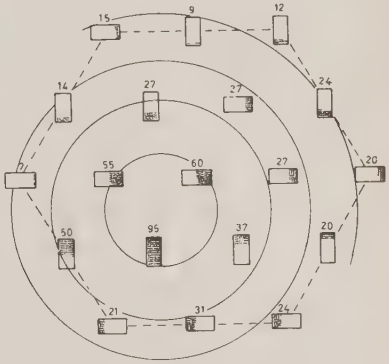

Fig. 6.

red in each tray. The error in determining the position of the shower axis did not exceed 1 meter. In some cases several counter trays were placed inside a thick lead block, thereby separating nuclear-active from nuclear-inactive penetrating particles.

In our latest experiments the number of hodoscope counters has been increased up to 2 500.

An example of the spatial distribution of counters discharged by a shower is shown in Fig. 6. Rectangles represent hodoscope counter sets; the number of black points in the rectangles and the figures represent the shower particle density at the given point.

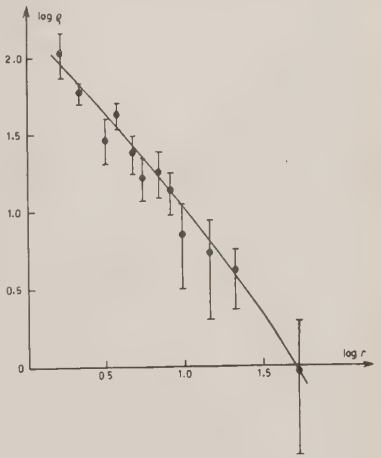

Fig. 7.

5. – Results.

In Fig. 7 the shower data are presented in graphical form. The ordinates give the logarithm of the density of particles, the abscissae are the logarithm of the distance from the axis (in meters).

Our results indicate that at mountain heights the spatial distribu-

tion of the particles' density can be expressed by a formula of the form $r^{-(0,95\pm0,05)}$ if the distance from the shower axis lies between 2 and 10 meters; it is $(\exp[-r/80])/r$ for distances of the order of tens of meters, and r^{-3} for distances of the order of hundreds of meters (200÷800 m).

Experiments show that the spatial distribution for $(2 < r < 10$ m) is insensitive to variations of the energy of the primary particles.

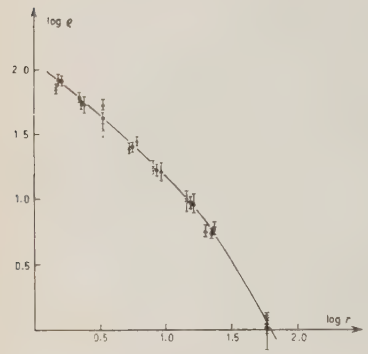

Fig. 8.

Thus, even if this energy changes by tens of times, the spatial distribution can be expressed by a law of the form r^{-1} irrespective of the shower energy. The spatial distribution of particles in showers formed by primaries of various energies E_0 is represented in Fig. 8; it will be noticed that all the values fit satisfactorily the same curve. In the graph the logarithm of the density of particles is plotted against the logarithm of the distance from the axis. Triangles refer to showers with total number of particles $N = 2 \cdot 10^4$ ($E_0 \sim 5 \cdot 10^{13}$ eV), points to $N = 7 \cdot 10^4$ ($E_0 \sim 1 \div 2 \cdot 10^{14}$ eV), crosses to $N = 6 \cdot 60^5$ ($E_0 \sim 10^{15}$ eV). The curves are fitted at the 9 meter point.

Similar measurements, performed at sea level, showed that the spatial distribution of shower particles (for a total number of shower particles between $N = 4 \cdot 10^4$ and $N = 4 \cdot 10^5$) can be expressed by the law $1/r$ for distances of the order of a meter and by the law $(\exp[-r/55])/r$ for that of tens of meters; when r is of the order of hundreds of meters the law is correspondingly $1/r^{2.6}$. These data also show that, excluding the far periphery of the shower, the spatial distribution at high altitudes as well as at sea level can be expressed by the same formula, on the condition that lengths are expressed in cascade theory radiation units.

The spatial ditribution of penetrating particles was also studied; the central and remote parts of the shower were investigated, nuclear-active particles being measured separately from nuclear-inactive particles.

Results obtained at the Pamir station for small distances from the axes of the showers can be represented by the curves plotted in Fig. 9; curve 1 represents the density of nuclear-active particles, curve 2, that of μ-mesons. The different character of the two curves is easily noticeable. At distances $r < 10$ m the density of nuclear-active particles exceeds that of μ-mesons, and the latter ceases to rise with decreasing r. At sea level the curves are similar, but the relative number of μ-mesons is larger by two times.

At small distances from the shower axis ($2\text{m} < r < 10$ m) the density of

nuclear active particles follows the law r^{-1} at high altitudes as well as at sea level. According to our data, the energy distribution of nuclear-active particles falls off even more steeply. This result shows that energetic nuclear-active particles are present in shower cores even at sea level, their relative number (with respect to the total number of charged particles) in this shower region being about the same ($\sim 1\%$) at various altitudes.

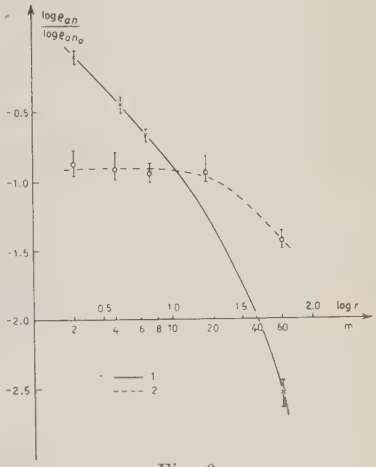

Fig. 9.

Nuclear collisions resulting in π^0-meson formation take place throughout the atmosphere and the electron-photon component of the shower is thus continuously represented; this explains why the function giving the spatial distribution of the particles is independent of the altitude. This absence of shower « aging » sharply contradicts the electromagnetic cascade theory, according to which in the central regions of the shower the spatial distribution of the particles should have the form $1/r^{(2-S)}$. The value of S increases as the shower penetrates the atmosphere and therefore in its central regions the shower should « smear out ». Our results however do not reveal any such « smearing out ».

The spatial distribution of shower particles near the shower axis ($r < 2$m) was investigated by us in 1953 at an altitude of 3860 m; showers with total number of particles $N \cong 8 \cdot 10^4$ were studied with the help of « correlated hodoscopes » containing a large number of small counters arranged inside a circle of diameter ~ 3 m [19] .

In agreement with HAZEN's results [20] obtained by a different method, it was found that for showers with a number of particles close to the above mentioned value, $\varrho(r) \sim r^{-0.5}$ if $0.3\text{m} < r < 1\text{m}$. The region $1\text{m} < r < 2\text{m}$ is an intermediate one, the density law changing from $\sim r^{-0.5}$ to $\sim r^{-1}$.

6. – Conclusions.

The foregoing experimental data on the structure of extensive air showers enable us to draw some important conclusions about the nature of the elementary interaction process for ultra high energy particles.

We shall first consider the conclusions referring to the angular distribution of particles produced in the elementary interaction process.

The decrease of the shower density as r^{-1} for $2\text{m} < r < 10\text{m}$ corresponds to such a spatial distribution of shower electrons (at the maximum shower development) that can be explained only by assuming multiple Coulomb scattering. Thus nuclear processes do not affect the electron divergence. This signifies that the angles of ejection of high energy particles produced in nuclear collisions are small. It can be shown [21] that the divergence of particles created in collisions of primary protons with the nuclei of the athmosphere will not influence the spatial distribution of the shower electrons only on the condition that the density of the energy flux of the particles decreases with the angle θ of emission more rapidly than θ^{-1} for all angles larger than $\theta_{\min} = r_{\min}/H$; according to our data, $r_{\min} = 2\text{m}$ (region in which $\varrho(r)$ begins to take the form $1/r$). H is the distance between the point of the proton-nucleon collision and the point at which the shower is recorded. A value of $H = 1.5 \cdot 10^4$ m can be accepted and hence $\theta_{\min} = 10^{-4}$.

A better conception of the elementary act can be obtained by considering the process in the center of mass system of the colliding particles.

For small angles θ the change from the laboratory system to the center-of-mass system can be carried out by using the relation: $\theta_c = 2\gamma_c\theta_L$, where $\gamma_c = \sqrt{E_0/2Mc^2}$. Here E is the primary particle energy and M is the mass of particle initially at rest; collisions with this particle lead to the formation of secondary particles.

Assuming $E_0 \sim 10^{14}$ eV and taking for M the mass of the nucleon column with which the primary nucleon collided in the air nuclei, one obtains $\theta_c \sim 2^\circ$. Even if one puts M equal to the mass of a single nucleon it will be found that $\theta \sim 4^\circ$.

Thus the density of the energy flux of secondaries produced by primaries of 10^{11} eV falls off with the divergence angle more rapidly than θ_c^{-1} (for $\theta \gtrsim 4^\circ$). This means that in the center of mass system the secondary particles are ejected in a very asymmetrical manner (*).

This conclusion is in sharp contradiction with the theory of FERMI [22], which treats the interaction of nucleons at high and ultra high energies from a statistical and thermodynamical viewpoint. According to FERMI, head-on collisions should lead to an isotropic distribution of the particles in the c. m. system. Forward and backward directions will predominate if collisions with finite impact parameter are taken into account. However, the calculations of I. L. ROZENTAL' and D. S. ČERNAVSKIJ [23] show that, according to Fermi's theory, the decrease of the energy flux density should be slower than θ^{-1} up to angles corresponding approximately to $r \sim 9\text{m}$. Thus, even if non-central collisions

(*) Asymmetry in the center of mass system of the colliding particles does not, of course, contradict the limiting case in which most of the energy of the incident particle is transmitted to a single secondary particle.

are taken into account, Fermi's theory still contradicts the experimental facts.

Fermi's theory, as is well known, is not a consistent theory inasmuch as it does not take into account the interaction of the particles created. An important development of Fermi's theory was made by L. D. Landau [24]; collisions of two nucleons were described by using the equations of relativistic hydrodynamics, allowance being made for the interaction of the emitted particles. The angular distribution of the secondaries is very different in Landau's and Fermi's theories. According to Landau, in the c. m. system the energy flux density should be very high near the collision axis (because of strong dependence of the particle energy on the angle of ejection). The energy flux density should increase as the angle relative to the collision axis decreases, and this should be true down to small angles θ_c of the order $(Mc^2/E_0)^{\frac{1}{2}}$. If the shower is produced by a primary particle of energy $E = 10^{14}$ eV, the angle defining the region in which the energy flux density is constant will be less than 1° in the c. m. system; beginning with an angle θ of the order of 1° the energy flux density decreases more rapidly than θ^{-1} and for $\theta > 4°$ the decrease is faster than θ^{-2}. A nuclear-cascade computation of the shower development and also the experimental data are not sufficient to permit one to carry out a quantitative comparison of the experimental data with Landau's theory on the angular distribution of particles participating in the elementary interaction act. However, it should be clear from the foregoing that Landau's theory yields a better description of the elementary interaction at ultra-high energies than does Fermi's original theory which sharply contradicts the experimental results.

From an analysis of our data on extensive air showers one is also able to draw some important conclusions relating to the distribution of energy between particles produced in the elementary interaction act.

In a first approximation this problem has been solved for intermediate energies by S. N. Vernov, N. L. Grigorov and collaborators [25, 26].

These authors made a detailed analysis of the data on the transition effect of the soft component in the stratosphere at various latitudes and also of the data on ionization bursts. It was convincingly shown that only about 30% of the energy of primary protons of $\sim 10^{10}$ eV is transmitted to mesons and slow secondary nucleons produced in single nuclear interactions. The main part of the primary particle energy ($\sim 70\%$) is retained by a single nucleon (which can undergo charge exchange). Thus, at energies $\sim 10^{10}$ eV, the partition of the primary particle energy is very weak.

As was mentioned above, the development of a real shower in the atmosphere considerably differs from what one would expect for an electron-photon cascade. In showers created by primaries of $3 \cdot 10^{13} \div 10^{15}$ eV and consisting of $10^4 \div 10^5$ particles, the difference of the number of particles between high altitudes and sea level is much less than that theoretically predicted for electron-photon cascades. This undoubtedly is due to continuous « rejuvenation » of the

shower at expense of the energy of nuclear-active particles. The fact that even at sea level the central region of the shower does not « smear out » shows that most of the energy transferred to π^0-mesons from the nuclear-active component is located in π^0-mesons of high energy ($E > 10^{10}$ eV) near the shower axis (not farther than 1 m from it). This can be possible only if the greater part of the energy of the nuclear-active shower component is carried by particles of very high energy which one can estimate to be larger than $10^{11} \div 10^{12}$ eV. We thus arrive at the conclusion that the energy of nuclear-active shower particles at sea level (i.e. after a path of about 15 nuclear interaction lengths) will differ from the primary particle energy by a factor of only $10^2 \div 10^3$. Assuming that in each collision a certain fraction of the energy is given to the secondary particle, we find from the relation $\alpha^{15} = 10^{-3}$ that $\alpha = 0.6$. This forces us to conclude that in nuclear collisions even very energetic nucleons retain most of the initial energy.

Experimental data on the absorption of single high energy nuclear-active particles also permits one to approach the problem of the degree of energy partition in nuclear collisions [27]; the reason for this is that the relation between the absorption (λ_{abs}) and interaction (λ_{inter}) paths is dependent on the probability of creation of nuclear-active particles possessing energies close to that which the particle had previous to the collision.

The absorption of nuclear-active particles of $\sim 10^{12}$ eV energy was investigated experimentally by K. P. Ryžkova and L. I. Saryčeva in 1952 [28]. The particles were selected by recording the showers produced by them in the absorbers. It was found that the absorption path λ_{abs} for particles possessing an energy 10^{12} eV is $1/\mu_{abs} = (112 \pm 11)$ g/cm^2. For nuclear-active particles of smaller energy ($10^{10} \div 10^{11}$ eV) the absorption path determined with the same apparatus was found to equal $1/\mu_{abs} = (130 \pm 3)$ g/cm^2 which agrees with the results of other authors. The absorption path of particles of 10^{12} eV obtained by Kaplon *et al.* [29] using emulsion chambers ($1/\mu_{abs} \sim 120$ g/cm^2) does not, at any rate, contradict the results of Ryžkova and Saryčeva.

The values of the absorption path should be compared with the interaction path of nuclear-active particles in media possessing an atomic number close to the mean atomic number of air.

We may cite in particular the value of λ_{inter} measured in graphite at the Pamir station by A. L. Ljubimov [30] which is of (70 ± 5) g/cm^2.

As is well known, μ_{abs} and μ_{inter} are related by the following formula

$$\mu_{abs} = \mu_{inter} [1 - \Delta(E)] .$$

The quantity $\Delta(E)$ accounts for the fact that particles of a given energy are not only absorbed, but may also be created in high energy collisions. In view of the sharp decrease of the energy spectrum of nuclear-active particles in the

atmosphere ($F(E) \sim E^{-\gamma}$, where $\gamma \cong 1.5$) the quantity $\Delta(E)$ will be sensitive to the probability of transfer of a considerable fraction of the energy of the generating nucleon to one of the secondary particles. From the data presented above it can be seen that Δ depends only weakly on the energy of the interacting particle: at $E \cong 10^{10}$ eV, $\Delta = 0.5 \pm 0.05$, and at $E \cong 10^{12}$ eV, $\Delta = 0.6 \pm 0.06$.

It was mentioned above that VERNOV, GRIGOROV *et al.* established that when nucleons having energies $E \cong 10^{10}$ eV interact with light atomic nuclei, approximately 2/3 of the primary particle energy is retained by one of the secondary nucleons. The fact that Δ practically does not change (*) when E changes between 10^{10} and 10^{12} eV, also indicates that in the region of $E \sim 10^{12}$ eV most of the primary particle energy is retained by one of the secondary particles.

At the same time it can be shown that these particles are not π-mesons or any other type of short-lived meson which emits a μ-meson on disintegration. This follows from a comparison of the intensity of the high energy primary particles with that of μ-mesons possessing the same energy. Computations show that on the average even the fastest π-meson created in a nuclear collision receives less than 1/7 of the energy of the incident nucleon.

One thus arrives at the conclusion that it is exactly the nucleons which retain the main part of the energy after collision.

The high degree of concentration of energy in a single secondary particle, and also the angular distribution of the energy flux of the secondary particle do not agree with the initial assumptions of the Fermi theory. The formation of secondary particles by decaying Fermi systems is determined by the statistical weights of the possible states. Without further argument, it is clear that this type of elementary process cannot explain the high degree of energy concentration in a single particle, or the fact that this fraction is independent of the energy of the colliding nucleons.

A more consistent treatment of the nucleon collision process also substantially changes the prediction relating to the energy distribution of secondary particles. According to Landau's hydrodynamic treatment of two-particle collisions, a considerable fraction of the primary particle energy is concentrated in the forward wave front moving in the system of the interacting nucleons, and therefore the energy is localized in only a few secondary particles.

The theory can be checked by comparing the calculations with the experimental data. It was noted above that the absorption coefficients substantially depend on the concentration of energy in separate particles. The absorption curve for high energy nuclear-active particles in the atmosphere and also the

---

(*) Assuming that: 1) the effective nucleon interaction cross-section is almost constant up to 10^{12} eV and 2) the fraction of energy transferred in the collision does not decrease.

altitude dependence of extensive air showers [34] were computed on the basis of the energy distribution obtained in Landau's theory by using the « successive generation » method [31-33]. It was assumed in the calculation that the nuclear collision effective cross-section remains equal to the « geometrical cross-section » ($1/\mu_{\text{inter}} = 65$ g/cm^2) up to the very highest energies.

These calculations give better agreement with the experimental data than similar calculations based on Fermi's theory. However the discrepancy which still remains indicates that the energy concentrated in one of the secondary particles is really larger than that one would expect from Landau's theory. Moreover, although in Landau's theory the probability of energy concentration in a single particle decreases with increasing energy of the colliding particles more slowly than in Fermi's theory, the discrepancies that this theory does not remove seem to show that the dependence is even weaker (if it exists at all).

There is no doubt that further theoretical work and accumulation of new experimental evidence will permit more quantitative comparison of theory and experiment; this should yield some important information about the elementary interaction process at ultra high energies. However already at the present time it can be stated that investigations of extensive air showers have established the following facts relating to the elementary nuclear interaction process at high and ultra high energies.

1) The effective interaction cross-section is close to the geometrical value up to the highest energies known ($10^{17} \div 10^{18}$ eV).

2) The multiplicity (number of secondaries created in one act) increases with the primary particle energy; the experimental evidence can be represented by a relation of the form $n \sim E_0^{\frac{1}{4}}$.

3) In the center of mass system, the angular distribution of secondary particles produced by high and ultra high energy particles is strikingly anisotropic with a predominance of particles moving in backward and forward directions.

4) Most of the primary particle energy (in the laboratory system) is concentrated in one or, at any rate, in only a few nucleons; this is true not only for particles of intermediate energy but also for high and ultra high energy particles.

REFERENCES

[1] D. V. SKOBEL'CYN: *Dokl. Akad. Nauk SSSR*, **37**, 16 (1942).
[2] D. V. SKOBEL'CYN, G. T. ZACEPIN and V. V. MILLER: *Phys. Rev.*, **71**, 315 (1947). G. T. ZACEPIN and V. V. MILLER: *Žu. Éksper. Teor. Fiz.*, **17**, 939 (1947).
[3] G. MOLIÈRE: *Die kosmische Strahlung. Herausgegeben von W. Heisenberg* (Berlin, 1943).
[4] A. B. MIGDAL: *Žu. Éksper. Teor. Fiz.*, **15**, 313 (1945).

[5] J. Daudin: *Compt. Rend.*, **216**, 411 (1943); V. Rogozinski: *Phys. Rev.*, **65**, 291 (1944).
[6] G. T. Zacepin, L. H. Ėjdus: *Žu. Ėksper. Teor. Fiz.*, **17**, 937 (1947); **18**, 259 (1948); G. T. Zacepin, S. A. Kučaj and I. L. Rozental': *Dokl. Akad. Nauk SSSR*, **61**, 47 (1948).
[7] G. Cocconi, A. Loverdo and V. Tongiorgi: *Phys. Rev.*, **70**, 852 (1946); G. Cocconi and K. J. Greisen: *Phys. Rev.*, **74**, 62 (1948);
[8] G. Salvini and G. Tagliaferri: *Phys. Rev.*, **73**, 261 (1948).
[9] D. Broadbent and L. Jánossy: *Proc. Roy. Soc.*, A **192**, 364 (1948).
[9] D. M. Alekseev, G. T. Zacepin amd I. G. Morosov: *Dokl. Akad. Nauk SSSR* **63**, 375 (1948).
[10] G. T. Zacepin, I. L. Rozental', L. I. Saryčeva, G. B. Hristiansen and L. H. Ėjdus: *Izv. Akad. Nauk SSSR, Ser. Fiz.*, **17**, N. 1 (1953); L. H. Ėjdus, M. I. Adamovič, I. A. Ivanovskaja, V. S. Nikolaev amd M. S. Tuliankina: *Žu. Ėksper. Teor. Fiz. SSSR*, **22**, 440 (1592).
[11] G. Cocconi, V. Cocconi-Tongiorgi and K. Greisen: *Phys. Rev.*, **76**, 1020 (1949).
[12] N. G. Birger, V. I. Veksler, N. A. Dobrotin, G. T. Zacepin, L. V. Kournosova, A. L. Ljubimov, I. L. Rozental' and L. H. Ėjdus: *Žu. Ėksper. Teor. Fiz. SSSR*, **19**, 826 (1949).
[13] G. T. Zacepin: *Dokl. Akad. Nauk SSSR*, **67**, 993 (1949).
[14] G. Cocconi: *Rev. Mod. Phys.*, **21**, 26 (1949).
[15] G. T. Zacepin and L. I. Saryčeva: *Dokl. Akad. Nauk SSSR*, **69**, 635 (1949).
[16] G. B. Hristiansen: *Dissertation* (Institute of Physics of the Academy of Sciences of the USSR, 1953).
[17] L. N. Korabl'ev: *Dokl. Akad. Nauk SSSR*, **69**, 643 (1949).
[18] G. N. Vavilov, S. I. Nikol'sky and E. I. Tukiš: *Dokl. Akad. Nauk SSSR*, **93**, 233 (1953); G. N. Vavilov, S. I. Nikol'skij and V. P. Sarancev: *Žu. Ėksper. Teor. Fiz. SSSR*, **28**, 505 (1955); A. T. Abrosimov, A. A. Bednjakov, V. I. Zacepin, Jv. A. Nečin, V. I. Solov'ev, G. B. Hristiansen and P. S. Čikin: *Žu. Ėksper. Teor. Fiz. SSSR*, **29**, 693 (1955).
[19] O. I. Dovženko and S. I. Nikol'skij: *Dokl. Akad. Nauk SSSR*, **102**, 241 (1955).
[20] W. E. Hazen: *Phys. Rev.*, **85**, 455 (1952).
[21] G. T. Zacepin: *Dissertation* (Institute of Physics of the Academy of Sciences of the USSR, 1954).
[22] E. Fermi: *Progr. Theor. Phys.*, **5**, 570 (1950); *Phys. Rev.*, **81**, 683 (1951).
[23] I. L. Rozental' and D. S. Černavskij: *Usp. Fiz. Nauk* **52**, 185 (1954).
[24] L. D. Landau: *Izv. Akad. Nauk SSSR. Ser. Fiz.*, **17**, 51 (1953).
[25] N. L. Grigorov and V. S. Murzin: *Izv. Akad. Nauk SSSR*, **17**, 21 (1953).
[26] N. L. Grigorov: *Dokl. Akad. Nauk SSSR*, **94**, 835 (1954).
[27] G. T. Zacepin: *Žu. Ėksper. Teor. Fiz. SSSR*, **19**, 1104 (1949).
[28] K. P. Ryžkova and L. I. Saryčeva: *Žu. Ėksper. Teor. Fiz. SSSR*, **28**, 618 (1955).
[29] M. F. Kaplon, J. Z. Klose, D. M. Ritson and W. D. Walker: *Phys. Rev.*, **91**, 1573 (1953).
[30] S. A. Asimov, N. A. Dobrotin, A. L. Ljubimov and K. P. Ryžkova: *Izv. Akad. Nauk SSSR, Ser. Fiz.*, **17**, 80 (1953).
[31] N. L. Grigorov: *Dissertation* (Institute of Physics of the Academy of Sciences of the USSR, 1954).
[32] G. T. Zacepin and I. L. Rozental': *Dokl. Akad. Nauk SSSR*, **99**, 369 (1954).
[33] U. Haber-Scheim and G. Yekutieli: *Nuovo Cimento*, **11**, 172 (1954).
[34] G. T. Zacepin and L. I. Saryčeva: *Dokl. Akad. Nauk SSSR*, **99**, 951 (1954).
[35] S. Z. Belen'kij: *Žu. Ėksper. Teor. Fiz. SSSR*, **28**, 111 (1955); *Dokl. Akad. Nauk SSSR*, **99**, 523 (1954).

SUPPLEMENTO AL VOLUME III, SERIE X
DEL NUOVO CIMENTO

N. 4, 1956
1° Semestre

High Energy Inelastic Diffraction Phenomena.

E. L. Feinberg and I. Pomerančuk
Academy of Sciences of the USSR - Moscow

Contents. — **1.** Introduction. – **2.** Electromagnetic phenomena accompanying nuclear collisions. – **3.** Purely electromagnetic processes. – **4.** Nuclear phenomena. – **5.** Conclusions.

1. – Introduction.

This is a survey of a series of theoretical papers by various authors [1-10] published during the last two years. Unified by a common physical idea, they pertain however to rather different particular phenomena. The problem is being developed further in the direction of including more particular phenomena, as well as along the line of generalization and improvement of the method.

We consider processes, arising in the course of collisions of *high energy* particles, mainly above 10^8 eV (in some cases peculiarities of the phenomenon appear only for energies, exceeding 10^{12} eV). We hope however that similar phenomena may occur at any energies. We keep in mind inelastic collisions, electromagnetic bremsstrahlung, π-meson pair formation by photons, splitting of fast deuterons etc. The processes under consideration are unified by the fact that all of them are connected with a diffraction of the particles on a target, this target playing the part of a « third body ». It may be for instance a « macroscopic » collection of other particles (bremsstrahlung of an electron in a medium, in particular in a crystal lattice; electromagnetic radiation accompanying diffraction of a π-meson by a nucleus etc.). It should be emphasized that energies are supposed to be so high, that all wave lengths are much smaller than the lattice constant, the radius of the nucleus, and so on. Nevertheless, diffraction phenomena are of the utmost value. This peculiarity first of all demands clarification.

The formal basis of the investigation is given by the following circumstance, which, we believe, has not yet attracted due attention. When energy increases, the angle of divergence of the particles involved in the collision diminishes. This leads to a decrease of the longitudinal component $q_{\|}$ of the momentum q, transferred to the « third body » (the crystal lattice, the nucleus etc.). For sufficiently high energies $q_{\|}$ may become small, as compared to the inverse value of the characteristic dimensions of the « third body », of the distance between atoms or of the nuclear radius R. In other words, for sufficiently high energy either of the following conditions may be fullfilled:

(1*a*) $$q_{\|} a \ll 1 ,$$

or

(1*b*) $$q_{\|} R \ll 1 .$$

According to indeterminacy relations, this means that the effective dimension of the essential region of space involved (*),

(2) $$r_{\text{eff}} = \frac{1}{q_{\|}} ,$$

becomes very large as compared to a or R, however small the wave length may be (cfr. X-ray diffraction on diffraction grating for glancing incidence, diffraction of light on the moon's edge etc.). Such region may contain in the case of electron bremsstrahlung many atoms, in the case of collision with a nucleus this nucleus as a whole.

This peculiarity has different influence on different phenomena and is used in the development of their theories in different ways.

On one side, it is important that besides the « third body », usually taken into account, other particles of the medium play equal part, and the interaction with all of them occurs simultaneously. Therefore, the process in the medium will differ from that occurring on an isolated body. This turns out especially important for purely electromagnetic processes: bremsstrahlung of an electron in the Coulomb field of a nucleus etc. (compare, however, section 4·3 of the present paper).

On the other side, if we deal with a process in which within the whole region there is a single body, the nucleus, for instance, then the scattering action of the body on other particles involved must be known only at large distances. The process is « *external* » with respect to the body. Here this action may be described phenomenologically, using for example the formulas of the diffraction theory, or some kind of independent evidences on the behaviour of

(*) $\hbar = c = 1$.

the scattered particles at a distance from the nucleus (radiation of a photon by a π-meson interacting with a nucleus etc.).

Let us consider the problems of the first kind. When an electron of energy E (its rest mass equal m, momentum p) suffers a bremsstrahlung (photon momentum k), then the momentum q transferred to nucleus has two components: the transversal one $q_\perp$ which is of the order of m (this may be seen by the fact that the divergence angle of particles involved is of the order of or less than $q_\perp/p \sim m/E$), and the longitudinal one, which for zero angle of divergence, equals

$$q_\parallel = \sqrt{E^2 - m^2} - \sqrt{(E-k)^2 - m^2} - k \approx \frac{m^2 k}{2E(E-k)} \tag{3}$$

(as long as the order of magnitude is considered this expression for $q_\parallel$ holds not only for $\theta = 0$, but for the whole essential range of angles $\theta \sim m/E$ as well).

The motion of the electron and of the quantum throughout the whole region of space stretched along p over the length $1/q_\parallel \sim 2E(E-k)/m^2 k$ tells on the emission essentially. Here at least the following phenomena should by mentioned.

1) If E is sufficiently large (or k sufficiently small) for the condition (1a) to by fulfilled, the bremsstrahlung of a particle moving along some crystallographic axis of the crystal will be affected by a *common* (coherent) action of all the N_{eff} nuclei, situated within the section $1/q_\parallel$

$$N_{\text{eff}} \sim \frac{1}{q_\parallel a}\,. \tag{4}$$

This means that the effective charge of a scattering center is $N_{\text{eff}} \cdot Ze$, instead of Ze, and the cross-section for the phenomenon is proportional to N_{eff}^2, i.e. the bremsstrahlung maxima of interferential origin will arise.

2) When moving in an amorphous, as well as in a crystalline medium, in the case of sufficiently high E or sufficiently low k the electron may suffer, over the path equal to $1/q_\parallel$, enough multiple scatterings to go out of the angle of the order of m/E. Therefore, the process of emission will be disturbed. Thus the bremsstrahlung in the medium must decrease when the energy surpasses some large value.

3) Both effects must tell on production of electron pairs, practically in the same conditions, since the interactions of pair components with the third body have the same features.

4) For soft bremsstrahlung photons the deviation from unity of the refractive index of the medium $\sqrt{\varepsilon}$ may tell. Over such a long path $r_{\text{eff}} = 1/q_\parallel$ the additional phase shift of the photon

$$(\sqrt{\varepsilon} - 1) k r_{\text{eff}}\,, \tag{5}$$

may increase sufficiently to destroy the coherence over the path and therefore destroy completely the whole process of radiation.

Let us turn now to nuclear interactions, in which case the most important is not the action of the medium, but the fact that the process is external with respect to the nucleus.

If a particle capable of nuclear interactions strikes the nucleus, it may emit a photon (if the particle possesses an electric charge), or a π-meson (particularly if the particle is a nucleon). For instance, if a charged π-meson (energy E, rest mass μ) impinging on a nucleus emits a photon having momentum k, then for a zero angle of divergence (neglecting the recoil of the nucleus)

$$q_{\parallel} \sim \frac{1}{2} \frac{\mu^2 k}{E(E-k)} . \tag{6}$$

If E is sufficiently high or k sufficiently low to satisfy the inequality (1b), then the essential region of space becomes much larger than the dimensions of the nucleus. The nucleus acts as a whole, while the formation of quanta will proceed at large distances from the nucleus.

This process may be clarified in another way. The possibility of absorption of a π-meson by the nucleus means that the diffraction of the π-meson by the nucleus must occur as well. In the course of the diffraction, the meson acquires some transverse recoil momentum, which equals $q_{\perp} \approx p\theta$ and for sufficiently large angles θ is sufficient to cause the emission of a photon.

In the high energy region, diffraction may be considered as caused by a black sphere. When the wave length of the meson is small enough, the Kirchhoff approximation of the diffraction theory may be used.

6) Quite similarly, a semi-phenomenological treatment of π-meson pair formation by a photon on a nucleon may be given.

7) If a nucleon of high energy E (rest mass M) interacts with a nucleus, then it may emit a π-meson (energy E_π). For small angles

$$q_{\parallel} = \sqrt{E^2 - M^2} - \sqrt{(E - E_\pi)^2 - M^2} - \sqrt{E_\pi^2 - \mu^2} \approx \frac{M^2 E_\pi}{2E(E - E_\pi)} + \frac{\mu^2}{2E_\pi} . \tag{7}$$

If the condition (1b) is satisfied, then the possibility of external production of π-mesons arises. In this case the scattering of the nucleon, as well as that of the meson must be phenomenologically taken into account.

8) If a fast nonrelativistic nucleus, for instance a deuteron, strikes a target's nucleus, diffraction must take place. Therefore, the striking nucleus acquires a transversal momentum and thus its splitting, which may be called diffractive or external splitting, may occur (quite apart from the splitting

caused by the nuclear electrostatic field). For example, for a deuteron with kinetic energy E (its binding energy being ε_d), assuming energies of the outgoing proton and neutron to be equal (this assumption is proved by subsequent calculations) we have:

$$q_{\parallel} = \sqrt{2(2M - \varepsilon_d)E} - 2\sqrt{2M\tfrac{1}{2}(E - \varepsilon_d)} \approx \sqrt{\frac{M}{E}}\,\varepsilon_d . \tag{8}$$

The condition (1*b*) may be satisfied even for energies exceeding few MeV.

In all the processes (5)-(8), in which the nucleus acts as a whole, the characteristic feature is that it acquires the transferred momentum as a whole as well. Assuming that $q = \sqrt{q_{\perp}^2 + q_{\parallel}^2} \approx q_{\perp}$ is not very large, namely that $q_{\perp} < \mu$ (this is particularly necessary if we want to consider the nucleus as having an abrupt edge), we may conclude that the energy acquired by the nucleus (its atomic weight being A) equals

$$\frac{q^2}{2MA} \lesssim \mu \frac{\mu}{2MA} \sim \frac{12\ \text{MeV}}{A} \tag{9}$$

and thus is so small, that the nucleus suffers some recoil, but, as a rule, is not disrupted.

9) One more application of the same principle may be found when considering head-on collisions of fast nucleons with nuclei, in the course of which the nucleus is disrupted and new particles are generated. Frequently in this case, in the energy region 10^9—10^{12} eV, one tries to investigate a cascade multiplication within the nucleus. It turns out, however, that in reality even the treatment of subsequent collisions is possible only if the divergence angle of particles and the recoil energy of nucleons are large enough. In the opposite case the impinging particle interacts simultaneously with all the intranuclear nucleons, situated on its path, i. e. with the whole « tunnel ».

2. – Electromagnetic Phenomena Accompanying Nuclear Collisions.

2·1. *Emission of Photons in the course of diffraction and of capture of mesons* [1]. – Let us consider electromagnetic processes accompanying collision of fast charged π-mesons with nuclei, mesonic momentum being assumed large enough for its wave length to be small as compared to nuclear radius R.

Nuclear interactions can not be included in theoretical calculations properly. It turns out, however, that the electromagnetic radiation process accompanying nuclear collision may be studied in details due to peculiarities of the collision described above.

The process in general is determined by the emission of the field accompanying the meson when it is scattered or captured by the nucleus. Therefore, at least for low energy quanta, their spectrum has the form $\mathrm{d}k/k$, and the probability of emission differs from that of a main process by a factor $e^2 \approx 1/137$ (and by factors logarithmically dependent on energy).

There are two kinds of π-meson interactions involved: that with e.m. radiation field and that with nuclear force field (e.m. interaction with nucleus may be omitted). The possibility of a rather full and sufficiently strict calculation is due to the possibility of applying the perturbation theory to the first of these interactions, while the second one is treated without this approximation (this being the essence of the method).

In fact, outside of the nucleus we may write down the wave function of the π-meson which takes into account the influence of the nucleus. Let us assume for instance, that the nucleus behaves with respect to mesons as a black body (which, as is shown by experiments, holds already for $E \sim 2 \div 3 \cdot 10^9$ eV). Then the pseudoscalar wave function of a π-meson is a superposition of an initial plane wave and of a wave due to the diffraction by the sphere. According to Kirchhoff's diffraction formula ($pR \gg 1$) we have:

$$\psi_{\boldsymbol{p}} = \psi_0 + \psi_1 = \frac{1}{\sqrt{V}}\left(\exp\left[i\boldsymbol{p}\boldsymbol{r}\right] + \frac{ip}{2\pi}\int\limits_{(S)} \frac{\exp\left[ip\,|\boldsymbol{r}-\boldsymbol{r}'|\right]}{|\boldsymbol{r}-\boldsymbol{r}'|}\,\mathrm{d}S'\right), \tag{10}$$

integration being extended over the nuclear cross-section normal to the meson momentum $\boldsymbol{p}$. In this expression plane waves are contained the momentum of which differs from $\boldsymbol{p}$; this is due to the acceleration acquired by the meson through diffraction scattering by the nucleus (the scattering in turn being a result of all the absorption π-meson processes; by « absorption » we mean every process, which takes the meson out of its initial state of momentum $\boldsymbol{p}$). This acceleration will suffice to cause the e.m. radiation by the π-meson, if in the system, in which the meson initially was at rest, it acquires the momentum $q_\perp \gtrsim \mu$. By means of selecting from the Fourier-series of $\psi_{\boldsymbol{p}}$ the terms with $q_\perp \sim \mu$, the magnitude of the cross section may be estimated. A fuller theory may be obtained either by applying the perturbation theory to the transition of a meson under the influence of radiation field from the state given by eq. (10) into the state:

$$\psi_{\boldsymbol{p}'}^{(-)} = \frac{1}{\sqrt{V}}\left(\exp\left[i\boldsymbol{p}'\boldsymbol{r}\right] - \frac{ip'}{2\pi}\int\limits_{(S')} \frac{\exp\left[-ip'\,|\boldsymbol{r}-\boldsymbol{r}'|\right]}{|\boldsymbol{r}-\boldsymbol{r}'|}\,\mathrm{d}S'\right) \tag{11}$$

(a plane wave plus a *convergent* wave, integration being extended over a nuclear cross-section normal to $\boldsymbol{p}'$), or by writing the equation for ψ in the presence

of the quantized e.m. wave with a vector potential $\boldsymbol{A}$:

$$\left(\frac{\partial^2}{\partial t^2} - \Delta + \mu^2\right)\psi = \frac{2e}{i}\,\boldsymbol{A}\nabla\psi\,, \tag{12}$$

substituting ψ by

$$\psi = \psi_{\boldsymbol{p}} \exp\left[-iE_p t\right] + \sum_{\boldsymbol{p}'} \exp\left[-iE_{p'}t\right]\psi_{\boldsymbol{p}'} \tag{13}$$

and using a Green function (accounting for the presence of a black sphere) of the resulting equation for $\psi_{\boldsymbol{p}'}$:

$$G(\boldsymbol{r}, \boldsymbol{r}') = \frac{\exp\left[ip'\,|\boldsymbol{r}-\boldsymbol{r}'|\right]}{4\pi|\boldsymbol{r}-\boldsymbol{r}'|} - \frac{p'}{2\pi i}\int \frac{\exp\left[ip'\,|\boldsymbol{r}-\boldsymbol{s}|\right]}{|\boldsymbol{r}-\boldsymbol{s}|}\,\frac{\exp\left[ip'\,|\boldsymbol{r}'-\boldsymbol{s}|\right]}{4\pi|\boldsymbol{r}'-\boldsymbol{s}|}\,\mathrm{d}S \tag{14}$$

(integration extending over the nuclear cross-section normal to the vector $\boldsymbol{r}-\boldsymbol{r}'$). In such a procedure we get an expression for the wave function of a meson going out with a momentum $\boldsymbol{p}'$ and accompanied by a photon of momentum $\boldsymbol{k}$.

When calculating the cross-section, the question arises whether it is allowable to consider a π-meson as a point particle. If a point meson is assumed, then its diffraction scattering by a nucleus having a radius R, leads to emission of a quantum $\boldsymbol{k}$, with a cross-section containing as a factor some function of a dimensionless parameter $\mathcal{T}(\mu R)$, tending to $0.56/\mu R$ if $\mu R \gg 1$. For $\mu R \gg 1$ $(A \gg 1)$ we have

$$\sigma^d(k) = 2.3e^2\,\frac{E-k}{E}\,\frac{1}{k}\,\frac{R}{\mu} \approx 2.3e^2\,\frac{E-k}{E}\,\frac{1}{k}\,\frac{A^{\frac{1}{3}}}{\mu^2}\,. \tag{15}$$

The total energy radiated is

$$\int k\sigma^d(k)\,\mathrm{d}k \approx 2ER^2e^2\mathcal{T}(\mu R)\,. \tag{16}$$

Quite similarly, a radiation due to absorption of a π-meson by a nucleus may be calculated. This is a radiation accompanying the π-meson current directed inside the nucleus. The cross-section integrated over frequencies $k > k_{\min}$, and over photon angles $\theta < \theta_{\max}$ equals

$$\sigma^c = e^2R^2\left(\ln\frac{\theta_{\max}E^2}{e^2\mu^2}\right)\left(\ln\frac{E}{k_{\min}} - 1\right). \tag{17}$$

Taking into consideration the relativistic arguments, the influence of the

π-meson form factor on the radiation of photons may be supposed to be represented by a factor

$$F = F\left(\frac{kE(\theta^2+(\mu^2/E^2))}{2\mu^2}\right). \tag{18}$$

Therefore, we may hope that in the future a detailed experimental investigation of e.m. radiation described above may lead to the possibility of determining such an important quantity as the π-meson form factor.

The total energy emitted due to capture turns out to have the order of magnitude of e^2R^2E. The cross-section is especially large for radiation emitted at small angles. In fact, for $\theta = \mu/E$ the differential cross-section of the capture radiation is

$$\frac{e^2}{4\pi}R^2\left(\frac{E}{\mu}\right)^2\frac{E-k}{E}\frac{1}{k} \tag{19}$$

and for $E/\mu \sim 40$ equals $R^2((E-k)/E)\cdot(1/k)$, which is of the order of magnitude of nuclear cross-sections.

A similar process for the case when the initial particle has spin equal to $\frac{1}{2}$ was investigated in papers [2]. In particular here the diffraction formula of Kirchhoff for half spin particles was deduced.

2·2. *π-meson pair formation by photons on nuclei* [3]. – The process considered above has quantitative characteristics the order of magnitude of which could be foreseen. Its investigation, however, enabled to get exact formulas, and, moreover, to develope a method applicable to some other processes. Thus, in ref. [3], the process mentioned in the title of the section was studied, the action of a nucleus, considered as a black body with respect to mesons, being taken into account by describing the generated mesons with the aid of eq. (11). Here, therefore, the meson-nucleus interaction is treated strictly (under the assumption, which by no means is a matter of principle, that the nucleus is absolutely black).

The expression obtained for the cross-section is rather complex. In the case of a heavy nucleus, however, if the radius is large as compared to the π-meson wave length, the formulas are considerably simplified. The cross-section for the production by a photon (having a momentum $\boldsymbol{k}$) of a pair of mesons with momenta $\boldsymbol{p}_1$ and $\boldsymbol{p}_2$, is

$$\mathrm{d}\sigma = \frac{e^2}{2\pi^2}\frac{R^2}{\varkappa^2}\frac{J_1^2(\varkappa R)\,E_1(k-E_1)\,\mathrm{d}E_1\,b^2\,\mathrm{d}\boldsymbol{b}\,\mathrm{d}\boldsymbol{\varkappa}}{k^3(\mu^2+b^2)^2}, \tag{20}$$

where

$$\boldsymbol{p}_1 = \frac{\boldsymbol{k}}{k}\left(p_1 - \frac{k_1^2}{2p_1}\right) + \boldsymbol{k}_1 ; \qquad \boldsymbol{p}_2 = \frac{\boldsymbol{k}}{k}\left(p_2 - \frac{k_2^2}{2p_2}\right) + \boldsymbol{k}_2 ;$$

$$\boldsymbol{\varkappa} = \boldsymbol{k}_1 - \boldsymbol{k}_2 , \quad \boldsymbol{b} = \tfrac{1}{2}(\boldsymbol{k}_2 - \boldsymbol{k}_1) , \qquad E_1 = \sqrt{p_1^2 + \mu^2} .$$

Here $\boldsymbol{k}_1$, $\boldsymbol{k}_2$ are two dimensional vectors which are perpendicular to the photon momentum, $k_1^2 \ll k^2$, $k_2^2 \ll k^2$. In the eq. (20) the π-mesons are considered as a point body. Otherwise the formula is supplemented by a factor, having the meaning of a form factor for the process considered. If the π^+-π^--mesons interaction is strong, then in eq. (20) appears another factor accounting for it.

Integration of eq. (20) over all $\boldsymbol{\varkappa}$ and over $\boldsymbol{b}$ which are less than some $b_{\max}$ yields the following distribution over energies:

$$(20a) \qquad \mathrm{d}\sigma = \frac{e^2R^2}{2}\left[\ln\frac{\mu^2 + b_{\max}^2}{\mu^2} + \frac{\mu^2}{\mu^2 + b_{\max}^2} - 1\right]\frac{E_1(k - E_1)}{k^3}\,\mathrm{d}E_1 .$$

The integral cross-section is:

$$(20b) \qquad \sigma = \frac{e^2R^2}{12}\left[\ln\frac{\mu^2 + b_{\max}^2}{\mu^2} + \frac{\mu^2}{\mu^2 + b_{\max}^2} - 1\right].$$

At high values of $b_{\max}$ the « non-point » character of π-mesons is essential.

The eqs. (20)-(20b) lead to the following conclusions.

1) The cross-section for the production of π^+-π^- pairs which are not accompanied by excitation of the nucleus, in the extremely relativistic case, does not depend on the photon energy. The cross-section is proportional to $R^2 \sim A^{\frac{2}{3}}$ and is of the order of magnitude of $(e^2/10)R^2$.

2) The sum of the transversal momenta of π^+ and π^- mesons ($\boldsymbol{\varkappa} = \boldsymbol{k}_1 + \boldsymbol{k}_2$) is of the order of $1/R$. The distribution with respect to $\boldsymbol{\varkappa}$ is given by eq. (20).

3) Effective values of $\boldsymbol{b} = \frac{1}{2}(\boldsymbol{k}_2 - \boldsymbol{k}_1)$ depend on the « size » of the elementary particles and on their interaction.

It should be emphasized, that the same process for the formation of two neutral mesons is forbidden due to the conservation of charge parity: a γ-quantum is odd (with respect to charge), while a π-meson is even (the nucleus acts as a black body and therefore should be considered as even). Thus at high energies the cross-section for $\gamma \to 2\pi^0$ is much smaller than for $\gamma \to \pi^+ + \pi^-$.

Besides the case of both mesons propagating to infinity, there may occur a process in which a γ-quantum is absorbed, a pair of mesons at a distance from a nucleus is virtually produced and only one of the components of the pair propagates away, while the other is absorbed in the nucleus and a star

arises (an explosion of a nucleus). The theory of this process was given by J. A. VDOVIN [4]. The order of magnitude of the cross-section obtained by him is of $(e^2/10)R(1/\mu)$ (for $R \gg 1/\mu$). The essential feature of the process is that the most part of the γ-quantum energy is taken by a single meson (namely by the one which goes out). The same author has studied also the formation of stars under the action of a photon in the case when *both* virtual π-mesons, which have arisen at large distance from the nucleus are captured by it. This mechanism of formation of photo-stars has a cross-section $\sigma \sim e^2 R^2 \ln k/\mu$ (in the case of point meson).

3. – Purely Electromagnetic Processes.

3·1. *Bremsstrahlung of electrons in a crystal lattice* [5]. – E. J. WILLIAMS [11] was the first to mention the possibility of the simultaneous action of different atoms of a crystal on bremsstrahlung. He gave however only an estimate which, as it is now clear, led him to an incorrect conclusion that the bremsstrahlung should decrease at very high energies due to regularities in the position of atoms. The criterium for the arising of the effect, given by him without any comment, is not confirmed by further investigation. Later FERRETTI [12] considered the influence of the crystal lattice much more consistently. Here, however, the results were also not of quantitative character and they are not confirmed by the results of the work which we intend to report here.

In the papers by M. L. TER-MIKAELJAN [5], the bremsstrahlung was investigated for a relativistic electron entering the crystal lattice (for simplicity a cubic one) in a given direction with respect to the crystallographic axis. The usual perturbation theory was used (practically for calculations the Weizsäcker-Williams procedure was taken, as in FERRETTI's work, but the same formulas were obtained in a frame of reference in which the lattice is at rest). The crystal potential is a sum of potentials of the screened nuclear fields. It is important that the thermal vibrations of the atoms be taken into account. As is readily seen, the cross-section for the emission of a photon in a process, in which the lattice receives the momentum $\boldsymbol{q}$, differs in this case from that of an isolated atom by an interference factor

$$|\sum_i \exp[i\boldsymbol{q}\boldsymbol{r}_i]|^2,$$

where the sum is taken over the instantaneous positions of nuclei, $\boldsymbol{r}_i$. The average over thermal vibrations transforms this factor, as is usual for the theory of X-ray scattering by crystals, into

$$N_1 N_2 N_3 (1 - \exp[-2M]) + \exp[-2M] |\sum \exp[i\boldsymbol{q}\boldsymbol{r}_{i0}]|^2 . \tag{21}$$

Here N_1, N_2, N_3, are the numbers of atoms along different axes, $2M = q^2u^2$, where u^2 is the mean square of the thermal displacements of an atom, $\boldsymbol{r}_{i0}$ the radius vector of the equilibrium position of the i-th atom. Correspondingly the cross-section is decomposed into an « amorphous part », which is proportionate to the total number of atoms within the crystal, N_1, N_2, N_3, and an « interference part ». The amorphous radiation cross-section is less than that for an isolated atom multiplied by the number of atoms; the difference depends on temperature and, for some elements, may become of the order of $10 \div 20\,\%$. When temperature increases this difference diminishes. This radiation does not depend on the initial direction of the electron motion.

The interference part is of a more complex structure. Since the transversal component of the momentum transferred to nucleus is always large, $q_\perp \sim m$, then the nuclei situated in the plane perpendicular to the electron motion do not give any interference, while the nuclei situated along the path of the electron contribute to this effect. A more precise evaluation than that expressed by eqs. (1a) and (3) gives the energy for which the effect is essential:

$$\frac{E}{m} \gtrsim \frac{am}{4\pi} \frac{\varepsilon}{1-\varepsilon} \sim \nu \frac{137}{2\pi} \frac{\varepsilon}{1-\varepsilon}. \tag{22}$$

Here $\nu = 10^8 a$, a being the lattice constant, $\varepsilon = k/E$ the fraction of the initial electron energy E radiated in the form of a photon. For $\nu \sim 3$, $\varepsilon \sim \frac{1}{2}$ this gives $E \gtrsim 50$ MeV. For higher energies (or for radiation of more soft quanta) the cross-section increases proportionally to the *square* of the effective number of atoms N_{eff} situated along the path of the electron. In the paper [5] the conditions for the arising of interference maxima are investigated, the case of the arbitrary thick crystal is calculated, the conditions of applicability of the formulae obtained are given and the dependence on the initial direction of the electron motion is studied. For instance, the interference part of bremsstrahlung of a beam of electrons with angular dimension θ, entering the lattice along one of its axes, equals, if divided through the total number of atoms in the lattice:

$$\frac{1}{N_1 N_2 N_3} \sigma_{\text{int}}(\varepsilon)\,\mathrm{d}\varepsilon = \sigma_{\text{B.-H.}}(\varepsilon)\,\mathrm{d}\varepsilon \frac{\pi\varrho}{a\theta}, \tag{23}$$

under the condition that $(2\pi/a)\sqrt{\overline{u^2}} = \theta_{\max} > \theta > \theta_{\min} = (\varepsilon/(1-\varepsilon))\, am\ (m/2E.)$ Here $\sigma_{\text{B.-H.}}$ is the usual Bethe-Heitler cross-section, $\varrho \approx a_0 Z^{-\frac{1}{3}}$ is the screening radius of the atom. The interference radiation decreases for $\theta < \theta_{\min}$. For tungsten, $\theta_{\max} = 2.4^\circ$ for $T = 0$, $\theta_{\max} = 4.8^\circ$ for the Debye temperature W. Since $\pi\varrho/a \approx (2\pi/\nu)(1/Z^{\frac{1}{3}}) \sim 1$, then for sufficiently small θ the intensity of radiation may exceed many times that for an isolated atom.

It is essential that the integral over all angles gives strictly the same in-

tensity as given by bremsstrahlung on a single atom. Therefore, for the case of a beam of electrons penetrating through a sufficiently thick polycrystal, the effect of the crystal structure disappears. The effect of the lattice, therefore, consists in forming sharp and narrow maxima compensated by a small decrease of the general background outside.

3·2. *Effect of multiple scattering on the bremsstrahlung of electrons* [6]. – In the case of an amorphous medium, when no interference phenomena arise, there appears, for sufficiently high energies, another important process, namely, the multiple scattering of electrons by the atoms of the medium tells on the bremsstrahlung (in the case of a crystal it plays a subdominant role [5]). The possibility of this circumstance was pointed out in ref. [6]. Here the estimates and the approximate formulas for limiting cases were also given in the case of classical treatment of bremsstrahlung (this is exact for the radiation of soft photons, $k \ll E$, and gives an estimation of the general effect), and to some degree for quantum case as well. A more rigorous classical quantitative theory of the effect and especially its quantum investigation turned out to be very complex. They were given by A. B. MIGDAL [7]. His results in particular support the results of classical approximate treatment.

If particles during the time of motion through the essential region with dimension $1/q_{\parallel} \sim 2E(E-k)/m^2k$ (see eq. (3)) suffer multiple scattering sufficient to decline them through an angle exceeding $\theta \sim m/E$, then the emission process will be violated. The mean square ot the scattering angle for this path (assuming, for the sake of estimation, $k \ll E$) is

$$\overline{\theta_s^2} = \left(\frac{E_s}{E}\right)^2 \frac{r_{\text{eff}}}{L} \sim \frac{2E_s^2}{m^2 k L},$$

where $E_s = \sqrt{4\pi \cdot 137}\, m \approx 21$ MeV, L is radiation length (in cm) for this medium. If $\overline{\theta_s^2}$ becomes $\gtrsim (m/E)^2$, i.e. if

$$\frac{E}{m} \gtrsim \frac{1}{60}\sqrt{kL} \tag{24}$$

then the intensity of radiation must diminish. Even for hard quanta, $k \sim \frac{1}{2}E$, this gives:

$$\frac{E}{m} > \frac{1}{7200}\, mL\,. \tag{25}$$

For Pb, $L \approx 5 \cdot 10^{-1}$ cm, for air at normal conditions $L \approx 3 \cdot 10^{4}$ cm. Correspondingly for $E > 2 \cdot 10^{6}$ m in Pb, or for $E > 10^{11}$ m in air, the bremsstrahlung cross-section must be smaller than is usually assumed. For softer

quanta the effect tells for lower energies. For a given energy E the effect appears for photons with

$$k < 3600 \left(\frac{E}{m}\right)^2 \frac{1}{Lm}, \tag{26}$$

i.e., for Pb, at $k < 4 \cdot 10^{-7}(E/m)E$. For instance, an electron with energy $E \sim 5 \cdot 10^{10}$ eV will give in Pb few photons with $k < 0.01E \sim 5 \cdot 10^{8}$ eV.

A more consequent estimation, within the region of applicability of classical treatment ($k \ll E$) shows that in distinction of the usual Bethe-Heitler formula:

$$\mathrm{d}I_{\text{B.-H.}} = \frac{e^2}{3\pi} \frac{\mathrm{d}k}{L} \frac{E_s^2}{m^2} = \frac{16}{3} \frac{n}{137} (Zr_0)^2 \ln (191 Z^{-\frac{1}{3}}) \, \mathrm{d}k \tag{27}$$

(n is the number of atoms of the medium per unit volume, Z the atomic number of the element, $r_0 = e^2/m$ the classical electron radius), the intensity is described by the equation

$$\mathrm{d}I = \frac{e^2}{2} \sqrt{k} \, \mathrm{d}k \frac{E_s}{E} \frac{1}{\sqrt{6\pi L}} \quad \text{for} \quad k \ll \left(\frac{EE_s}{m^2}\right)^2 \frac{1}{6L}. \tag{28}$$

Thus, the bremsstrahlung cross-section at high energies decreases as $1/E$, while the photon spectrum behaves as $\mathrm{d}I/k \sim \mathrm{d}k/\sqrt{k}$. At sufficiently high energies the electrons and positrons become a penetrating component. As it has been already remarked above, the same pertains for pair production by photons as well. Therefore, they also become penetrating.

This result is obtained by considering a classical equation for the energy, emitted at frequency $\omega = k$ into an element of solid angle $\mathrm{d}\Omega$ by an electron, moving along a trajectory:

$$\mathrm{d}I = \frac{e^2}{4\pi^2} k^2 \, \mathrm{d}k \, \mathrm{d}\Omega \left| \int_{-\infty}^{\infty} [\boldsymbol{nv}] \exp [i(\boldsymbol{kr} - \omega t)] \, \mathrm{d}t \right|^2, \tag{29}$$

where $\boldsymbol{r} = \boldsymbol{r}(t)$ and $\boldsymbol{v} = \boldsymbol{v}(t)$ are the radius vector and the velocity of the electron, given as a function of time t, $\boldsymbol{n}$ the unit vector of propagation of photon, $\boldsymbol{k} = \omega \boldsymbol{n}$. A classical approximation to the Bethe-Heitler formula is obtained if we put $\boldsymbol{r} = \boldsymbol{v}t$, and $\boldsymbol{v}$ changes within some region with dimension a from one constant value $\boldsymbol{v}_1$ to some other value $\boldsymbol{v}_2$ (the resulting formula being valid for wave lengths of photon $\lambda \gg a$). In particular, for $\boldsymbol{v}_2 = 0$, a stopping radiation is obtained. Within the medium, however, due to multiple scattering, $\boldsymbol{v}$ is varying all the time around $\boldsymbol{v}_1$ and, later, around $\boldsymbol{v}_2$. It is sufficient to consider as fluctuating components of velocity only those, which are

perpendicular to $\boldsymbol{v}_1$ and, correspondingly, to $\boldsymbol{v}_2$. Their squares increase proportionally to time. For instance, in the case of emission of a radiation directed exactly along the line of initial motion, $\boldsymbol{kv}_1(-\infty) = kv_1(-\infty)$, the phase at $-\infty < t < 0$ will contain, in the average, expressions of the type of $[v_1(1 - \frac{1}{2}\overline{\theta_s^2}(t)) - 1]\omega t$ instead of $\boldsymbol{kr} - \omega t = \omega t(v_1 - 1)$, $\theta_s(t)$ being the angle of multiple scattering. For $kv_1\overline{\theta_s^2} \gtrsim 2k(1 - v_1)$ an essential term arises, and due to fast fluctuations of the expression integrated, $\mathrm{d}I$ (given by form. (29)) decreases. The true value of the intensity must be obtained by averaging the expression for $\mathrm{d}I$ with respect to the transversal components of velocity. In paper [6], instead of averaging $\mathrm{d}I$, the phase alone was averaged. This leads to the estimation given by eq. (28). Later, however, strict calculations, using a very elegant method, were performed for $E \gg m$ by A. B. MIGDAL [7], who also succeeded in giving a quantum theory of the phenomenon.

Averaging over scatterings the eq. (29) for $\mathrm{d}I$ in the classical case, MIGDAL transforms it by expressing its average through Fourier components of the probability of a given value of the velocity W_k (the Fourier components arise from exponentials occurring in eq. (29)). In the space of angular variables W_k obeys an equation of the Fokker-Planck type. Solving this equation he obtains:

$$\text{(30)} \qquad \begin{cases} \mathrm{d}I = \{\mathrm{d}I\}_0 \Phi(s) = \dfrac{4e^2Q}{3\pi(1-v)}\,\Phi(s)\,, \\ s = \dfrac{1-v}{4}\sqrt{\dfrac{\omega}{Q}}\,, \quad Q = 4\pi n(Zr_0)^2(\ln 191Z^{-\frac{1}{3}})(1-v^2)\,. \end{cases}$$

Here $\{\mathrm{d}I\}_0$ is the energy radiated when scattering is neglected (classical approximation to the Bethe-Heitler formula), while $\Phi(s)$ is a tabulated function:

$$\text{(30}a\text{)} \qquad \Phi(s) = 3s\int_0^\infty \exp[-sx]\,\frac{\cos sx + \sin sx}{\mathrm{ch}^2(x/2)}\,\mathrm{d}x - \\ + 24s^2\int_0^\infty \exp[-sx]\,\frac{\sin sx}{\mathrm{sh}\,x}\,\mathrm{d}x - 6\pi s^2\,.$$

For $s \to \infty$ (scattering is negligible) $\Phi(s) \to 1 - (48/7s^4)$ and we come to eq. (27); for $s \to 0$, $\Phi(s) \to 6s$: the result differs from the eq. (28) by a numerical coefficient of the order of unity. This complete formula shows that in Pb for photons with $k = \frac{1}{2}E$, the deviation from the Bethe-Heitler formula attains 50 %, if $E = 3 \cdot 10^{12}$ eV.

The quantum treatment, necessary for the region $k \sim E$, is much more difficult to handle. The radiating particle, owing to scattering, is not describable by a wave function, and the density matrix is introduced. The author obtains

for it a quantum kinetic equation, which he subsequently solves. The result in main part supports the classical treatment, but it contains also some peculiar features.

3·3. *Effect of Polarization of the Medium* [8]. – It was shown in paper [8] that the above investigation of the influence on the bremsstrahlung of multiple scattering must be supplemented by the account of polarization of the medium. In fact, the difference of the velocity of photons from unity must be taken into consideration. This may be effected by introducing a general factor $\sqrt{\varepsilon}$ into eq. (29) and by putting $\boldsymbol{k}$ equal to

$$\boldsymbol{k} = \sqrt{\varepsilon}\,\omega\boldsymbol{n} \tag{31}$$

instead of $\boldsymbol{k} = \omega\boldsymbol{n}$. Here the dielectric constant of the medium ε may be supposed to have the form:

$$\varepsilon = 1 - \frac{4\pi n Z e^2}{m\omega^2}\,. \tag{32}$$

This means that the effect is essential for the softest quanta. Therefore, the classical formulae suffice. After introducing in eq. (29) the modifications just mentioned and averaging the phase of the integrated function over possible scatterings, we notice that, besides the scattering term $\omega t(1 - \frac{1}{2}\overline{\theta_s^2}(t))$, the phase contains another term, $\omega t(\sqrt{\varepsilon} - 1) \approx (2\pi n Z e^2/m\omega)t$. If it exceeds the scattering term (low frequencies), then the polarization plays a predominant role. The results of investigation [8] may be summarized as follows.

a) Unless the energy of the electron exceeds some critical value

$$E < E_{\text{crit}} = \left(\frac{m}{E_s}\right)^2 6L\sqrt{\frac{4\pi n Z e^2}{m}}\,m \tag{33}$$

(for dense media, assuming the elements to be in the middle or in the end of the periodical table, $E_{\text{crit}} \sim 10^4 m \sim 10^{10}$ eV), the multiple scattering has no chance to produce any effect, since the polarization of the medium predominates. For different frequency regions we have the following cases. If

$$\omega \gg \sqrt{\frac{4\pi n Z e^2}{m}}\,\frac{E}{m}\,,$$

then

$$\mathrm{d}I = \frac{1}{3\pi}\,\frac{\mathrm{d}k}{L}\left(\frac{E_s}{m}\right)^2, \tag{34}$$

i.e. the influence of the medium may be neglected and the formula, which is a classical analogous of the Bethe-Heitler formula (and coincides with it for $k \ll E$), holds. If

$$\sqrt{\frac{4\pi n Z e^2}{m}} \ll \omega \ll \sqrt{\frac{4\pi n Z e^2}{m}} \frac{E}{m},$$

(for frequencies $\omega \lesssim \sqrt{4\pi n Z e^2/m}$ the approximate eq. (32) is not valid), then

$$\mathrm{d}I = \frac{m}{12\pi^2 L n Z} \frac{E_s^2}{E^2} k^2 \,\mathrm{d}k \,. \tag{35}$$

b) if the electron energy increases and becomes $E \gtrsim E_{\mathrm{crit}}$, then a region of frequencies arises, where the multiple scattering plays the main part, namely: for

$$\left(\frac{4\pi n Z e^2}{m}\right)^{\frac{3}{2}} \left(\frac{6E^2 L}{E_s^2}\right)^{\frac{1}{2}} = \omega_p \ll \omega \ll E \frac{E}{m} \left(\frac{E_s}{m}\right)^2 \frac{1}{6L} = \omega_s \,, \tag{36}$$

the eq. (28) holds. For $E \gtrsim E_0 = m \cdot mL(E_s/m)^2$ the region given by relation (36) covers almost the whole high frequency part of spectrum, excluding the interval $E - E_0 < \omega < E$, where the Bethe-Heitler formula still holds. For $\omega \ll \omega_p$ again eq. (35) is valid, for $\omega \gg \omega_s$ eq. (27) holds.

On the whole the situation may be schematically represented by Fig. 1, where, however, the scale is not represented quantitatively: in reality $\omega_p \ll E$. An interesting feature of the influence of the medium is that the so called infra-red catastrophe disappears. Therefore, when checking experimentally the radiative corrections usually calculated for various processes and strongly influenced by infra-red catastrophe, the presence of the medium must be taken into account.

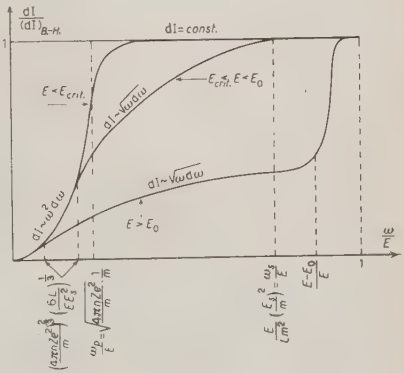

Fig. 1.

4. – Nuclear Phenomena.

4·1. *Emission of mesons by nucleons in the course of diffraction scattering* [9]. – This process differs from others considered above in the fact that it cannot be calculated quantitatively with the same degree of accuracy. This is due to the lack of a consistent meson theo-

ry and to the non-applicability of the perturbation theory. Here the perturbation theory may give no more than an uncertain suggestion of a possible order of magnitude of the cross-section.

The condition (1*b*), when eq. (7) is used, gives the energetic threshold of the effect. If the meson acquires a small fraction of the energy (of the order of $(\mu/M)E$), then the condition is:

$$E \ll \mu R M \approx A^{\frac{1}{3}} M \,. \tag{37}$$

If, on the contrary, the meson energy is of the same order as that of the nucleon, then the condition is:

$$E \gg \frac{M}{\mu} A^{\frac{1}{3}} M \,, \tag{38}$$

i.e. the threshold increases considerably. In the case of generation of several mesons the threshold increases proportionally to their number. The peculiar feature of such a process would be the absence of the so called « second cone », the generated mesons would move (in the center of mass system) only forward.

In evaluating the cross-section we must keep in mind the fact that the process cannot be considered as caused by the nucleus as a whole, if the transversal component of transferred momentum is too large, namely if it exceeds the inverse value of the mutual distance of nucleons in the nucleus. This distance may be taken equal to $1/\mu$. Therefore, we must restrict ourselves to $q \lesssim \mu$. In that case the velocity acquired by the nucleon (in its rest system) is small: $v \sim \mu/M$. Accordingly the emission of mesons cannot be very intensive. In fact, by applying (in the same way as used in sect. 2·1) the perturbation theory and assuming pseudoscalar coupling of pseudoscalar mesons, we get for the emission of a single meson:

$$\sigma \sim g^2 \frac{A^{\frac{1}{3}}}{\mu^2} \left(\frac{\mu}{M}\right)^2 \approx \frac{g^2}{A^{\frac{1}{3}}} \left(\frac{\mu}{M}\right)^2 \sigma_0 \,. \tag{39}$$

Here g is the coupling constant, σ_0 the geometrical cross-section of the nucleus. Even for $g^2 \sim 10 \div 20$, the cross-section is much smaller than σ_0. Due to the value of the threshold, as well as according to eq. (39), this phenomenon must be comparatively more noticeable in the case of light nuclei.

Since meson interactions are strong, we may believe that a similar process is possible for the production of π-mesons by a π-meson suffering diffraction by a nucleus. In this case the smallness of meson mass is favourable to the process.

4·2. *Diffractive splitting of deuteron.* – The calculation of the process may be performed consistently notwithstanding the fact that the law of interaction of nucleons is not known with certainty. The knowledge of the deuteron wave

function alone is necessary. This function is known definitely only for proton-neutron distances exceeding the range of nuclear forces, $1/\mu$. Therefore the detailed calculations are possible only for some of the processes, namely for the cases of transfer of not very large momenta, $q \ll \mu$. The investigation was performed for deuterons having kinetic energy within the interval $50 \div 170$ MeV, in which case the target nucleus may be considered opaque. In order to obtain an estimate of the cross-section we may proceed as follows. Let us take the wave function of the deuteron, suffering, as a whole, diffraction by a black sphere representing the target nucleus (here the finite dimensions of the deuteron should be taken into account; this is why its wave function of internal motion $\varphi(|\boldsymbol{r}_p - \boldsymbol{r}_n|)$ will enter into the calculations). Selecting in this function the cases of scattering with transferred momentum q sufficiently large for the splitting of deuteron, i.e., with $q \sim \mu$, we get for the order of magnitude of the cross-section: $\sigma \sim RR_d$, R being the target nucleus radius, R_d that of deuteron. Thus σ is of the same order of magnitude as for stripping, and is much smaller than the geometrical cross-section, $\pi(R+R_d)^2$. Assuming $R \ll R + R_d$ (this assumption has no fundamental meaning, and the more general case is now under consideration) we may apply the perturbation theory. It can be shown that the cross-section for diffractive splitting, which gives a neutron having the momentum $\boldsymbol{p}_n$ and a proton having the momentum $\boldsymbol{p}_p$, is

$$(40) \qquad d\sigma(\boldsymbol{p}_n, \boldsymbol{p}_p) = 2\pi |\langle \psi^{(-)}_{\boldsymbol{p}_n} \psi^{(-)}_{\boldsymbol{p}_p} | U | \psi_d \rangle|^2 \delta(E - E_0) ,$$

$\psi^{(-)}_{\boldsymbol{p}_n}$ and $\psi^{(-)}_{\boldsymbol{p}_p}$ being the neutron and proton functions, given by eq. (11), ψ_d the wave function of the deuteron, suffering diffraction as a whole, while U is an operator, describing the proton-neutron interaction. Restricting ourselves to that part of all processes which corresponds to $q < \mu$, we may assume that the target nucleus edge is abrupt, substitute for the deuteron function $\varphi \sim \exp[-\alpha |\boldsymbol{r}_p - \boldsymbol{r}_n|]$, $\alpha = \sqrt{M\bar{\varepsilon}_d}$ and consider U as a δ-function of the mutual distance of the nucleons. This last simplification is possible since the mutual velocity of nucleons in final states is low, being of the same order of magnitude, as the velocity inside the deuteron.

Thus, suffering the splitting due to a feeble push, the deuteron gives a proton and a neutron with the same distribution with respect to angles and energies, as when the stripping occurs. In fact, in both cases these distributions are prescribed essentially by their distributions within the deuteron. However, contrary to stripping, in the case considered, both the proton and the neutron are produced in every elementary process. The cross-section is

$$(41) \qquad \sigma \approx RR_d^2 \mu \frac{q_{max}}{\mu} .$$

Here $q_{\max}$ is the highest of the values of transferred momenta, allowed for by the above condition. Putting $q_{\max} \sim \mu$ we get: $\sigma \sim RR_d$.

In order to check these results experimentally one needs the coincidence measurements. We may, however, mention that all the experiments in which the yield of protons was examined have always given for the stripping cross-section unreasonably high values. For instance, a group of investigators [13], having paid no attention to the process described here, calculated from experiments an astonishingly high value of the nuclear radius, namely, $R = r_0 A^{\frac{1}{3}}$ with $r_0 \approx 1.6 \div 1.7 \cdot 10^{-13}$ cm. It seems quite probable that these experiments in reality were influenced by diffractive splitting.

We should like to mention that such a diffractive splitting is possible for some other nuclei as well, if the activation energy for the corresponding reaction is sufficiently low. Since the process is of a purely kinematical nature and is determined by the transversal components of momentum (it may be seen, in particular, by the independence of the cross-section from the deuteron energy), then the situation should not alter when going over to relativistic energies of the deuteron (for which case the nucleus again becomes opaque).

The process considered was investigated independently by one of the present authors (E.F.) and also by A. I. AHIEZER and A. G. SITENKO.

4·3. *Collision of a Nucleon with a Nucleus* [10]. – As it has been already pointed out (Section **1**, form. (9)), due to large size of the essential region, it may happen that a collision of an impinging fast nucleon (or of a π-meson) with the nucleons of a nucleus, leading to π-mesons formation, cannot be considered according to the scheme of subsequent collisions. A somewhat more detailed estimate shows that such a cascade scheme is permissible only if the particles produced in the collision of two nucleons diverge isotropically in their center of mass system, and, therefore, if in the laboratory system the angle is of the order of $\sqrt{M/E}$ and the recoil energy exceeds approximately 100 MeV per nucleon. For smaller angles, and lower recoil energies, the whole tunnel is involved in every collision. There is some experimental evidence [14] which seems to be against the scheme of subsequent collisions, not only at very high energies, where the Fermi-Landau theory holds, but for the energies of the order of $10^{10} \div 10^{11}$ eV as well.

5. – Conclusions.

The results surveyed above are, of course, only examples of the method developed. This method may be extended on different other phenomena (this extension is in fact now being performed). In particular, the formation of pairs accompanying the diffraction of a particle by a nucleus and some other effects

have been considered. In some cases it has turned out reasonable to consider the nucleus as being partly transparent. The behaviour of a diffracted particle may be represented in the essential region in a more general way than that offered by the Kirchhoff formula etc. All these and similar other possibilities deserve further investigation.

REFERENCES

[1] L. D. Landau and I. Ja. Pomerančuk: *Žu. Éksper. Teor. Fiz.*, **24**, 505 (1953).
[2] A. I. Ahiezer: *Dokl. Akad. Nauk SSSR*, **94**, 651 (1954); A. I. Ahiezer and I. Ja. Pomerančuk: *Dokl. Akad. Nauk SSSR*, **94**, 821 (1954).
[3] I. Ja. Pomerančuk: *Dokl. Akad. Nauk SSSR*, **96**, 481 625, (1954).
[8] J. A. Vdovin: *Some Processes of Interaction of High Energy γ-quanta with π-mesons and Nucleons*, Thesis (Moscow, 1955).
[5] M. L. Ter-Mikaeljan: *Žu. Éksper. Teor. Fiz.*, **25**, 289, 296 (1954).
[6] L. D. Landau and I. Ja. Pomerančuk: *Dokl. Akad. Nauk SSSR*, **92**, 535, 735 (1953).
[7] A. B. Migdal: *Dokl. Akad. Nauk SSSR*, **96**, 49 (1954).
[8] M. L. Ter-Mikaeljan: *Dokl. Akad. Nauk SSSR*, **94**, 1033 (1954).
[9] I. Ja. Pomerančuk and E. L. Feinberg: *Dokl. Akad. Nauk SSSR*, **93**. 439 (1953).
[10] E. L. Feinberg: *Žu. Éksper. Teor. Fiz.*, **28**. 242 (1955).
[11] E. J. Williams: *K. Danske Vidensk. Selsk., Mat.-fys. Medd.*, **13**, 276 (1935).
[12] B. Ferretti: *Nuovo Cimento*, **7**, 118 (1950).
[13] G. P. Millburn, W. Birnbaum, W. E. Crandall and L. Schecter: *Phys. Rev.*, **95**, 1268 (1954); W. Heckrote: *Phys. Rev.*, **95**, 1279 (1954).
[14] J. L. Rozental' and D. S. Černavskij: *Usp. Fiz. Nauk*, **52**, 185 (1954); **55**, 121 (1955).

SUPPLEMENTO AL VOLUME III, SERIE X
DEL NUOVO CIMENTO

N. 4, 1956
1° Semestre

Optical Spectrum of Excitons in the Crystal Lattice.

E. F. Gross

Institute of Technical Physics of the Academy of Sciences - Leningrad

Contents. — **1.** Introduction. – **2.** Study of the structure of the long-wave edge of cuprous oxyde crystals. Fundamental absorption at room temperature. – **3.** Structure of the edge of the fundamental absorption of Cu_2O crystals at $T=77.3$ °K (liquid nitrogen). Hydrogen-like series of narrow lines of absorption. – **4.** Optical spectrum of excitons in the crystal lattice. Yellow series of excitons in Cu_2O crystals. – **5.** Green series of excitons in Cu_2O crystals at $T=77.3$ °K (liquid nitrogen). – **6.** The exciton spectrum in Cu_2O at $T=4.2$ °K (liquid helium). New lines. – **7.** The exciton spectrum in Cu_2O at $T=1.3$ °K (liquid helium). – **8.** Stark effect in the lines of the exciton spectrum. – **9.** Zeeman effect in the lines of the exciton yellow series. – **10.** The structure of the edge of the fundamental absorption band in other crystals.

1. – Introduction.

It is well known that crystals have wide ranges of continuous spectrum, the so-called characteristic or fundamental absorption band, where the absorption coefficient goes up to very high values of the order of $10^5 \div 10^6$ cm $^{-1}$. On the side of long waves the continuous absorption range possesses an edge which, for some crystals, undergoes an abrupt fall. The position of the long-wave absorption edge in the spectrum depends on the composition of a crystal and is defined, as is known, by the width of the forbidden zone in a crystal. In many substances the characteristic absorption is connected with the photoconductivity, and this effect is caused mostly by the lengths of waves falling upon the long-waves edge of the fundamental absorption. For instance, this may be clearly seen in Fig. 1 which provides with the curve of absorption and that of the spectral distribution of the photoconductivity in the crystal of cuprous oxide according to the data obtained by A. V. Ioffe and A. F.

IOFFE [1]. That empirical rule was stated already by GUDDEN and POHL [2] in 1923. But, up to now, the cause of the photosensitivity fall within the strong absorption range in the fundamental band remains unknown. GUDDEN [3] considered this phenomenon to be a mistery. As it is known, J. FRENKEL [4] in 1931 introduced the idea of the exciton in order to explain the absorption of light in the fundamental band without the rise of photoconductivity.

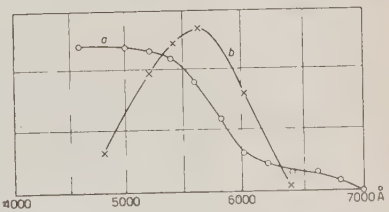

Fig. 1. – Absorption curve (*a*) and spectral distribution curve of photoconductivity (*b*) in Cu_2O crystal, according to A. V. IOFFE and A. F. IOFFE [1].

Being interested in that phenomenon, we have undertaken at the Institute of Technical Physics of the Academy of Sciences a systematic study of the absorption spectrum of crystals in order to obtain detailed data on the energetic levels of electrons in crystal lattices.

Selecting the object of investigation, we have first of all taken the cuprous oxide (Cu_2O) crystal. This selection was made for the following reasons. The electrical properties of the cuprous oxide as a « classical » semi-conductor had been studied in details long before. In 1947-1950 the thorough study of the photoelectric properties of this crystal was carried out by V. P. ŽUZE and S. M. RYVKIN [5] at the Institute of Technical Physics. They came to the conclusion of the impurity nature of the Cu_2O photoconductivity. ŽUZE and RYVKIN were the first to point out [6] the role of excitons in the phenomenon of the photoconductivity. For the external photoeffect, the exciton mechanism was suggested by APKER and TAFT [7].

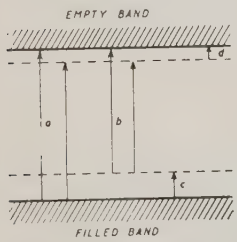

Fig. 2. – Diagram of electronic levels in Cu_2O crystals, according to data obtained by ŽUZE and RYVKIN [5, 6] for photoconductivity.

Depending on the electron levels distribution in the crystal, the absorption of light may be observed in various spectral ranges. In the case of the Cu_2O crystal, basing upon the study of photoconductivity by ŽUZE and RYVKIN [5, 6], we should expect that the absorption of light might be connected with the electron transitions, which are schematically shown in Fig. 2. The energy difference between the levels in the case of electron transitions of the *a* or *b* type is relatively higher than in the case of *c* or *d* type transitions. The energies of the *c* and *d* transitions are small, and, therefore, the absorption of light connected with them might be expected to be in the long-wave (infrared) part of the spectrum, while the absorption connected with the *a* and *b* transitions must be observed near the fundamental absorption band (for Cu_2O, about $\lambda = 6300$ Å) on its long wave side.

The absorption of light in Cu_2O was studied little. The visible range of the spectrum was studied by A. V. IOFFE and A. F. IOFFE [1], M. PIGAREV and S. GOLUB [8], and by G. MÖNCH [9].

2. – Study of the Structure of the Long-wave Edge of Cuprous Oxide Crystals. Fundamental Absorption at Room Temperature.

In order to study more thoroughly the long-wave edge of the main absorption band, we used spectral instruments whose dispersion (25 Å/mm in the range of $\lambda \simeq 6300$ Å) exceeded by approximately 10 times that of the instruments previously used.

Our first experiments on the study of the characteristic absorption in cuprous oxide were performed at room temperature ($t = 20$ °C) with macrocrystalline Cu_2O plates of various thickness, from dozens up to hundreds of microns. These experiments (performed together with N. A. KARRYEV) have proved [10] that the edge of the Cu_2O crystal fundamental absorption band possesses a complicated structure. The absorption of light near the edge does not continuously increase with decreasing wavelength but is of a stepped character. One may clearly observe two points where the curve of absorption undergoes a break and forms a sort of step. These points at $t = 20$ °C are located in the following way: 1) at 6371 Å (1.945 eV) and 2) at 6284 Å (1.972 eV), so that the width of the step is about 87 Å (0.027 eV). The absorption of light within the range of the step between these two points is comparatively small. Behind the step ($\lambda = 6284$ Å) the absorption undergoes a fast increase in the direction of short waves, and the curve of absorption goes up. All these phenomena are clearly seen in Fig. 3, where the microphotogram of the absorption spectrum near the edge of the Cu_2O fundamental band is shown.

Another interesting phenomenon is observed at both edges of the step: a bright narrow line is seen against the background of absorption on the long-wave side before each limit of the step.

These lines are contacting the limits, where the abrupt breaks in the curve of absorption are observed. Thus, the bright lines are located at $\lambda = 6371$ Å and $\lambda = 6284$ Å and are nothing but the narrow lines of radiation (*).

When the temperature of the crystal decreases, the edge of the Cu_2O crystal fundamental absorption together with the step and its sharp limits shifts to the short-wave side of the spectrum. The absorption of light on the step is greatly dependent on the temperature and undergoes a strong fall

(*) NIKITIN and his colleagues (see reference [29]) have also observed the bright lines at the step edges.

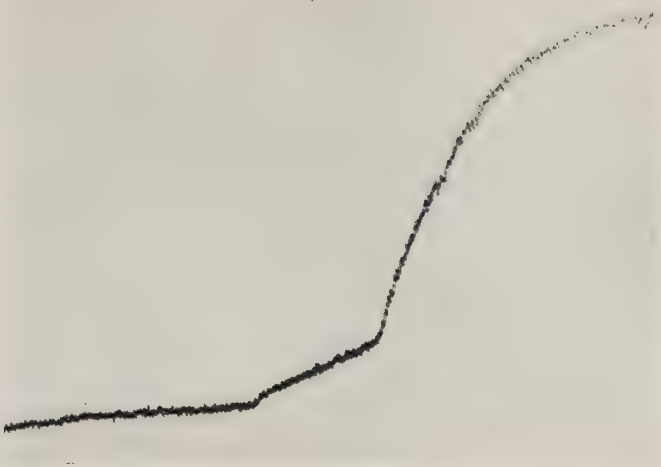

Fig. 3. – Microphotometric record of the «step» at the edge of the fundamental absorption curve of Cu_2O crystal at 20 °C.

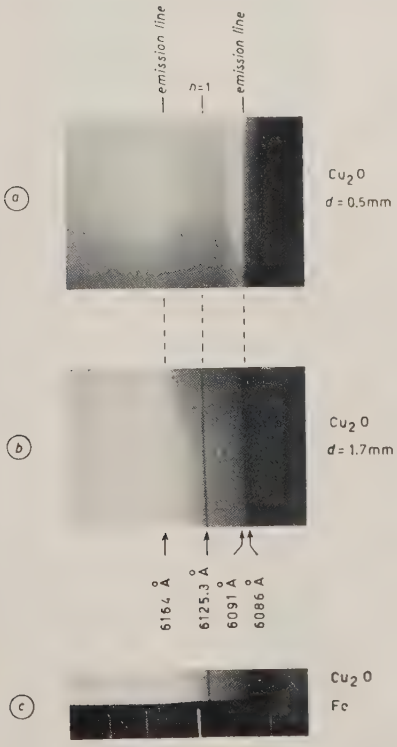

Fig. 4. – Spectrograms of the «step», of a narrow line and lines of emission at the edge of the fundamental absorption curve of Cu_2O crystal at $T = 77.3$ °K. *a*) Cu_2O plate of thickness $d = 0.5$ mm; *b*) $d = 1.7$ mm; *c*) comparison of the Cu_2O line with those of Fe.

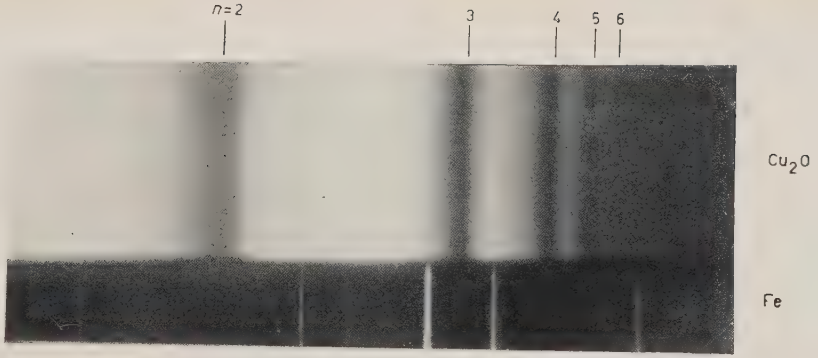

Fig. 5. – Spectrogram of the exciton yellow series in Cu_2O crystal at $T = 77.3$ °K.

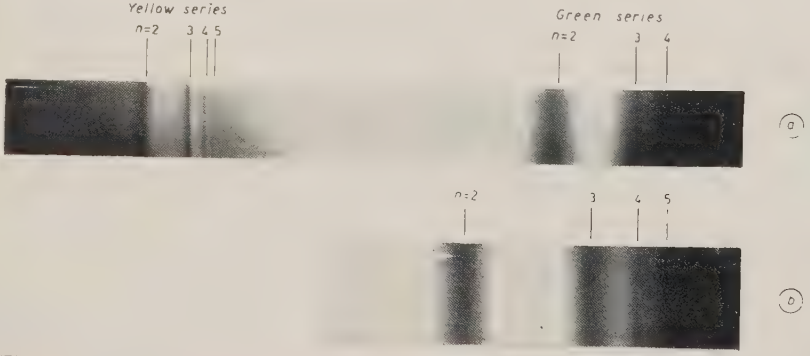

Fig. 7. – Spectrograms of yellow and green series in Cu_2O crystal (*a*), and magnified green series (*b*), at $T = 77.3$ °K.

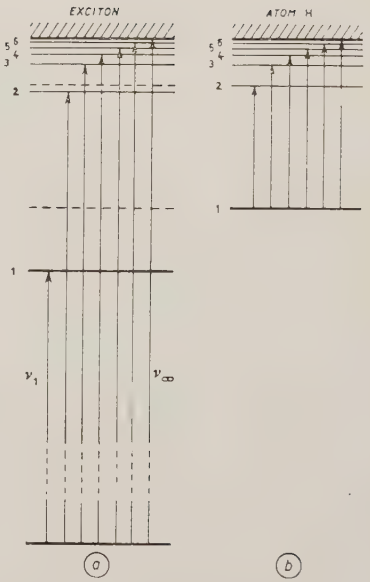

Fig. 6. – Diagram of exciton and hydrogen atom.

(evidently, according to an exponential law) when the crystal is cooled. The edges of absorption at the step shift and remain sharp, if the crystal temperature is reduced up to that of the liquid nitrogen ($T = 77.3$ °K). At $T = 77.3$ °K the edges of the step are located: 1) at $\lambda = 6164$ Å (2.010 eV) and 2) at $\lambda = 6086$ Å (2.034 eV). The distance between the first and the second edge, i.e. the step width, at $T = 77.3$ °K is of 78 Å (0.024 eV). Thus, the step width scarcely changes with the temperature alteration, while the absorption in it undergoes such a decrease at $T = 77.3$ °K that it becomes hardly noticeable at this temperature.

The above-mentioned results were independently obtained by the Japanese scientists HAYASHI and KATSUKI [11]. These authors have reported that they observed the absorption edges only in the Cu_2O absorption spectrum.

We went further in the study of the structure of the Cu_2O crystal fundamental absorption edge and succeeded in the discovery of a new interesting phenomenon.

3. – Structure of the Edge of the Fundamental Absorption of Cu_2O Crystals at $T = 77.3$ °K (Liquid Nitrogen). Hydrogen-like Series of Narrow Lines of Absorption.

If the temperature decreases, the edge of the Cu_2O crystal fundamental absorption together with the range of the stepped absorption, as it was mentioned above, shifts to the shortwave side of the spectrum (the orange part) and a very narrow absorption line [12] comes out against the weak continuous background of the step. At $T = 77.3$ °K this line becomes exceedingly sharp and thin, so that its width becomes comparable with that of the narrow lines of atomic spectra. Its location is greatly dependent on the temperature, and it

TABLE I. – *Position of the lines of the exciton yellow series in the* Cu_2O *absorption spectrum at* $T = 77.3$ °K.

Quantum number n	Wavelengths λ_n in Å	Energy in eV	Frequencies ν_n in cm^{-1}	$\Delta\nu_n$ in cm^{-1}	
				observed	calculated
1	6125.3	2.0234	16325.7	1134.3	785
2	5792.7	2.1396	17263.2	196.8	196.3
3	5756.6	2.1530	17371.2	88.8	87.2
4	5743.8	2.1578	17410.1	49.9	49.1
5	5738.1	2.1599	17427.5	32.5	31.4
6	5734.1	2.1615	17439.4	20.6	21.8
⋮	⋮	⋮	⋮	⋮	⋮
∞	5727.4	2.1640	17460	0	0

shifts to the short-wave part of the spectrum together with the step, when the Cu_2O crystal is cooled. At $T = 77.3$ °K this line is located at $\lambda = 6125.3$ Å (see Table I, $n = 1$). Fig. 4 shows the simultaneous existence of the wide step and of the narrow line upon it.

If the temperature goes down, not only the absorption coefficient on the step decreases, but the continuous spectrum behind the step undergoes a strong weakening as well, so that the limit of the beginning of the strong absorption shifts to the short-wave side of the spectrum quicker than the step. A series of separate absorption lines, located before the strong absorption edge, gradually opens in the yellow part of the spectrum as a result of the continuous weakening of the spectrum caused by low temperature. At $T = 77.3$ °K these lines become very narrow. We have succeded in discovering 5 of these sharp lines which get closer as the frequency increases i.e. six lines including the first one, against the background of the step. The disposition of these lines greatly depends on the temperature, so that the whole series of lines shifts to the short-wave part of the spectrum, when the crystal is cooled. The disposition of the above-mentioned lines in the spectrum at $T = 77.3$ °K is given in Table I (n from 1 to 6). Fig. 5 shows the spectrogram of the yellow series of absorption lines in Cu_2O.

When the temperature tends to 0 °C, the lines widen and become hardly visible against the background of continuous absorption, whose intensity strongly increases with the increase of temperature and which comes from the side of the short waves (*).

The widening of lines goes on asymmetrically, and is stronger at the long-wave part of the spectrum. The short-wave side of the lines remains sharper in this case.

The system of narrow lines drawing together, converges to the limit after which the continuous spectrum of absorption begins. The continuum limit (series limit) is located near $\lambda = 5727{,}4$ Å (Table I, $n = \infty$). The discrete lines with the continuous spectrum behind them form a sequence which is similar to the series observed in the line spectra of absorption of the atom (ion) near the limit of the series.

We have attempted to find a certain regularity in the alteration of narrow lines in the absorption spectrum of the Cu_2O crystal, analogous to the serial one. It has turned out that the frequencies ν_n of these new lines satisfy the simple serial relation

$$(1) \qquad \nu_n = A - \frac{B}{n^2} = \nu_\infty - \frac{B}{n^2} = \left(17\,460 - \frac{785}{n^2}\right) \text{cm}^{-1}, \qquad n = 1, 2, 3, 4, 5, 6;$$

(*) Even at room temperature, one may notice the traces of the first members of the series, $n=1$ and $n=2$.

n is the quantum number, A and B are constants. $A = \nu_\infty$ has the value of the serial limit ($n = \infty$), i.e. corresponds to the red border of the photodissociation of the system of charges in the crystal lattice; that system causes the appearence of the series of lines in the Cu_2O spectrum.

Table I gives the experimental values of the frequencies ν_n of the serial lines. It gives also the comparison in wave numbers of the observed and calculated differences $\Delta\nu_n$ between the frequency ν_∞ of the series limit and the frequencies ν_n of the serial lines:

$$\Delta\nu_n = \nu_\infty - \nu_n = \frac{B}{n^2}, \qquad n = 1, 2, 3, 4, 5, 6.$$

As it follows from Table I, the agreement between the observed and calculated values of the frequencies ν_n is quite good, with the only exception of the first serial line ($n = 1$), where there is no agreement between the two values; this is particularly evident in the differences $\Delta\nu_1$.

Relation (1) and Table I show that the series of lines observed in the Cu_2O crystal is hydrogen-like. The continuous spectrum behind the limit of the series of lines should be explained by the extraction of the electron, resulting from the photodissociation of the system of charges which causes the series of lines in the crystal spectrum.

The existence of narrow absorption lines in crystals at low temperature was observed many times, e.g. in molecular crystals (Obreimov and Prihot'ko [13, 14], Špol'skij [15]), in alkali-halide coloured salts with the introduction of metal atoms (e.g. in KI – Tl by Yuster and Delbecq [16], by Pringsheim [16]) in the salts of rare earths etc.

But, up to now, there have been no groups of lines in the crystals satisyfing the serial regularities observed.

4. – Optical Spectrum of Excitons in the Crystal Lattice. Yellow Series of Excitons in Cu_2O Crystals.

The experiments described in the previous paragraph state a new interesting fact: that series of narrow lines with greater number of members, regularly converging to the series limit, analogous to those observed in free atoms and ions, can be observed in the solid.

Hence, natural is the question, how the hydrogen-like series appears in the cuprous oxide crystalline lattice, and what is its origin. The position of the series of lines in the spectrum, just near the long-wave edge of the fundamental absorption band, and the high absorption coefficient of the lines of the series permits to assert that the phenomenon is connected with the main lattice of the Cu_2O crystal but not with its local defects, impurities

and deviation from the stoichiometric correlations (*). The serial regularity (1) of a hydrogen-like atom shows that the system of electric charges in the crystal, causing the appearance of the hydrogen like series, is bound by Coulomb forces.

All these facts have led us to the thought that the hydrogen-like series of narrow lines in the cuprous oxide is caused by the absorption of light, related to the exciton formation in the Cu_2O lattice.

The conception of the exciton as an excited state of the lattice which can migrate around in the crystal, was suggested by J. FRENKEL [4] in 1931.

Later on, excitons and their properties were studied by WANNIER [17], MOTT [18], SLATER and SHOCKLEY [19], FRANCK and TELLER [20], and by SEITZ [21]. Recently, various properties of excitons were considered by SEITZ [22, 35] as well as by HELLER and MARCUS [23], ANSEL'M and FIRSOV [24], SAMOJLOVIČ and KORENBLIT [25], SAMOJLOVIČ and KONONOVA [26].

WANNIER [17] and MOTT [18] consider the exciton to be a hydrogen-like atom (+) in which the electron and the hole, bound by Coulomb forces, are rotating around their mutual centre of gravity.

The coupled electron and hole state are characterized by discrete energetic levels of the hydrogen-like atom. The absorption spectrum of such a system should therefore consist of discrete lines (×) corresponding to the transitions of the system under the influence of light into various excited states of the exciton. In these states the exciton is not a carrier of current. The photoconductivity should be originated when the light of a higher frequency can dissociate the exciton and transfer it into the state with a free electron and a hole, when they become the current carriers.

Hence, it follows that the discrete energy levels of the excited states of the exciton should be located below the edge of the empty band, while the red limit of the exciton dissociation should coincide with its lower edge (defined from the optical data) (−).

Hence, it is evident that the discrete absorption lines, corresponding to the electron transitions into the exciton states, should be located in the spec-

---

(*) It is known that there is usually surplus oxygen in the Cu_2O crystal, which may be removed by way of continuous heating of Cu_2O at high temperatures in the vacuum. But, despite such a processing of the Cu_2O, the series of absorption lines was preserved in Cu_2O spectrum. This testifies to the fact that the origin of the series is not connected with the surplus oxygen in the crystal.

(+) The positive hole mass approaches that of the electron and, therefore, it is more natural to consider the exciton to be analogous to the positronium, than to the atom of hydrogen.

(×) The possibility of the existence of narrow lines in absorption spectra of crystals was shown also by PEIERLS [27].

(−) The definition of the zone edge by the spectroscopic data may not coincide with the thermic one.

trum on the red side of the characteristic absorption edge, and converges to the limit of the series, located at the edge of the characteristic absorption.

The following serial relation of the hydrogen-like atom for the frequencies of the exciton absorption spectrum results from theoretical considerations:

$$\nu_n = \nu_\infty - \frac{R'}{n^2}, \qquad n = 1, 2, 3, \ldots,$$

where ν_n is the frequency of the n-th absorption line in the exciton spectrum; ν_∞ is a constant corresponding to the value of the frequency of the serial limit in the exciton absorption spectrum, i.e. corresponding to the energy of the exciton photodissociation; n is the quantum number, assuming the value of integers 1, 2, 3, ...; R' is a quantity defined by the relation

$$R' = \frac{R(\mu/m)}{n_0^4},$$

where R is the Rydberg constant; n_0 is the index of refraction; m is the electron mass in the vacuum; μ is the reduced effective mass of the exciton,

$$\frac{1}{\mu} = \frac{1}{\mu_1} - \frac{1}{\mu_2},$$

where μ_1 and μ_2 are the effective masses of the electron and the hole.

If we pass now to the experimental results described above, it turns out that the experimental data agree well with the concept of exciton. Then, the experimental data make it possible to determine the reduced exciton mass μ for Cu_2O from the values of the constant B of the exciton series, and to calculate by that either the effective mass μ_1 of the electron or the effective mass μ_2 of the hole, if one of these values is known.

Assuming that $\mu_2 = 1$ (*) and $n_0 = 2.5$, we obtain the value $\mu_1 = 0.4$ from the data for the exciton spectrum.

Thus, we obtain from the exciton spectrum a reasonable value for the effective masses, which demonstrates the good agreement between theory and experiment.

The above-mentioned considerations drive us to the conclusion that the hydrogen-like series of narrow lines in the yellow part of the absorption spectrum of the Cu_2O crystal observed by us [10, 12] is the optical spectrum of the

(*) The value $\mu_2 \cong 1$ may be taken as an average from the values for $\mu_2 = 1.5 \div 1.8$ obtained from the data for the F-centre in the Cu_2O crystal and the value $\mu_2 = 0.5$ obtained from the thermoelectric electromotive force and from the Hall effect. These data were kindly given us by S. I. Pekar and V. P. Žuze.

exciton and serves as a direct proof of the existence of excitons in the crystal lattice.

These results were first obtained by us in the spring of 1951 (*).

Several months later, the fact of the existence of the hydrogen-like series of narrow lines in the solid, found in our experiments [10, 12] with the Cu_2O crystal, was confirmed by the Japanese physicists HAYASHI and KATSUKI [28] who observed in the yellow part of the Cu_2O spectrum the series of lines, which was erroneously ascribed to the polaron (self-trapped electron). In 1954 our experiments on Cu_2O were repeated in France and once more confirmed by NIKITIN and his colleagues [29].

The exciton formation in the crystalline lattice under the influence of the quanta of light may be presented by the diagram plotted in Fig. 6-*a*. In Fig. 6-*b* is plotted the diagram of a hydrogen atom, whose scale is decreased by R/R' times in order to compare it with the energetic scheme of the exciton. The comparison of the two diagrams demonstrates the difference between the scheme of the exciton formation from the main level in the crystal:

$$\nu_n = \nu_\infty - \frac{R'}{n^2}\,, \qquad n = 1, 2, 3, \ldots,$$

and the scheme of the excitation of the hydrogen atom from the main (normal) state of the hydrogen atom:

$$\nu_n = R\left(\frac{1}{1^2} - \frac{1}{n^2}\right); \qquad n = 2, 3, \ldots .$$

Contrary to the hydrogen atom, to generate an exciton it is necessary to spend the energy ν_1, i.e. the energy of the exciton formation in the state $n = 1$ (+). The theory does not give this value, but ν_1 can be experimentally determined from the exciton spectrum in the same way, as the

---

(*) The results of these researches were reported on 19 September 1951 at the Institute of Technical Physics of the Academy of Sciences of the USSR (Leningrad) and on 12 December 1951 at the Institute of Physics of the Academy of Sciences of the Ukr. SSR (Kiev).

(+) If the number of excitons having the quantum number $n = 1$ were sufficiently large, the series of transitions of the exciton from the state $n = 1$ into the excited states with quantum numbers $n = 2, 3, 4, \ldots$, could have been observed. This series of lines, similar to the Lyman series of the hydrogen atom, should lie in the infra-red. It is possible, that in certain crystals with a very narrow forbidden zone, the concentration of excitons generated thermically might be sufficiently high to observe this « infra-red series » of the exciton.

value ν_∞ of the exciton photodissociation. For the cuprous oxide $\nu_1 = 2.023$ eV, $\nu_\infty = 2.164$ eV. The frequency of the first member of the exciton series defines the lowest energy of the exciton formation. The exciton may be formed in the excited states, and higher energies are required for this purpose (Fig. 6-*a*).

It is evident from the comparison of the exciton spectrum with that of the hydrogen atom by the differences: $\Delta\nu_n = \nu_\infty - \nu_n$, given in the last column of Table I, that considerable deviations from the hydrogen-likeness take place in the first member of the exciton series, $n = 1$. Hence, the Coulombian law of interaction between the electron and the hole in the crystal considered as a dielectric medium, introduced by MOTT [18]:

$$\nu = -\frac{e^2}{r \cdot n_0^2},$$

is not verified for the small exciton orbits. The corresponding levels of energy lie deeper than the hydrogen ones, as it is evident from Fig. 6.

The first member of the exciton series in Cu_2O stands out not only thanks to its position but also thanks to its exceptional narrowness, sharpness and exceedingly low intensity, if compared to the other members of the series. In order to ensure good observation, it is necessary to take thick plates of Cu_2O. Fig. 4-*a* and *b* give the spectrograms obtained with plates of Cu_2O 0.5 and 1.7 mm thick. The first member of the series, $n = 1$, is quite clearly seen in this case. One may also see here the « step » and the emission lines on its edges, of which we spoke above. Fig. 4-*c* gives the spectrogram of the first line of the series next to the comparison spectrum of iron, wherefrom it is seen that the width of the first member of the series is comparable with the width of the Fe atomic lines. The very weak absorption of the first line of the series and its small width show that the transition from the main level of the Cu_2O crystal to the first level of the exciton $n = 1$ takes place with a very low probability and is forbidden by the selection rules. The strong absorption in other lines of the exciton series shows that in the cuprous oxide there is higher probability of formation of excitons in the excited states.

According to FRENKEL [4] there can be two main types of excitons in the crystal. He called them « free » and « trapped ». These two types of excitons were recently considered by DAVYDOV [30] for the case of molecular crystals (« free » and « localized » excitons) and by DYKMAN and PEKAR [31] and DYKMAN [32] for the ion crystals (« non-polarizing » and « polarizing » excitons).

The very small width not only of the first, but of the other lines of the exciton yellow series in the Cu_2O crystal, leads to the conclusion that the exciton quickly migrates around the Cu_2O crystal, i.e. is a free, nonpolarizing exciton.

5. – Green Series of Excitons in Cu_2O Crystals at $T = 77.3$ °K (Liquid Nitrogen).

For the forthcoming study of the discovered phenomena, it was interesting to advance into the region of continuous absorption of Cu_2O behind the limit of the yellow series of the exciton. The study of this region presents great difficulties because of the very high absorption coefficient. Still, at a very large exposition, already in our first experiments, we found [12] a heterogeneity in the continuous spectrum of the Cu_2O absorption behind the limit of the yellow series of the exciton. The strong continuous absorption, beginning just behind the line series, gradually decreases with the advance into the short-wave region and reaches a certain wide minimum located (at $T = 77.3$ °K) approximately near $\lambda = 5500$ Å (2.25 eV). This pointed out to a certain heterogeneous structure of the conduction band in the Cu_2O crystal. Therefore, we undertook together with B. P. ZAHARČENJA [33], a new study of that phenomenon with thin plates. Careful polishing made the Cu_2O plates about 20 μ thick.

In the absorption spectrum of the Cu_2O thin plates, at the temperature of the liquid nitrogen ($T = 77.3$ °K), after the minimum of absorption on the short-wave side of the yellow series a new « green » series of narrow lines appears. These lines converge to the short-wave side to the limit after which the continuous absorption is observed [33]. We have succeeded in the observation of the 4 lines of the second series on a spectrogram. The absorption of light in the lines of the green series is much stronger than in the lines of the yellow one, and they are wider. The measurements have proved that the frequencies ν_n of these four lines also well correspond to the serial regularity of the hydrogen-like atom:

$$\nu_n = \nu_\infty - \frac{B}{n^2} = \left(18\,507 - \frac{1\,246}{n^2}\right) \text{cm}^{-1}; \qquad n = 2, 3, 4, 5, \ldots . \tag{2}$$

At the liquid nitrogen temperature we could neither visually, nor spectrographically observe the line which might have been interpreted as the first member $n = 1$ of the green series.

Fig. 7 (a, b) gives a part of the spectrum, where one may see both series (a), the green series being magnified (b).

Table II gives the frequencies ν_n of the lines of the green series, as well as the differences $\Delta\nu_n$ between the frequencies ν_∞ of the series limit and those ν_n of the lines observed:

$$\Delta\nu_n = \nu_\infty - \nu_n = (18\,507 - \nu_n) \text{ cm}^{-1} .$$

TABLE II. – *Position of the lines of the exciton green series in the* Cu_2O *absorption spectrum at* $T = 77.3\,^{\circ}K$.

Quantum number n	Wavelengths λ_n in Å	Energy in eV	Frequencies ν_n in cm^{-1}	$\Delta\nu_n$ in cm^{-1}	
				observed	calculated
1	—	—	—	—	1246
2	5496	2.255	18195	312	311
3	5444	2.277	18369	138	138
4	5426	2.284	18429	78	77
5	5419	2.287	18454	53	50
⋮	⋮	⋮	...	0	⋮
∞	5404	2.294	18507	⋮	0

The experimental values of the differences $\Delta\nu_n$ are confronted in Table II with the values $\Delta\nu_n$, calculated from the relations (2)

$$\Delta\nu_n = \frac{B}{n^2} = \frac{1246}{n^2}\ cm^{-1}; \qquad n = 2, 3, 4, 5.$$

As it follows from Table II, also the frequencies of the second series satisfy very well the serial regularity of the hydrogen-like atom.

We assume that the second hydrogen-like series in the cuprous oxide, as the first series, is caused by excitons in the crystal lattice of Cu_2O.

One of the possible explanations of the appearance of the two series in the absorption spectrum may be the assumption of the existence of the two overlapping free bands in the Cu_2O crystal, as it is shown in Fig. 8. Each series converges to its conduction band.

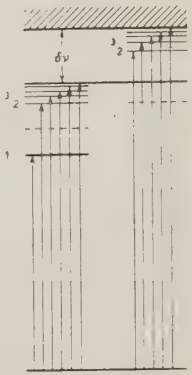

Fig. 8. – Alternative diagram of excitation of the yellow and green series in Cu_2O.

One should pay attention to the fact that the difference in frequencies of the limits of the yellow and green exciton series, $\delta\nu = 0.131$ eV, within the limits of measurement errors, coincides with the energy of one of the infra-red absorption bands in Cu_2O [10], which is of 0.138 eV.

The green series in the cuprous oxide was also observed by the Japanese physicists HAYASHI and KATSUKI [28] who also ascribe it to the exciton, while they relate the yellow (first) series in Cu_2O, to the polaron (self-trapped electron). This seems to us to be wrong for the following considerations:

1) The polaron dissociation energy is of the order of 0,1 eV [34], and therefore the absorption spectrum of the polaron

should be located in the infra-red region, but not in the visible one, as the yellow series in Cu_2O, the excitation energy of which is of the order of 2 eV.

2) By its polarization nature, the polaron is tightly bound to the lattice vibrations, and therefore the optical spectrum of its excitation must consist mainly of one wide band, as it is in case of F-centres [34, 35], but not of a series of several very narrow lines, as in the case of the yellow series.

3) The temperature going down, the absorption of light caused by polarons should sharply decrease, as the polaron concentration in the crystal decreases according to an exponential law [34]. Nothing of the sort can be observed in the Cu_2O yellow series.

6. – The Exciton Spectrum in Cu_2O at $T = 4.2$ °K (Liquid Helium). New Lines.

The following phenomenon was observed [36] with a prism spectrograph having a dispersion of 7 Å/mm near $\lambda = 5800$ Å, when the Cu_2O crystal is cooled down to the temperature of the liquid helium ($T = 4.2$ °K). The lines of the yellow series as well as of the green one became much narrower than at the liquid nitrogen temperature, and both series shifted ever more to the shortwave part of the spectrum.

One more step was found [36], where the continuous absorption undergoes a leap. That step is located at $\lambda = 5841$ Å (2.1219 eV). We found also another very weak line on this step at $\lambda = 5817$ Å (2.1306 eV). We assume that this line is the first member ($n = 1$) of the exciton green series.

Table III gives the wavelength of the absorption lines of the yellow and green exciton series in Cu_2O at $T = 4.2$ °K.

TABLE III. – *Position of the lines of the exciton yellow and green series in* Cu_2O *at* $T = 4.2$ °K.

Quantum number n	Yellow series			Green series		
	Wavelengths λ_n in Å	Energy in eV	Frequencies ν_n in cm^{-1}	Wavelengths λ_n in Å	Energy in eV	Frequencies ν_n in cm^{-1}
1	6095.8	2.0332	16404.7	5817	2.131	17191
2	5770.8	2.1477	17328.6	5469	2.266	18285
3	5735.0	2.1611	17436.8	5419	2.287	18454
4	5722.8	2.1657	17473.9	5402	2.294	18512
5	5716.8	2.1618	17492.3	5394	2.298	18539
6	5713.1	2.1694	17503.6	⋮	⋮	⋮
⋮	⋮	⋮	⋮	⋮	⋮	⋮
∞	5706.6	2.1719	17523.3	5380	2.303	18587

The frequencies of the lines of the yellow as well as of the green series at $T = 4.2$ °K (with the exception of the first members) satisfy the hydrogen-like serial relation

$$\text{for the yellow series: } \nu_n = \left(17\,523.3 - \frac{780.7}{n^2}\right) \text{cm}^{-1}, \quad n = 1, 2, 3, \ldots,$$

$$\text{for the green series: } \nu_n = \left(18\,587 - \frac{1\,200}{n^2}\right) \text{cm}^{-1}, \quad n = 1, 2, 3, \ldots.$$

At the liquid helium temperature in the absorption spectrum of the Cu_2O crystal, we discovered [36] 7 new weak thin lines of absorption, located between the lines of the yellow exciton series, as it is shown in Fig. 9. The frequencies of these new lines are given in Table IV.

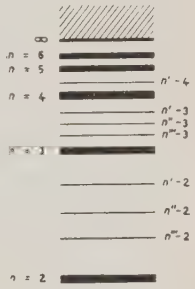

Fig. 9. – Diagram of the disposition of the weak absorption lines between the exciton yellow series members at $T = 4.2$ °K.

TABLE IV – *Position of the new weak lines in the* Cu_2O *exciton spectrum at* $T = 4.2$ °K *and* $T = 1.3$ °K.

Designation	$T = 4.2$°K		$T = 1.3$°K	
	Wavelengths in Å	Frequencies in cm^{-1}	Wavelengths in Å	Frequencies in cm^{-1}
$n''' - 2$	5758.7	17 365.0	5758.8	17 367.1
$n'' - 2$	5753.2	17 381.6	5752.5	17 383.7
$n' - 2$	5746.3	17 402.5	5745.1	17 406.1
$n''' - 3$	5731.8	17 446.5	5731.8	17 446.5
$n'' - 3$	5729.0	17 455.0	5729.5	17 453.5
			5728.0	17 458.1
			5727.3	17 460.2
$n' - 3$	5726.5	17 462.7	5726.5	17 462.7
			5726.0	17 464.2
			5725.4	17 466.0
$n' - 4$	5719.8	17 483.1	5719.3	17 484.7
			5718.1	17 488.3
			5714.7	17 498.7
			5713.9	17 501.2

Fig. 10 gives the photographs of the yellow series members, and the weaker lines, observed at $T = 4.2$ °K, are seen among them. The new lines possess different absorption coefficients and therefore cannot be revealed with

sufficient clearness simultaneously in the same spectrogram. Therefore, Fig. 10 gives three spectrograms (*a*, *b*, and *c*) which are taken with different exposures: 20 min, 5 min and 5 s, in order to reveal the new lines. These new lines are marked with pointers in Fig. 10.

7. – The Exciton Spectrum in Cu_2O at $T = 1.3$ °K (Liquid Helium).

Further study of the absorption spectrum of the Cu_2O was undertaken with a spectrograph having a diffraction grating with a dispersion of about 4 Å/mm. Besides that, the Cu_2O crystal was cooled down to the ever lower temperatures which may be attained by the evaporation of the liquid helium at low pressure.

At $T = 1.3$ °K, when the exciton spectral lines become ever narrower, it was possible to observe [37] that certain lines of the exciton yellow series, beginning with the second, showed a fine structure.

At $T = 1.3$ °K, due to the narrowing of lines and to the very strong weakening of the continuous background, we could observe distinctly [37] the highest members of the exciton yellow series near the series limit, the 9-th member of the series included (*).

Fig. 11 gives the spectrogram of the yellow exciton series at $T = 1.3$ °K. The spectrogram of the same series at $T = 77.3$ °K taken from the same Cu_2O plate 160 μm thick, is compared to it. It is seen from these spectrograms what a strong weakening (in the transition from $T = 77.3$ °K to $T = 1.3$ °K) characterizes the continuous spectrum laying upon the series, and what a narrowing the series lines undergo at $T = 1.3$ °K.

Table V (second column) gives the frequencies of the lines of the exciton yellow series we observed at $T = 1.3$ °K. The measurements concern the middle parts of the lines, their fine structure being not taken into account.

The narrowing of the absorption lines at $T = 1.3$ °K makes it possible to measure the frequencies of the lines of the yellow series, and, particularly, its highest members $n = 7$ and $n = 8$, with relatively greater accuracy. One may use the measurements of these lines of the series, for which the hydro-

(*) Attention should be paid to the size of the exciton orbits which should correspond to the highest members of the series ($n \simeq 10$) observed in the experiment at $T = 1.3°$ K. For such high quantum numbers, the radii of the exciton orbits in the crystal are enormous. Assuming $\mu_1 = \mu_2 = m$, we obtain for the radii of the orbits of the electron and hole in the exciton:

$$r_{n\ \mathrm{exciton}} = 2 r_{1H} \cdot n^2 \cdot n_0^2 \cong n^2 \cdot n_0^2 \text{ Å}$$

r_{1H} is the first orbit radius in the hydrogen atom, n_0 is the refractive index of the crystal. Assuming $n_0 = 2.5$ and $n = 10$, we obtain $r_{10\ \mathrm{exciton}} \cong 600$ Å.

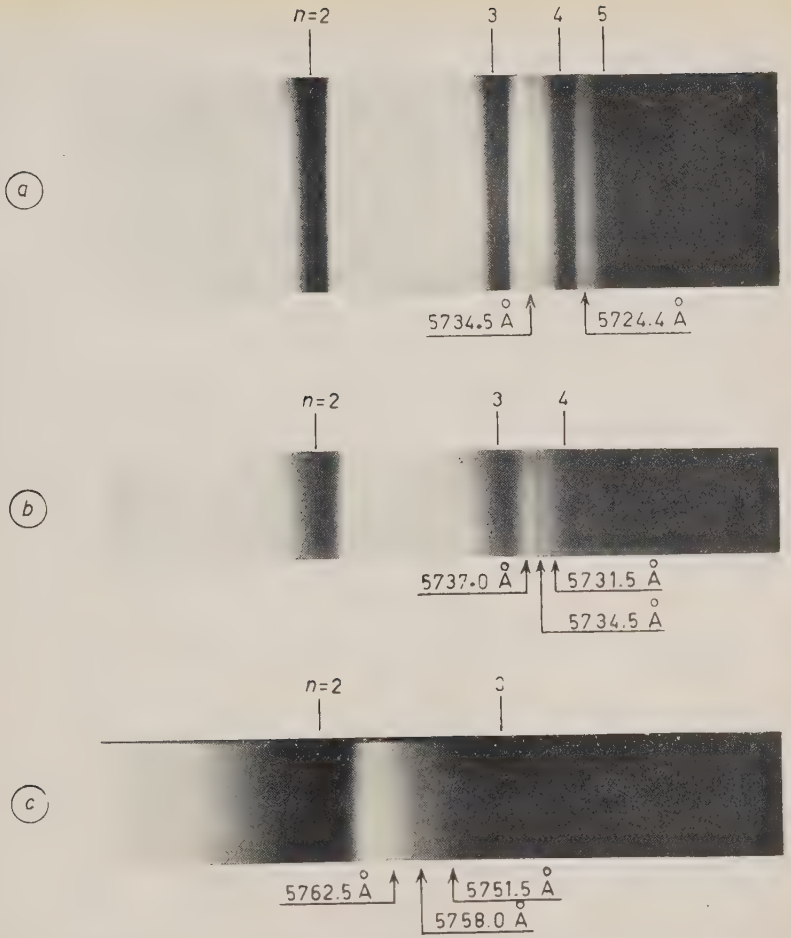

Fig. 10. - Spectrograms of the exciton yellow series members at $T = 4.2$ °K, with weak lines between them, obtained with the following exposures: (*a*) 20 min; (*b*) 5 min; (*c*) 5 s.

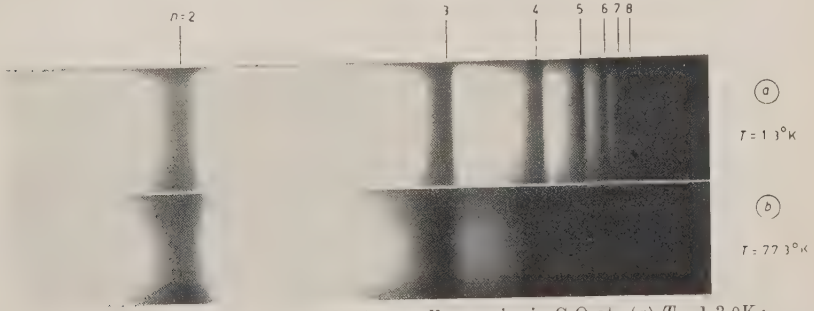

Fig. 11. – Spectrograms of the exciton yellow series in C_2O at: (*a*) $T = 1.3$ °K; (*b*) $T = 77.3$ °K.

TABLE V. – *Position of the members of the* Cu_2O *exciton yellow series at* $T = 1.3$ °K.

Quantum numbers n	Observed values of frequencies ν_n in cm^{-1}	Calculated values of frequencies ν_n in cm^{-1}	$\Delta\nu$ in cm^{-1}
1	16406.8	16814.0	407.2
2	17331.3	17346.9	15.6
3	17438.3	17445.6	7.3
4	17477.3	17480.1	2.8
5	17949.4	17496.1	1.7
6	17504.5	17504.8	0.3
7	17510.0	17510.0	0
8	17513.4	17513.4	0
9	17515.8	17515.8	0
⋮	⋮	⋮	⋮
∞	—	17524.5	—

gen-likeness can be well observed, to calculate (*) the constants ν_∞ and B of the serial relation of the yellow series frequencies. We obtain:

$$\nu_n = \left(17524.5 - \frac{710.5}{n^2}\right) \text{cm}^{-1}, \qquad n = 1, 2, 3, \ldots .$$

The values of the frequencies of the yellow series, calculated by this formula, are given in Table V, column 3. The differences between the observed and the calculated values of frequencies demonstrate deviations from the hydrogen-likeness of the yellow series members. Table V shows that this discrepancy takes place not only in the first member of the series $n = 1$, but also in the other serial lines $n = 2, 3, 4, 5$, and the value of these deviations decreases with the increase of the quantum numbers. Thus, the smaller the exciton orbits are, the greater deviation from the hydrogen-likeness is observed. This may be explained, on one hand, by the fact that one may neglect the crystal microstructure and consider it macroscopically, as a medium with a certain dielectric constant, only in case of large exciton orbits. On the other hand, the deviations for small orbits might be explained by the fact that the hole in the crystal is not a point charge.

At $T = 1.3$ °K, we found [37], between the serial members $n = 4$ and $n = 5$ and between $n = 5$ and $n = 6$, new lines besides the lines we observed [36] at $T = 4.2$ °K.

Besides that, some of the previously observed weak lines between the members of the yellow series splitted at $T = 1.3$ °K into several very narrow thin lines, due to the narrowing of the lines.

(*) These calculations were performed by B. P. ZAHARČENJA.

All lines observed at $T = 4.2$ °K and $T = 1.3$ °K, located between the members of the exciton yellow series, are compared in Table IV (*).

According to our study of the Stark effect of the exciton yellow series [38, 39] (see § 8 below), the lines observed between the members of the exciton series at the liquid helium temperature (Table IV) appear under the influence of the external electric field at the liquid nitrogen temperature and increase in intensity with increasing field. Therefore, they can be ascribed to the forbidden electronic transitions appearing under the influence of the external electric field.

Now it is yet difficult to formulate a conception on the energetic levels, between which these forbidden transitions take place. Probably, the existence of these levels is connected with the incomplete hydrogen-likeness of the exciton energetic scheme.

Deviations from the hydrogen-likeness in the exciton structure should lead to the elimination of degeneration in relation to the quantum number l (determining the orbital angular momentum) and to the appearance of new levels in the exciton energetic scheme. The appearance of new forbidden lines in the exciton spectrum between the members of the yellow series should be then related to the violation of the selection rules: $\Delta l = \pm 1$.

8. – Stark Effect in the Lines of the Exciton Spectrum.

a) *Homogeneous electric field.* – It is a fact well-known, that the splitting of the lines of atomic spectra in magnetic and electric fields is of great aid in the analysis of complex spectra. Therefore, we have undertaken the study of the influence of the external electric and magnetic fields on the exciton series lines in the cuprous oxide. These experiments, interesting in themselves, might give us the opportunity, as we expected, of studying more comprehensively the complicated spectrum of Cu_2O and help us in the interpretation of the new lines we discovered at the liquid helium temperature.

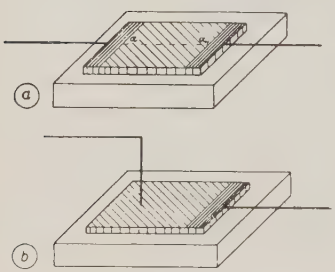

Fig. 12. – Scheme of electrodes for the study of Stark effect in Cu_2O crystal: (*a*) linear electrodes for the formation of a « homogeneous » electric field; (*b*) point by which the inhomogeneous field is obtained.

We might expect a great Stark effect in the exciton spectrum, due to its hydrogen-likeness and to large orbits of the exciton's electron and hole.

(*) In the region of the first serial member $n=1$ at the temperature of liquid helium, we have noticed a weak hazy line at $\lambda = 6039$ Å (2.0523 eV).

Placing the Cu_2O crystal in the electric field, we found [38] new phenomena leading to great changes in the exciton spectrum.

At the first stage of our experiments we examined the exciton yellow series at $T = 77.3$ °K. We used for the study of the Stark effect two sources of electric field, of 20 and 70 kV, which were applied to the Cu_2O plates by the electrodes shown in Fig. 12-*a*. The study of the behaviour of the exciton absorption lines in the electric field was performed by means of a prism spectrograph with a dispersion of 7 Å/mm in the yellow region of the spectrum (*).

In the Cu_2O plates used in these experiments, we succeeded [38] in following the influence of the electric field on 5 members of the exciton yellow series ($n = 1, 2, 3, 4, 5$). As it might be expected according to the theory of the Stark effect, the highest members of the series, with quantum numbers $n = 5$, 4 and 3, turned to be mostly affected. The electric field influence is found, at first, only on the $n = 5$ line and becomes noticeable already at comparably weak fields (approximately 5 kV/cm) (+).

With the increase of the electric field, the $n = 5$ line first widens and then, approximately at 6 kV/cm, a triplet appearing at its place becomes noticeable. The field being stronger, the widening of the $n = 4$ line becomes visible, and a new line appears between $n = 4$ and $n = 5$, which is the line $n' - 4$ observed between these members of the exciton series at the liquid helium temperature [36] (Table IV). Then the field being increased up to approximately 8 kV/cm, two components replace the $n = 4$ line, thus forming a triplet together with the line $n' - 4$, the intensity of which has increased with increasing field. The distance between the triplet components increases with the increase of the applied field.

The field being increased within the interval $8 \div 10$ kV/cm, 3 more lines appear between $n = 3$ and $n = 4$, corresponding to the lines $n' - 3$, $n'' - 3$, and $n''' - 3$, which we also found at the temperature of the liquid helium (Table IV). Further increase of the electric field leads to great changes in the exciton spectrum. The lines $n'' - 3$ and $n''' - 3$ increase in intensity: when the field is strengthened, they widen and move together from the line $n = 3$ of the exciton series to the violet part of the spectrum. The series member $n = 3$, on the contrary, shifts to the red part of the spectrum with the increase of the field and, widening, it merges in the wide band which appears on the long-wave side of the line $n = 3$ and increases in intensity with increasing field;

(*) A. A. Kalinjak and L. G. Fedorovič, in *Dokl. Akad. Nauk SSSR*, **96**, 1137 (1954), studied the influence of the electric field on the exciton spectrum.

(+) We could judge on the average value of the electric field only by the applied potential and by the distance between the electrodes.

by its position in the spectrum, this band corresponds to the lines $n'-2$ and n^*-2 observed at the liquid helium temperature (Table IV).

Simultaneously with this band, a clear and wide line corresponding to the $n''-2$ line observed in the liquid helium appears between $n=3$ and $n=2$, with the increase of the field (Table IV) (*).

We have observed only a small widening and a certain weakening in the intensity of the serial member $n=2$ under the influence of an electric field of the order of $20 \div 25$ kV/cm. Even at maximum fields of about 50 kV/cm used in our experiments, we could not notice any changes in the first serial member $n=1$, despite of its exceeding narrowness.

We discovered a very interesting phenomenon, simultaneously with the above-mentioned alterations in the exciton spectrum in case of a gradually increasing electric field. When the electric field increases, the highest members of the exciton series, together with their components, widen and, together with their satellites (new lines), weaken in intensity and gradually disappear: first, the line $n=5$; then, at a higher field, $n=4$; and at last, at an even stronger field, $n=3$. Simultaneously, the continuous spectrum advances from the limit of the series to the place previously occupied by the series members, which had gradually disappeared together with their components under the influence of the field (+). We succeeded in observing the fact, that at sufficiently strong fields, only the two first members $n=1$ and $n=2$ remained practically out of the whole exciton series (×).

The phenomenon of the disappearing of the highest members of the exciton series under the influence of the electric field is caused, in our opinion, by the extraction of an electron from the exciton levels by the field, i.e. by the ionization (dissociation) of the exciton by the electric field.

This effect in the exciton is analogous to the phenomenon of the ionization of the hydrogen atom in a strong electric field, forecast first by Oppenheimer [40] and found in the hydrogen atom by Rausch von Traubenberg [41]. The theory of this phenomenon for the hydrogen atom was developed by Lanc-

---

(*) Although the wavelengths of all the new lines in the liquid nitrogen and in the helium differ, due to the difference of temperatures, their location in relation to the serial members in both cases is identical, which leaves no doubts as to their identity.

(+) The same phenomenon was observed in the green exicton series as well.

(×) The disappearing of the highest members of the exciton series, in case of the electric field increase, might be apparently interpreted as the result of the Cu_2O heating by the electric current, increasing with the increase of the field. But this is not correct. Specially designed experiments have proved that the disappearing of the highest series members up to $n=3$ included, in case of the crystal heating, is connected with a very strong shift of the whole series of lines, the first members $n=1$ and $n=2$ among them, to the red part of the spectrum, which is not observed in the electric field.

zos [42]. The probability of the exciton destruction by the electric field was examined by Seitz [43]. According to the experiments of Rausch von Traubenberg, a field of the order of 10^6 V/cm is necessary to observe the ionization of the hydrogen atom by the electric field. The value of the critical electric field for exciton ionization, as our experiments prove, decreases down to the value of the order of 10^4 V/cm, because of the big electron orbits, of the hole in the exciton and of the influence of the dielectric constant of the crystal.

The alterations we observed in the exciton spectrum, under the influence of the increasing electric field, are schematically shown in Fig. 13. Fig. 14 gives the spectrogram of the Stark effect in the Cu_2O crystal exciton spectrum, where one may see the widening and the separate components of the exciton series members, the appearance of new lines and the gradual disappearing of the highest members of the exciton series, with the increase of the field.

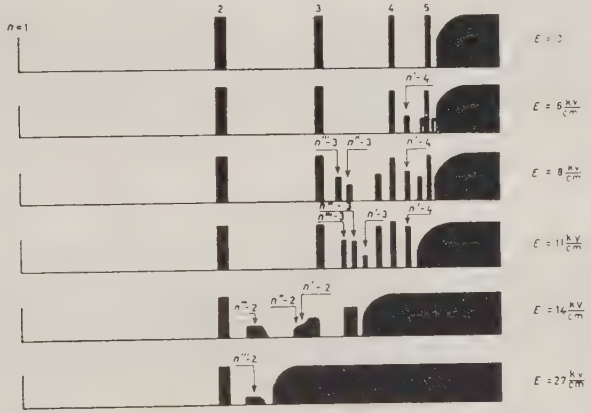

Fig. 13. – Diagram of changes which take place in the spectrum of the exciton yellow series in Cu_2O crystal, under the influence of the increasing external electric field at $T = 77.3$ °K.

As it has been already mentioned above, we consider the new lines as the « forbidden » ones, resulting from the appearance, due to the influence of the electric field, of the transitions between the exciton levels in the Cu_2O crystal forbidden by the selection rules.

We have also investigated the state of polarization of the exciton lines in the electric field. The experiments have proved that one may observe in the exciton spectrum under the action of the electric field, as usually in the Stark effect, the components polarized in the direction parallel to the field (π components) as well as those polarized in the direction perpendicular to the field (σ components). So, the line $n''' - 3$ is polarized parallel to the field,

while the line $n''-3$ is perpendicular to it. The π and σ components are also observed in the serial member $n = 4$.

The quantitative determinations of the values of the shifts of excitons spectral lines in the electric fields are difficult, because the determination of the field strength in the crystal is affected by grave errors. Having taken Cu_2O plates, in which the electric field was comparably homogeneous (*), and the Stark splitting uniform along the whole length of the Cu_2O plate, projected upon the spectrograph slit, we have performed the quantitative measurements of the shift of the exciton lines, depending on the average strength of the electric field E, determined from the potentials and from the distance between the electrodes (Table VI). The data of the table may give an idea of the values of the shift of the exciton lines in the electric field, but not of the laws (linear or quadratic) to which the shift of lines in the field obeys.

TABLE VI. – *Shift of the exciton lines of* Cu_2O *in the electric field.*

$n = 3$		$n''' = 3$		$n = 4$		$n' = 4$	
E in kV/cm	$\Delta\lambda$ in Å	E in kV/cm	$\Delta\lambda$ in Å	E in kV/cm	$\Delta\lambda$ in Å	E in kV/cm	$\Delta\lambda$ in Å
10	+ 0.4	9	0	7	+ 1.0	7	0
14	+ 1.2	12	— 0.7	12	+ 1.8	10	— 0.5
18	+ 2.1	14	— 1.1	13	+ 2.0	12	— 0.9

The results of the above-mentioned experiments show that the Stark effect on the exciton lines in the Cu_2O crystal greatly differs from that in the atom of hydrogen. This indicates the deficiency of a hydrogen-like Mott's model of the exciton.

b) *Inhomogeneous electric field.* – In order to study more thoroughly the observed phenomena, it is easier to follow the behaviour of the exciton lines in a gradually increasing electric field; with the aim of attaining stronger fields, we have undertaken the study of the Stark phenomenon in an inhomogeneous electric field [39].

As it is known, the observation of the Stark effect on atomic spectra in inhomogeneous fields is performed by the LO SURDO [44] method near the cathode of the discharge tube, where there is a strong decrease of the potential difference and high gradients of the electric field. We have used a point for the formation of strong inhomogeneous electric fields with high gradients in the

(*) As far as it can be attained in the Cu_2O crystals with the electrodes shown in Fig. 12-*a*.

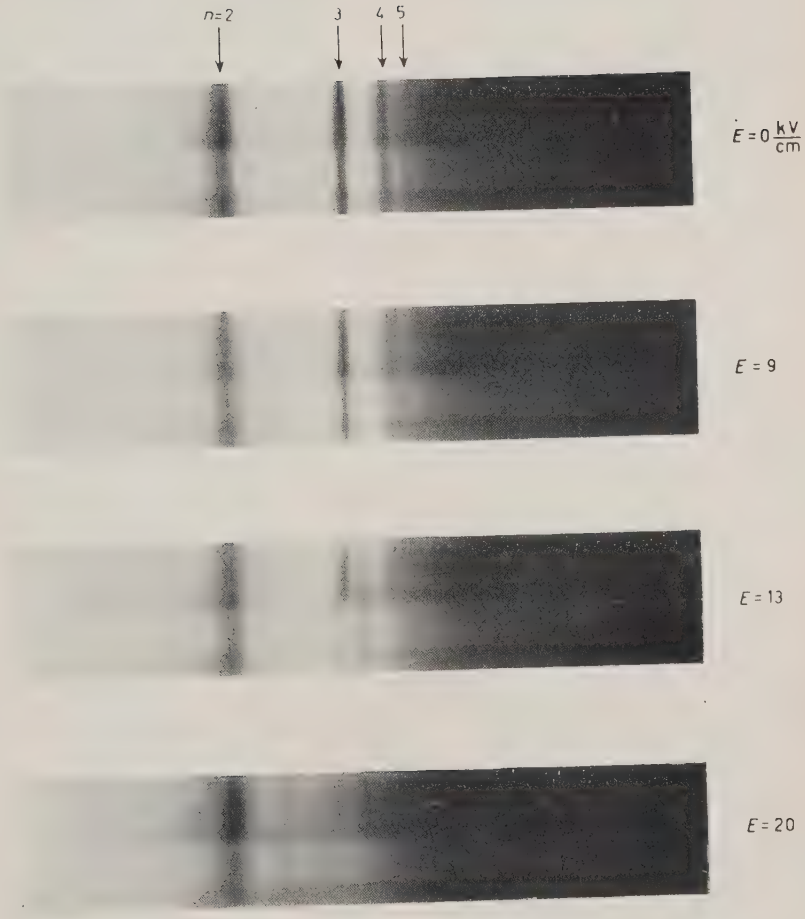

Fig. 14. – Spectrograms of the Stark effect in a « homogeneous » electric field E on the lines of the exciton yellow series in the Cu_2O crystal at $T = 77.3$ °K, with various values of E.

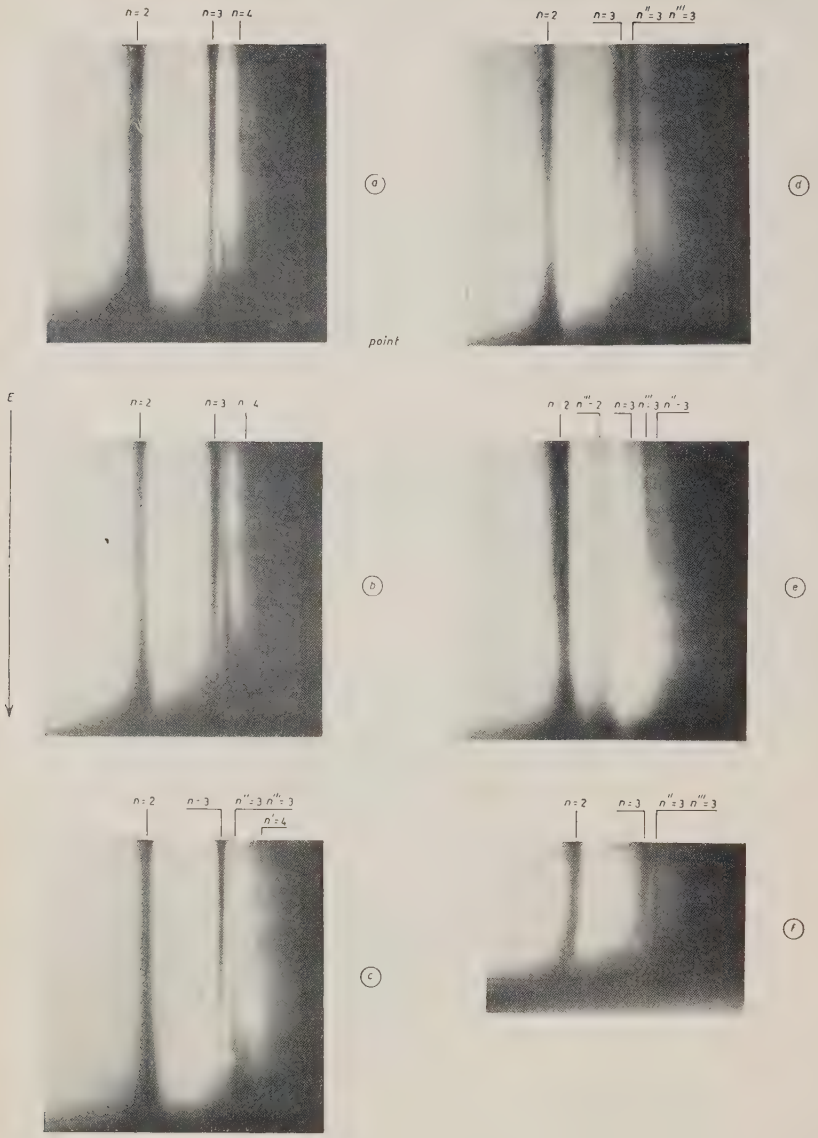

Fig. 15. – Spectrograms of the Stark effect in an inhomogeneous electric field E on the lines of the exciton yellow series in the Cu_2O crystal at $T=77.3$ °K: (*a*) with point electrode and difference of potential 8 kV/cm; (*b*), (*c*), (*d*), (*e*) and (*f*), with linear electrodes, the difference of potential being correspondingly: 10, 12, 15, 20 and 25 kV/cm.

cuprous oxide crystal. One of the electrodes, through which the electric field was applied to the Cu_2O plate, was linear and sufficiently long, the other one was the point. The scheme of the electrodes is given in Fig. 12-*b*. With such a disposition of electrodes, the decrease of the potential should have been concentrated near the point, where the field should have been strong and inhomogeneous.

Forcing the light through the Cu_2O crystal near the point, and projecting the point on the spectrograph slit, we observed the absorption spectrum of the exciton in the range of the strong electric field near the point. Using this method, we could observe [39] in the exciton spectrum a characteristic picture of the splitting of lines in the electric field, which is analogous to that observed in atomic spectra by the Lo Surdo method. Fig. 15-*a* gives the photograph of the Cu_2O exciton spectrum in the inhomogeneous electric field, obtained by means of the point, with a difference of potential between the electrodes of about 8 kV/cm.

In some particular cases, we could observe a clearer picture of the Stark effect in the inhomogeneous field. Studying the Stark phenomenon in various specimens of Cu_2O with the electrodes of Fig. 12-*a* (without the point), we found on the spectrogram that the splitting of the exciton lines in various specimens is different along the line aa_1, projected on the slit of the spectrograph. This pointed out to an inhomogeneity of the electric field in some Cu_2O plates along the lines aa_1, connected with certain peculiarities in the structure of the plates, or with defects in the electrodes contacts.

In one of these Cu_2O plates, these properties were exceedingly clearly expressed, and the Stark phenomenon was very strong. Fig. 15-*b*, *c*, *e* and *f* show the spectrograms we obtained with this Cu_2O plate, the difference of potential being correspondently 10, 12, 15, 20 and 25 kV/cm.

Very strong electric fields, generated in the Cu_2O crystal by inhomogeneous electric fields, made it possible for us to state new facts escaping our observation in « homogeneous » electric fields. We have succeeded in discovering the electric field influence on the second and first members of the exciton series ($n = 2$ and $n = 1$). In strong fields the line $n = 2$ weakens in intensity, widens a little and shifts to the red side of the spectrum, as it is seen on Fig. 15-*f* by the bending of the end of the line $n = 2$ on the lower edge of the spectrogram.

Even in strong electric fields, we could observe neither the shift, nor the splitting of the first line $n = 1$ of the exciton series, despite of its exceeding narrowness. Only on the lower edge of the spectrum, corresponding to the region of the Cu_2O crystal near the point, where the field is most intensive, we have found a considerable increase in intensity of the line $n = 1$. In this respect the behaviour of the line $n = 1$ in the electric field is similar to that of the lines forbidden by the rules of selection.

The absence of splitting of the first serial line even in strong electric fields confirms its interpretation, as the first member 1*S* of the exciton series.

As it is evident from the spectrograms (Fig. 15), all the characteristic features of the Stark phenomenon appear more clearly in the exciton spectrum with inhomogeneous electric fields:

1) Appearance of components of the lines in the electric field and increase of distances between them, with the increase of the field.

2) Shift of the lines to the red and violet sides of the spectrum, with the increase of the field.

3) Widening of the lines with the field.

4) Appearance of new forbidden lines in the electric field, increase of their intensity and shift of them to the red or violet sides of the spectrum, with the increase of the field.

5) Gradual disappearing of the highest members of the exciton series with the increase of the field.

These phenomena are so characteristic and similar to the splitting of the lines of free atoms spectra in the electric field, that they leave no doubts as to the fact, that here the Stark effect takes place, though, according to our knowledge, this effect has never been observed up to now in crystal spectra in external electric fields.

9. – Zeeman Effect in the Lines of the Exciton Yellow Series.

The splitting of spectral lines of the free atoms does not depend on the radii of electron orbits (principal quantum members n). Therefore, one should expect that the Zeeman splitting of lines of the exciton, contrary to the Stark phenomenon, would be of the same order of magnitude, as the splitting of lines in the atomic spectra.

The experimental study of the Zeeman effect on the exciton lines was performed with a diffraction grating spectrograph having a dispersion of 4 Å/mm. The studies were performed with unpolarized light, as well as with polarized one, with the application of polarizing prisms permitting the passage of light with the electric vector directed perpendicularly or parallelly to the direction of the magnetic field. All these studies were performed at the liquid nitrogen temperature ($T = 77.3\,°\mathrm{K}$). Some experiments were performed at the liquid helium temperature (4.2 °K).

In these conditions, we observed the splitting of the first member $n = 1$ of the yellow exciton series in the magnetic field. We obtained a most clear picture of the Zeeman splitting, when studying the phenomenon with pola-

rized light. In case of such a position of the polarizing prism-analyser, that the light is polarized with the electric vector perpendicular to the magnetic field direction (σ components), the Zeeman splitting of the first member of the exciton yellow series gives a doublet, the components of which are symmetrically disposed in respect to the initial position of the line $n = 1$, when the magnetic field is zero. In case of another polarization (π components) we observed the absorption line located in the same place of the initial line, when the field is zero, but widened. Without the polarizing prism analyser the picture of splitting is not clear and, therefore, it is difficult to state wheather there is a triplet or a more complicated splitting, connected with the splitting of the π component. The above mentioned widening of the line of the π component also drives to the thought of an unresolved, more complicated structure of this line.

Fig. 16 gives the photographs of the Zeeman splitting of the first member of the exciton yellow series taken at the temperature $T = 4.2$ °K. Table VII gives the numeric values of the distances between the σ doublet components we obtained in magnetic fields of 26000 and 32000 oersteds. It follows from the data of Table VII, that the numeric values of the Zeeman splitting of the exciton are the same, as in free atoms. The splitting $\Delta\nu$, as it should be in the Zeeman effect, is proportional to the magnetic field H.

TABLE VII. – *Values of the Zeeman splitting of the first member of the* Cu_2O *exciton yellow series* (σ-*components*).

H in oersted	$\Delta\lambda$ in Å	$\Delta\nu$ in cm^{-1}	$(\Delta\nu/H)\cdot 10^6$
26000	0.9	2.4	92
32000	1.1	2.9	91

We could not observe the Zeeman splitting in other members of the exciton series because of their great width.

In the paper recently published by SAMOJLOVIČ and KORENBLIT [25], the authors have considered the magneto-optical properties of the exciton. Taking Mott's ideas for the exciton (quasipositronium model), the authors have computed a formula for the Zeeman splitting in the exciton spectrum for the case of strong fields, when the Paschen-Back effect takes place:

$$\Delta\nu = \frac{\Delta m}{M}\cdot\frac{eH}{2\mu c}\cdot\Delta m_l\,; \qquad \Delta m_l = 0,\ \pm 1\ldots, \tag{3}$$

where e is the electron charge, c is the velocity of light, H is the magnetic field intensity; $M = \mu_1 + \mu_2$, $\Delta m = \mu_1 - \mu_2$, $\mu = \mu_1\cdot\mu_2/M$, μ_1 and μ_2 are the effective masses of the electron and the hole.

The Zeeman splitting of the exciton lines on one hand, and the exciton optical spectrum without the magnetic field influence on the other, give us the possibility to determine separately the electron and hole effective masses only from spectroscopic data.

If we assume, that the observed Zeeman splitting $\Delta\nu$ of the first member of the exciton yellow series in Cu_2O is the splitting of a normal triplet, and that formula (3) can be applied to it, then, using for μ the data obtained from the exciton optical spectrum, one may calculate the effective electron and hole masses in the Cu_2O crystal. They have turned out to be: $\mu_1 = 0.54$ and $\mu_2 = 0.60$.

Thus, the spectroscopic determination of the effective electron and hole masses does not considerably deviate from the data obtained by means of other methods for the determination of these quantities.

10. – The Structure of the Edge of the Fundamental Absorption Band in Other Crystals.

The existence of the two hydrogen-like series in the Cu_2O absorption spectrum puts the natural question, whether such a structure of the edge is observed or not in the characteristic absorption spectra of other crystals.

The absorption spectra of the crystals near the long-wave edge of the characteristic absorption band with high dispersion and at low temperatures have been studied but little till now. There are available data only for a few crystals. So, in the spectrum of the cadmium sulfide, near the edge of the characteristic absorption band, at the liquid helium temperature (4.2 °K) a complicated structure was found, consisting of a group of 11 narrow lines and 4 narrow bands [45]. The frequencies of these lines and bands are confronted in Table VIII (brackets indicate the band edges) (*).

Fig. 17 gives the absorption spectrum of the CdS crystal (+).

The absorption spectrum of CdS is almost as complicated, as that of the cuprous oxide, and this fact points out to the great number of electron levels in the CdS crystal. The picture becomes still more complicated due to the fact, that the structure of the CdS absorption edge depends on the state of the polarization of the absorbed light.

We consider it natural to relate the structure of the edge of the fundamental absorption band in CdS to the formation of excitons in the lattice

(*) Only the line $\lambda = 4869$ Å and a wider band $\lambda = 4864 \div 4858$ Å are observed [12] near the edge of the absorption band in CdS at the liquid nitrogen temperature.

(+) The CdS crystal spectrogram given in Fig. 17 is composed of two photographs, taken at different exposures, in order to reveal simultaneously the lines and bands.

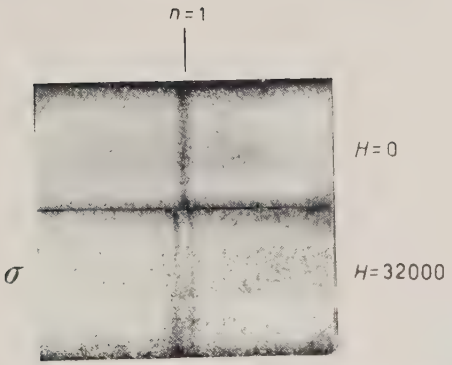

Fig. 16. – Spectrogram of the Zeeman splitting (σ components) of the first member of the exciton yellow series in the Cu_2O crystal at $T = 4.2$ °K in a magnetic field of 32 000 oersted.

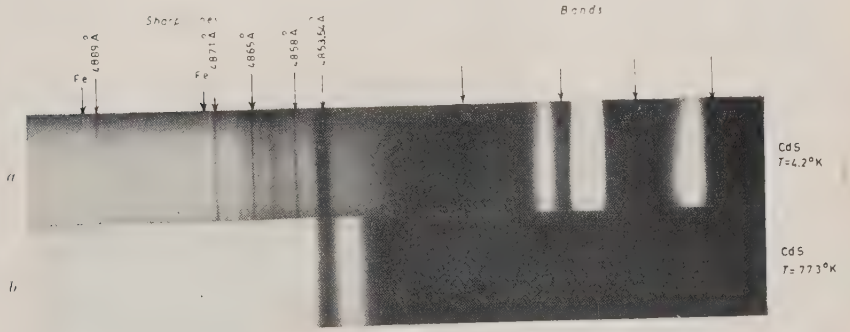

Fig. 17. – Spectrograms of the structure of the fundamental absorption edge in the CdS crystal: *a*, at $T = 4.2$ °K; *b*, at $T = 77.3$ °K.

of the cadmium sulfide. It is therefore necessary to suppose the existence of two types of excitons in the CdS lattice, which are polarized perpendicularly to each other according to the double refraction of light in the CdS crystal (dichroism of the exciton).

Then, the structure of the edge of the absorption band in the HgI_2 crystal was discovered (*).

TABLE VIII. – *Position of lines and bands near the edge of the fundamental absorption band in the* CdS *crystal spectrum.*

Wavelengths in Å	Frequencies in cm^{-1}	Energy in eV
4889.5	20452	2.5348
4870.8	20530	2.5448
4869.2	20537	2.5454
4868.2	20541	2.5459
4867.1	20546	2.5465
4866.2	20549	2.5469
4865.6	20552	2.5472
4864.9	20555	2.5476
4863.5	20561	2.5483
4861.8	20567	2.5492
4858.0	20585	2.5512
4854.2	20601	2.5532
4853.5	20603	2.5536
4836	20679	2.563
4820	20748	2.572
4817	20759	2.573
4815	20770	2.574
4809	20793	2.577
4800	20832	2.582
4793	20862	2.586
4791	20872	2.587

Interesting results were obtained with the PbI_2 crystal by NIKITIN and PERNY [47], who discovered at the liquid helium temperature ($T = 4.2$ °K) a group of four narrow lines near the absorption edge of this crystal.

We have obtained [48] data (at $T = 77.3$ °K) for several more crystals: MoO_3, Bi_2O_3, TiO_2, V_2O_5, As_2S_3, in which the structure of the edge of the absorption band is not observed at all, and the absorption curve at the edge undergoes a monotonous increase.

Attention should be paid to the fact, that the latter crystals have no (or

(*) In the works by NIKITIN, COUTURE, SIESKIND and PERNY [46] as well as in the experiments by B. P. ZAHARČENJA and the author of this article.

very weak) photoconductivity. On the contrary, in case of crystals, where we can observe the exciton structure of the absorption edge with narrow and intensive lines (Cu_2O, CdS, HgI_2, PbI_2), there is a very strong photoeffect, and its spectral curve possesses a maximum located at the absorption edge, where the exciton absorption lines are observed.

Hence, we may draw the conclusion, that, in order to generate a strong photoeffect, the existence of a structure at the fundamental absorption edge with sharp, strong and discrete absorption lines is probably necessary. This testifies to the relation between the exciton spectrum and the photoelectric phenomena: in the crystals, where the excitons may be formed by the light, a strong photoeffect can be generated.

The above described results, obtained for different crystals, do not yet give the ground to draw general conclusions. Nevertheless, they provide with the possibility to draw some conclusions.

The poor data, which are now at our disposal, show that we do not have the clear similarity among the exciton spectra of various crystals which we should have if the Mott model of the exciton should be correct. For instance, in the spectra of other crystals, we do not observe the well expressed hydrogen-like series of lines, as in Cu_2O crystals. In some cases, the spectra of these crystals consist only of two or three lines (at the liquid nitrogen temperature).

This can be explained by the fact, that strong internal electric fields in crystals might ionize (dissociate) excitons, as it is observed in Cu_2O, when it is influenced by a strong external field (Sect. 8 of this paper). The highest members of the series disappear from the exciton spectrum under the influence of the internal electric field, and only the first members with small quantum numbers remain.

Another explanation lies in the fact that, in some crystals, excitons may be polarizing, and then, according to the theory of Dykman and Pekar [31], the frequencies of the exciton spectrum should not satisfy the serial relation of the hydrogen-like atom. But it should be noted that in this case the exciton lines must be wide. Further on, it follows from the theory of Dykman and Pekar that in certain cases the lower states of the exciton may be non-polarizing, while the upper, excited states, should be polarizing. This will result in the fact that the first (long-wave) exciton lines will be narrow, while the next ones (short-wave) will be wide, and the hydrogen-likeness of the spectrum will not be preserved. As the wide lines of the upper states, overlapping each other, may coincide with the region of the continuous absorption band of the crystal, then only the first narrow exciton lines will be mostly observed in the experiments. The results of the Dykman and Pekar theory [31] are obtained from the consideration of the Mott exciton with account of the interaction of the electron and hole with the oscillations of ions.

From this interaction comes the polarizing exciton spectrum, as well as its deviations from the hydrogen-likeness. The non-polarizing exciton should be the hydrogen-like one.

We can hardly doubt of the fact that the excitons in the Cu_2O crystals are non-polarizing. But it was pointed out, during the analysis of the absorption spectrum of the Cu_2O crystal, that the deviations from the hydrogen-likeness are observed in the Cu_2O non-polarizing exciton spectrum as well. This is confirmed by the study of the Stark effect in the exciton spectrum of the Cu_2O crystal (Sect. **8** of this paper).

Basing upon the rather poor experimental material, which is now at our disposal, we think that the exciton should be considered as a system, which is rather similar to a more complicated atom, than to the atom of hydrogen. The hole in the crystal cannot be treated as point charge. The complicated exciton structure, and, consequently, the structure of the absorption edge as well, depends on the substance, on atoms and ions forming the crystal lattice, and is evidently connected with the structure of the crystal. Then the optical spectrum of the exciton may be more complicated and will be rather similar to the spectrum of a complicated atom (or ion), than to the simple spectrum of the hydrogen atom. The demonstration of this fact is clear in the cuprous oxide crystals and particularly in the spectra of the other examined crystals.

The conception of the exciton as a hydrogen-like system of the electron and point hole should be considered only as a first approximation, which gives the correct schematic conception of the most general characteristics of the phenomenon.

(Translated by L. Zolotarevskij).

REFERENCES

[1] A. V. Ioffe and A. F. Ioffe: *Žu. Éksper. Teor Fiz.*, **6**, 737 (1936).

[2] B. Gudden and R. Pohl: *Zeits. f. Phys.*, **17**, 331 (1923); **18**, 199 (1923).

[3] B. Gudden: *Lichtelektrische Erscheinungen* (Berlin, 1928).

[4] J. Frenkel: *Phys. Rev.*, **37**, 17, 1276 (1931); J. Frenkel: *Žu. Éksper. Teor. Fiz.*, **6**, 647 (1936); *Phys. Zeits. d. Sowjet.*, **9**, 158 (1936).

[5] V. P. Žuze and S. M. Ryvkin: *Žu. Éksper. Teor. Fiz.*, **20**, 152 (1950). Translated in: *Abhandlungen aus der sowjetischen Physik*, Folge II, p. 91 (Berlin, 1951).

[6] V. P. Žuze and S. M. Ryvkin: *Collection of articles published on the occasion of the 70-th birthday of the Academician A. F. Ioffe* (Moscow, 1950), p. 216; *Dokl. Akad. Nauk SSSR*, **76**, 241 (1951); *Izv. Akad. Nauk SSSR, Ser. Fiz.*, **76**, 93 (1952).

[7] L. Apker and E. Taft: *Phys. Rev.*, **79**, 964 (1950); **81**, 698 (1951); **82**, 814 (1951).

[8] M. Pigarev and S. Golub: *Phys. Zeits. d. Sowjet.*, **6**, 603 (1934).
[9] G. Mönch: *Zeits. f. Phys.*, **78**, 728 (1932).
[10] E. F. Gross and N. A. Karryev: *Dokl. Akad. Nauk SSSR*, **84**, 261 (1952).
[11] M. Hayashi and K. Katsuki: *J. Phys. Soc. Japan*, **5**, 381 (1950).
[12] E. F. Gross and N. A. Karryev: *Dokl. Akad. Nauk SSSR*, **84**, 471 (1952).
[13] I. V. Obreimov and A. F. Prihot'ko: *Phys. Zeits. d. Sowjet.*, **1**, 203 (1932); **9**, 34, 48 (1936); I. V. Obreimov, A. F. Prihot'ko and K. G. Šabaldas: *Žu. Éksper. Teor. Fiz.*, **6**, 1062 (1936); I. V. Obreimov and K. G. Šabaldas: *J. of Phys USSR*, **7**, 168 (1943).
[14] A. F. Prihot'ko: *J. of Phys. USSR*, **8**, 257 (1954); *Žu. Éksper. Teor. Fiz.*, **19**, 383 (1949); I. V. Obreimov, A. F. Prihot'ko and I. V. Rodnikova: *Žu. Éksper. Teor. Fiz.*, **18**, 409 (1948).
[15] E. V. Špol'skij and L. A. Klimova: *Izv. Akad. Nauk SSSR, Ser. Fiz.*, **18**, 673 (1954).
[16] P. H. Yuster and C. J. Delbecq: *J. Chem. Phys.*, **21**, 892 (1953); P. Pringsheim: *Zeits. f. Phys.* **136**, 573 (1954).
[17] G. H. Wannier: *Phys. Rev.*, **52**, 191 (1937).
[18] N. F. Mott: *Proc. Roy. Soc.*, A **167**, 384 (1938).
[19] J. Slater and W. Shockley: *Phys. Rev.*, **50**, 705 (1936).
[20] J. Franck and E. Teller: *J. Chem. Phys.*, **6**, 859 (1938).
[21] F. Seitz: *Trans. Faraday Soc.*, **35**, 74, (1939); *J. Chem. Phys.*, **6**, 150 (1938); *Modern Theory of Solids* (New York, 1940).
[22] F. Seitz: *Imperfections in Nearly Perfect Crystals* (New York, 1952), p. 25; *Rev. Mod. Phys.*, **23**, 328 (1951).
[23] W. R. Heller and A. Marcus: *Phys. Rev.*, **84**, 808(1951).
[24] A. I. Ansel'm and Iu. A. Firsov: *Žu. Éksper. Teor. Fiz.*, **28**, 151 (1955).
[25] A. G. Samojlovič and L. L. Korenblit: *Dokl. Akad. Nauk SSSR*, **100**, 43 (1955).
[26] A. G. Samojlovič and M. V. Kononova: *Dokl. Akad. Nauk SSSR*, **101**, 55 (1955).
[27] R. Peierls: *Ann. der Phys.*, **13**, 905 (1932).
[28] M. Hayashi and K. Katsuki: *J. Phys. Soc. Japan*, **7**, 599 (1952).
[29] S. Nikitin, G. Perny and M. Sieskind: *Compt. Rend.*, **238**, 67 (1954); S. Nikitin, L. Couture, M. Sieskind and G. Perny: *Compt. Rend.*, **238**, 1786 (1954); S. Nikitin, M. Sieskind and G. Perny: *Compt. Rend.*, **238**, 1987 (1954); S. Nikitin, R. Reiss and G. Perny: *Compt. Rend.*, **240**, 505 (1955); S. Nikitin: *Compt. Rend.*, **240**, 1415 (1955).
[30] A. S. Davydov: *Izv. Akad. Nauk SSSR. Ser. Fiz.*, **12**, 608 (1948); *Theory of light absorption in molecular crystals* (Kiev, 1951).
[31] I. M. Dykman and S. I. Pekar: *Works of the Institute of Physics of the Acad. Sci. Ukr. SSR*, n. 3, p. 92 (1952).
[32] I. M. Dykman: *Works of the Institute of Physics of the Acad. Sci. Ukr. SSR*, n. 5, p. 48 (1954).
[33] E. F. Gross and B. P. Zaharčenja: *Dokl. Akad. Nauk SSSR*, **90**, 745 (1953).
[34] S. I. Pekar: *Researches on the electron theory of crystals* (Moscow, 1951).
[35] F. Seitz: *Rev. Mod. Phys.*, **26**, 27 (1954).
[36] E. F. Gross, B. P. Zaharčenja and N. M. Rejnov: *Dokl. Akad. Nauk SSSR*, **92**, 265 (1953).
[37] E. F. Gross, B. P. Zaharčenja and N. M. Rejnov: *Dokl. Akad. Nauk SSSR*, **99**, 231 (1954).

[38] E. F. Gross, B. P. Zaharčenja and N. M. Rejnov: *Dokl. Akad. Nauk SSSR*, **97**, 57 (1954).
[39] E. F. Gross, B. P. Zaharčenja and N. M. Rejnov: *Dokl. Akad. Nauk SSSR*, **97**, 221 (1954).
[40] J. R. Oppenheimer: *Phys. Rev.*, **31**, 66 (1928).
[41] H. Rausch von Traubenberg and R. Gebauer: *Zeits. f. Phys.*, **54**, 307 (1929); **56**, 254 (1929); **62**, 289 (1930); **71**, 291 (1931).
[42] C. Lanczos: *Zeits. f. Phys.*, **62**, 518 (1930); **68**, 204 (1931).
[43] F. Seitz: *Phys. Rev.*, **76**, 1376 (1949).
[44] A. Lo Surdo: *Rend. Accad. Lincei*, **22**, 665 (1913).
[45] E. F. Gross and M. A. Jakobson: *Žu. Tehn. Fiz.*, **25**, 364 (1955); *Dokl. Akad. Nauk SSSR*, **102**, 485 (1955).
[46] S. Nikitin, L. Couture, M. Sieskind and G. Perny: *Compt. Rend.*, **238**, 1786 (1954); S. Nikitin and M. Sieskind: *Compt. Rend.*, **240**, 1324 (1955).
[47] S. Nikitin and G. Perny: *Compt. Rend.*, **240**, 64 (1955).
[48] E. F. Gross and M. L. Belle: *Žu. Tehn. Fiz.*, **25**, 948 (1955).

SUPPLEMENTO AL VOLUME III, SERIE X
DEL NUOVO CIMENTO

N. 4, 1956
1° Semestre

On Thermal Conduction in Semiconductors.

A. F. IOFFE

Academy of Sciences of the USSR - Moscow

CONTENTS. — **1.** Introduction. – **2.** Measurements of the thermal conductivity coefficient. – **3.** Temperature dependence of $\varkappa_{ph}$. – **4.** Investigations on the electrical conductivity $\varkappa_e$: deviations from the Wiedemann-Franz law. - **5.** Theory of excitons. – **6.** Discussion.

1. – Introduction.

An interest to the questions of thermal conductivity of semiconductors arose in connection with two practical problems: 1) the use of semiconductor thermoelements, and 2) the application of physics to agriculture. The first problem had led us to an investigation of phonon heat transfer and the relation of this process to electrical properties of semiconductors (A. F. IOFFE and collaborators) [1], while the second has suggested an investigation of the thermal properties of soil and of the influence of humidity and porosity over them (A. B. ČUDNOVSKIJ and collaborators) [2].

The present paper deals with the results obtained by the first problem. As the problem made indispensable our investigation of a large number of different substances we decided to use the unsteady flow method. On eliminating or making corrections for the more important sources of errors, the apparatus used [1] allowed to measure specific thermal conductivity with an accuracy up to $2 \div 3\%$ over a period of $3 \div 5$ minutes. Our method consisted in measuring the rate of heating $\Delta T/\Delta t$ of a copper block through the sample under a measured temperature difference $(T_1 - T_2)$. This block had been surrounded with a copper cylinder the temperature of which was being kept equal to the temperature of the block. The heat transfer through air and the thermal resistance of the contacts had been determined before and taken account of at computation. The non-linear character of the temperature distri-

bution over the sample had also been born in mind. The results obtained in this manner had been verified on standard substances of various thermal conductivities (amorphous quartz, lead and others). The accuracy for substances with specific thermal conductivity less than 0.1 and more than 0.001 cal $^{\circ}C^{-1}$ cm^{-1} s^{-1} did not exceed 5%. While working with this apparatus it has been observed that the plastic deformation of rock salt as well as the transition through Curie point in seignet to electrics (ferroelectrics) does not change the thermal conductivity over 3%. The change of the crystal state into amorphous reduces thermal conductivity significantly not only in quartz but also in selenium and sulphur. V. P. ŽUZE and A. R. REGEL' [3] and V. VOL'KENSTEJN [4] have designed other apparata for the measurement of thermal conductivity. In the apparatus used by ŽUZE and REGEL the rate of heating dT/dt is determined directly by induced currents. The apparatus gives sure results for substances with high thermal conductivity. Thermal conductivity measurements within a range of 90° K to 800° K were being conducted by E. D. DEVJATKOVA [5] and P. V. GULTJAEV with the usual method of stationary flow.

2. – Measurements of the Thermal Conductivity Coefficient.

An investigation of the thermal conductivity of many semiconductors had been accomplished by A. V. IOFFE partly in cooperation with the author of the dresent paper. The heat transfer in semiconductors is obtained by two physical processes: namely by propagation of thermal vibration waves (phonons) and by electron diffusion. The thermal conductivity coefficient may be assumed to be the sum:

$$\varkappa = \varkappa_{ph} + \varkappa_{e}\,, \tag{1}$$

the electron part of thermal conductivity is directly related to electrical conductivity

$$\varkappa_{e} = L\sigma\,, \tag{2}$$

where L for the atomic crystal lattice with non-degenerate electrons is:

$$L = 2\left(\frac{k}{e}\right)^{2} T\,, \tag{2a}$$

and for concentrations of electrons corresponding to the degenerate state is:

$$L = 3.3\left(\frac{k}{e}\right)^{2} T\,. \tag{2b}$$

The relation between $\varkappa_e$ and σ (equation (2)) generally known as the Wiedemann-Franz law, is verified not only in metals but also in semiconductors.

I. A. Dounaev and I. P. Maslakovec [6] have proved this law to hold for lead sulfide with non-degenerate electrons, E. D. Devjatkova has proved the same for degenerate electrons, whereas our experiments on semiconductors having electrical conductivities in the range of 1 000 Ω^{-1} cm^{-1} to 4 500 Ω^{-1} cm^{-1} showed it good for both cases. Fig. 1 shows that taking the value $\varkappa_{ph} = 2.3 \cdot 10^{-3}$ cal cm^{-1} °C^{-1} s^{-1}, given by extrapolation to $\sigma = 0$, to be constant, the value of $\varkappa_e$ is increasing linearly with σ, while the coefficient L has the theoretical value of about 10^{-3} cal cm^{-1} °C^{-1} s^{-1} for 1 000 Ω^{-1} cm^{-1} at $\sigma < 2\,500$ Ω^{-1} cm^{-1}, and of $1.5 \cdot 10^{-3}$ cal cm^{-1} °C^{-1} s^{-1} at $\sigma < 3\,500$ Ω^{-1} cm^{-1}. The increase of L from $1 \cdot 10^{-6}$ up to $1.5 \cdot 10^{-6}$ corresponds to the beginning of the degeneration at concentrations of the order of 10^{19} cm^{-3}.

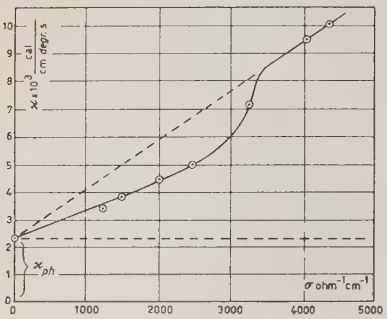

Fig. 1.

The additivity of $\varkappa_{ph}$ and $\varkappa_e$ is by far not yet evident; it does not take into account the scattering of thermal waves (phonons) by electrons. The validity of the Wiedemann-Franz ratio for light as well as for heavy metals indicates the high magnitude of such a scattering. As will be shown below, one may suppose that the thermal conductivity of light metal lattice under absence of free electrons would reach the same order of magnitude as the whole conductivity $\varkappa = \varkappa_{ph} + \varkappa_e$ (about (0.2÷0.3) cal cm^{-1} °C^{-1} s^{-1}). This contradiction to a certain extent reminds us of the paradox of the classical theory of metals concerning the heat capacity of electrons: here is lacking the thermal conductivity of crystal lattice, whereas in the case of the heat capacity of metals it was the electron heat capacity that disappeared.

It seems natural to attempt the explanation of the weak participation of phonon thermal conductivity by the scattering of phonons by free electrons.

It follows that at concentrations of electrons exceeding 10^{20} cm^{-3}, the scattering of phonons on electrons has to be considered.

As Debye has shown as early as 1914, the phonon part of thermal conductivity may be expressed, with analogy to the diffusion of gases, as

$$\varkappa_{ph} = \tfrac{1}{3} C V \bar{\lambda} \quad \text{or} \quad \varkappa_{ph} = \tfrac{1}{4} C V \hat{\lambda} \tag{3}$$

where

C = volume heat capacity,

V = velocity of sound (phonons),

$\bar{\lambda}$ = mean free path of phonons.

The value $\bar{\lambda}$ is defined by the degree of unharmonicity of thermal vibrations and by their intensity, the latter may be represented as $\int_0^T c\,dT$. At temperatures exceeding the Debye temperature θ, when the thermal energy is being distributed equally between all the degrees of freedom, one may assume:

$$\frac{1}{\bar{\lambda}} = A\int_0^T c\,dT\,, \tag{4}$$

while the unharmonicity factor A may be considered as independent on temperature. For thermal vibrations of a continuous solid with the number of vibrations in the interval $d\nu$ proportional to ν^2, we get a detailed tabulated integral that can be represented for temperatures above θ as:

$$\left(\int_\theta^T c\,dT\right)_{T>\theta} \cong C\left(T-\frac{\theta}{3}\right). \tag{5}$$

Thus for these conditions:

$$\frac{1}{\varkappa_{ph}} = \frac{3A}{V}\left(T-\frac{\theta}{3}\right). \tag{6}$$

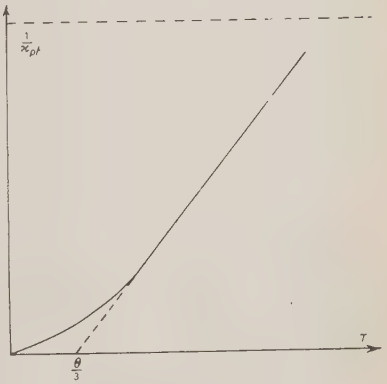

Fig. 2.

The relation of $1/\varkappa_{ph}$ to T is shown in Fig. 2.

As one should have expected, the equation (6) holds good while we consider the body as a continuum. As soon as $\bar{\lambda}$ approaches the value of the lattice constant a, $1/\varkappa_{ph}$ does not satisfy the relation (6). We did not succeed in lowering $\varkappa_{ph}$ to the magnitude of $\bar{\lambda} < a$.

The corresponding limiting value $1/\varkappa_{ph}$ is shown by a dotted line in Fig. 2.

Further development of the theory of phonon thermal conductivity by PEIERLS and other scientists still does not provide an answer to the most important question concerning the determination of the magnitude of thermal heat conductivity and its relation to other characteristics of the

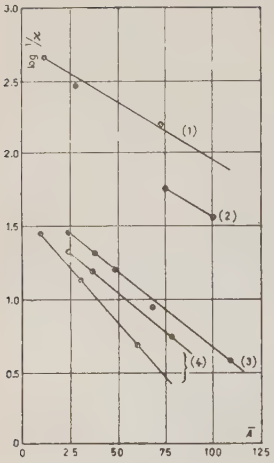

Fig. 3.

substance. And still $\varkappa_{ph}$ varies within a broad range, from 0.5 cal $^{o}C^{-1}$ cm^{-1} s^{-1} for diamond to 0.0005 cal $^{o}C^{-1}$ cm^{-1} s^{-1} for sulphur.

3. – Temperature Dependence of $\varkappa_{ph}$.

Up to recent times, experimental researches were mostly directed on investigating the temperature dependence of $\varkappa_{ph}$ at low temperatures. Simple considerations allow us to assume that the thermal conductivity under the same conditions will be the less, the lower is the temperature θ of the metal, i.e. the lower are the atomic vibration frequencies determined by atomic weight and by elastic modulus or sound velocity. Besides, $\varkappa_{ph}$ will be smaller in crystal lattices when the unharmonicity of thermal vibrations is the greatest.

The first conclusion to be made is that $\varkappa_{ph}$ decreases with increasing atomic weight for substances with the same type of lattices. This conclusion is actually justified both on the basis of the available thermal conductivity data and of those we have got. In fact, the thermal conductivity $\varkappa_{ph}$ of the elements of the first two periods of Mendeleev's system is measured in tenths of cal $^{o}C^{-1}$ cm^{-1} s^{-1}, in the middle part of the system it is measured in hundredths and in the lower part in thousandths of the same unity. The results of measurements and the magnitudes of Log $1/\varkappa_{ph}$ as a function of the average atomic weight $\bar{A}$ of the components are given in Fig. 3. Substances with the same chemical types of crystals are connected with lines: 1) elements of the 4-th group, 2) diamond-like lattices of the compounds of the 3-rd and 5-th groups, 3) oxides of the elements of the 2-nd group, compounds of elements of the 2-nd and 6-th groups, 4) alkali halid crystals of the compounds of the 1-st and 7-th groups with ions of equal atomic weights, and with ions of different atomic weights. There is no doubt that as a rule $\varkappa_{ph}$ decreases with the increase of A. The thermal conductivity plays a decisive role for the efficiency of thermoelements: the lesser is $\varkappa_{ph}$, the higher is the efficiency. It was therefore important to choose

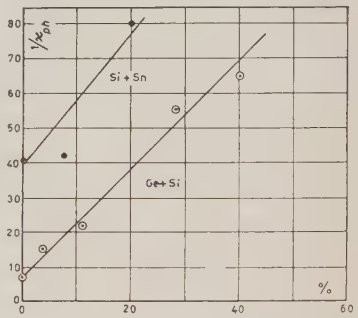

Fig. 4.

the right way for selecting semiconductors with a small $\varkappa_{ph}$ and for lowering $\varkappa_{ph}$ in the cases when it is too high. One must also take into account the mobility of electrons. The higher is the ratio of the mobility of electrons to the thermal conduction of phonons, the more is this semiconductor suitable for thermoelements. If we introduce defects or impurity atoms into the crystal lattice we get a lower value of $\bar{\lambda}$ and, as a consequence, a lower value of $\varkappa_{ph}$: this is shown in Fig. 4, where $1/\varkappa_{ph}$ is plotted as a function of the concentration of impurity atoms added to Ge and to Si. One can estimate the influence of admixtures: each of these introduces an additional centre of scattering of phonons with cross-section pa^2, where a is the lattice period.

$\bar{\lambda}$ for Ge is of 200 Å or of about 35 a. At room temperatures, 3% of the atoms take part in the scattering of phonons in Ge. If one adds 3% of impurity atoms and each of them produces an equal scattering, then $\varkappa_{ph}$ must decrease by a factor 2, and in fact $1/\varkappa_{ph}$ increases about as much.

$\bar{\lambda}$ for lead telluride has the value of 15 Å $= 3a$. In order to lower the thermal conduction by a factor 2, one requires 30% of impurity atoms. This difference is clearly seen from comparison of Fig. 4 and Fig. 5. Still one can meet admixtures producing a more effective scattering: for example an addition of 7% Te lowers the thermal conduction of GaSe from $60 \cdot 10^{-3}$ to $12 \cdot 10^{-3}$. Here $p > 1$; but sometimes there are such defects that have an average value of $p < 1$. Thus the influence of admixtures is determined not only by their concentration, but also by the conditions of their incorporation in the lattice. Interstitial admixtures deforming the lattice over a few atomic distances seem to possess a larger cross-section of scattering than substitutional admixtures.

Of some interest was the investigation of the influence of admixtures of a broad range of concentrations especially for the solid solutions of isomorphous substances. Fig. 5 gives the curve of the thermal resistance $1/\varkappa_{ph}$ for the solutions PbSe and PbTe.

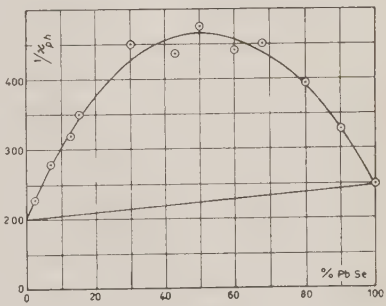

Fig. 5.

For the solutions Bi_2Te_3 and Sb_2Se_3 the solubility is limited on both edges.

It has been proved also that for solutions containg 50% of both components the substance behaves as amorphous to phonon scattering and $\bar{\lambda}$ approaches the interatomic distance a; for PbTe and PbSe, $\varkappa_{ph}$ in this case is near $2 \cdot 10^{-3}$ and does not depend on temperature (curve 2 of Fig. 6). Even for solutions of Si in Ge, $\varkappa_{ph}$ decreases from $145 \cdot 10^{-3}$ to $8 \cdot 10^{-3}$ (20 times) and $\bar{\lambda}$ is of about 6 Å, the lattice period. In solid solutions, where

the phonon free path is reduced to the magnitude of the lattice period, the mobility and the electron free path are still keeping high values. A solid solution amorphous for phonons still keeps its periodical properties or electrons.

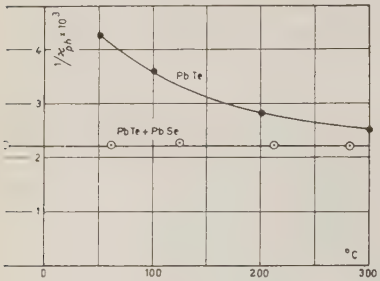

Fig. 6.

One may suppose that this difference is due to the difference of wavelength. The wavelength of the major part of phonons is of the order of $10^{-8} \div 10^{-7}$ cm; that is why scattering is produced even by defects having the dimensions of interatomic distances. The electron wavelength of a semiconductor is about 20 lattice periods; for such waves it is important to keep up the periodicity of a long range. Local fluctuations are not more effective than fluctuations of thermal motion.

4. – Investigations on the Electrical Conductivity $\varkappa_e$. Deviations from the Wiedemann-Franz Law.

Let us turn to the electron part $\varkappa_e$ of the thermal conduction: there seems to exist an opinion that the Wiedemann-Franz law has already reproduced the whole picture. Subtracting $L\sigma$ from the total value of $\varkappa$ we should have expected to get for $\varkappa_{ph}$ a linear dependence on temperature (equation (2) and Fig. 2).

E. D. DEVJATKOVA has noticed some years ago that with the appearance of intrinsic conductivity the Wiedemann-Franz law for $\varkappa_e$ does not reproduce the behaviour of the curve; there is an extra thermal conductivity $\Delta\varkappa$ growing with the rise of intrinsic electrical conductivity (Fig. 7).

In 1954 BUSCH [7] has noted the same deviation for the alloy InSb. $\varkappa_e$ is by 100 times greater compared to the correction predicted by the Wiedemann-Franz law (Fig. 8).

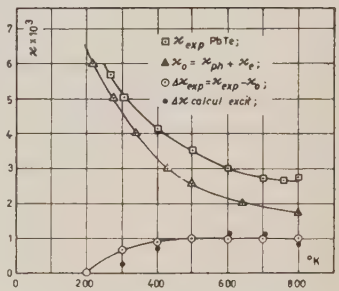

Fig. 7.

Further investigation of the observations made by E. D. DEVJATKOVA at higher temperatures has been achieved by P. V. GULTJAEV and has confirmed the fact of the existence of a deviation of the curve towards higher thermal conductivity (Fig. 7). The rise of thermal conductivity is still more

pronounced for the compound Bi_2Te_3 (Fig. 9), as E. D. Devjatkova and P. V. Gultjaev have shown. Judging by the temperature range where a rise of thermal conduction is observed, one may suppose that here also it is connected with the appearance of intrinsic conductivity. A number of other compounds show a similar rise of thermal conductivity ($\varkappa - L\sigma$).

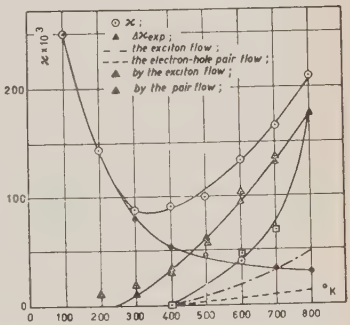

Fig. 8.

Thus the simultaneous appearance of the higher thermal conductivity, exceeding the value $L\sigma$ given by the Wiedemann-Franz law (equation (2)), and of the intrinsic conductivity in a semi-conductor is not a chance phenomenon. It does not contradict the results of experiments given above and the applicability of the Wiedemann-Franz law for semi-conductors, but completes them. These experiments concerned the extrinsic conductivity with current carriers all of the same sign (either electrons or holes). Deviations from this law arise within that temperature range where one can expect the appearance and the following predominance of intrinsic conductivity, that generates charges of both signs.

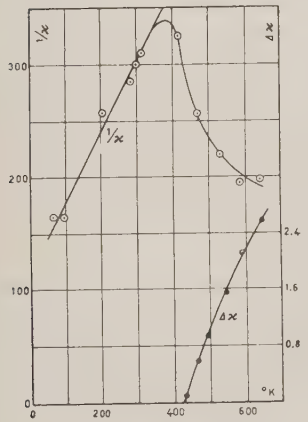

Fig. 9.

The simultaneous partaking of holes and electrons in a current or in a diffusion process substantially changes the relations between charge transfer and heat transfer. While only electrons or only holes are present, their run from the hot end to the cold one produces an electric field counterbalancing the diffusion process. A statistical balance is produced, under which an equal quantity of electrons passes through every cross-section in both directions, but with different kinetic energies. Such is the process of the temperature levelling by free charges having the same sign. Matter looks different when there are current carriers of two signs. A diffusion flow of holes and electrons (bipolar diffusion) does not carry a charge and does not produce a counteracting field. When the mobilities of the charge carriers are different, those having greater mobility go ahead the diffusion process and produce an electrical field E that accelerates the slower charges and slackens down the more rapid ones to an equal velocity of diffusion. This electrical field, as in the

case of electrolitic diffusion, is

$$E = \frac{kT}{e}\frac{1}{n}\frac{\mathrm{d}n}{\mathrm{d}x}\frac{u_- - u_+}{u_- + u_+} = \frac{\Delta E}{2eT}\frac{u_- - u_+}{u_- + u_+}\frac{\mathrm{d}T}{\mathrm{d}x}. \tag{7}$$

This bipolar diffusion field is due only to the difference in the mobilities of carriers; so that in the case $u_- = u_+$,

$$E = 0\,.$$

As early as 1940, B. J. Davydov and J. M. Šmuškevič [2] (and Price in 1954 [9]) derived the equation for $\varkappa_e$ for the case of simultaneous partaking of holes and electrons. Here not only other conditions for the movement of charges are considered, but also the fact that running from a hot end, where the concentrations are higher, to the cold one, the pairs of electron-holes are recombining on their way and generating energy ΔE. The equation given by Davydov and Šmuškevič may be written as follows:

$$\varkappa_e = L(\sigma_+ + \sigma_-) + 2L\frac{\sigma_+\cdot\sigma_-}{\sigma_+ + \sigma_-}\left(\frac{\Delta E}{2kT} + r + 2\right)^2. \tag{8}$$

Here σ_+ and σ_- are the specific electrical conductivities due to holes and electrons separately, ΔE is the width of the forbidden band and r is the exponent in the equation for the mean free path of free charges as a function of their velocity. In the particular case of atomic lattices with one acoustic branch of thermal vibrations, $r = 0$. The additional thermal conduction produced by the flow of the pairs electron-hole is

$$\Delta\varkappa_{\text{pair}} = 2L\frac{\sigma_+\cdot\sigma_-}{\sigma_+ + \sigma_-}\left(\frac{\Delta E}{2kT} + 2\right)^2.$$

The magnitude of the factor out of brackets depends on the ratio σ_+/σ_-.

When $\sigma_+ = \sigma_-$ this factor has the value $L\sigma$ or $\frac{1}{2}L(\sigma_+ + \sigma_-)$, so that eq. (8) becomes

$$\varkappa_e = L(\sigma_+ + \sigma_-)\left[1 + \tfrac{1}{2}\left(\frac{\Delta E}{2kT} + 2\right)^2\right]. \tag{9}$$

As long as σ_+/σ_- is only 1.5 :-2, the factor $\frac{1}{2}$ is changing insignificantly. When σ_+ is much greater or much lesser than σ_-, then the quantity $(2L\sigma_+\cdot\sigma_-)/(\sigma_+ + \sigma_-)$ is of about $2L\sigma_i$, where σ_i is the lesser of the two values σ_+ or σ_-. For instance, for the alloy InSb in the intrinsic conductivity range, when $n_- = n_+$, and the ratio of mobilities is $u_-/u_+ = 80$, the equation (8)

may be represented as

$$\varkappa_e = L(\sigma_+ + \sigma_-)\left[1 + \frac{1}{40}\left(\frac{\Delta E}{2kT} + 2\right)^2\right]. \tag{9a}$$

In the region of available temperatures the intrinsic conductivity $(\sigma_+ + \sigma_-)$, as well as $\varkappa_e$, reach a considerable magnitude if ΔE does not exceed 0.6 eV. Then the factor in square brackets of the second member of equation (9) reaches a magnitude of about 70; in other words with the transition to the intrinsic conductivity range the coefficient increases by 70 in comparison to the magnitude it should have according to the Wiedemann-Franz law. In the case of InSb, when $\Delta E \simeq 0.3$ eV, L increases, according to the equation (9*a*), only by a factor 2, whereas BUSCH observed an increase of L nearly by 100.

5. – Theory of Excitons.

The effect of bipolar diffusion of free charges however is not the only process that can lead to an increase of thermal conduction. The appearance of intrinsic conductivity may, for example, be accompanied also by generation of excitons. Excitons were introduced into the theory of semiconductors by J. I. FRENKEL in 1931. They were very successfully applied by V. P. ŽUZE and S. M. RYVKIN for an explanation of peculiarities of the inner photo-effect in cuprous oxide. E. F. GROSS investigated the spectra of excitons generated by light in Cu_2O and CdS. A. I. ANSEL'M computed the mean free path of unlocalized excitons. If light can produce such an excitation of the crystal lattice, it may be produced by thermal motion also. In this case the concentration of excitons N may be represented as a function of temperature and of a certain activation energy $\Delta E'$. Unlocalized excitons, that can be regarded as connected hole-electron pairs, diffuse freely from the hotter part of a body to the colder one without carrying a charge. During this path the number of excitons decreases, and the energy $\Delta E'$ of their recombination converts into heat or light.

Under these assumptions the additional thermal conductivity $\Delta\varkappa_{ex}$ may be expressed, in analogy to $\Delta\varkappa_{pair}$ for intrinsic conductivity, as follows:

$$\Delta\varkappa_{ex} = \frac{k^2}{e^2} CT \frac{N}{n} \frac{U}{u}\left[\frac{\Delta E'}{kT} + 2\right]^2, \tag{10}$$

where N is the concentration of excitons and $U = (e/kT)D$ (D coefficient of exciton diffusion), n and u are the same as for free charges.

According to the theory of A. J. ANSEL'M, U and u are quantities of the

same order. G. E. PIKUS obtained the following equation for $\Delta\varkappa_{ex}$:

$$(10a)\quad \Delta\varkappa_{ex} = ND\left[\frac{\Delta E'}{kT} + 2\right]^2, \quad \text{where} \quad N = 2\frac{(2\pi m^* kT)^{\frac{3}{2}}}{h^3}\exp\left[-\frac{\Delta E'}{kT}\right].$$

In the case of InSb, where one may suppose that electrons are already in a degenerate state, N is considerably greater than n. According to equation (10), $\Delta\varkappa_{ex}$ may reach values far greater than those given by equation (9a) and may thus be successfully applied to the explanation of the results obtained by BUSCH.

Two more processes increasing the thermal conductivity of semiconductors are to be considered when the intrinsic conductivity becomes appreciable.

Bipolar diffusion of holes and electrons presumes their continuous flow from the hot part of the body to the cold one. If, as it has been supposed, phonons are scattered by electrons, then the interaction of electrons and holes with phonons must lead to the carrying along of phonons by the flow of free charges. This carrying is the more intensive the more often does the scattering of electrons by phonons take place, and the less is therefore the mean free path and the mobility u. One can therefore assume that the additional thermal conductivity due to the carrying along of phonons by the flow of electrons and holes may be represented as:

$$(11)\qquad \Delta\varkappa_{\text{pair drag}} \sim \frac{n}{l} \sim \frac{n}{u}\, T^{\frac{1}{2}}.$$

Supposing the flow of electrons and holes in the intrinsic conductivity range is accompanied by a flow of excitons, one must also expect a « drag » of phonons by the flow of excitons.

The additional conductivity called forth by this process may be represented as:

$$(12)\qquad \Delta\varkappa_{\text{ex, drag}} \sim \frac{N}{D}.$$

Finally the raise of temperature makes noticeable the energy transfer by thermal radiation. GENZEL computed this additional thermal conductivity brought in by energy radiation to be

$$(13)\qquad \Delta\varkappa_{\text{rad,}} = \frac{16}{3}\,\frac{a\varepsilon}{k}\,T^3,$$

where ε = square of refraction coefficient,
k = coefficient of infrared absorption,
a = coefficient in the equation for the radiation of an absolutely black body $u = aT^4$.

The magnitude of k depends on the free charges concentration n.

6 – Discussion.

From the facts cited above one may conclude that equations (1) and (2) hold approximately for extrinsic conductivity only, and till $n < 10^{20}\,\mathrm{cm}^{-3}$. At greater values the scattering of phonons by the current carriers may come forth, so that the division of $\varkappa$ into two independent terms $\varkappa_{\mathrm{ph}}$ and $\varkappa_e$ would become impossible: the value of $\varkappa$ is less than the sum of $\varkappa_{\mathrm{ph}}$ and $\varkappa_e$.

With the appearance of the intrinsic conductivity, owing to the simultaneous partaking of electrons and holes in the diffusion process, a number of new phenomena arise, which change the relation between $\varkappa$ and σ.

We have considered the additional thermal conductivity $\Delta\varkappa$ due to:

1) diffusional flow of electron-hole-pairs and also a number of other processes that might accompany bipolar diffusion at high temperatures;
2) the exciton flow;
3) the « drag » of phonons by the pair flow;
4) the « drag » of phonons by the exciton flow;
5) heat transfer due to radiation.

All these phenomena overlapping one another can change the value of L in equation (2*a*) and (2*b*) sometimes by 10 and 100 times. Each of the above mentioned processes may gain a predominant significance in its dependence on the properties of a semiconductor. For quantitative computation we have the necessary data only for $\varkappa_{\mathrm{pair}}$ that is caused by the pair flow. This quantity can be computed by the equation of Davydov and Šmuškevič.

When we have an exciton flow (provided excitons are generated by thermal motion) we are not yet able in appreciating their concentration and temperature dependence. Only in a few cases [Cu_2O, CdS, PbTe] we can evaluate their energy levels and also the magnitude of $\Delta E'$ with the help of absorption spectra.

We have not yet evaluated the thermal conductivity due to the « drag » of phonons by the pair flow and by the exciton flow.

The number of experimental facts that can be drawn for discussing the causes of the thermal conductivity increase at high temperatures and for the explanation of the relation of this phenomena to the intrinsic conductivity is still quite insufficient. Considering all the data on thermal conductivity accumulated up to the present we come to the conclusion that the equation (2): $1/\varkappa_{\mathrm{ph}} = 3A/v(T - \theta/3)$ plotted in Fig. 2 is verified in insulating crystals until $\bar{\lambda} < a$ (lattice constant). The presence of extraneous scattering centres introduces an additional term S into the equation for $1/\varkappa_{\mathrm{ph}}$. In this case the

extrapolation of the curve $(1/\varkappa_{ph})_{T>0} = f(T)$ must intersect the abscissa axis at $T < \theta/3$ and sometimes at $T < 0$ also. If impurity scattering significantly exceeds the phonon scattering, the quantity $1/\varkappa_{ph}$ in the equation $1/\varkappa_{ph} = 3A/v(T - \theta/3) + S$ does not change appreciably with temperature, as is shown by Fig. 5, where the data got by P. V. GULTJAEV for the quantity $\varkappa_{ph}(T)$ are given for pure PbTe and for the alloy PbTe – PbSe.

In semiconductors with extrinsic conductivity, equation (6) and Fig. 2 are fully verified, as well as in insulators, if $\varkappa_{ph}$ is defined by electrical conductivity according to the law $\varkappa_{ph} = \varkappa - L\sigma$. Yet, with the appearance of intrinsic conductivity the temperature dependence is changing pronouncedly: the curve $1/\varkappa_{ph}(T)$ deviates to the bottom towards greater values of $\varkappa$. This is clearly seen in Fig. 10, showing the thermal resistance $1/(\varkappa - L\sigma)$ for $BiTe_3$ measured by E. D. DEVJATKOVA and P. V. GULTJAEV. Fig. 9 gives the same relation $(\varkappa - L\sigma) = f(T)$, obtained by the same authors, for PbTe.

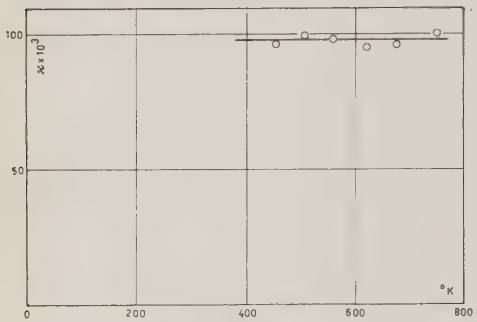

Fig. 10.

Fig. 8 gives the data for pure samples of InSb obtained by BUSCH. Fig. 10 gives P. V. GULTJAEV's measurements for InSb that have such a number of impurities that up to the high temperatures prevails the impurity scattering.

The impurity scattering of phonons seems to prevail over the thermal vibration scattering. Therefore, as in the case of solid solution (Fig. 6), $\varkappa$ is practically independent on T.

In this case the thermal conductivity increase at high temperatures discovered by BUSCH was not observed. At the bottom of Figs. 7-9 a continuous curve represents the values of $\Delta\varkappa$, that have been computed as a difference between the values observed at a given temperature T and those extrapolated by the curve of Fig. 2.

A dotted line shows the computed values of $\Delta\varkappa$, and for $\Delta\varkappa_{ph}$ one of the points is being joined by the value of $\Delta\varkappa$. The coincidence of the continuous and dotted curve would have meant that the above mechanism might have been responsible for the observed effect. The value $\Delta E'$ for excitons is defined for PbTe with the aid of absorption spectrum near the edge of proper absorption. For other substances $\Delta E'$ is accepted to be $0.1 \div 0.2$ eV lesser than ΔE.

Summarizing these facts, we are not yet able of drawing definite conclusions on the comparative role of different effects producing the increase of $\varkappa$. It is only

possible to state that the sole effect of energy transfer by electron-hole pairs computed by DAVYDOV and ŠMUŠKEVIČ does not give us a full explanation of the experimental values of Δz. This circumstance makes us involve in the description of the experimental results other phenomena such as exciton flow, exciton and pair « drag ». We are still carrying on an investigation on thermal conductivity of other semiconductors with small width of the forbidden band and we hope to get a more thorough analysis of the phenomenon of thermal conduction in semiconductors.

REFERENCES

[1] A. F. IOFFE: *Semiconductors in modern physics* (Leningrad, 1954); A. V. IOFFE and A. F. IOFFE: *A simple method of measuring the heat conductivity*, in *Žu. Tehn. Fiz.*, **22**, 2005 (1952); *Dokl. Akad. Nauk SSSR*, **97**, 821 (1954); **98**, 757 (1954).
[2] A. F. ČUDNOVSKIJ: *Heat conduction in porous media* (Leningrad, 1954).
[3] V. P. ŽUZE and A. P. REGEL': *Žu. Èksper. Teor. Fiz.*, **22**, 1376 (1952).
[4] V. S. VOL'KENSTEJN: *Žu. Èksper. Teor. Fiz.*, **22**, 1043 (1952).
[5] E. D. DEVJATKOVA and L. S. STIL'BANS: *Žu. Èksper. Teor. Fiz.*, **22**, 968 (1952).
[6] I. A. DOUNAEV: *Žu. Èksper. Teor. Fiz.*, [*], 1101 (1946).
[7] G. BUSCH and M. SCHNEIDER: *Physica*, **20**, 1084 (1954).
[8] J. B. DAVYDOV and J. M. ŠMUŠKEVIČ: *Progress in Physical Science*: [*] 21 (1940).
[9] P. J. PRICE: *Phys, Rev.*, **95**, 596 (1954).

[*] Manca l'indicazione del volume (*N. d. R.*)

SUPPLEMENTO AL VOLUME III, SERIE X
DEL NUOVO CIMENTO

N. 4, 1956
1° Semestre

Some Problems of the Dynamic Theory of Non-Ideal Crystal Lattices.

M. LIFŠIC (*)

Academy of Sciences of the USSR - Moscow

CONTENTS. — **Introduction.** – **1. Influence of a local irregularity on the oscillations of lattice atoms.** 1. Appearance of discrete frequencies. 2. Scattering of short elastic waves by local irregularities. – **2. Influence of a local irregularity on the crystal free energy.** – **3. Spectrum of frequencies of disordered crystals.** 1. Trace method. 2. Calculations of the free energy of a disordered crystal. 4. The spectrum structure. 4. Some thermodynamical conclusions. – **4. Other applications of the method.** 1. Infra-red absorption by disordered crystals. 2. Surface oscillations of the lattice.

Introduction.

Problems of the dynamic theory of non-ideal crystals may be of interest from many points of view.

It is known that the presence of the translation symmetry simplifies very much the mathematical aspect of the problem and offers the opportunity of studying comprehensively the oscillations of ideal lattices. A part of the physical results obtained is connected to a great extent with the presence of the translation symmetry (e.g. selective character of the absorption of infrared rays). Other results, qualitatively at least, are not connected with this circumstance, but this cannot be proved within the limits of the existing theory, the methods of which are totally based upon the periodic structure of the crystal.

One should also draw attention to the analogy between the theory of the oscillations of lattice atoms and the wave mechanics of the electron moving in the field of the crystal.

The equation for the amplitude $\chi^s(\boldsymbol{r})$ of the atomic oscillations in the ideal crystal (which may be considered as the equation for the wave function of the

phonon in the quantum theory of crystals) is

$$\sum A^{sx,\,s'x'}_{\boldsymbol{r}-\boldsymbol{r}'}\chi^{s'x'}(\boldsymbol{r}') = m_s\omega^2\chi^{sx}(\boldsymbol{r})\,, \tag{1}$$

where $\boldsymbol{r}$ are the points of the crystal lattice ($\boldsymbol{r} = r_i\boldsymbol{a}_i$; $i = 1, 2, 3$: r_i are integers, $\boldsymbol{a}_i$ are the principal periods), m_s is the mass of the atom which occupies the s place in the cell ($s = 1, ..., p$; where p is the number of atoms in the cell), and $A^{sx,\,s'x'}_{\boldsymbol{r}-\boldsymbol{r}'}$ are the interaction coefficients. The solution of this equation yields the plane waves

$$\boldsymbol{\chi}^s(\boldsymbol{r}) = \boldsymbol{q}(s)\exp[2\pi i\boldsymbol{k}\cdot\boldsymbol{r}] \tag{2}$$

and the spectrum of the oscillation frequencies consists of $3p$ partially overlapping branches,

$$\omega^2 = \omega^2_r(\boldsymbol{k})\,; \qquad r = 1, ..., 3p \tag{3}$$

three of which begin with zero (the acoustic branches); for the other branches $\omega_r(0) \neq 0$.

Equation (1) represents a generalized discrete analog of the differential equation for the wave functions of an electron in the periodical field. Accordingly, if one takes into account that the variable s characterizes the «coordinate» inside the cell, while $\boldsymbol{r}$ is the cell coordinate, the wave function of the phonon (2) appears as a modulated plane wave, and, thus, corresponds to the wave function of a zone electron $\psi = c(\boldsymbol{r})\exp[2\pi i\boldsymbol{k}\cdot\boldsymbol{r}]$. The number of the oscillation branch corresponds to that of the zone for the electron functions, while the dependence $\omega^2 = \omega^2(\boldsymbol{k})$ corresponds to the law of dispersion $E = E(\boldsymbol{k})$ for the zone electrons. Analogously, the alteration of the phonon wave functions and of the spectrum of phonon energies caused by the appearance of irregularities in the crystal has qualitatively the same character as the corresponding alteration of the wave functions and of the energy spectrum of the electrons. This circumstance makes it possible to extend certain results obtained for the phonons, and the methods used to obtain them, to the electrons in the crystal.

Usually, the study of the differential equations is considered to be an easier task than the study of their discrete analogs. However it turns out that some problems (especially those connected with the theory of local perturbations) are considerably simplified and become more transparent just owing to the possibility of operating with discrete variables. We should point out that the determination of the dispersion law for phonons $\omega = \omega(\boldsymbol{k})$, for the non-perturbed problem, with given coefficients A_r, requires the solution of an algebraic equation of $3p$ degree, while the same problem for the three-dimensional differential equation with periodical coefficients has transcendent character.

This paper deals with certain results obtained in the field of the dynamic

theory of the crystalline lattice which are connected with the use of the methods of the theory of local perturbations developed in the papers published in the period 1943-1953 (*) [1-9].

The first two Sections give a short account of the results connected with the role of separate « local » disturbances of the periodicity of the lattice. Section 3 is devoted to the determination of the phonon energy spectrum in disordered lattices. Section 4 deals with certain other applications of the method discussed above, namely the problem of the surface oscillations of the lattice and the infrared absorption of a disordered crystal.

1. – Influence of a Local Irregularity on the Oscillations of Lattice Atoms.

To illustrate a simple case, we consider an idealized simple lattice with all oscillations polarized in one direction and we assume that the local « disturbance » is simply the alteration of the mass of the atom, which is at the origin of the coordinates. These assumptions simplify considerably all derivations without changing the fundamentals of the problem. We shall try to formulate the final conclusions for a general case giving the corresponding formulae when they are not too complicated.

The equation of the lattice oscillations is:

$$\sum A_{r-r'}\chi(\boldsymbol{r}') - m_r\omega^2\chi(\boldsymbol{r}) = 0\,. \tag{4}$$

For the non-perturbed lattice all atoms are alike ($m_r = m$). For a foreign atom at the origin of the coordinates we would evidently have

$$m_r = m(1 - \varepsilon\delta_{r_0}); \qquad \varepsilon = \frac{m - m'}{m}; \tag{5}$$

Equation (4) may be written in the matrix form:

$$(\hat{L} - z(1 - \varepsilon\hat{\Delta}))\chi = 0\,; \qquad z = \omega^2 \tag{6}$$

$$L_{rr'} \equiv L_{r-r'} = \frac{A_{r-r'}}{m}; \qquad \Delta_{rr'} = \delta_{r0}\delta_{r'0}\,, \tag{7}$$

where $\hat{L}$ will be treated as a non-perturbed operator, and $\varepsilon z\hat{\Delta}$ as the local perturbation operator (ε is not supposed to be small). The eigenfunctions of

(*) It should be pointed out that recently analogous methods were partially developed in the papers by G. F. Koster, J. C. Slater and M. Lax [10-13], who, evidently, did not know our results.

the operator $\hat{L}$ are the plane waves

$$\chi_k^0(\boldsymbol{r}) = \exp[2\pi i \boldsymbol{k}\cdot\boldsymbol{r}]; \tag{8}$$

the corresponding eigenvalues are the squares of the frequencies

$$z = \omega^2 = \omega^2(\boldsymbol{k}); \qquad \omega^2(\boldsymbol{k}) = \sum L_r \exp[2\pi i \boldsymbol{k}\cdot\boldsymbol{r}]. \tag{9}$$

Equation (9) is the law of dispersion of elastic waves and determines the spectrum of frequencies of the non-perturbed lattice.

The presence of the local perturbation $\varepsilon z\hat{\Delta}$ leads, on the one hand, to the scattering of waves propagating in the crystal, and on the other hand, to the possible appearance of new discrete eigenfrequencies, outside the interval of the non-perturbed spectrum. The study of these effects may be completed owing to the fact that the local perturbation operator has a finite number of dimensions, i.e. it is a matrix of a finite rank; here, the operator $\hat{\Delta}$ is a matrix of the first rank ($\Delta_{rr'} = \delta_{r0}\delta_{r'0}$). The general theory of such perturbations has been developed in previous papers of the writer [1-3, 7, 8]. In the very simpe case that we consider here some of the results are obtained directly. We shall only refer to the other results.

1·1. *Appearance of discrete frequencies.* – In order to obtain new discrete frequencies, assuming that z is outside the continuous spectrum interval, we shall write the initial equation (6) as:

$$\chi = -\varepsilon z(\hat{L} - z)^{-1}\hat{\Delta}\chi = \varepsilon z\int \frac{(\Delta\chi, \hat{\chi}_k^0)\chi_k^0}{z - \omega^2(\boldsymbol{k})}\,\mathrm{d}\boldsymbol{k}\,, \tag{10}$$

where $\mathrm{d}\boldsymbol{k}$ is the differential of volume in $\boldsymbol{k}$ space and the integration extends over the cell volume of the inverse lattice $V^* = 1$ (*).

Hence, taking into consideration (7) and (8) we obtain

$$\chi(\boldsymbol{r}) = \varepsilon z\chi(0)\int \frac{\exp[2\pi i \boldsymbol{k}\cdot\boldsymbol{r}]\,\mathrm{d}\boldsymbol{k}}{z - \omega^2(\boldsymbol{k})}\,. \tag{11}$$

Finally assuming that $\boldsymbol{r} = 0$ in (11), we obtain the equation for the determination of the discrete frequencies

$$1 = \varepsilon z\int \frac{\mathrm{d}\boldsymbol{k}}{z - \omega^2(\boldsymbol{k})}\,. \tag{12}$$

(*) Here and further on the period of the lattice is taken as unit of length: the lattice is supposed to be a cubic one.

Taking into account that, in the three-dimensional case, the integral which is on the right-hand side remains finite on the border of the continuous spectrum z_g^0, while outside of this interval it decreases gradually with the removal from the border, we see that for sufficiently small ε the discrete frequencies cannot take place (+). Since the frequency spectrum begins with zero ($\omega(0) = 0$), in our case the discrete frequency appears only for sufficiently large positive $\varepsilon > \varepsilon_{cr}$, where

$$\varepsilon_{cr} = \frac{1}{z_g^0 \int \mathrm{d}\boldsymbol{k}/[z_g^0 - \omega^2(\boldsymbol{k})]}. \tag{13}$$

This corresponds to the case of a lighter impurity atom. In the general case of a multi-atom lattice, the discrete frequencies may split from each branch of the oscillations spectrum, and the maximum number of discrete frequencies splitting from each band does not exceed the rank of the local perturbation operator. The general equations determining these frequencies have been given previously [6,3].

The waves corresponding to such discrete frequencies naturally undergo a fast attenuation with the removal from the local irregularity. In our case equation (11) determines the wave function corresponding to such « local » levels.

1·2. *Scattering of short elastic waves by local irregularities.* – Let us pass now to the study of the solutions of equation (6) in the region of the continuous spectrum. Physically such solutions should reflect the process of the scattering of elastic waves [7]. The simplicity of the picture of wave scattering by single scattering centres in the elastic theory of continuum is connected with the simple relation between the energy of a single wave and its wave vector $\boldsymbol{k}$ ($\omega^2 \sim k^2$), resulting from the differential equations of the theory of elasticity. However this picture changes considerably with the transition to the discrete crystalline lattice, i.e. for wave lengths comparable with the atomic dimensions. The study, which can be completed, reveals in this case several unusual peculiarities of the scattering picture [7]. Qualitatively, all the results obtained hold also for the other cases of scattering in presence of a complicated law of dispersion (e.g. scattering of electrons in a metal, scattering of spin waves, etc.).

The solution of the principal equation in the range of the continuous spectrum is obtained in a way similar to that used in section 1·1. However in this case there are additional difficulties connected with degeneracy; a precise analysis is necessary, as the direct solution of the equation analogous

(+) In the one-dimensional case the corresponding integral in (12) diverges at $z = z_g^0$ and the discrete frequencies appear at arbitrary small ε.

to (11) has no meaning, owing to the divergency of the integral in it. We shall not dwell upon the details, but we shall give only the final results.

The solution of equation (6) describing the incoming and scattered waves is

$$(14)\qquad \begin{cases} \chi(\boldsymbol{r}) = \exp\left[2\pi i \boldsymbol{k}\cdot\boldsymbol{r}\right] - \tau\varepsilon\omega^2 \int \left(\dfrac{\exp\left[2\pi i \boldsymbol{k}\cdot\boldsymbol{r}\right]\mathrm{d}\boldsymbol{k}}{\omega^2(\boldsymbol{k}) - z}\right)_{z=\omega^2+i0} \\ \dfrac{1}{\tau} = 1 + \varepsilon\omega^2 \int \left(\dfrac{\mathrm{d}\boldsymbol{k}}{\omega^2(\boldsymbol{k}) - z}\right)_{z=\omega^2+i0} \end{cases}$$

The given formulae are valid for all distances $\boldsymbol{r}$. The most interesting result is the limit of this expression for $r \to \infty$. Calculations which are not given here yield [7]

$$(15)\qquad \chi(\boldsymbol{r}) = \exp\left[2\pi i \boldsymbol{k}\cdot\boldsymbol{r}\right] - \frac{\varepsilon\tau\omega^2}{r} \sum_{\nu} \frac{\exp\left[2\pi i u_\nu r\right]}{\left|\nabla\omega^2(\boldsymbol{k}_\nu)\right| \sqrt{\left|\mathcal{K}_\nu\right|}}\,. \qquad (u_\nu = \boldsymbol{k}_\nu\cdot\boldsymbol{n})$$

Here $\boldsymbol{k}_\nu = \boldsymbol{k}_\nu(\boldsymbol{n})$ is the radius-vector which is drawn to the contact point of the surface $\omega^2(\boldsymbol{k}) = z$ with the plane normal to the direction $\boldsymbol{n}$, $(\boldsymbol{r} = r\boldsymbol{n})$. $\mathcal{K}_\nu$ is the Gauss curvature of the surface $\omega^2(\boldsymbol{k}) = z$ in this point; the summation is performed over all points of contact for which $\mathrm{d}u_\nu/\mathrm{d}z > 0$ and $\nabla\omega^2(\boldsymbol{k})$ is the gradient in $\boldsymbol{k}$ space.

In case of sufficiently long waves (small $\boldsymbol{k}$) the signs of u_ν and $\mathrm{d}u_\nu/\mathrm{d}z$, are evidently the same ($\boldsymbol{k}$ increases with the frequency). Thus, formula (15) has only the terms of the type $\exp\left[2\pi i u_\nu r\right]/r$ with $u_\nu > 0$, which correspond to diverging waves. On the contrary, in case of sufficiently short waves there may be difference in the signs: $u_\nu \cdot \mathrm{d}u_\nu/\mathrm{d}z < 0$. Here, the sum (15) must contain the terms with $u_\nu < 0$ i.e., seemingly converging waves. This result, which may at first seem paradoxical, is explained by the fact that the wave-vector $\boldsymbol{k}$ is determined up to a vector $\boldsymbol{H}$ of the reciprocal lattice having integer components. Thus, the negative quantity $u_\nu = -\alpha$ is equivalent to the positive quantity $u_\nu^* = -\alpha + \boldsymbol{H}\cdot\boldsymbol{n} > 0$.

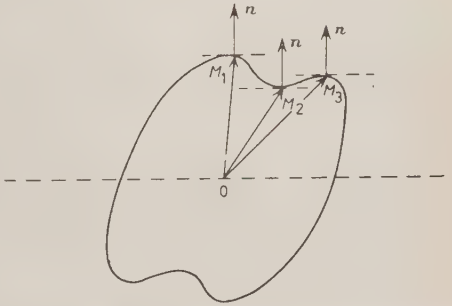

Fig. 1. – $OM_\nu = \boldsymbol{k}_\nu(\boldsymbol{n})$ is the radius vector drawn to the contact points of the surface $\omega^2(\boldsymbol{k}) = z$ with the planes normal to the direction $\boldsymbol{n}$ satisfying the additional condition $(\mathrm{d}u_\nu/\mathrm{d}z) > 0$.

The configuration of the wave surface is determined by the equation $(\boldsymbol{r}\cdot\boldsymbol{k}_\nu) = \mathrm{const}$ and is polar in relation to the surface of constant frequency

$\omega^2(\boldsymbol{k}) = z$. In the simplest case $\omega \sim k$ we will have $\boldsymbol{k}_\nu = k\boldsymbol{n}$, and we obtain a spherical wave $\sim \exp\,[2\pi ikr]/r$.

In case of a convex surface with many branches, the number of diverging waves equals the number of the surface branches; each wave has its own configuration and its velocity of propagation.

Peculiarly interesting is the case when the surface $\omega^2(\boldsymbol{k}) = z$ ceases to be convex and hyperbolic points appear on the surface. Fig. 1 shows that in this case there are in some directions three planes with $u_\nu > 0$, while in others there is only one. Correspondingly, in some directions we shall have the propagation of three waves and in other directions of only one wave. The section of the wave surface in this case should appear as it is schematically plotted in Fig. 2.

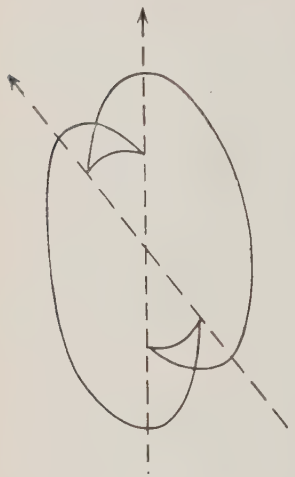

Fig. 2. – The approximate form of the wave surface of the section when the surface $\omega^2(\boldsymbol{k}) = z$ is not convex.

Considering the expression (15) as the wave function of the phonon and taking into account that $\boldsymbol{v} = (1/2\pi)\cdot\nabla\omega(\boldsymbol{k})$ is its velocity, we may obtain the value of the effective cross-section for scattering in the given direction,

$$(16) \qquad \sigma = \frac{\varepsilon^2\omega^2}{16\pi^2 v(\boldsymbol{k}) v(\boldsymbol{k}_\nu)\cdot \mathcal{K}_\nu}\cdot \left[1 + \varepsilon\omega^2 \int \frac{\mathrm{d}\boldsymbol{k}}{\omega^2(\boldsymbol{k}) - \omega^2 - i0}\right]^{-2}.$$

In the general case the formulae have the same structure, but the expression for the amplitude, which is not given here, has a considerably more complicated character [7].

2. – Influence of a Local Irregularity on the Crystal Free Energy.

Here we shall calculate the alteration of the vibrational part of the crystal free energy connected with the replacement of one atom by another which differs only in mass [8].

With this aim in view, we shall write the initial equation (6) with the preliminary multiplication of it from the left by $(1 - \varepsilon\hat{\Delta})^{-1}$ in the form

$$(17) \qquad (\hat{L} + \varepsilon'\hat{\Delta}\hat{L})\chi = z\chi; \qquad \varepsilon' = \frac{\varepsilon}{1-\varepsilon}.$$

Thus, the squared oscillation frequencies $z = \omega^2$ of the lattice with the

impurity atom are the eigenvalues of the operator $\hat{L}+\varepsilon'\hat{\Delta}\hat{L}$ or, what is just the same, of a similar hermitian operator $\hat{L}+\varepsilon'\hat{L}^{\frac{1}{2}}\hat{\Delta}\hat{L}^{\frac{1}{2}}$.

The free energy of the oscillations is given, as it is known, by the expression

$$F=\sum_j\left\{\theta\ln\left(1-\exp\left[-\frac{\hbar\omega_j}{\theta}\right]\right)+\frac{\hbar\omega_j}{2}\right\},\qquad \theta=kT\,, \tag{18}$$

where the summation is performed over all eigenfrequencies ω_j.

Assuming the dimensions of the crystal to be finite (*) in order that the expression (18) should have any meaning, we shall write the free energy in the presence and in the absence of the impurity atom respectively in the form

$$\begin{cases} F_0=\mathrm{Sp}\ \varphi(L) \\ F\ =\mathrm{Sp}\,\varphi(\hat{L}+\hat{\Delta})\,, \qquad \hat{\Delta}=\varepsilon'\hat{L}^{\frac{1}{2}}\hat{\Delta}\hat{L}^{\frac{1}{2}}\,, \end{cases} \tag{19}$$

$$\varphi(z)=\theta\ln\left(1-\exp\left[-\frac{\hbar\sqrt{z}}{\theta}\right]\right)+\frac{\hbar\sqrt{z}}{2}\,. \tag{20}$$

Thus, the free energy change upon the replacement of one atom by an impurity atom will be

$$\Delta F=\mathrm{Sp}\,\{\varphi(\hat{L}+\hat{\Delta})-\varphi(\hat{L})\}\,. \tag{21}$$

In the case of an infinite crystal the spectrum of the operator $\hat{L}$ is continuous and $\mathrm{Sp}\,\varphi(\hat{L})$ does not exist. However the difference (21) remains finite: the increment of the free energy caused by the replacement of one atom by another tends to this limit in case of infinite growth of the crystal. Therefore, calculating ΔF we shall consider the limiting case of an infinite crystal, i.e. we shall assume the spectrum of $\hat{L}$ to be continuous.

As it has been already pointed out, the operator $\hat{\Delta}$ and, consequently, $\hat{\Delta}=\varepsilon'\hat{L}^{\frac{1}{2}}\hat{\Delta}\hat{L}^{\frac{1}{2}}$ is a first rank matrix; the matrix elements $\Lambda_{kk'}$ in the $\boldsymbol{k}$ representation will be

$$\Lambda_{\boldsymbol{kk'}}=(\hat{\Delta}\chi^0_{\boldsymbol{k}},\ \chi^0_{\boldsymbol{k'}})=\varepsilon'(\hat{\Delta}\hat{L}^{\frac{1}{2}}\chi^0_{\boldsymbol{k}},\ \hat{L}^{\frac{1}{2}}\chi^0_{\boldsymbol{k'}})=\varepsilon'\omega(\boldsymbol{k})\omega(\boldsymbol{k'}). \tag{22}$$

Thus, the problem is the calculation of the trace of the operator difference (21), where $\varphi(z)$ is a function of the general type, $\hat{L}$ is a hermitian operator

(*) For this purpose it is sufficient to impose on the solution (17) the cyclical condition without changing the type of the matrix $\hat{L}$.

with a continuous spectrum, and $\hat{A}$ is a hermitian operator of a finite number of dimensions (in this case one-dimensional). Such a problem was put and solved in paper [8]; its further complete mathematical analysis is given in paper [9].

The above mentioned papers give the « trace formulae »

$$\mathrm{Sp}\{\varphi(\hat{L}+\hat{A})-\varphi(\hat{L})\} = \int \varphi'(z)\xi(z)\,\mathrm{d}z\,, \tag{23}$$

where $\xi(z)$ is computed in a certain way by the given operators $\hat{L}$ and $\hat{A}$; outside the range of the continuous spectrum of the operator $\hat{L}$ the function $\xi(z)$ is of a step character and corresponds to separate discrete eigenvalues. In our case

$$\Delta F = \int_{\gamma}^{z_g^0} \varphi'(z)\xi_1(z)\,\mathrm{d}z + [\varphi(z_1)-\varphi(z_g^0)]\,, \tag{24}$$

$$\xi_1(z) = \frac{1}{\pi}\,\mathrm{arctg}\,\frac{\pi\varepsilon z\nu_0(z)}{1+\varepsilon z\,\mathrm{S}\int_0^{z_g^0}[\nu_0(\mu)/(\mu-z)]\,\mathrm{d}\mu}\,, \tag{25}$$

$$\nu_0(z) = \int_{\omega^2(\boldsymbol{k})=z} \frac{\mathrm{d}\Omega}{|\nabla\omega^2(\boldsymbol{k})|}\,, \tag{26}$$

where $\mathrm{d}\Omega$ is the element of the surface $\omega^2(\boldsymbol{k}) = z$ over which the integration is performed and S is the principal value of the integral. The last component in (24) appears when the discrete eigenvalue comes into being. This eigenvalue is located in the point determined by the equation (12):

$$1 = \varepsilon z_1 \int \frac{\mathrm{d}\boldsymbol{k}}{z-\omega^2(\boldsymbol{k})}\,. \tag{27}$$

The formulae (24)-(27) solve completely the problem.

To explain these formulae, we shall give an idea of their derivation in our simplest example.

We shall introduce the sequence of operators $\hat{L}_\alpha$ with eigenfunctions $\chi_{\boldsymbol{k}}^0 = \exp[2\pi i\boldsymbol{k}\cdot\boldsymbol{r}]$ and eigenvalues $\lambda_n = n\alpha$, where $n = [\omega^2(\boldsymbol{k})/\alpha]$ (*). Each eigenvalue λ_n of the operator $\hat{L}_\alpha$ for the infinite crystal is infinitely degenerate. As it was shown in paper [2], for the operator with the degenerate spectrum

(*) We indicate with $[p]$ the entire part of any number p.

the addition of a one-dimensional operator $\hat{A}$ decreases by 1 the multiplicity of each eigenvalue of the spectrum: the degenerate values remain in the former place, and the separated eigenvalues settle between the neighbouring eigenvalues λ_n and λ_{n+1}. Thus, the new eigenvalues (the separated ones) of the operator $\hat{L}_\varkappa + \hat{A}$ may be written in the following way, with accuracy up to terms small compared with α:

$$z_n = \lambda_n + \alpha\xi(\lambda_n)\,. \tag{28}$$

The equation for the eigenfunctions of the operator $\hat{L}_\varkappa + \hat{A}$ corresponding to these separated values reads

$$(\hat{L}_\alpha - z_n)\chi = -\hat{A}\chi\,. \tag{29}$$

From (22) we have, for arbitrary f and g,

$$(\hat{A}f, g) = \varepsilon'(f, h)\cdot(h, g), \qquad h = \int \omega(\boldsymbol{k})\chi^0_{\boldsymbol{k}}\,\mathrm{d}\boldsymbol{k}; \tag{30}$$

this yields, with the procedure used to obtain (10), (11)

$$\chi = \varepsilon'(\chi, h)\cdot\sum \frac{1}{z_n - \lambda_n}\int\limits_{\lambda_n<\omega^2(\boldsymbol{k})<\lambda_{n+1}} \omega(\boldsymbol{k})\chi^0_{\boldsymbol{k}}\mathrm{d}\boldsymbol{k}\,. \tag{31}$$

Multiplying scalarly both members of the equality by h and eliminating (χ, h), we obtain

$$1 = \varepsilon' \sum_n \frac{\alpha\lambda_n \nu_0(\lambda_n)}{z_n - \lambda_n}; \qquad \nu_0(z) = \int\limits_{\omega^2(\boldsymbol{k})=z} \frac{\mathrm{d}\Omega}{|\nabla\omega^2(\boldsymbol{k})|}\,. \tag{32}$$

If we assume, according to (28), that $z_n = \lambda_n + \alpha\xi_n$ and we pass to the limit $\alpha \to 0$, we have after some transformations

$$1 = \pi\varepsilon' z\nu_0(z)\operatorname{ctg}[\pi\xi(z)] + \varepsilon' \int \frac{\mu\nu_0(\mu)}{z-\mu}\,\mathrm{d}\mu\,, \tag{33}$$

from which, taking into consideration that $\int \mathrm{d}\boldsymbol{k} = 1$ and $\varepsilon = \varepsilon'/(1-\varepsilon')$ we obtain formula (25). The considered eigenvalues in the limit $\alpha \to 0$ form a continuous spectrum. If a discrete eigenvalue appears, it will be determined from the equation (27).

The expressions obtained for the eigenvalues of the perturbed operator

provide the opportunity of computing the differences of traces by the limit transition $\alpha \to 0$:

$$\Delta F = \lim_{\alpha \to 0} \mathrm{Sp}\{\varphi(\hat{L}_\alpha + \hat{\Lambda}) - \varphi(\hat{L}_\alpha)\} =$$

$$= \lim_{\alpha \to 0} \sum_n \{\varphi[\lambda_n + \alpha\xi(\lambda_n)] - \varphi(\lambda_n)\} + [\varphi(z_1) - \varphi(z_g^0)] =$$

$$= \int_0^{z_g^0} \xi(z)\varphi'(z)\,\mathrm{d}z + [\varphi(z_1) - \varphi(z_g^0)]\,,$$

which corresponds to formula (24).

3. – Spectrum of Frequencies of Disordered Crystals.

3·1. *Trace method.* – The considerations of the preceeding paragraph were applied to the determination of the spectrum of frequencies of the oscillations in disordered crystals (solid solutions) [14, 15].

The paper recently published by Dyson [16] considers such a problem for the particular case of a disordered chain with interaction of nearest neighbours only, but Dyson's method cannot be extended to three-dimensional systems.

The method given below is free from these restrictions. In order to simplify the description, we shall again illustrate it on the idealized case of isotope solution in a simple lattice with one direction of polarization. Thus, we should again proceed from the principal equation (4). However we shall now consider the masses m_r as random quantities capable of two values (two-component solution) with a priori probabilities equal to the concentrations of the corresponding isotopes. The quantity to be defined is the mathematical expectation of the spectral density, i.e. the number of levels for the interval of frequencies. (For a sufficiently large crystal, the practical value of the spectral density coincides with its mathematical expectation).

Considering the deviation of the mass m_r from a certain « principal » mass m as a perturbation (not a small one!) we may prove in the same way as it was done at the beginning of Section 2, that the squares of the eigenfrequencies of the solid solution are the eigenvalues of the operator L^*

$$\hat{L}^* = \hat{L} + \hat{\Lambda}\,, \qquad \hat{\Lambda} = \hat{L}^{\frac{1}{2}}\hat{E}\hat{L}^{\frac{1}{2}}\,, \tag{34}$$

$$E_{rr'} = \varepsilon_r'\delta_{rr'}\,, \qquad \varepsilon_r' = \frac{m - m_r}{m_r}\,. \tag{35}$$

The operator $\hat{E}$, and the perturbation operator $\hat{A}$ as well, are random-operators, because ε_r' are random quantities.

We shall find the difference of the vibrational parts of the free energy of a non-perturbed and perturbed crystal, i.e. the expression

$$F - F_0 = \mathrm{Sp}\,\{\varphi(\hat{L}+\hat{A}) - \varphi(\hat{L})\}\,, \tag{36}$$

($\varphi(z)$ is given by formula (20)). The expression (36) is connected with the difference of spectral densities of oscillations by the immediate relation

$$F - F_0 = N\int\varphi(z)[\nu(z) - \nu_0(z)]\,\mathrm{d}z = -N\int\varphi'(z)\mathrm{d}z\int_0^z[\nu(\mu) - \nu_0(\mu)]\,\mathrm{d}\mu\,, \tag{37}$$

N is the number of atoms in the lattice; $N\nu(z)$ is the spectral density, $\nu_0(z)$ is given by formula (26) for the non-perturbed problem.

In substance, the choice of the function $\varphi(z)$ is not decisive; but the calculation of the free energy is of independent interest.

Let us choose the mass m_1 of the first isotope as the « principal » one. In case of the correlation in the disposition of atoms of the second isotope, of mass m_2, it is necessary to give the correlation functions W_r, $W_{r-r'}$, ... determining the probabilities $P_{r_1 r_2 \ldots r_n}$ of the distribution of n « alien » atoms in the points $\boldsymbol{r}_1, \ldots, \boldsymbol{r}_n$ respectively, along with their concentration c

$$P_r = c\,; \qquad P_{r_1 r_2} = c^2 W_{r_1 - r_2}\,; \quad \ldots\,. \tag{38}$$

In case of absence of long-range order $(W_r)_{r\to\infty} \to 1$; when there is no correlation at all, all $W = 1$.

The spectral density $\nu(z)$, as a function of the concentration c, possesses singularities connected with the appearance of new ranges of frequencies and with the shift of the non-perturbed border of the spectrum. Since the free energy $F - F_0$, on the contrary, does not possess such singularities, we shall perform the development of this quantity in series of powers of the concentration and then, using equation (37), we shall draw the conclusions on the spectral density.

3·2. *Calculations of the free energy of a disordered crystal.* – The development of $F - F_0$ in series of powers of c (asymptotically at high N) is

$$F - F_0 = Ncf_1 + N\frac{c^2}{2}f_2 + \ldots\,, \tag{39}$$

$$Nf_1 = \left(\frac{\partial F}{\partial c}\right)_{c=0} = N(\bar{F}_1 - F_0);$$

$$Nf_2 = \left(\frac{\partial^2 F}{\partial c^2}\right)_{c=0} = N^2(\bar{F}_2 - 2\bar{F}_1 + F_0);$$

. . . . . .

Here F_n is the free energy of the lattice (in which there are n impurity atoms) averaged over all possible configurations of these atoms. Let us denote by the symbol $\psi_n(\boldsymbol{r}_1, ..., \boldsymbol{r}_n)$ these «alien» atoms which are distributed accordingly in the points $\boldsymbol{r}_1, ..., \boldsymbol{r}_n$; evidently $\psi_1(\boldsymbol{r}) = \psi_1$; $\psi_2(\boldsymbol{r}_1, \boldsymbol{r}_2) = \psi_2(\boldsymbol{r}_1 - \boldsymbol{r}_2)$; and $(\psi_2(\boldsymbol{r}))_{r\to\infty} \to 2\psi_1$.

Then it is evident that

$$f_1 = \psi_1 ; \qquad f_2 = \sum_{r\neq 0} W_r[\psi_2(\boldsymbol{r}) - 2\psi_1] ; \quad ... \tag{40}$$

wherefrom

$$F - F_0 = N\left\{c\psi_1 + \frac{c^2}{2}\sum_{r\neq 0} W_r[\psi_2(\boldsymbol{r}) - 2\psi_1] + ...\right\}. \tag{41}$$

Thus, it is enough to calculate the additions to the free energy in case of replacement of no more than n atoms, in order to determine $F - F_0$ of the solution with an approximation up to terms $\sim c^n$.

In replacing n atoms, such an addition runs as follow:

$$\psi_n(\boldsymbol{r}_1, ..., \boldsymbol{r}_n) = \mathrm{Sp}\,\{\varphi[\hat{L} + \hat{\Lambda}_n(\boldsymbol{r}_1, ..., \boldsymbol{r}_n)] - \varphi(\hat{L})\}, \tag{42}$$

$$(\hat{\Lambda}_n)_{\boldsymbol{k}\boldsymbol{k}'} = (\hat{\Lambda}_n\chi_{\boldsymbol{k}}, \chi^0_{\boldsymbol{k}'}) = \varepsilon'\omega(\boldsymbol{k})\omega(\boldsymbol{k}')\sum_{p=1}^{n}\exp[2\pi i(\boldsymbol{k} - \boldsymbol{k}')\cdot\boldsymbol{r}_p]. \tag{43}$$

The perturbation operator $\hat{\Lambda}_n$ has a finite number of dimensions equalling that of the replaced atoms. Using the results mentioned in the preceeding paragraph, we obtain:

$$\psi_n(\boldsymbol{r}_1, ..., \boldsymbol{r}_n) = \int \xi_n(z, \boldsymbol{r}_1, ..., \boldsymbol{r}_n)\cdot\varphi'(z)\mathrm{d}z, \tag{44}$$

$$\xi_n = \frac{1}{\pi}\arg D\left(\delta_{ik} + \varepsilon z\int\frac{J_{r_i - r_k}(\mu)\,\mathrm{d}\mu}{\mu - z - i0}\right), \tag{45}$$

$$J_r(z) = \int_{\omega^2(\boldsymbol{k})=z}\frac{\exp[2\pi i\boldsymbol{k}\cdot\boldsymbol{r}]}{|\nabla\omega^2(\boldsymbol{k})|}\,\mathrm{d}\Omega, \tag{46}$$

where $D(\alpha_{ik})$ denotes the determinant of the n-th order composed of the elements α_{ik}. Particularly, for $\xi_1(z)$ we immediately obtain the formula (25). Formulae (41) and (44) yield finally

$$\begin{cases} F - F_0 = N\int\varphi'(z)Q(z, c)\mathrm{d}z; \\ Q(z, c) = c\xi_1(z) + \dfrac{c^2}{2}\sum W_r[\xi_2(z, \boldsymbol{r}) - 2\xi_1(z)] + ... \end{cases} \tag{47}$$

If there are the discrete eigenvalues $z_j^{(n)}$ which are determined from the equation

$$D\left(\delta_{ik} + \varepsilon z \int_0^{z_g^0} \frac{J_{r_i - r_k}(\mu)}{\mu - z}\,\mathrm{d}\mu\right) = 0\,, \tag{48}$$

then the function ξ_n has a step character outside the interval $(0, z_g^0)$ of the continuous spectrum of the non-perturbed operator. Taking into account the contribution to the free energy determined by these values, we shall write:

$$\frac{F - F_0}{N} = \int_0^{z_g^0} Q(z, c)\cdot\varphi'(z)\,\mathrm{d}z + c[\varphi(z^{(1)}) - \varphi(z_g^0)] + \\ + \frac{c^2}{2}\sum_{r\neq 0} W_r[\varphi(z_1^{(2)}) + \varphi(z_2^{(2)}) - 2\varphi(z^{(1)})] + \ldots . \tag{49}$$

As $z^{(2)}(r) \to z^{(1)}$ at $r \to \infty$, then the values in square brackets quickly decrease and the sum over r converges.

The expression (49) obtained above assumes a particularly simple form at small ε ($\varepsilon \ll 1$). When there is no correlation, the summation may be performed in a closed form and we obtain, with an approximation of the order of $\sim \varepsilon^2$ (at arbitrary concentration):

$$\frac{F - F_0}{N} = \varepsilon c \int_0^{z_g^0} z\varphi'(z)\nu_0(z)\,\mathrm{d}z + \varepsilon^2\left\{c^2\int_0^{z_g^0}\left[z\varphi'(z) + \frac{z^2}{2}\varphi''(z)\right]\nu_0(z)\,\mathrm{d}z - \right. \\ \left. + \frac{c(1-c)}{2}\int_0^{z_g^0}\int_0^{z_g^0}\frac{z^2\varphi'(z) - \mu^2\varphi'(\mu)}{z-\mu}\cdot\nu_0(\mu)\cdot\nu_0(z)\,\mathrm{d}\mu\,\mathrm{d}z\right\} \quad \ldots . \tag{50}$$

At last we shall give, without deducing it, the formula for the addition to the free energy at $\varepsilon \ll 1$ in the actual case of arbitrarily polarized crystal oscillations. The lattice with the average atomic mass $m = m_1(1 - c\varepsilon)$ may be chosen here as a « non-perturbed » one. In this case

$$\begin{cases} F - F_0 = \dfrac{1}{2}\sum\limits_{r,r'}\varepsilon_r\varepsilon_{r'}\displaystyle\int\int \Phi(\boldsymbol{k}, \boldsymbol{k}')\exp\left[2\pi i(\boldsymbol{k} - \boldsymbol{k}')\cdot(\boldsymbol{r} - \boldsymbol{r}')\right]\mathrm{d}\boldsymbol{k}\,\mathrm{d}\boldsymbol{k}'\,, \\ \Phi(\boldsymbol{k}, \boldsymbol{k}') = \sum\limits_{j,j'}(\boldsymbol{q}^j(\boldsymbol{k})\cdot\boldsymbol{q}^{j'}(\boldsymbol{k}'))^2\,\dfrac{\omega_j^2(\boldsymbol{k})\varphi'[\omega_j^2(\boldsymbol{k})] - \omega_{j'}^2(\boldsymbol{k}')\cdot\varphi'[\omega_{j'}^2(\boldsymbol{k}')]}{\omega_j^2(\boldsymbol{k}) - \omega_{j'}^2(\boldsymbol{k}')}\,, \end{cases} \tag{51}$$

($\boldsymbol{q}^j$ are the normalized vectors of polarization corresponding to j vibration branches with frequencies $\omega_j(\boldsymbol{k})$).

If there is no correlation, we obtain

$$F - F_0 = \frac{1}{2} Nc(1-c)\varepsilon^2 \iint \varphi(\boldsymbol{k}, \boldsymbol{k}')\,\mathrm{d}\boldsymbol{k}\,\mathrm{d}\boldsymbol{k}' . \tag{52}$$

3·3. *The spectrum structure.* – The formal comparison of the formulae (46), (47) and (37) at arbitrary $\varphi(z)$ yields for the internal range of the continuous spectrum of the non-perturbed problem

$$\nu(z) - \nu_0(z) = -\frac{\mathrm{d}}{\mathrm{d}z}\left\{c\xi_1 + \frac{c^2}{2}\sum_{r\neq 0}[\xi_2(\boldsymbol{r}) - 2\xi_1]\cdot W_r + \ldots\right\}, \tag{53}$$

and in case $\varepsilon \ll 1$, correspondently,

$$\begin{aligned}\nu(z) - \nu_0(z) = -\frac{\mathrm{d}}{\mathrm{d}z}\Big\{&\varepsilon c z \nu_0(z) - \\ &- \varepsilon^2\left[c(1-c)z^2\nu_0(z)\int\frac{\nu_0(\mu)}{\mu - z}\,\mathrm{d}\mu - \frac{c^2}{2}z^2\nu_0'(z)\right] + \ldots\Big\}.\end{aligned} \tag{54}$$

However, the expressions written above do not hold near the border of the unperturbed spectrum z_g^0, where $\nu_0(z)$ has a singularity $(\nu_0(z) \sim \sqrt{z - z_g^0})$. We shall show how to write the expression for $\nu(z)$ in such a form which does not contain divergencies and which makes it possible to define the shift of the spectrum boundaries. We shall start with the case of the development in series of powers of ε. Let us point out that the expression (50) may be written in the form

$$\begin{cases} F = N\int_0^{z_g^0}\nu_0(z)\{\varphi(z) + \varepsilon a_1\varphi'(z) + \varepsilon^2 a_2\varphi''(z) + \ldots\}\,\mathrm{d}z\,, \\ a_1 = cz + \varepsilon c^2 z + \varepsilon c(1-c)z^2\int_0^{z_g^0}\nu_0(\mu)\,\dfrac{\mathrm{d}\mu}{z-\mu}; \qquad a_2 = \dfrac{c^2z^2}{2}; \ldots . \end{cases} \tag{55}$$

Taking into consideration the fact that the point z_g^0 is not a singularity for the function $\varphi(z)$ and that the coefficients $a_1, a_2, \ldots$ remain finite in the point z_g^0, we may consider the whole expression in the brackets as the development in series of powers of ε of the value

$$\varphi[z + \varepsilon cz + \varepsilon^2\eta(z)]; \qquad \eta(z) = c^2 z + c(1-c)z^2\int_{z_g^0}\frac{\nu_0(\mu)\,\mathrm{d}\mu}{z-\mu}\,. \tag{56}$$

Then a simple substitution of variables in the integral yields

$$\begin{cases} F = \int_0^{z_g} \nu_0[t(z)] \cdot \frac{\mathrm{d}t}{\mathrm{d}z} \cdot \varphi(z)\,\mathrm{d}z\,, \\ z = t + \varepsilon c t + \varepsilon^2 \eta(t)\,, \qquad z_g = z_0^g + \varepsilon c z_g^0 + \varepsilon^2 \eta(z_g^0)\,. \end{cases} \tag{57}$$

Hence

$$\nu(z) = \nu_0[t(z)] \cdot \frac{\mathrm{d}t}{\mathrm{d}z}\,. \tag{58}$$

Analogously, in the case of the development in series of powers of the concentration (at arbitrary ε) we obtain (with an approximation up to the terms $\sim c$)

$$\nu(z) = \frac{\nu_0\left[z - c\dfrac{\xi_1}{\nu_0}\right]}{1 + c\dfrac{\mathrm{d}}{\mathrm{d}z}\left(\dfrac{\xi_1}{\nu_0}\right)}; \tag{59}$$

$$z_g = z_g^0 + \frac{c\varepsilon z_g^0}{1 + \varepsilon z_g^0 \int_0^{z_g^0} \dfrac{\nu_0(\mu)}{\mu - z_g^0}\,\mathrm{d}\mu}\,. \tag{60}$$

Referring to the expression (13) for the critical value ε_{cr} corresponding to the appearence of a discrete eigenvalue, we obtain

$$z_g = z_g^0 \cdot \left(1 + \frac{c\varepsilon\varepsilon_{cr}}{\varepsilon_{cr} - \varepsilon} + \ldots\right). \tag{61}$$

Let us consider now the second part of the free energy in (49) determined by the outsplitted discrete eigenvalues. In the limit case of infinite crystal, these values form a new branch of the continuous spectrum which, generally speaking, may coincide with the principal branch. As to the structure of the expression (49), it should be noted that the point $z^{(1)}$ appearing in the replacement of one atom is the limit-point for the sequence of points $z^{(2)}$, which enter in the terms $\sim c^2$; analogously each point of the sequence $z^{(2)}$ is the limit-point for the sequences $z^{(3)}$ of the spectrum points resulting from the replacement of three atoms and entering the term of the order $\sim c^3$ etc. It should be noted that though the addition to the free energy determined by the range of the separated eigenvalues may be developed in series of powers

of the concentration, the expression for the spectrum density in this interval of z cannot be obtained directly; (the formal transition gives sums of the δ functions which have no meaning).

But, as we are always interested not in the spectral density itself, but in the mathematical expectation of the type (36) computed by means of that density, the developments in series of powers of the concentration (49) obtained above solve the problem.

An analogous method may be used for the study of the influence of the ordering processes on the energetic spectrum of phonons [14]. But we shall not dwell upon this problem in this paper.

3·4. *Some thermodynamical conclusions.* – The expressions obtained for the vibrational part of the free energy make it possible to draw certain thermodynamic conclusions [4].

At low temperatures the main role is played by the zero energy of oscillations which depends on the mutual disposition of atoms. In order to obtain it, we shall assume that in (51), (52): $\varphi(z) = \hbar\sqrt{z}2$. A simple analysis proves that in case of isotopes solution, the zero energy makes the two-phase solution decomposition efficient from the thermodynamic point of view (*).

The thermodynamic potentials obtained above offer the opportunity to consider in principle the thermodynamic properties and the equilibrium diagram of the isotopes solution. But in this case, one should remember that the expression for the correlation functions W_r should themselves be obtained thermodynamically by way of minimization of the sum of the free energy, and the corresponding configuration term $-kT \ln \Omega$, where $\Omega = \Omega(W_r)$, is the number of configurations corresponding to the given values of W_r. It turns out that such a problem may be also solved by way of development in powers of the concentration.

4. – Other Applications of the Method.

In the preceeding Sections we tried mostly to underline the methodological side of the problem and naturally we could not dwell upon the major part of the physical results obtained in this field. Therefore, to conclude, we would like to mention some other problems of the dynamic theory of crystals which can be solved by analogous methods.

(*) It should be noted that a similar conclusion was recently reached by I. Prigogine and J. Jeener (*Physica*, **20**, 516 (1954)), who, by the usual method of quantum mechanical perturbation theory, have found the correction to the ground level connected with a slight difference in masses of the disordered isotopes.

4'1. *Infra-red absorption by disordered crystals.* This problem in connected with the solution of the equation of the forced oscillations of a lattice under the influence of incoming waves. The selective character of absorption in ideal crystals (« residual rays ») is connected with the translational symmetry. Its disturbance leads to the appearance of absorption in the whole range of the phonon spectrum. The frequency dependence of this absorption is found in several limiting cases by determining the complex dielectric constant of the disordered crystal.

4'2. *Surface oscillations of the lattice.* – The method of the local perturbation theory may be applied successfully to the study of the surface oscillations of the lattice [17-20]. In this case its essence consists in the fact that the crystal border is considered as a local perturbation in the infinite crystal, which is expressed by the « exclusion » of the interaction between the atoms lying on both sides of the section.

The surface waves appearing in this case attenuate quickly along the direction normal to the surface and correspond to the « local oscillations » near an irregularity described in Section 1. It should be noted that, due to the regularity of the crystal in the directions parallel to the boundary, the problem has a one-dimensional character and the footnote of pag. 720 applies to it.

The energy spectrum of such « surface phonons » has a peculiar character. One of its branches, in the limiting case of long waves, transforms into the well-known Rayleigh surface waves. The other oscillations form the peculiar surface optical branches which have no analog in the theory of continuum. The consideration of the translation symmetry in the direction parallel to the free surface leads to the fact that only limiting frequencies corresponding to infinitely long surface waves may be optically active, also for the surface optical branches. The presence of such frequencies may lead to the appearance of additional spectral lines in the infra-red absorption spectra of crystals and in those of combinational scattering.

A similar method may be applied to the solution of other problems of mechanics of the crystalline lattice limited by a free surface; such problems appear particularly in the microscopic theory of crystal twinning [21] which describes the initial stage of the process.

In conclusion, it should be noted that the method of local perturbations can be applied also outside the theory of crystals, but these applications did not constitute the topic of this paper.

REFERENCES

[1] I. M. Lifšic: *Dokl. Akad. Nauk SSSR*, **48**, 83 (1945)
[2] I. M. Lifšic: *Žu. Éksper. Teor. Fiz.*, **17**, 1017 (1947).
[3] I. M. Lifšic: *Žu. Éksper. Teor. Fiz.*, **17**, 1076 (1947).
[4] I. M. Lifšic: *J. of Phys. USSR*, **7**, 211 (1943).
[5] I. M. Lifšic: *J. of Phys. USSR*, **7**, 249 (1943).
[6] I. M. Lifšic: *J. of Phys. USSR*, **8**, 89 (1944).
[7] I. M. Lifšic: *Žu. Éksper. Teor. Fiz.*, **18**, 293 (1943).
[8] I. M. Lifšic: *Usp. Matemat. Nauk*, **7**, 170 (1952).
[9] M. G. Krein: *Matemat. Sbornik*, **33**, (75), 597 (1953).
[10] M. Lax: *Phys. Rev.*, **94**, 1391 (1954).
[11] G. F. Koster and J. C. Slater: *Phys. Rev.*, **94**, 1392 (1954).
[12] G. F. Koster and J. C. Slater: *Phys. Rev.*, **95**, 1167 (1954).
[13] G. F. Koster: *Phys. Rev.*, **95**, 1436 (1954).
[14] I. M. Lifšic and G. I. Stepanova: *Žu. Éksper. Teor. Fiz.* (1955) (in the press).
[15] I. M. Lifšic and G. I. Stepanova: *Fiz. Sbornik*, L'vov University, **1** (1955).
[16] F. J. Dyson: *Phys. Rev.*, **92**, 1331 (1953).
[17] I. M. Lifšic and L. N. Rozencvejg: *Žu. Éksper. Teor. Fiz.*, **18**, 1012 (1948).
[18] L. N. Rozencvejg: *Učen. Zap. Hark. Gosud. Univ.*, **2**; *Trudy Fiziko-Matemat. Otdel.*, **2**, 19 (1950).
[19] I. M. Lifšic and L. N. Rozencvejg: *Izv. Akad. Nauk SSSR, Ser. Fiz.*, **12**, 667 (1948).
[20] I. M. Lifšic and S. I. Pekar: *Usp. Fiz. Nauk*, **56**, 531 (1955).
[21] I. M. Lifšic and I. V. Obreimov: *Izv. Akad. Nauk SSSR, Ser. Fiz.*, **12**, 65 (1948).

SUPPLEMENTO AL VOLUME III, SERIE X
DEL NUOVO CIMENTO

N. 4, 1956
1° Semestre

Hydrodynamics of Liquid Helium.

E. M. LIFŠIC and I. M. HALATNIKOV
Academy of Sciences of the USSR - Moscow

CONTENTS. — 1. Introduction. – 2. Hydrodynamical equations of the superfluid. – 3. Dissipative processes.

1. – Introduction,

The aim of the present paper is to give a brief account of the theoretical work, done by L. LANDAU and by the authors on the hydrodynamics of the superfluid helium (the microscopical problems of the theory of superfluidity are entirely omitted in this paper). We hope that such a survey can be so much the more useful, as these questions are widely discussed in the current literature and there exists the opinion that even the problem of the fundamental hydrodynamical equations of liquid helium is not yet entirely solved. J. G. DAUNT and R. S. SMITH, e.g., discuss in their recent survey [1] on an equal basis eight different equations.

2. – Hydrodinamical Equations of the Superfluid.

Meanwhile, the exact system of hydrodynamical equations of the superfluid liquid can be obtained quite unambiguously starting from the conditions imposed by the conservation laws and by the Galilean relativity principle, and also from certain properties of the motion, which are the consequence of the microscopic theory of superfluidity [2-4]. The properties are the following: in the liquid two different motions take place simultaneously with two different velocities $\boldsymbol{v}_s$ and $\boldsymbol{v}_n$; the « superfluid motion » is always conservative (rot $\boldsymbol{v}_s = 0$), and does not transfer entropy; the entropy transport is entirely due to the « normal motion » with the velocity $\boldsymbol{v}_n$.

We write the mass flow density of the liquid $\boldsymbol{j}$ in the form of a sum

$$\boldsymbol{j} = \varrho_s \boldsymbol{v}_s + \varrho_n \boldsymbol{v}_n \,, \tag{1}$$

of two terms, correspondingly due to the superfluid and normal motions. The quantity $\boldsymbol{j}$ is also the volume density of the momentum of the moving liquid. The sum $\varrho_s + \varrho_n$ is the actual density of the liquid ϱ; the quantities ϱ_s and ϱ_n are functions of temperature, pressure and of the relative velocity $\boldsymbol{w} = \boldsymbol{v}_n - \boldsymbol{v}_s$. The conservation of the mass is expressed by the continuity equation

$$\frac{\partial \varrho}{\partial t} + \operatorname{div} \boldsymbol{j} = 0 \,, \tag{2}$$

and the conservation of the momentum, by an equation of the form

$$\frac{\partial j_i}{\partial t} + \frac{\partial \Pi_{ik}}{\partial x_k} = 0 \,, \tag{3}$$

Π_{ik} being the momentum flow tensor (here and in the following the summation is implied over the tensor indices which occur twice).

We shall start from the equations which do not take into account the dissipative processes in the liquid. The first is the equation of the entropy conservation:

$$\frac{\partial (\varrho s)}{\partial t} + \operatorname{div} (\varrho s \boldsymbol{v}_n) = 0 \,, \tag{4}$$

s being the entropy per 1 g of the liquid. The expression $\varrho s \boldsymbol{v}_n$ for the « entropy flow density » corresponds to the fact that entropy is transferred only by the normal motion.

One more equation is to be added which determines the acceleration of the superfluid motion. This equation must be constructed in such a manner, as to ensure the conservative character of the motion:

$$\frac{\partial \boldsymbol{v}_s}{\partial t} = - \operatorname{grad} \varphi \,, \tag{5}$$

where φ is a scalar function.

The hydrodynamical equations (2)-(5) must automatically give the energy conservation law, which is expressed by an equation of the form

$$\frac{\partial E}{\partial t} + \operatorname{div} \boldsymbol{q} = 0 \,, \tag{6}$$

E being the energy per 1 cm³ of the liquid and $\boldsymbol{q}$ the energy flow density. As to the yet undetermined quantities Π_{ik}, $\boldsymbol{q}$, φ, their form can be found on the basis of the Galilean relativity principle.

Let K be the laboratory reference system, and K_0 the system, which is moving relative to K with a velocity equal to the velocity $\boldsymbol{v}_s$ of the superfluid motion in the system K. According to the general mechanical transformation formulae, the values of all the quantities in the system K are connected with their values in the system K_0 (which we supply with an index 0) by means of the following relations:

$$\boldsymbol{j} = \varrho \boldsymbol{v}_s + \boldsymbol{j}_0 , \tag{7}$$

$$E = E_0 + \boldsymbol{j}_0 \cdot \boldsymbol{v}_s + \frac{\varrho v_s^2}{2} , \tag{8}$$

$$\boldsymbol{q} = \left(\frac{\varrho v_s^2}{2} + \boldsymbol{j}_0 \cdot \boldsymbol{v}_s + E_0 \right) \boldsymbol{v}_s + \frac{v_s^2}{2} \boldsymbol{j}_0 + (\Pi_0 \boldsymbol{v}_s) + \boldsymbol{q}_0 , \tag{9}$$

$$\Pi_{ik} = \varrho v_{si} v_{sk} + v_{si} j_{0k} + v_{sk} j_{0i} + \Pi_{0ik} . \tag{10}$$

(here $(\Pi_0 \boldsymbol{v}_s)$ stands for the vector with the components $\Pi_{0ik} v_{sk}$). Since in the system K_0 only the normal motion takes place with the velocity $\boldsymbol{w} = \boldsymbol{v}_n - \boldsymbol{v}_s$, all the quantities with the subscript 0 depend only on the difference $\boldsymbol{w}$, but not on $\boldsymbol{v}_n$ or $\boldsymbol{v}_s$ alone. In particular the vectors $\boldsymbol{j}_0$ and $\boldsymbol{q}_0$ are directed along $\boldsymbol{w}$, and $\boldsymbol{j}_0$ is simply $\varrho_n \boldsymbol{w}$. Thus the formulae (7)-(10) determine the dependence of the required quantities on $\boldsymbol{v}_s$ for a given $\boldsymbol{w}$.

The energy E_0 satisfies the thermodynamic relation

$$\mathrm{d}E_0 = \Phi \, \mathrm{d}\varrho + T \, \mathrm{d}(\varrho s) + \boldsymbol{w} \, \mathrm{d}\boldsymbol{j}_0 . \tag{11}$$

Φ is the Gibbs free energy per 1 g of the liquid and the last term expresses the fact that by differentiating the energy with respect to the momentum we obtain the velocity of the motion.

Further calculations proceed in the following way. We insert E and $\boldsymbol{q}$ from (8) and (9) into equation (6) and calculate $\partial E_0 / \partial t$ from (11). If then all the time derivatives are excluded by means of hydrodynamic equations (2)-(5), equation (6) must be automatically fulfilled. If one takes also into account that the quantities $\boldsymbol{q}_0$, Π_{0ik}, φ depend only on the thermodynamic variables and on the velocity $\boldsymbol{w}$, then it turns out that the energy conservation law is identically fulfilled only for a unique choice of the expressions for $\boldsymbol{q}_0$, Π_{0ik}, φ. The final expressions for φ, $\boldsymbol{q}$, Π_{ik} are:

$$\varphi = \frac{v_s^2}{2} + \Phi , \tag{12}$$

$$\boldsymbol{q} = \left(\Phi + \frac{v_s^2}{2}\right)\boldsymbol{j} + T\varrho s\boldsymbol{v}_n + \varrho_n \boldsymbol{v}_n(\boldsymbol{w}\boldsymbol{v}_n)\,, \tag{13}$$

$$\Pi_{ik} = \varrho_n v_{ni} v_{nk} + \varrho_s v_{si} v_{sk} + p\delta_{ik} \tag{14}$$

with

$$p = -E_0 + T\varrho s + \Phi\varrho + \varrho_n w^2\,. \tag{15}$$

The quantity p is to be regarded as a natural definition of the pressure in the moving liquid; for $w = 0$ it coincides with the usual definition.

The equations (2)-(5) with the definitions (1), (12)-(15) constitute the complete set of the equations of the « two-fluid » hydrodynamics. As such, it is exact in the sense that its derivation implies no assumptions as to the magnitude of the velocities. Of course, it is to be held in mind that actually liquid helium II loses its superfluidity when the velocities are too large. At present the nature of these « critical velocities » is not yet clear, but in any case it has nothing to do with the derivation of hydrodynamical equations as such.

In the physically interesting case of velocities not too large, all the quantities can be developed in powers of w. If we wish to obtain equations correct up to the terms of the second order we must leave in ϱ_s and ϱ_n only the terms of the order zero, that is consider ϱ_s, ϱ_n as independent of w. By differentiating the expression (15) and making use of (11) we get an exact relation:

$$\mathrm{d}\Phi = -s\,\mathrm{d}T + \frac{\mathrm{d}p}{\varrho} - \frac{\varrho_n}{\varrho} w\,\mathrm{d}w\,.$$

Hence it is seen, that the first two terms of the expansion of Φ are:

$$\Phi(p, T, w) = \Phi(p, T) - \frac{\varrho_n}{2\varrho} w^2\,, \tag{16}$$

and by differentiating

$$\begin{cases} s(p, T, w) = s(p, T) + \dfrac{w^2}{2}\dfrac{\partial}{\partial T}\dfrac{\varrho_n}{\varrho}\,, \\ \varrho(p, T, w) = \varrho(p, T) + \dfrac{\varrho^2 w^2}{2}\dfrac{\partial}{\partial p}\dfrac{\varrho_n}{\varrho}\,. \end{cases} \tag{17}$$

The quantities Φ, ϱ, s in the right hand sides of these equalities are the usual Gibbs free energy, entropy and density of the stationary liquid.

By inserting (16) and (17) into the equations (2)-(5) and omitting the terms of the higher order we obtain the approximate equations, which were sought for. In the usual « acoustical » approximation also the second order terms in these equations can be omitted [2, 5]. The second order terms must be taken

into account, e.g. for correct consideration of the temperature « shock waves » which arise in the intensive second sound pulses [6].

It is to be stressed that the unambiguous derivation of the approximate hydrodynamical equations is possible only by means of performing appropriate neglections in the exact equations. If one performs these neglections from the very beginning, then we lose the possibility of an unambiguous derivation on the basis of the conservation laws and of the relativity principle.

3. – Dissipative Processes.

We proceed now to dissipative processes which can occur in the moving helium II. In order to take into account these processes, one must introduce into the hydrodynamical equations additional terms which are proportional to the space derivatives of the velocities and of the temperature. The form of these terms can be established in a most general manner starting from the conditions imposed by the second law of thermodynamics and by Onsager's reciprocity relations [7].

Let ϱ and $\boldsymbol{j}$ be, as above, the mass and the momentum per unit volume of the liquid. Then the continuity equation preserves its original form (2). But into equations (3), (5), (6) additional terms are to be inserted which we write on their right hand sides:

$$\frac{\partial j_i}{\partial t} + \frac{\partial \Pi_{ik}}{\partial x_k} = -\frac{\partial \Pi'_{ik}}{\partial x_k}, \tag{18}$$

$$\frac{\partial \boldsymbol{v}_s}{\partial t} + \operatorname{grad} \varphi = -\operatorname{grad} \varphi', \tag{19}$$

$$\frac{\partial E}{\partial t} + \operatorname{div} \boldsymbol{q} = -\operatorname{div} \boldsymbol{q}'. \tag{20}$$

The entropy equation has no more the form of the continuity equation (4) because the entropy is not conserved. On the contrary, the quantities Π'_{ik}, φ', $\boldsymbol{q}'$ are to be determined so as to ensure the increase of the entropy. For this sake we insert E out of (8) into the energy conservation equation (20) and exclude the time derivatives $\dot{\varrho}$, $\dot{\boldsymbol{j}}$, $\dot{\boldsymbol{v}}_s$ by means of the equations (2), (18), (19). After some calculations the following entropy equation is obtained:

$$T\left\{\frac{\partial(\varrho s)}{\partial t} + \operatorname{div}(\varrho s \boldsymbol{v}_n)\right\} = \tag{21}$$

$$= -\operatorname{div}\{\boldsymbol{q}' + \varphi' \varrho_s \boldsymbol{w} - (\Pi' \boldsymbol{v}_n)\} + \varphi' \operatorname{div}(\varrho_s \boldsymbol{w}) - \Pi'_{ik} \frac{\partial v_{ni}}{\partial x_k}.$$

The most general form of Π'_{ik}, $\boldsymbol{q}'$, φ' which depend linearly on the space derivatives of the velocities and the temperature and which ensure the monotonous increase of the entropy, is the following:

$$\Pi'_{ik} = -\eta\left(\frac{\partial v_{ni}}{\partial x_k} + \frac{\partial v_{nk}}{\partial x_i} - \frac{2}{3}\delta_{ik}\frac{\partial v_{nl}}{\partial x_l}\right) - \delta_{ik}\zeta_1 \operatorname{div} \varrho_s \boldsymbol{w} - \delta_{ik}\zeta_2 \operatorname{div} \boldsymbol{v}_n , \tag{22}$$

$$\varphi' = \zeta_3 \operatorname{div} (\varrho_s \boldsymbol{w}) + \zeta_4 \operatorname{div} \boldsymbol{v}_n , \tag{23}$$

$$\boldsymbol{q}' = -\varphi' \varrho_s \boldsymbol{w} + (\boldsymbol{v}_n \Pi') - \varkappa \nabla T , \tag{24}$$

(in Π'_{ik} we have put in evidence a combination of the derivatives of $\boldsymbol{v}_n$ which has a zero trace, in analogy to what is made in ordinary hydrodynamics). By using Onsager's reciprocity relations one can deduce

$$\zeta_1 = \zeta_4 . \tag{25}$$

All the other coefficients are independent of each other.

By inserting (22)-(24) into (21) and performing some simple transformations, we obtain the following entropy equation:

$$T\left\{\frac{\partial(\varrho s)}{\partial T} + \operatorname{div}\left(\varrho s \boldsymbol{v}_n - \frac{\varkappa \nabla T}{T}\right)\right\} = \tag{26}$$

$$= \frac{\eta}{2}\left(\frac{\partial v_{ni}}{\partial x_k} + \frac{\partial v_{nk}}{\partial x_i} - \frac{2}{3}\delta_{ik}\frac{\partial v_{nl}}{\partial x_l}\right)^2 + 2\zeta_1 \operatorname{div} \boldsymbol{v}_n \operatorname{div} \varrho_s \boldsymbol{w} +$$

$$+ \zeta_2 (\operatorname{div} \boldsymbol{v}_n)^2 + \zeta_3 (\operatorname{div} \varrho_s \boldsymbol{w})^2 + \frac{\varkappa}{T}(\nabla T)^2 .$$

The expression at the right hand side of this equation is the dissipative function which determines the entropy increase. The conditions for this expression to be positive are

$$\eta > 0 , \quad \zeta_2 > 0 , \quad \zeta_3 > 0 , \quad \varkappa > 0 , \quad \zeta_1^2 \leqslant \zeta_2 \zeta_3 . \tag{27}$$

Hence we see that the dissipative processes in helium II are characterized by five independent coefficients: η, φ_1, ζ_2, ζ_3, $\varkappa$. The first is analogous to the usual viscosity coefficient of the ordinary liquids. The next three ones present an analogy to the « second viscosity » coefficient of the ordinary liquids. The last coefficient, $\varkappa$, is analogous to the usual coefficient of thermal conduction. All these quantitiest appear, e.g., in the first and second sound attenuation in helium II. The absorption coefficients of the first and the second sound are

respectively [7, 8]:

$$\alpha_1 = \frac{\omega^2}{2\varrho u_1^3}\left(\frac{4}{3}\eta + \zeta_2\right),$$

$$\alpha_2 = \frac{\omega^2}{2\varrho u_2^3}\left[\frac{\varrho_s}{\varrho_n}\left(\frac{4}{3}\eta + \zeta_2 + 2\varrho\zeta_1 + \varrho^2\zeta_3\right) + \frac{\varkappa}{C}\right]$$

(u_1, u_2 are the first and second sound velocities, C is the heat capacity per 1 g of helium).

We shall discuss now the hydrodynamical equations for ^{3}He-^{4}He mixtures. Besides the conservation equations of the mass (2), momentum (3), entropy (4), and superfluid motion potentiality (5), the complete set of the hydrodynamical equations of a mixture must contain also an equation which expresses the conservation of each of the two substances separately. It can be written in the form:

$$\frac{\partial(\varrho c)}{\partial t} + \operatorname{div} \boldsymbol{g} = 0\,, \tag{28}$$

c being the mass concentration of ^{3}He in the mixture and $\boldsymbol{g}$ the density of the hydrodynamical flow of ^{3}He. It turns out, however, that the general conditions imposed by the conservation laws and by the Galilean relativity principle are insufficient for an unambiguous determination of all the quantities in these equations. It appears to be necessary to make certain additional assumptions on the properties of ^{3}He transfer in the moving liquid. The general conditions mentioned above allow only to draw a definite conclusion for the liquid at the absolute zero temperature: it turns out that in mixtures of arbitrary concentrations ^{3}He can be transferred only by the normal motion. On the other hand it follows from the microscopical theory of superfluidity that, for small impurity concentrations, ^{3}He takes part only in the normal motion at all temperatures from zero up to the λ-point [9]. Hence it appears natural to assume that ^{3}He (which, being pure, is not superfluid) takes part only in the normal motion at arbitrary temperatures and concentrations of the mixture. Thus we have the following expression for the ^{3}He flow:

$$\boldsymbol{g} = \varrho c \boldsymbol{v}_n\,. \tag{29}$$

After this assumption is made, all the other quantities can be determined unambiguously [4]. The equations (2), (3), (4) with the definitions of $\boldsymbol{j}$ and Π_{ik} by (1) and (14)-(15) are not changed, Φ being as before the Gibbs free energy per 1 g of the liquid mixture. For the scalar function φ in the equation (5) and for the energy flow vector $\boldsymbol{q}$ in (6) the following expressions are

obtained:

$$\varphi = \frac{v_s^2}{2} + \frac{\mu_4}{m_4}, \tag{30}$$

$$\boldsymbol{q} = \boldsymbol{j}\left(\frac{\mu_4}{m_4} + \frac{v_s^2}{2}\right) + \varrho c\left(\frac{\mu_3}{m_3} - \frac{\mu_4}{m_4}\right)\boldsymbol{v}_n + \varrho s T \boldsymbol{v}_n + \varrho_n \boldsymbol{v}_n(\boldsymbol{v}_n \boldsymbol{w}) . \tag{31}$$

Here m_3, m_4 stand for the masses of ^{3}He and ^{4}He atoms and μ_3, μ_4 are the chemical potentials of ^{3}He, ^{4}He in the mixture. The potentials μ_3, μ_4 are connected with the Gibbs free energy by means of

$$\Phi = \frac{c}{m_3}\mu_3 + \frac{(1-c)}{m_4}\mu_4 .$$

The equations thus formulated are formally exact in the sense that their derivation implies no assumptions as to the magnitude of the velocities or of the concentration. For small velocities, in the linear approximation, these equations allow us to calculate the sound velocities in dilute solutions of ^{3}He in ^{4}He [10] and in mixtures of arbitrary concentrations [11]. The equations with terms up to the second order can be used in the problem of shock waves which appear in the intensive sound pulses in mixtures [6].

The number of dissipative coefficients in mixtures is of course greater than in pure ^{4}He. A detailed analysis shows, that besides the five quantities which were discussed above there appear another two. These are analogous to the diffusion and thermal diffusion coefficients in ordinary solutions. They too participate in the sound attenuation in ^{3}He-^{4}He mixtures [11].

REFERENCES

[1] J. G. Daunt and R. S. Smith: *Rev. Mod. Phys.*, **62**, 172 (1954).
[2] L. D. Landau: *J. of Phys. USSR*, **5**, 71 (1941); **8**, 1 (1944).
[3] L. D. Landau and E. M. Lifšic: *Mechanics of the continuous media*, 2nd edition, chap. XVI (Moscow, 1953).
[4] I. M. Halatnikov: *Žu. Éksper. Teor. Fiz.*, **23**, 169 (1952).
[5] E. M. Lifšic: *J. of Phys. USSR*, **8**, 110 (1944).
[6] I. M. Halatnikov: *Žu. Éksper. Teor. Fiz.*, **23**, 253 (1952); *Dokl. Akad. Nauk SSSR*, **79**, 237 (1951).
[7] I. M. Halatnikov: *Žu. Éksper. Teor. Fiz.*, **23**, 8, 21 (1952).
[8] I. M. Halatnikov: *Zu. Éksper. Teor. Fiz.*, **20**, 243 (1950).
[9] L. D. Landau and I. Pomerančuk: *Dokl. Akad. Nauk SSSR*, **59**, 669 (1949).
[10] I. Pomerančuk: *Žu. Éksper. Teor. Fiz.*, **19**, 41 (1949).
[11] I. M. Halatnikov: *Žu. Éksper. Teor. Fiz.*, **23**, 265 (1952).

SUPPLEMENTO AL VOLUME III, SERIE X
DEL NUOVO CIMENTO

N. 4, 1956
1° Semestre

On the Relativistic Motion of Electrons in Magnetic Fields when Quantum Effects are Taken into Account.

A. SOKOLOV

State University - Moscow

CONTENTS. — **1.** Introduction. – **2.** Adiabatic invariants. – **3.** Electron motion in a constant and homogeneous magnetic field. – **4.** Study of radial and axial oscillations.

1. – Introduction.

The behaviour of an electron moving in the magnetic field with an energy E which is much higher than its rest energy mc^2 has several peculiar characteristics.

As it was pointed out in the paper by IVANENKO and POMERANČUK [1], the radiation of the relativistic electron at high energies becomes so intensive that the loss of energy may considerably affect the electron motion, e.g. in accelerators, for, according to the laws of classical electrodynamics, the quantity of energy radiated per time unit must increase in proportion to the fourth power of energy:

$$W_0 = \frac{2}{3}\frac{e^2 c\beta^4}{R^2}\left(\frac{E}{mc^2}\right)^4, \tag{1}$$

where e is the electron charge, R is the orbit radius, $c\beta$ is the electron velocity.

Then, ARZIMOVIČ and POMERANČUK [2] found the approximate shift of the spectral distribution of the radiation intensity and proved that the maximum of the radiation intensity does not fall on the main harmonic component, as in the case of the non-relativistic radiation, but on a high overtone ν_{max}, having the order:

$$\nu_{max} \sim \left(\frac{E}{mc^2}\right)^3.$$

Another peculiarity of this radiation is given by the fact that the electromagnetic waves are radiated mostly along the electron motion.

The following task was put before the theoreticians: to determine more precisely the dependence of the radiation intensity on the overtone number.

After several papers had thrown more light upon this problem [3, 4], it was found out that SCHOTT [5] had comparatively long ago obtained a precise formula for the spectral distribution of the radiation of the rotating electron:

$$W_\nu = \frac{e^2 c\beta\nu}{R^2}\left[2\beta^2 J'_{2\nu}(2\nu\beta) - (1-\beta^2)\int_0^{2\nu\beta} J_{2\nu}(x)\,\mathrm{d}x\right], \tag{2}$$

where $J_{2\nu}$ is the Bessel function of the order 2ν.

We should remind you here of the fact that SCHOTT himself has applied this formula to several electrodynamic problems and in particular he attempted to explain the spectral laws of the first atom models.

It is quite difficult, however, to plot the diagram of the dependence of the radiation intensity of the relativistic electron on the harmonic number ν, for the reason that the index ν appears both in the argument and in the order of the Bessel function.

Then we used [6] (see also [7]) the limit formula for the Bessel function of a high order ($x \sim \nu$, $x \leqslant \nu$):

$$J_\nu(x) = \frac{\sqrt{2}}{\pi\sqrt{3}}\left(1-\frac{x}{\nu}\right)^{\frac{1}{2}} K_{\frac{1}{3}}\left(\frac{\sqrt{8}\nu}{3}\left(1-\frac{x}{\nu}\right)^{\frac{3}{2}}\right),$$

for the transformation of the following formula given by SCHOTT:

$$\mathrm{d}W = \frac{9\sqrt{3}}{8\pi} W_0 y\,\mathrm{d}y \int_y^\infty K_{\frac{5}{3}}(x)\,\mathrm{d}x\,, \tag{3}$$

where: $y = (2/3)\nu(mc^2/E)^3$, and the function K is in a simple relation with the Hankel function:

$$K_s(x) = \tfrac{1}{2}\pi i \exp[\pi s i/2] H_s^{(1)}(ix)\,.$$

The formula (3) gives us the possibility to plot comparatively easily the diagram of the $\mathrm{d}W/\mathrm{d}y$ dependence from y (i.e. practically on the overtone number ν as well).

The theory of the relativistic electron radiation has been used in various aspects of physics.

Thus, POMERANČUK [8] has proved that the radiation of the relativistic

electron in the magnetic field of the earth gives us a limit of the energy at which electrons from the interplanetary space can reach the earth.

Developing the ideas of POMERANČUK, VLADIMISRKIJ [9] has studied the influence of the magnetic field of the earth on the Auger extensive showers. The theory of the radiation of the relativistic electron constituted the basis of his work.

He has plotted a curve of the dependence of the radiation intensity on the harmonic ν through the numeric integration of a more complicated expression, but not by means of the formula (5).

In a way the non-thermal radiation of the galaxy appears to be nothing but the radiation of relativistic electrons in the galactic magnetic fields [10-12].

The new radiation is of a particular importance for the study of the electron motion in cyclic accelerators.

One of the main results of that theory was formulated already in the first paper by IVANENKO and POMERANČUK [1], which treated the problems concerned. They proved that at energies of the order

$$E \sim mc^2 \left(\frac{R^2}{r_0 c T}\right)^{\frac{1}{4}},$$

where $r_0 = e^2/mc^2$ and T is the time of the electron motion, this radiation cannot be neglected.

This conclusion was experimentally confirmed by BLEWETT [13] who has shown that the orbit radius decreases by approxymately 3 cm in the betatron calculated for 100 MeV; and this is in good agreement with the theoretical calculations performed by ARZIMOVIČ and POMERANČUK [2] as well as by BLEWETT himself.

This radiation turns out to be strongly polarized, that is, as it was proved in one of our latest papers [14], 7/8 of the radiation consists of a radiation whose electric field vector is perpendicular to the external magnetic field, and only 1/8 of the radiation has the vector almost parallel to that field.

This radiation (i.e. the radiation of the so-called optical electron) was experimentally discovered by POLLOCK and others [15, 16].

The losses of energy in the betatron turned out to be very large, and so a new method for accelerating electrons in cyclic installations (synchrotrons) at high energies was introduced. That method was based upon the principle of autophasing.

This principle was worked out first by VEKSLER [17] and by MC MILLAN [18] with the aim of accelerating electrons in such a way that not only the relative mass increase should be taken into consideration, but the losses of energy on radiation must be compensated as well.

Thus, the theoretical formulae for the losses of energy on radiation quickly found their practical application.

The problem of taking into account the quantum effects in the optical electron theory has turned out to be far from being a trivial one.

SCHWINGER [7] and VLADIMIRSKIJ [9] considered it possible to neglect the quantum effects when the radiated photon energy $\varepsilon = \hbar(c/R)(E/mc^2)^3$ was smaller than the electron energy $E(\varepsilon < E)$.

The qualitative data of these authors established the condition for a classical approximation:

$$E < E_{\frac{1}{2}} = mc^2\left(\frac{mcR}{\hbar}\right)^{\frac{1}{2}}. \tag{4}$$

The last formula testifies to the fact that the quantum corrections would become noticeable at the minimum energy of several 100 GeV in the now existing cyclic installations.

In an earlier paper [19] on the quantum theory of the optical electron we quantized not only the rotatory motion (quantum number l) but the radial oscillation (quantum number s) as well. We have proved that in the classical case the radiation does not affect the amplitude of radial oscillations, i.e. the quantum number s. According to our calculations, based on the quantum theory, starting with the energies

$$E > E_{\frac{1}{5}} = mc^2\left(\frac{mcR}{\hbar}\right)^{\frac{1}{5}}, \tag{5}$$

the quantum number s should change. That has driven us to the conclusion that the quantum effects must to a certain extent be taken into account, beginning with the energies $E \sim E_{1/5}$, where the energy $E_{1/5}$ is of the order of several hundred MeV.

We did not succeed in obtaining any quantitative result in our first paper on the quantum theory of the optical electron.

After that we brought more light to this problem (see [20] pp. 288, 289). In particular we came to the conclusion that the terms of the order $E/E_{1/5}$ decrease when we considerer the total radiation intensity (i.e. the radiation summed on all final values of the radial quantum number s') and the criterium (4) for quantum corrections did take place in this particular case. Though we did not neglect the possibility that a weaker criterium (5) may appear in other cases.

Then PARZEN's [21] work was published, and again the author used our criterium (5). But he did not notice here that, beginning with the energies $E \sim E_{1/5}$, the quantum number s would change as well. PARZEN limited his calculations by the assumption that $s = s' = 0$ and thus obtained the following expression for the integral radiation intensity

$$W_{qu} = W_0 \exp\left[-\alpha(E/E_{1/5})^5\right], \tag{6}$$

where $\varkappa$ is a coefficient of the order of unity. Hence PARZEN came to a wrong conclusion, according to which at high energies the quantum effects would sharply decrease the radiation intensity. But, as we had proved [20] even before the paper by PARZEN appeared, and as it was shown in other articles subjecting PARZEN's works to criticism [22-25], the terms of the order $E/E_{1/5}$ disappeared in the calculation of the total radiation intensity when summed on all final values of s'.

After that, the problem became somewhat more difficult and some authors assumed (see [26]) that the criterium (5) for the appearance of certain quantum effects is not correct.

We obtained several qualitative formulae and proved that beginning with the energies hardly exceeding $E_{1/5}$, a quantum excitation of macroscopic radial oscillations appears, which quickly covers the classical damping.

These quantum radial oscillations may in a way affect also the angular distribution of the radiation intensity.

It is difficult to draw a final conclusion on how strongly the quantum effects would influence the work of cyclic electron accelerators, until these effects have not been experimentally found. But in this article we treat the fundamentals of the quantum theory of the optical electron which has been developing up to now independently from experiments.

2. – Adiabatic Invariants.

The relativistic electron motion in the magnetic field will be described with the cylindrical coordinates: $r = \sqrt{x^2+y^2}$, z, φ.

As it is known, the following relation should take place in a betatron near the stationary orbit ($r \sim R_0$, $z \sim 0$):

$$\tfrac{1}{2}\bar{H} = H \,. \tag{7}$$

and the magnetic field H, as well as its average value $\bar{H}$, are directed along the axis z.

Together with the condition:

$$\operatorname{div} \boldsymbol{H} = 0 \tag{8}$$

there is also another condition in the plane $z = 0$:

$$\operatorname{rot} \boldsymbol{H} = 0 \,, \tag{9}$$

which expresses the absence of sources in the orbit plane.

We shall satisfy the last equality admitting that

$$\tfrac{1}{2}\bar{H}(r, z) = \frac{B}{(2-q)r^q}\left(1 + \frac{q(2-q)}{2}\frac{z^2}{r^2}\right) + \frac{1-q}{2-q}\frac{B}{r^2 R_0^{q-2}}, \tag{10}$$

where R_0 is the radius of the stationary orbit, and B is a constant coefficient.

The vector potential $\boldsymbol{A}$ is:

$$A_x = -\tfrac{1}{2}y\bar{H}, \qquad A_y = \tfrac{1}{2}x\bar{H}, \qquad A_z = 0, \tag{11}$$

while the magnetic field in the stationary orbit plane ($z = 0$) will change in accordance with the law:

$$H = \frac{B}{r^q}. \tag{12}$$

The Lagrange function and the generalized impulses are in this case:

$$L = -mc^2\sqrt{1 - \frac{1}{c^2}(\dot{r}^2 + r^2\dot{\varphi}^2 + \dot{z}^2)} - \frac{e}{2c}Hr^2\dot{\varphi}, \tag{13}$$

$$p_\varphi = \frac{e}{c}r^2(H - \tfrac{1}{2}\bar{H}), \qquad p_r = \frac{E}{c^2}\dot{r}, \qquad p_z = \frac{E}{c^2}\dot{z}, \tag{14}$$

and the electron energy is given by:

$$E = \frac{mc^2}{\sqrt{1-\beta^2}}. \tag{15}$$

The quantum numbers are simply introduced by quantization of the adiabatic invariants:

$$\oint p_\varphi \mathrm{d}\varphi = 2\pi\hbar l, \qquad \oint p_r \mathrm{d}r = 2\pi\hbar s, \qquad \oint p_z \mathrm{d}z = 2\pi\hbar k. \tag{16}$$

According to the well-known Erenfest adiabatic principle, the adiabatic invariants should remain unchanged in case of slow alteration of the magnetic field.

As it is evident in particular from (14) and (7), all adiabatic invariants must vanish ($l = s = k = 0$) on the stationary orbit ($r = R_0 = \mathrm{const}$, $z = 0$).

Let us consider the electron motion when the adiabatic invariants do not vanish. In this case the electron energy is connected with the moments

by the equality:

$$\frac{E^2}{c^2} - m^2c^2 = p_r^2 + p_z^2 + V(r, z)\,, \tag{17}$$

where

$$V = \left(\frac{\hbar l}{r} + \frac{e}{c}\frac{r\overline{H}}{2}\right)^2. \tag{18}$$

The radius R of the instantaneous equilibrium orbit can be obtained from the condition:

$$\frac{\partial V}{\partial r} = \frac{\partial V}{\partial z} = 0\,. \tag{19}$$

Hence we obtain

$$R = R_0\left[1 + \frac{c\hbar l(2-q)}{eR_0^2 H(R_0)(1-q)}\right]^{1/(2-q)}. \tag{20}$$

The radial and axial oscillations will go on in accordance with the law:

$$x = r - R = a\sin\omega_1 t\,, \qquad z = b\sin\omega_2 t\,. \tag{21}$$

where

$$\omega_1 = \sqrt{1-q}\,\frac{c}{R}\,, \quad \omega_2 = \sqrt{q}\,\frac{c}{R}\,. \tag{22}$$

Thus, the motion will be stable if $0 < q < 1$.

Introducing the solution (21) into (16) and taking (14) into consideration, we shall obtain

$$a^2 = \frac{2c\hbar s}{eH(R)\sqrt{1-q}}\,, \tag{23}$$

$$b^2 = \frac{2c\hbar k}{eH(R)\sqrt{q}}\,. \tag{24}$$

It is evident from the formulae (20), (23) and (24) that together with the increase of the magnetic field H, when one can neglect the radiation (l, s, $k = \text{const}$), the radius R of the instantaneous equilibrium orbit will tend to the stationary orbit radius R_0, while the amplitudes of the radial and axial oscillations will go down according to the law $H^{-\frac{1}{2}}$.

Even if one takes into account the radiation, then in the classical case the adiabatic invariants $\hbar s$ and $\hbar k$ will remain unchanged. In this case the ra-

diation has only the result of decreasing the adiabatic invariant $\hbar l$, i.e. the orbit radius.

First of all, using the quantum theory, we should determine the radiation influence on the alterations of the adiabatic invariants $\hbar s$, $\hbar k$.

3. Electron Motion in a Constant and Homogeneous Magnetic Field.

It is quite difficult to find a general solution to this problem in the field (10) using the quantum theory only. Therefore we shall first of all consider the case of a constant and homogeneous magnetic field, when the vector potential undergoes changes in accordance with the law:

$$A_x = -\tfrac{1}{2}yH\,, \qquad A_y = \tfrac{1}{2}xH\,, \qquad A_z = 0\,. \tag{25}$$

We shall use the Dirac equation in order to solve this problem:

$$(E - e(\boldsymbol{\alpha}\cdot\boldsymbol{P}) - mc^2\varrho_3)\psi = 0\,, \tag{26}$$

where

$$\boldsymbol{P} = \frac{\hbar}{i}\boldsymbol{\nabla} + \frac{e}{c}\boldsymbol{A}\,.$$

We can obtain now the solution of the Dirac equation. It runs as follows:

$$\psi_\mu = \frac{\exp\,[ik_z z]}{\sqrt{L}}\,\frac{\exp\,[il_\mu\varphi]}{\sqrt{2\pi}}\,f_\mu(r)\,, \tag{27}$$

where $\mu = 1, 2, 3, 4$; L is the normalization length; $l_{1,3} = l - 1$, $l_{2,4} = l$; while for the function $f_\mu(r)$ we have the expression:

$$f_{1,2,3,4}(r) = \frac{\sqrt{\gamma}}{1 + (k_0/K)} \begin{cases} C_1\left(1 + \dfrac{k_0}{K}\right) I_{n-1,s}(\varrho)\,, \\ iC_2\left(1 + \dfrac{k_0}{K}\right) I_{n,s}(\varrho)\,, \\ \left(\dfrac{\sqrt{4\gamma n}}{K}\,C_2 + \dfrac{k_z}{K}\,C_1\right) I_{n-1,s}(\varrho)\,, \\ i\left(\dfrac{\sqrt{4\gamma n}}{K}\,C_1 - \dfrac{k_z}{K}\,C_2\right) I_{n,s}(\varrho)\,. \end{cases} \tag{28}$$

where

$$\varrho = \gamma r^2, \qquad \gamma = \frac{eH}{2c\hbar}, \qquad k_0 = \frac{mc}{\hbar}.$$

K is related with the energy by the following formula:

$$E = c\hbar K = c\hbar\sqrt{k_0^2 + k_z^2 + 4\gamma n}. \tag{29}$$

The function $I_{n,s}$ has the expression:

$$I_{n,s}(\varrho) = \frac{1}{\sqrt{n!s!}} \exp\left[-\tfrac{1}{2}\varrho\right]\varrho^{(n-s)/2} Q_s^{n-s}(\varrho). \tag{30}$$

Here $Q_s^l(\varrho)$ are the generalized Laguerre polynomials:

$$(-1)^l \varrho^{-l} Q_{s+l}^{-l}(\varrho) = Q_s^l(\varrho) = (-1)^s \sum_{\mu=0}^{s} (-1)^\mu \frac{s!(s+l)!\varrho^{s-\mu}}{\mu!(s-\mu)!(s+l-\mu)!}. \tag{31}$$

The coefficients C_1 and C_2 characterize the spin state of the electron.

We assume for the initial condition that

$$|C_1|^2 = |C_2|^2 = \tfrac{1}{2},$$

and for the final one:

$$|C_1'|^2 + |C_2'|^2 = 1.$$

The principal quantum number $n = l + s$ assumes the values: 0, 1, 2, 3,..., the radial quantum number s changes from 0 to ∞, and the azimuth l from $-\infty$ to n.

One should notice that in the case of a constant and homogeneous magnetic field the motion along the axis z is free.

First of all we should calculate the radiation intensity for the electron transition from the quantum state n, s, $k_z = 0$ (plane case) into another state $n' = n - \nu$, $s' = s - \nu'$ and k_z'.

For that purpose we shall use the formula which is known from the theory of radiation:

$$W_{\nu,\nu'} = \int_0^\pi \sin\theta c\hbar\varkappa w_{\nu,\nu'}(\theta)\,\mathrm{d}\theta, \tag{32}$$

where

$$\varkappa = K - K' = \frac{K}{\sin^2\theta}\left(1 - \sqrt{1 - \frac{\nu}{n}\beta^2 \sin^2\theta}\right),$$

θ is the angle between the wave vector $\boldsymbol{\varkappa}$ and the axis z. We have the following value for the probability $w(\theta)$ of the transition:

$$w_{\nu,\nu'}(\theta) = \frac{e^2\varkappa}{\hbar}\,(\boldsymbol{a}\cdot\boldsymbol{j}^+)(\boldsymbol{a}^+\cdot\boldsymbol{j})\,.$$

Here $\boldsymbol{a}$ are the amplitudes of the photon field which satisfy the relation (s, $s' = 1, 2, 3$):

$$a_s a_{s'}^+ = \delta_{ss'} - \frac{\varkappa_s \varkappa_{s'}}{\varkappa^2}\,,$$

and the matrix element $\boldsymbol{j}$ equals:

$$\boldsymbol{j} = \int \psi^+_{n',s',k'_z} \exp\,[i\boldsymbol{\varkappa}\cdot\boldsymbol{r}]\boldsymbol{\alpha}\psi_{n,s,k_z}\,\mathrm{d}^3x\,. \tag{33}$$

Hence we obtain the following expression for the value of the probability $w_{\nu,\nu'}(\theta)$ (see [14])

$$\begin{aligned} w_{\nu,\nu'}(\theta) = \frac{e^2\varkappa}{\hbar}\, I^2_{s,s'}(x)\,\frac{n\gamma}{KK'}\Bigg\{\sqrt{\frac{n'}{n}}\,[(I_{n,n'-1} - I_{n-1,n'})^2 + \cos^2\theta(I_{n,n'-1} + I_{n-1,n'})^2 + \\ + \sin^2\theta(I_{n,n'} - I_{n-1,n'-1})^2] + 2\sqrt{\frac{x}{n}}\cos^2\theta\cdot(I_{n-1,n'-1}I_{n,n'-1} + I_{n-1,n'}I_{n,n'}) + \\ + \frac{1}{2}\,\frac{x_0}{n}\cdot\left(1 - \frac{x}{x_0}\right)\cdot[(1 + \cos^2\theta)(I^2_{n,n'-1} + I^2_{n-1,n'}) + \sin^2\theta\cdot(I^2_{n,n'} + I^2_{n-1,n'-1})]\Bigg\}, \end{aligned} \tag{34}$$

where

$$x = \frac{\varkappa^2 \sin^2\theta}{4\gamma}\,,\quad x_0 = (\sqrt{n} - \sqrt{n - \nu})^2\,,$$

and the function $I_{n,n'}(x)$ is determined by the equality (30).

We have combined the Bessel function $J_{2\nu}$ with the function $K_{\frac{1}{3}}$ in order to obtain the classical formula for the radiation (see [6]). In this case, i.e. in the quantum case we should combine the function $I_{n,n'}$ with $K_{\frac{1}{3}}$ as well.

Using the method described in [20] (see § 42), we shall obtain (see also [28]):

$$I_{n,n'}(x) \cong \frac{1}{\pi\sqrt{3}}\left(1 - \frac{x}{x_0}\right)^{\frac{1}{2}} K_{\frac{1}{3}}\left(\frac{2}{3}\,(nn')^{\frac{1}{4}}x_0^{\frac{1}{2}}\left(1 - \frac{x}{x_0}\right)^{\frac{3}{2}}\right). \tag{35}$$

For $\beta \cong 1$ we have:

$$1 - \frac{x}{x_0} = \sqrt{\frac{n}{n'}} (1 - \beta^2 \sin^2 \theta) .$$

Hence we obtain the following formula for the radiation intensity (see [27-29]), taking into account the terms proportional to $\hbar$ and $\hbar^2$:

$$W = \sum_{\nu,\nu'} \int_0^{\pi} \sin\theta c\hbar\varkappa w_{\nu,\nu'}(\theta) \mathrm{d}\theta = W_0 \left(1 - \frac{55\sqrt{3}}{24}\zeta - \frac{64}{3}\zeta^2 - \ldots\right), \quad (36)\ (*)$$

where

$$\zeta = \frac{3}{2} \frac{\hbar}{mcR_0} \left(\frac{E}{mc^2}\right)^2 .$$

Here we have taken into consideration that

$$\sum_{s'} I^2_{s,s'}(x) = 1 . \quad (37)$$

Hence it is evident that the quantum corrections would influence the total intensity of the optical electron radiation only within the range of energies comparable with $E_{\frac{1}{2}}$, where:

$$E_{\frac{1}{2}} = mc^2 \left(\frac{mcR_0}{\hbar}\right)^{\frac{1}{2}} . \quad (38)$$

If $\hbar \to 0$ the last expression turns into the classical one.

We shall now appraize the influence of spin corrections on the radiation intensity.

With this aim in view we shall determine the magnitude w^0 for the corresponding spinless wave equation (see [14-30]):

$$w^0_{\nu,\nu'}(\theta) = \frac{e^2\varkappa}{\hbar} I^2_{s,s'}(x) \frac{n\gamma}{KK'} \cdot \left[(I_{n+1,n'} - I_{n-1,n'})^2 + \cos^2\theta (I_{n+1,n'} + I_{n-1,n'})^2\right] . \quad (39)$$

Then, instead of the formula (36) we shall have the expression obtained

(*) We shall have the following expression (see [27]) for the radiation spectral intensity with the account of the terms proportional to $\hbar$:

$$\mathrm{d}W = \frac{9\sqrt{3}}{8\pi} W_0 y \mathrm{d}y \left[\int_y^{\infty} K_{\frac{5}{3}}(x)\,\mathrm{d}x - \zeta y^2 K_{\frac{2}{3}}(y)\right] .$$

(see [14]) for the radiation intensity:

$$W = W_0\left(1-\frac{55\sqrt{3}}{24}\varsigma+\frac{56}{3}\varsigma^2+\ldots\right). \tag{40}$$

Let us prove that the additional radiation is due to the spin magnetic moment of the Dirac electron.

In fact, the energy of the spinless particle is

$$E^0 = c\hbar\sqrt{k_0^2+k_z^2+4\gamma(n+\tfrac{1}{2})}\,. \tag{41}$$

Then, equalling the difference of the electron energy with the spin (see (29)) and that without it (see (41)) to the magnetic moment energy $-\mu H$, we obtain:

$$\mu \cong \mu_0\frac{mc^2}{E},$$

where

$$\mu_0 = \frac{e\hbar}{2mc},$$

while the ratio of the intensity W_μ of the radiation resulting from the magnetic moment and that coming from the charged particle, W_e, is of the order

$$\frac{W_\mu}{W_e}\sim\left(\frac{\mu}{e}\frac{\omega_{\max}}{e}\right)^2\sim\varsigma^2, \tag{42}$$

where

$$\omega_{\max}\sim\frac{c}{R_0}\left(\frac{E}{mc^2}\right)^3. \tag{43}$$

Hence it is evident that, in keeping with the formulae (36) and (40), the account of the intrinsic magnetic moment yields the corrections only in quantum terms of the second order in ζ^2.

That is why SCHWINGER [31], calculating the spinless electron radiation intensity taking account only of the quantum terms of the first order, has obtained a formula which perfectly coincides with that for the Dirac particles obtained by us (see [14, 29]).

We shall now examine in the quantum case the possibility of variations of the adiabatic invariants $\hbar s$ due to the radiation.

The time variation of $\hbar s$ may be determined by means of the equality

$$\frac{\mathrm{d}\hbar s}{\mathrm{d}t} = -\hbar\sum_{\nu,\nu'}\nu'\int_0^\pi \sin\theta w_{\nu,\nu'}(\theta)\mathrm{d}\theta\,. \tag{44}$$

We substitute in (44) the following approximate expression of $w_{\nu,\nu'}$, obtained from (34) neglecting higher powers of $\hbar$:

$$w_{\nu,\nu'} = \frac{e^2\nu}{3\pi^2 R\hbar}\, I^2_{s,s'}(x)\left\{\varepsilon^2 K^2_{\frac{2}{3}}\left(\frac{\nu}{3}\,\varepsilon^{\frac{3}{2}}\right) + \varepsilon\cos^2\theta K^2_{\frac{1}{3}}\left(\frac{\nu}{3}\,\varepsilon^{\frac{3}{2}}\right)\right\}, \tag{45}$$

where

$$\varepsilon = 1 - \beta^2\sin^2\theta\,.$$

Further on, summing over ν', we shall take into consideration the equality which characterizes the variation of s in one transition:

$$\Delta s = \sum_{s'}(s - s')I^2_{s,s'}(x) = x \approx \frac{c\hbar\nu^2}{2R^2 eH}\,, \tag{46}$$

while the sum over ν will be replaced by the integration over μ. Then we obtain (see also [27]):

$$\frac{\mathrm{d}\hbar s}{\mathrm{d}t} = \frac{55}{48\sqrt{3}}\,\frac{e^2\hbar}{mcR^2}\left(\frac{E}{mc^2}\right)^6. \tag{47}$$

Hence it is evident that in the classical case ($\hbar \to 0$) the adiabatic invariant $\hbar s$ given by (32) does not change.

4. – Study of Radial and Axial Oscillations.

First of all we shall generalize the formula (46) obtained for a constant and homogeneous field which changes in keeping with the law (12).

Together with that we shall consider the case when the amplitudes of the radial and axial oscillations are much smaller than the orbit radius $s \ll n$, $k \ll n$.

As it is evident from formula (20), the photon radiation with the energy $\Delta E = \hbar\nu(c/R)$ will lead to the decrease of the orbit radius by the value

$$\Delta R = \frac{1}{2 - q}\,\frac{\nu}{n}\,R = \frac{1}{1 - q}\,\frac{\Delta E}{E}\,R\,, \tag{48}$$

where:

$$n = l + l_0, \qquad l_0 = \frac{R_0^2 eH(R_0)(1 - q)}{c\hbar(2 - q)}\,. \tag{49}$$

On the other hand, as it follows from formula (23), the minimum change of the square of the radial oscillations amplitude, corresponding to $\Delta s = 1$, is

$$\Delta(a^2)_1 = \frac{2c\hbar}{eH\sqrt{1 - q}}\,. \tag{50}$$

If

$$(\Delta R)^2 < \Delta(a^2)_1 , \tag{51}$$

the radius fluctuation due to the radiation will not change the amplitude of radial oscillations (case of classical approximation).

If, on the contrary,

$$(\Delta R)^2 > \Delta(a^2)_1 , \tag{52}$$

the radiation may strongly influence the amplitude of radial oscillations.

With the help of (18) and (50) we find the energy at which the condition (52) will be satisfied:

$$E > E_{\frac{1}{5}} = mc^2 \left(\frac{mcR_0}{\hbar} \right)^{\frac{1}{5}} . \tag{53}$$

The last inequality was obtained in [19], and in [20] the authors proved (see p. 290) that it conditions the possibility of quantum transitions with variation of the radial quantum number s.

Taking into account the statical independence of the photonic radiation in the quantum range, one may prove that at high energies $E > E_{1/5}$ the radius variation ΔR during the emission of a single quantum of radiation will cause a variation in the square of the radial oscillations amplitude by

$$\Delta(a^2) = (\Delta R)^2 , \tag{54}$$

i.e. during a single emission the adiabatic invariant increases by

$$\Delta s = \frac{c\hbar\nu^2}{2(1-q)^{\frac{3}{2}} R^2 eH(R)} . \tag{55}$$

We have deduced this equality only for a constant and heterogeneous field: $q = 0$ (see (46)). Therefore in a general case, instead of formula (47), we shall have the following expression characterizing the variation per time unit of the adiabatic invariant $\hbar s$:

$$\frac{d\hbar s}{dt} = \frac{55}{48\sqrt{3}(1-q)^{\frac{3}{2}}} \frac{e^2\hbar}{mcR^2} \left(\frac{E}{mc^2} \right)^6 . \tag{56}$$

Hence we can deduce the law of variation for the square of the amplitude of

radial oscillations (see [33, 34]):

$$a^2 = a_0^2 \frac{H_0}{H} + \frac{55}{24\sqrt{3}} \frac{e^2\hbar R}{mE(1-q)^2} \int_0^t \left(\frac{E}{mc^2}\right)^6 \frac{\mathrm{d}t}{R^2} . \tag{57}$$

The first term characterizes the classical damping of the square of amplitude, inversely proportional to H (a_0^2 is the square of the oscillations amplitude, H_0 is the magnetic field at $t = 0$), the second term gives the excitation of radial oscillations resulting from the quantum character of the radiation.

As the classical term quickly vanishes with increasing energy, for sufficiently large energies we should draw our attention to the quantum excitation of the radial oscillations only.

Recently SANDS [35] has examined the problem of the influence of quantum fluctuations of the radiation upon the radial phase-oscillations in the synchrotron.

We should first of all notice that the quantum fluctuations connected with the radiation yield directly a variation of the radius, and thus must not depend on the frequency of the oscillations. SANDS' theory and ours should therefore differ in the method of accounting for the damping. The damping of the square amplitude of radial oscillations is inversely proportional to H, while the square amplitude of the radial-phase oscillations goes down in keeping with the exponential law $\exp[-t/\tau]$ and the time of the damping is

$$\tau = \frac{1-q}{3-4q} \frac{E}{W_0} . \tag{58}$$

In order to obtain SANDS' formula from our formulae one should place the attenuation factor $\exp[-t/\tau]$ in the integral of the expression (57) and assume $E = \text{const}$.

Then, leaving aside the first classical term of the series expansion we find

$$\frac{\overline{(\Delta r)^2}}{R^2} = \frac{55}{32\sqrt{3}} \frac{1}{(1-q)(3-4q)} \frac{\hbar}{mcR} \left(\frac{E}{mc^2}\right)^2 . \tag{59}$$

Deducing the last formula, we have taken into consideration the fact that the increase of the square average fluctuation of the radius is:

$$(\Delta r)^2 = \tfrac{1}{2}\Delta(a^2) .$$

In analogy to this fact it is quite easy to prove that the excitation of axial

oscillations resulting from the quantum fluctuations will go on at energies

$$E > E_{\frac{1}{3}} = mc^2 \left(\frac{mcR}{\hbar}\right)^{\frac{1}{3}}. \tag{60}$$

More precise calculations, performed with the participation of TERNOV, yielded the following formula, which characterizes the alteration of the amplitude of axial oscillations:

$$b^2 = b_0^2 \frac{H_0}{H} + \frac{13}{24\sqrt{3}} \frac{e^2\hbar R}{mEq} \int_0^t \left(\frac{E}{mc^2}\right)^4 \frac{\mathrm{d}t}{R^2}. \tag{61}$$

Let us prove that the electron passes from the classical condition to the quantum one, when, owing to spontaneous radiation, the quantum number s changes at least by a unity.

In fact, according to formulae (23) and (14), the coordinate $x = r - R$ and the radial impulse p will be of the order:

$$x \sim \sqrt{\frac{c\hbar s}{eH}}, \qquad p \sim \sqrt{\frac{eH\hbar s}{c}}.$$

If s changes by a unity, then $\Delta x \sim x/s$, while $\Delta p \sim (\hbar/\Delta x) \sim p$.

Therefore the classical approximation cannot be used.

Leaving aside the problem of the necessity of taking into account the quantum effects in designing the high-energy cyclic accelerators for electrons, we should point out the fact that in these accelerators we will have to deal with a sort of a « macroatom », as the amplitude of radial oscillations assumes a macroscopic size, while the laws of the oscillation become the quantum ones. There is also the possibility to observe the region of the electron transition from the classical condition to the quantum one.

REFERENCES

[1] D. IVANENKO and I. JA. POMERANČUK: *Phys. Rev.*, **65**, 343 (1944); see also *Dokl. Akad. Nauk SSSR*, **44**, 343 (1944).
[2] L. ARZIMOVIČ and I. JA. POMERANČUK: *J. of Phys. USSR*, **9**, 267 (1945).
[3] J. SCHWINGER: *Phys. Rev.*, **70**, 798 (1946).
[4] L. SHIFF: *Rev. Sci. Instr.*, **17**, 6 (1946).
[5] G. SCHOTT: *Ann. d. Phys.*, **24**, 641 (1907); *Phil. Mag.*, **13**, 189 (1907); see also *Electromagnetic Radiation*, (Cambridge, 1912) pp. 109, 110.
[6] D. IVANENKO and A. SOKOLOV: *Dokl. Akad. Nauk SSSR*, **59**, 1551 (1948).
[7] J. SCHWINGER: *Phys. Rev.*, **75**, 1912 (1949).

[8] I. Ja. Pomerančuk: *Žu. Éksper. Teor. Fiz.*, **9**, 915 (1939).
[9] V. Vladimirskij: *Žu. Éksper. Teor. Fiz.*, **18**, 392 (1948).
[10] H. Alfvén and N. Herlofson: *Phys. Rev.*, **78**, 616 (1950).
[11] V. Ginzburg: *Dokl. Akad. Nauk SSSR*, **76**, 376 (1951).
[12] G. Getmancev: *Dokl. Akad. Nauk SSSR*, **83**, 557 (1952).
[13] Y. Blewett: *Phys. Rev.*, **69**, 87 (1946).
[14] A. Sokolov, A. Matveev and I. Ternov: *Dokl. Akad. Nauk SSSR*, **102**, 65 (1955).
[15] F. R. Elder, A. M. Gurewitsch, R. V. Langmuir and H. C. Pollock: *Phys. Rev.*, **71**, 829 (1947).
[16] F. R. Elder, R. V. Langmuir and H. C. Pollock: *Phys. Rev.*, **74**, 52 (1948).
[17] V. Veksler: *Dokl. Akad. Nauk SSSR*, **44**, 393 (1944).
[18] E. M. McMillan: *Phys. Rev.*, **68**, 143 (1946).
[19] A. Sokolov: *Dokl. Akad. Nauk SSSR*, **67**, 1013 (1949).
[20] D. Ivanenko and A. Sokolov: *Classical Theory of Fields* (Moscow-Leningrad, 1951).
[21] G. Parzen: *Phys. Rev.*, **84**, 235 (1951).
[22] D. L. Judd, J. V. Laporé, M. Ruderman and P. Wolff, *Phys. Rev.*, **86**, 123 (1952).
[23] H. Olsen and H. Wergeland: *Phys. Rev.*, **86**, 123 (1952).
[24] A. Sokolov, N. Klepikov and I. Ternov: *Žu. Éksper. Teor. Fiz.*, **23**, 632 (1952); **24**, 249 (1953).
[25] A. Sokolov: *Žu. Éksper. Teor. Fiz.*, **24**, 488 (1953).
[26] V. Ginzburg: *Usp. Fiz. Nauk*, **51**, 350 (1953).
[27] A. Sokolov and I. Ternov: *Žu. Éksper. Teor. Fiz.*, **25**, 698 (1953); see also *Dokl. Akad. Nauk SSSR*, **92**, 537 (1953).
[28] A. Sokolov, N. Klepikov and I. Ternov: *Dokl. Akad. Nauk SSSR*, **89**, 665 (1953).
[29] N. Klepikov: *Žu. Éksper. Teor. Fiz.*, **26**, 19 (1954).
[30] M. Neuman: *Phys. Rev.*, **90**, 682 (1953).
[31] J. Schwinger: *Proc. Nat. Ac. Sci., U.S.A.*, **40**, 132 (1954).
[32] W. Pauli and M. Fierz: *Nuovo Cimento*, **15**, 167 (1938).
[33] A. Sokolov and I. Ternov: *Dokl. Akad. Nauk SSSR*, **97**, 823 (1954).
[34] A. Sokolov and I. Ternov: *Žu. Éksper. Teor. Fiz.*, **28**, 431 (1955).
[35] M. Sands: *Phys. Rev.*, **97**, 470 (1955).

SUPPLEMENTO AL VOLUME IN, SERIE X
DEL NUOVO CIMENTO

N. 4, 1956
1° Semestre

On Dynamically Deformable Form Factors in the Theory of Elementary Particles.

M. MARKOV

Academy of Sciences of the USSR - Moscow

CONTENTS. — Introduction. 1. Dynamically deformable form factors. 2. Transition to point particles ($\lambda \to 0$).

Introduction.

Numerous attempts have been made to introduce the extension of elementary particles into modern theory by the aid of the so-called form factors [1].

It is well known that by the introduction of these form factors, the $\Delta(x - x')$ function changes in such a way that it is no longer zero outside the light cone, e.g., for $(x_0 - x_0') < |\bar{x} - \bar{x}'|$ (see [2]).

Thus on space-like surfaces the commutability of physical quantities is violated, and hence the conditions necessary for the existence of any conventional type of relativistic mathematical formalism are no longer fulfilled.

This conflict between extension and relativity is especially apparent if the equations are written in a consistently relativistic manner in the form of the Tomonaga interaction representation

$$\left\{\frac{\hbar}{i}\frac{\delta}{\delta\sigma_x} + H_{12}(x)\right\}\Psi(\sigma) = 0\,.$$

The conditions of integrability of these equations require that the commutator $[H_{12}(x), H_{12}(x')]$ becomes zero on space-like surfaces.

Several attempts have been made in recent years to introduce form factors into the equation of motion in Heisenberg representation; a priori, however,

it should be obvious that the difficulties of the interaction representation, the essence of which is clear (appearance of signals with a velocity exceeding that of light), cannot probably disappear when any other mathematically equivalent formulation is used.

As a matter of fact, the authors who attempted to carry out this plan, encountered difficulties which are equivalent to those arising from an interaction representation. If the problem is considered in Heisenberg representation, one is forced to sacrifice the Hamiltonian method [3] and to seek the solution in non-Hamiltonian methods, such as the S-matrix method.

However, one gets the impression that the advantages of introducing a form factor by the S-matrix method are no greater than those which the Hamiltonian method presents [4] and that only a non-rigorous approach to this problem gives rise to illusions that the opposite may be true.

The hope remained that deviations from causality might arise only in small non-local regions and that macroscopic causality would not be affected [5]. This view rests on assumptions, mostly intuitive, that one cannot accurately verify the existence of deviations from relativity in a small region (*) or detect « small » deviations from relativity in macroscopic effects. At any rate the principal point has not been proved, namely, that these restrictions are inherent in the mathematical formalism of the theory and they therefore restrict the validity of relativistic conceptions, just as the Heisenberg relation restricts the applicability of classical conceptions.

Correspondingly, an attempt was made to introduce a length in the theory of elementary particles by applying new commutation relations such as the following [6]

$$[x_\mu, \varphi] = i r_\mu \varphi \,, \tag{1}$$

where φ is a scalar field and r_μ is a new vector; x_μ is the coordinate of the scalar field source.

These relations were interpreted in the sense that they restrict the field measurement in a small region. It is natural that relations of this type give rise to cut-off factors, but nevertheless it has been impossible to set up a consistent mathematical formalism for the theory (+). YUKAWA has shown that

---

(*) Only one example attests the opposite: in Fermi's theory of multiple particle creation for colliding particles the velocity of propagation of the interaction is important in a region $\sim \hbar/mc$. This means that, in principle, problems of this type may be the object of experimental study.

(+) In a particular case relation (1) turned out to be equivalent to Born's reciprocity principle. Thus, from (1) one may write

$$[x_\mu, [x^\mu, \varphi]] = \lambda^2 \varphi \tag{2}$$

if it is assumed

$$\Sigma (i, r_\mu)^2 = \lambda^2 .$$

commutation relations of this type are equivalent to the introduction of internal degrees of freedom of the elementary particles.

V. Ginzburg and I. Tamm [7] had previously considered equations for elementary particle with internal degrees of freedom; it was their purpose to describe in this way the excited states of the nucleon. After the discovery of hyperons, interest in such equations has greatly increased and there is a tendency to combine the problem of excited states of nucleons with the divergence problem.

The main defect of all non-local field theories proposed up to now is that form factors representing the particle dimensions are described by functions whose form is independent of the forces acting on the particle. In an «absolutely rigid medium» of this sort the signal velocity would exceed that of light and that, of course, is incompatible with relativity. Apparently, it is exactly this fact that explains the failure of all previous attempts carried out in this direction.

The following questions arise:

1) Is it possible to construct a form factor extending over a region in which interactions are propagated with retardation? We shall call the form factors of this type «dynamically deformable» [8].

2) Can form factors of this type eliminate the well known difficulty of divergencies?

Unfortunately, a final answer to these questions cannot be given at present, but a number of remarks, both optimistic and pessimistic, will be made here.

1. – Dynamically Deformable Form Factors.

As a graphic, although imperfect model of a dynamically deformable form factor, one may mention the hydrogen electron cloud. If the point interaction between the atomic electron and the light quantum is taken into account then, as result of this interaction, a deformation of the electron cloud will take place. The electron-photon interaction will be transmitted to the nucleus with retardation and the atom as a whole will receive a corresponding momentum increment.

In other words, in this case the model of an elementary particle is a «system» consisting of two point «particles» connected by the relativistic interaction law. It is moreover assumed that one of the two «particles» interacts with the external field in a point-like manner.

In this sense the theory becomes more local. This model gives some assurance in the possibility of a consistent relativistic formulation of the problem (the hydrogen atom as a two body system exists in reality); however, the model

described here should not be understood too literally. It is to be remembered that this equation must describe one particle only.

It is also obvious that no continuous spectrum of the internal states should exist and this restricts the form of the «internal potential function», as otherwise the self energy of the system would diverge (example: self energy of an electron bound in a hydrogen atom). This condition may be considered as a definition of an elementary particle in the sense that disintegration into two particles (e.g. photoeffect) is, as a matter of principle, impossible. Interaction can only lead to excitation of the internal states of the particle or to creation of new particles.

It seems that there exists a mathematical formalism that is adequate to express the idea of a dynamically deformable form factor in its particular aspect. We are speaking here of equations of the Bethe-Salpeter type with prescribed interaction between x_1 and x_2 coordinates ($L(x_1; x_2)$), e.g. equations of the type:

$$[\mathcal{D}x_1 + gw(x_1)][\mathcal{D}x_2]\,\psi(x_1; x_2) = L(x_1; x_2)\,\psi(x_1; x_2)$$

where $\mathcal{D}x_1 = \gamma_\mu(\partial/\partial x_{\mu_1})$, $w(x_1)$ is an external scalar field. $L(x_1; x_2)$ may be taken, for example, as $L \sim \sum (x_{\mu_1} - x_{\mu_2})^2$.

A correctly written equation of this type certainly will not contradict causality and relativity, but as long as the investigation of these equations is not yet performed, it is impossible to predict whether the divergencies will really be removed.

It is necessary to remember that $L(x_1; x_2)$ must be of such kind that the density of internal states should not be too high: in any case the internal continuous spectrum must be absent.

There is, however, a class of simpler equations with internal degrees of freedom which might be investigated at first. We are speaking about equations of the following kind:

$$\left\{\gamma_\mu \frac{\partial}{\partial x'_\mu} + \gamma_\mu \frac{\partial}{\partial x''_\mu} + f\left(\frac{\partial^2}{\partial x'^2}\,;\, \frac{\partial^2}{\partial x''^2}\,;\, \frac{\partial^2}{\partial x' \partial x''}\right) + m_0 + v(x';\, x'') + gw(x')\right\} \psi(x';\, x'') = 0.$$

With the position: $x_\mu = (x'_\mu + x''_\mu)/2$ and $r_\mu = x'_\mu - x''_\mu$, we may obtain in particular cases the equations of the Born-Yukawa type:

$$\left\{\gamma_\mu \frac{\partial}{\partial x_\mu} + a\left[-\frac{\partial^2}{\partial \xi_\mu\, \partial \xi_\mu} + \xi_\mu \xi_\mu\right] + m_0 + gw(x')\right\} \psi(x; \xi) = 0\,. \tag{3}$$

Here x_μ is the «center of mass» coordinate of some «cloud»; the dimensionless variables $\xi_\mu = r_\mu/\lambda$, $\xi_4 = i\xi_0$ will be interpreted as the coordinates of a cloud element (r_μ) in the center of mass system.

x' is the coordinate of a cloud element relative to the origin of coordinates.

Equations of type (3), which do not include the external field, have received considerable attention in the literature (Yukawa, Minardi, Rayski, Ginzburg and Silin, Ju. M. Širokov and others [9]). In this case, as is well known, a new difficulty arises: one must set up an equation with an increasing mass spectrum and a ground state that is not infinitely degenerate.

An equation of this type may be suggested in the following form [10]

$$\left\{i\gamma_\mu k_\mu + m_0 + a\left[-\frac{\partial^2}{\partial\xi_\mu\partial\xi_\mu} + \xi_\mu\xi_\mu + 2\,\frac{(k_\mu(\partial/\partial\xi_\mu))^2 - (k_\mu\xi_\mu)^2}{k_\mu k_\mu}\right]^e\right\}\psi(k,\xi) = 0\,. \tag{4}$$

In the system in which the particle is at rest ($\boldsymbol{k} = 0$) the mass operator in equation (4) takes the simple form

$$m_0 + a\left[\xi_0^2 + \xi_1^2 + \xi_2^2 + \xi_3^2 - \frac{\partial^2}{\partial\xi_0^2} - \frac{\partial^2}{\partial\xi_1^2} - \frac{\partial^2}{\partial\xi_2^2} - \frac{\partial^2}{\partial\xi_3^2}\right] \tag{5}$$

with a mass spectrum

$$M_{n_0 n_1 n_2 n_3} = m_0 + 2a(n_1 + n_2 + n_3 + n_0 + 2)\,. \tag{6}$$

This means that in the frame of rest we have a four dimensional oscillator in the literal sense of the word as the real time component (ξ_0) appears in (5) with the same sign as the other three components. For the sake of simplicity it has been assumed in equation (5) that $e = 1$. Another equation can be proposed

$$\left\{i\gamma_\mu k_\mu + m_0 + a\left[-\frac{\partial^2}{\partial\xi_\mu\partial\xi_\mu} + \xi_\mu\xi_\mu + \frac{(k_\mu(\partial/\partial\xi_\mu))^2 - (k_\mu\xi_\mu)^2}{k_\mu k_\mu}\right]\right\}\psi = 0\,. \tag{7}$$

In the frame of rest, equation (7) leads to a purely spatial oscillator possessing the mass spectrum

$$M_{n_1 n_2 n_3} = m_0 + 2a(n_1 + n_2 + n_3 + \tfrac{3}{2})\,. \tag{8}$$

For particles of integral spin an equation similar to (4) may be written in the form

$$\left\{k_\mu k_\mu + m_0^2 + a^2\left[-\frac{\partial^2}{\partial\xi_\mu\partial\xi_\mu} + \xi_\mu\xi_\mu + 2\,\frac{(k_\mu(\partial/\partial\xi_\mu))^2 - (k_\mu\xi_\mu)^2}{k_\mu k_\mu}\right]\right\}\psi = 0\,. \tag{9}$$

For some points of view the following simple equation may be of interest [9]

$$\left\{i\gamma_\mu\frac{\partial}{\partial x_\mu} + a\left[-\frac{\partial^2}{\partial\xi_\mu\partial\xi_\mu} + \xi_\mu\xi_\mu\right]\right\}\psi = 0 \tag{10}$$

the mass operator is

$$L = a\left[-\frac{\partial^2}{\partial\xi_\mu\partial\xi_\mu} + \xi_\mu\xi_\mu\right]. \tag{11}$$

The variables in equation (10) can be separated and therefore the solution is of the form

$$\psi = \varphi(x)\,\chi(\xi)\,, \tag{12}$$

where

$$\chi_{n_0 n_1 n_2 n_3} = H_{n_0} H_{n_1} H_{n_2} H_{n_3} \exp\left[-\frac{\xi_0^2 + \xi_1^2 + \xi_2^2 + \xi_3^2}{2}\right]$$

H_{ni} are Hermite polynomials.

Equation (10) yields the following mass spectrum

$$\sim (n_1 + n_2 + n_3 - n_0 + 1)\,. \tag{13}$$

As

$$n_1 + n_2 + n_3 - n_0 = 0\,, \tag{14}$$

can be realized in an infinite number of ways, the ground state is degenerate.

In most investigations this degeneracy is removed by introducing some auxiliary conditions. It should be noted that, as a rule, the auxiliary conditions are not compatible with equation (10).

Mathematically, the correct conditions (*) can be expressed only by the equations:

$$N\psi = 0\,, \qquad N = k_\mu \xi_\mu - k_\mu(\partial/\partial\xi_\mu)\,. \tag{15}$$

In the coordinate system in which the particle is at rest ($\boldsymbol{k} = 0$), the condition (15) becomes

$$\left(\frac{\partial}{\partial\xi_0} - \xi_0\right)\psi = 0\,. \tag{16}$$

Solution (12) satisfies condition (16) if

$$\frac{\partial H_{n_0}}{\partial\xi_0} = 2n_0 H_{n_0 - 1} = 0\,,$$

e.g., if $n_0 = 0$.

Condition (15) is compatible with equation (10)

$$[N, L] = 2N\,. \tag{17}$$

(*) The condition $k_\mu\xi_\mu = 0$ has also been proposed (e.g. RAYSKI, loc. cit.). However, generally speaking, this condition is incompatible with equation (10) as

$$[k_\mu\xi_\mu, L] = 2k_\mu(\partial/\partial\xi_\mu)\,.$$

This signifies that the condition of compatibility of (10) and (15) does not require any new condition.

In the frame of rest, the wave function χ of the lowest state has the form

$$\chi_{0000} = \frac{1}{\lambda^2 \pi} \exp\left[-\frac{r_1^2 + r_2^2 + r_3^2 + r_0^2}{2\lambda^2}\right]. \tag{18}$$

In an arbitrary coordinate system

$$\chi_{0000} = \frac{1}{\lambda^2 \pi} \exp\left[-\frac{1}{\lambda^2} \sum \frac{r_\mu r_\mu}{2} + \frac{(k_\mu r_\mu)^2}{m^2}\right]. \tag{19}$$

Equation (10) and condition (15) apparently yield all the physically permissible solutions that can be obtained from a more complicated equation recently proposed by YUKAWA [11]. Solutions (18) and (19) also satisfy equation (4). Unfortunately, due to auxiliary conditions (15), some difficulties arise when the external field is introduced. In this sense equations of type (4) are preferable, although equation (10) with auxiliary conditions of type (15) may be (as will be demonstrated below) of certain methodological interest when transition to a point particle ($\lambda \to 0$) is made. We realize that the considerations set forth here are almost exclusively of methodological value. Nevertheless, we wish to point out some peculiar features of theories containing deformable form factors; it appears that these features are common to a whole class of theories [12].

1) The lifetime of excited nucleons (decay time with respect to π-meson emission) varies in wide limits, depending on the decay energy, on the relation between n_0, n_1, n_2, n_3 of the respective transitions and on λ (particle extension).

Thus, for the first excited state ($n = 1$) the life-time may be of the order of 10^{-10} s if the decay energy is of ~ 40 MeV and $\lambda \sim 10^{-19}$ cm (Λ^0-particle?). A lifetime of the same magnitude is obtained in the paper [13] if $\lambda \sim 10^{-13}$, but then $n = 5$ (see appendix I).

2) Naturally, direct excitation of nucleons by π-mesons is practically impossible in these cases; creation of a highly excited nucleon-antinucleon pair, however, is quite possible. It is characteristic that production of nucleon pairs with large excitation numbers is more probable at high energies. This simply means that highly excited states are very degenerate, and thus a large statistical factor appears in the corresponding cross-sections.

In the particular case of the oscillator model (5), this factor equals the number of combinations of four positive integers the sum of which equals the excitation level number: $n = n_1 + n_2 + n_3 + n_0$.

For π-mesons of energy ~ 5 GeV nucleon pairs can be produced too, not

only in the zero $(p_0, \bar{p}_0)$ but in the first $(p_1, \bar{p}_1)$, $(n_1, \bar{p}_1)$ state as well (*). Here $\bar{p}$ designates an antiparticle, 0 and 1 the respective excitation level numbers.

If the π-meson energy is lower (~ 1 GeV), then the two excited nucleons can be produced only in intermediate states:

$$\pi^- + p_0 \to p_0 + \bar{p}_1 + n_1 . \tag{20}$$

If one identifies the excited neutron (n_1), with the Λ^0-particle, then it is necessary to assume that an excited antiproton, $\bar{p}_1$, and a proton in the normal state, p_0, can unite (+) to form a new particle [12, 14]

$$(\bar{p}_1 + p_0) \to \theta^0; \qquad \pi^- + p_0 \to (p_0 + \bar{p}_1) + n_1 . \tag{21}$$
$$\downarrow$$
$$\theta^0 + \Lambda^0 .$$

After a certain time the Λ^0- and θ^0-particles should emit a π-meson. The creation of single Λ^0- and θ^0-particles is excluded.

It is obvious that in order to develop any particular hyperon theory one must have reliable data on the spins of the θ^0, Λ^0, Λ^+ and Ω^--particles.

Information of this type could be of decisive importance for the theory as this would permit one to substantially decrease the number of possibilities.

By considering the creation of highly excited nucleon pairs in intermediate states it should be possible to set up a table containing the nucleon family (hyperons) and excited π-meson family ($\theta^0 \rightleftarrows \pi_{01}$ etc.).

It should be noted that reaction (20) yields one other possibility, the transformation of the $(\bar{p}_1 + n_1)$ particle into a new single particle π_{11}. This new particle should inevitably be nuclear-active in the same sense as the π-meson is

$$\pi^- + p_0 \rightleftarrows (\bar{p}_1 + n_1) + p_0 \rightleftarrows \pi_{11} + p_0 . \tag{22}$$

If the π_{11}-particle mass is sufficiently large and there are no unexpected restrictions, then it should disintegrate into two π-mesons: the decay time would be shorter than that of a π^0-meson decaying into two γ-rays, and the disintegration mechanism should also be quite similar.

At high energies it is principally possible that in reactions similar to (22)

(*) From this point of view the production of a $(n_1, \bar{p}_1)$ pair should be four times more probable than the production of a $(n_0, \bar{p}_0)$ pair.

(+) If understood in the literal sense of the word, combination of the particle and anti-particle would mean that we have here a generalization of the well known FERMI-YANG hypothesis.

highly excited nucleon pairs and nuclear-active particles can be produced; for example,

$$\pi^- + p_0 \to p_0 + (\bar{p}_n + n_n) \to p_0 + \pi^-_{nn}.$$

The π^-_{nn}-particle has a small lifetime and can decay into two particles, e.g.

$$\pi^-_{nn} \to \pi^-_{kk} + \pi^0_{mm},$$

each of these particles in turn could rapidly disintegrate and a π-meson shower would eventually be formed.

This peculiar mechanism of multiple particle creation may take place for relatively small interaction constants.

However promising the possibilities outlined here may seem, it must be borne in mind that as yet no consistent theory has been developed and the initial equations practically have not been subjected to investigation.

We may note, however, that in spite of the enormous number of new intermediate states over which one must now sum, the nucleon self-energy may be finite in some variants of the theory.

Thus, in equation (4) it is sufficient to put $e = 2$. In this sense, theories in which $n_0 = 0$ are the most favourable.

It should also be mentioned that the many-time formalism equations (3) written for n particles are compatible. We have here in view the system

$$(23)\qquad \begin{cases} \gamma^{(1)}_\mu \dfrac{\partial}{\partial x^{(1)}_\mu} + a\left[-\dfrac{\partial^2}{\partial \xi^{(1)}_\mu \, \partial \xi^{(1)}_\mu} + v(\xi^{(1)}_\mu \xi^{(1)}_\mu) + m^{(1)}_0 + g_1 w(x^{(1)}_1) \right] \psi = 0 . \\ \cdots\cdots\cdots\cdots\cdots\cdots\cdots\cdots\cdots\cdots \\ \gamma^{(i)}_\mu \dfrac{\partial}{\partial x^{(i)}_\mu} + a\left[-\dfrac{\partial^2}{\partial \xi^{(i)}_\mu \, \partial \xi^{(i)}_\mu} + v(\xi^{(i)}_\mu \xi^{(i)}_\mu) + m^{(i)}_0 + g_i w(x^{(i)}_1) \right] \psi = 0 , \end{cases}$$

where i is the number of particles. The integrability condition for these equations reduces to the usual requirement that

$$(24)\qquad [w(x^{(i)}_1),\ w(x^{(k)}_1)] = 0 .$$

Condition (24) can be satisfied because of the point-like nature of the interaction introduced by us. If one were to introduce a form factor into $w(x^i_1)$ or prematurely integrate over the internal variables (ξ), then equations (23) would become incompatible [9].

The danger exists, however, that the initial free equations, which do not lead to divergencies, may have an unsatisfactory Δ_F-function. Unfortunately, correct quantization of similar equations has not been carried out. It is clear, however, that in the general case the propagation function will not only depend

on x but also on the internal coordinate r, i.e., $\Delta(x - x', r, r')$. Significantly, in solutions (12) of eq. (10) (without auxiliary condition [15]) the internal variables (ξ) and center of mass variables (x, k) can be separated in any coordinate system. This apparently permits one to express the corresponding Δ-function in the form of a product

$$\Delta m'(x - x', \xi, \xi') = \Delta m(x - x') f(\xi, \xi'), \tag{25}$$

where $\Delta m(x - x')$ is the Δ-function with its usual properties; m is the particle mass.

This peculiarity of equations of type (10) is closely associated with infinite degeneracy (in particular of the ground state) since upon transformation the set of functions goes over into itself. As the degeneracy is very considerable, it again leads to divergencies in spite of the exponential fator in the matrix elements (exp $[-\lambda^2 k^2 \ldots]$).

Any attempt to remove the infinite degeneracy of the ground state inevitably leads to the result that the « center of mass » momentum vector (k) appears in the internal wave function χ; in (19) we have an example of this state of affairs. If one constructs the respective Δ-functions and integrates over momentum space k one finds that, in contrast to (25), coordinates χ and r in the Δ-function are no longer separable and generally speaking, function $\Delta(x - x', r, r')$ no longer vanishes (*) on the space-like surface. It should be remembered, however, that in our method of introducing the interaction the « center of mass » coordinate x is no longer an observable quantity (+).

Further development of the mathematical formalism may show that the property of the Δ-function discussed above, nevertheless, leads to formal internal contradictions in the theory. If this really happens, it will merely signify that equations of type (4) are not equivalent to the dynamically deformable form factor conception.

2. – Transition to " point „ particles ($\lambda \to 0$).

A characteristic feature of the equations under consideration, e.g., (4), (7), (18), is the appearance of two independent constants a and λ.

The constant λ determines the « dimensions » of the particle or the dimen-

---

(*) It is important to note that $\int \Delta(x, r, r')\, dr\, dr' = \Delta(x)$ where $\Delta(x)$ is the usual Δ-function.

(+) In a real system consisting, say, of two particles, the position of the center of mass instantaneously changes when the mass of one of the particles is instantaneously increased (e.g. by absorption of a meson) and this, of course, is compatible with relativity.

sions of the « oscillator » (18), while the constant a determines the energy differences between the nucleon excited levels.

Any decrease of the constant λ will leave the mass spectrum of the equation unchanged. For $a \to 0$ equation (4) changes into Dirac's equation, but for $a \neq 0$ and an arbitrarily small λ, equation (4) sharply differs from the equation of a point particle in the usual sense of the word. Although equation (4) has sense for any λ, however small, one nevertehless cannot put $\lambda = 0$ (*).

When $\lambda \to 0$ the internal wave functions (18) acquire the properties of a δ-function and this exactly corresponds to the physical meaning of a point particle. This limiting transition ($\lambda \to 0$) however can be carried out in the matrix elements. The value of this type of analysis is that the divergencies that subsequently emerge are by two powers smaller than those which follow from Dirac's equation.

As an example, let us first consider for $\lambda \neq 0$ that part of the self energy of a nucleon in the ground state which corresponds to the self-energy of a nucleon obeying Dirac's equation.

Suppose transitions to other mass states do not take place.

This is reasonable because in certain variants of the theory such transitions are absolutely forbidden for $\lambda \to 0$ (see for example matrix element M_{01}. with $\lambda \to 0$, Appendix I).

The initial nucleon function and the intermediate state function have, respectively, the following form

$$\psi_0 = \varphi c \exp\left[-\frac{\xi_0^2 + \vec{\xi}^2}{2}\right]; \qquad \psi_k = \varphi' c \exp\left[-\frac{\xi_\mu \xi_\mu}{2} + \frac{(k_\mu \xi_\mu)^2}{m^2}\right]. \tag{27}$$

In its initial state the nucleon is at rest ($\boldsymbol{k} = 0$); in the intermediate state a momentum $\boldsymbol{k} \neq 0$ is transferred to the nucleon.

In accord with (3), interaction with the scalar field is taken in the form $gw(x + \lambda\xi)$, which, for $\lambda \to 0$, changes into the usual $gw(x)$, φ and φ' are the initial and final spinor functions and are completely similar to the corresponding functions of the usual Dirac equation.

The expression for the nucleon self-energy will have the form

$$H''_{00} = \sum_k \{\ldots\} \left| \int \ldots \mathrm{d}^4\xi \right|^2, \tag{28}$$

where the expression in brackets is the usual Dirac theory expression and

$$\int \ldots \mathrm{d}^4\xi = \int \exp\left[-\tfrac{1}{2}(\xi_0^2 + \xi^2)\right] \exp\left[i\lambda(\xi, k)\right] \exp\left[-\frac{\xi_\mu \xi_\mu}{2} + \frac{(k_\mu \xi_\mu)^2}{m^2}\right] \mathrm{d}^4\xi \tag{29}$$

(*) In some of the terms λ appears in the denominator.

is determined by the internal wave functions of the initial and intermediate states

$$\int \ldots \mathrm{d}^4\xi = \frac{m}{\sqrt{k^2+m^2}} \exp\left[-\lambda^2 k^2 \ldots\right] = \frac{m}{E} = \sqrt{1-v^2/c^2}\,. \tag{30}$$

This behaviour of integral (29) is connected with the deformation of the internal function of the particle which appears when the latter recoils in the intermediate state. The spherically symmetrical « cloud » of the initial state transforms into an elliptical one. The difference between integral (29) and unity is a measure of the degree of overlapping of the « clouds » (e.g., of functions ψ_0 and ψ_k). In the case under consideration this peculiar feature of cloud deformation remains even when the limiting transition is carried out.

These considerations seem to furnish evidence of ambiguity of the point particle conception.

A better understanding of this limiting transition and of its validity can be obtained by analyzing the corresponding Δ_F-functions for $\lambda \to 0$. Some unexpected features may arise in this case (e.g. contradiction with causality).

In our analysis we purposely ignored electrodynamics.

Due to smallness of the constant $e^2/\hbar c$ electrodynamic difficulties appear only at very high energies for which the electromagnetic field cannot be separated from other fields such as meson field, β -field [15], and even gravitation fields. In the latter case the gravitation electron radius could serve as a natural limiting length [16].

Notwithstanding its shortcomings, modern electrodynamics can explain all known experimental data with an accuracy that may truly be envied.

Appendix I

The matrix element for transition from state $n=1$ to $n=0$ has the form [15]

$$M_{01} \sim g \frac{(\varphi_0^* \beta \gamma_\xi \varphi_1)}{\sqrt{E\pi}} \frac{(p,\,\lambda)}{\hbar} \exp\left[-\frac{\lambda^2}{4\hbar^2}\left(p_1^2+p_2^2+p_3^2+p_0^2\right)\right]. \tag{α}$$

Pseudoscalar coupling is considered here and it is assumed that

$$n=1\,, \qquad n_1=1\,; \qquad n_0=n_2=n_3=0\,.$$

p_ν are the momentum components of the particle. Relativistic deformation of the internal χ-function due to recoil is not taken into account.

From α it follows that the decay probability (lifetime) of the first excited state can be expressed in the form

$$\omega = \frac{1}{q} \sim \frac{g^2}{\hbar c} \frac{p^2}{M_\mu^2 c^2} \left(\frac{p\lambda}{\hbar}\right)^2 \frac{pc}{\hbar} \exp\left[-\frac{\lambda^2}{2}\left(p_1^2+p_2^2+p_3^2+p_0^2\right)\right].$$

REFERENCES

[1] G. Wataghin: *Zeits. f. Phys.*, **88**, 92 (1934).
[2] M. A. Markov: *Dokl. Akad. Nauk SSSR*, **40**, 18 (1943).
[3] C. Bloch: *K. Danske Vidensk. Selsk., Mat.-fys. Medd.*, **27**, N. 28 (1952).
[4] E. C. G. Stueckelberg and G. Wanders: *Helv. Phys. Acta*, **27**, 667 (1954).
[5] D. I. Blohincev: *Žu. Éksper. Teor. Fiz.*, **16**, 480 (1946); M. Chrétien and R. E. Peierls: *Nuovo Cimento*, **10**, 668 (1953).
[6] M. Markov: *J. of Phys. USSR*, **2**, 452 (1940).
[7] V. L. Ginzburg and I. E. Tamm: *Žu. Éksper. Teor. Fiz.*, **17**, 227 (1947).
[8] M. A. Markov: *Žu. Éksper. Teor. Fiz.*, **25**, 527 (1953).
[9] H. Yukawa: *Phys. Rev.*, **91**, 415 (1953); Ju. M. Širokov: *Žu. Éksper. Teor. Fiz.*, **21**, 748 (1951); V. L. Ginzburg and V. P. Silin: *Žu. Éksper. Teor. Fiz.*, **27**, 116 (1945); J. Rayski: *Nuovo Cimento*, **10**, 1729 (1953); **12**, 815 (1955); E. Minardi: *Nuovo Cimento*, **11**, 694 (1954).
[10] M. A. Markov: *Dokl. Akad. Nauk SSSR*, **101**, 449 (1955).
[11] H. Yukawa: *Phys. Rev.*, **91**, 416 (1953).
[12] M. A. Markov: *Dokl. Akad. Nauk SSSR*, **101**, 51 (1955).
[13] P. S. Isaev and M. A. Markov: *Žu. Éksper. Teor. Fiz.*, **29**, 111 (1955).
[14] M. M. Levy and R. E. Marshak: *Suppl. Nuovo Cimento*, **11**, 253 (1954).
[15] V. P. Silin: *Žu. Éksper. Teor. Fiz.*, **21**, 462 (1951).
[16] M. A. Markov: *Žu. Éksper. Teor. Fiz.*, **17**, 661 (1947).

SUPPLEMENTO AL VOLUME III, SERIE X
DEL NUOVO CIMENTO

N. 4, 1956
1° Semestre

Structure Analysis by Electron Diffraction.

B. K. VAJNŠTEJN

Institute of Crystallography of the Academy of Sciences of the USSR - Moscow

CONTENTS. — **1.** Introduction. – **2.** Experimental technique. – **3.** Geometric theory of electron diffraction patterns. – **4.** Reflexion intensities of electron diffraction patterns. – **5.** The Fourier method in electron diffraction analysis. – **6.** Experimental structure studies.

1. – Introduction.

Along with X-ray analysis, the principal method of studying the atomic structure of matter, another diffraction method, the electron diffraction technique (as well as neutron diffraction) is becoming increasingly important.

The early Soviet theoretical and experimental works on electron diffraction accomplished in the late '20ies and '30ies by P. S. TARTAKOVSKIJ [1], A. A. LEBEDEV [2, 3], V. E. LAŠKAREV [4] and other workers have laid solid foundations for the further development of the new method in the Soviet Union. At the present time electron diffraction analysis has found a number of various applications. Among these are: study of the structure of molecules of vapours and gases, phase analysis of surface layers, study of the shape and mutual orientation of microcrystals of different phases, and finally electron diffraction structure analysis, i.e. a complete determination of new crystalline structures, previously unknown.

In 1937-1938 Z. G. PINSKER [5] called attention to the possibility of using electron diffraction analysis for structure determinations, independent of X-ray analysis data. Later on, jointly with his co-workers, he carried out a number of studies of this kind. In 1949 he published a monograph under the title of *Electron diffraction* [6] (subsequently translated into English), in which Soviet and foreign studies on the theory and diverse uses of the method were discussed. In addition to studies of the atomic structure of crystals, electron

diffraction analysis is used in the Soviet Union in the study of oxidation processes of surface layers and their phase analysis (P. D. Dankov, N. A. Šišakov) [7-10], studies of the structure of molecules [11-13], high polymers [14-18], metals [10, 19-23, 62-66], etc.

The present paper is concerned only with problems of electron diffraction structure analysis, mainly with the new results obtained in developing the theory and technique of the method, as well as with the experimental structure determinations made by the author and other workers of the Electron Diffraction Laboratory of the Institute of Crystallography of the Academy of Sciences of the USSR.

Prior to a discussion of this material it would be useful to review the fields of application and the possibilities of electron diffraction structure analysis as compared to the X-ray and neutron diffraction methods. The principal object of structure analysis, viz. to reveal the arrangement of atoms in the unit cell, may be, in principle, achieved by any one of the three methods. However, differences in the nature of the interaction between any one radiation and a given substance call forth, on the one hand, limitations of the experimental possibilities of each method, and, on the other hand, a difference in the physical sense of the ultimate result, if the scope of the work is wider than a mere determination of the co-ordinates of atoms.

X-rays are scattered by electron clouds of atoms; accordingly, a treatment of X-ray diffraction data with the aid of the Fourier synthesis shows the electron density distribution in which the peaks correspond to atoms. The scattering of neutrons takes place on atomic nuclei; it may be used to obtain a map of «nuclear density». The scattering of electrons takes place on the electrostatic potential produced by atomic nuclei with a screening effect of electron clouds, due to which it is possible to obtain the potential distribution of the crystalline lattice, of which the peaks also correspond to atoms. The difference in the nature of interaction brings about a considerable difference in the absolute value of amplitudes of atomic scattering, as well as in the nature of the f-curves depending on the atomic number and on the value of $(\sin\vartheta)/\lambda$ for all the three radiations. The atomic amplitudes of scattering of X-rays, f_X, have a value of $\sim 10^{-11}$ cm; those of neutrons, $f_n \sim 10^{-12}$ cm, and those of electrons, $f_e \sim 10^{-8}$ cm. When passing to intensities which are proportional to f^2, this means that electrons interact with the substance about a million times as strongly as X-rays or neutrons do. Owing to this the thickness of specimens in electron diffraction work is about $10^{-5} \div 10^{-6}$ cm, and the exposition time when producing electron diffraction patterns is of a few seconds.

It is most adequate to use electron diffraction structure analysis for the study of substances occurring only in a finely dispersed state and hence hardly lending themselves to X-ray analysis. It may be, however, generally used

for the study of any compound, specimens of which may be prepared as thin films, as well as in a number of cases when large specimens are to be investigated by reflection diffraction.

Suitable objects for electron diffraction are furnished by some phases, the X-ray analysis of which is difficult because of their poor stability (e.g. a number of oxides and hydrates of some compounds). An important aspect of the application of electron diffraction analysis is the possibility of locating light atoms (hydrogen atoms included) in the presence of heavy ones in crystalline lattices. Finally, by revealing the potential distribution within atoms and between them by the use of Fourier synthesis it is possible to study the problems of chemical bonding, ionization of atoms, their thermal movement etc.

2. – Experimental Technique.

In the Soviet Union various models of electron diffraction cameras have been constructed [6, 24-28], some of which designed to serve some special purpose, and some of universal applicability. In the different cameras the value of the accelerating potential ranges from 40 to 100 kV; the specimen-screen distances, from 350 to 1100 mm; the dimensions of the photographic plates, from 4.5 cm × 6 cm to 13 cm × 18 cm. Moreover, the technique of using electron microscopes to obtain the electron diffraction has been developed.

Fig. 1 shows the latest model of electron diffraction camera designed at

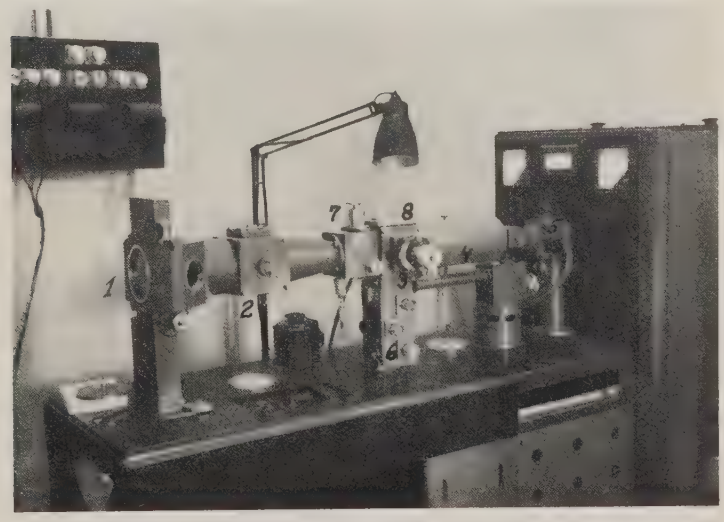

Fig. 1. – General view of the electron diffraction camera of the Institute of Crystallography of the Academy of Sciences of the USSR.

the Institute of Crystallography, working at voltages from 50 to 100 kV. The horizontal design is convenient for an easy handling of all the parts of the apparatus. The specimen-screen distance is 700 mm; with a size of the photoplates of 13 cm × 18 cm this permits to fix completely the diffraction pattern. An intermediate camera (2) being provided, photographs can be taken at a distance of 250 mm. With the aid of limiting shields it is possible to produce on a single 13 cm × 18 cm plate not one but several photographs of a smaller size (e.g. when photographs are taken with multiple expositions). The diffraction pattern can be observed by several persons on the large screen of the photographic camera (1), supplied in addition by two more windows. The crystal holder (3) has four movements necessary in making structure studies: two displacements, an azimuth rotation and a tilt about a horizontal axis perpendicular to the beam. The electron optic system comprising a double magnetic lens (4) and an electron gun (5) insure a high resolving power. The tungsten filament inside the focusing cap has three movements, the gun as a whole is also mobile, which makes it possible to place the beam precisely onto the axis of the apparatus. The vacuum adjustement is made by valves (6); the apparatus is furnished also with an intermediate valve (7) which serves to supply air into the photographic chamber and to replace the plates without disturbing the vacuum in the central chamber (8), where the speciment is placed, and vice-versa.

According to the properties of the substance to be investigated, the specimens are prepared by crystallization from solution, settling from suspensions, and sublimation. By varying the solvent, the temperature of drying the specimen, etc., on the celluloid support single-crystal, mosaic films, textures, polycrystalline aggregates can be produced. The method of sublimation in vacuum onto orienting single-crystal supports is extensively used in the study of metals, alloys, and a number of other substances.

3. - Geometric Theory of Electron Diffraction Patterns.

The geometric theory of electron diffraction patterns is based on the conception of a reciprocal lattice. An electron diffraction interference image is a flat section of a reciprocal lattice on a $L\lambda$ scale (L specimen-screen distance, λ wave length). According to the secondary structure of the specimen three types of electron diffraction patterns are produced. The first type is presented by spot patterns from mosaic single-crystal films (Fig. 2). The second type comprises patterns from textures, i.e. from aggregates of small crystals oriented on the support with one degree of freedom (Figs. 3-6). The third type includes patterns from polycrystalline specimens analogous to powder diagrams in X-ray work (Fig. 7). According to the nature of the substance to be investigated, and to the mode of preparing the specimen, patterns of one, two or all the three types may be produced.

Spot electron diffraction patterns reveal all the points of a given plane of the reciprocal lattice. A quantitative consideration of the factors of simultaneously revealing all of these points shows that the most important of these is the mosaic structure of the specimen, i.e. the distribution of the crystallites within a small angular range, generally of the order of $2^{\circ} \div 3^{\circ}$. Experience

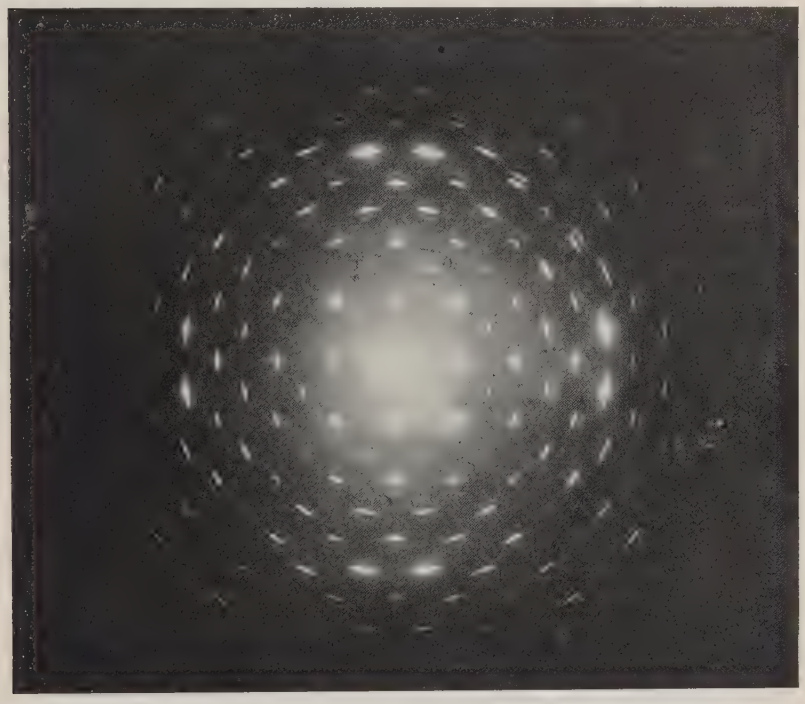

Fig. 2. - Electron diffraction pattern from a mosaic single-crystal of pentaeritritol. Specimen produced by crystallization at room temperature from aqueous solution.

gained from the investigations of various inorganic and organic substances shows that the two-dimensional diffraction, which has been previously regarded as the principal cause of the formation of spot electron diffraction patterns, is actually rather rarely encountered.

From a symmetry of spot electron diffraction patterns which is bounded by six flat groups with an inversion centre: $C_2 = 2$; $C_4 = 4$; $C_6 = 6$; $C_{2v} = m\,m$; $C_{4v} = 4\ m\,m$; $C_{6v} = 6\ m\,m$ [29], some direct inferences may be made as to the Laue symmetry of the crystal. To this purpose, in the general case no more than three photographs are required, corresponding to the different planes of the reciprocal lattice.

One spot electron diffraction pattern makes it possible to directly measure the parameters of a given net plane of the reciprocal lattice on the basis of the formula $H_{hkl} = r(L\lambda)^{-1} = d_{hkl}^{-1}$ (where r is the distance on the electron diffraction pattern). To determine the unit cell in the general case it is sufficient to have either two electron diffraction patterns and to know the angle

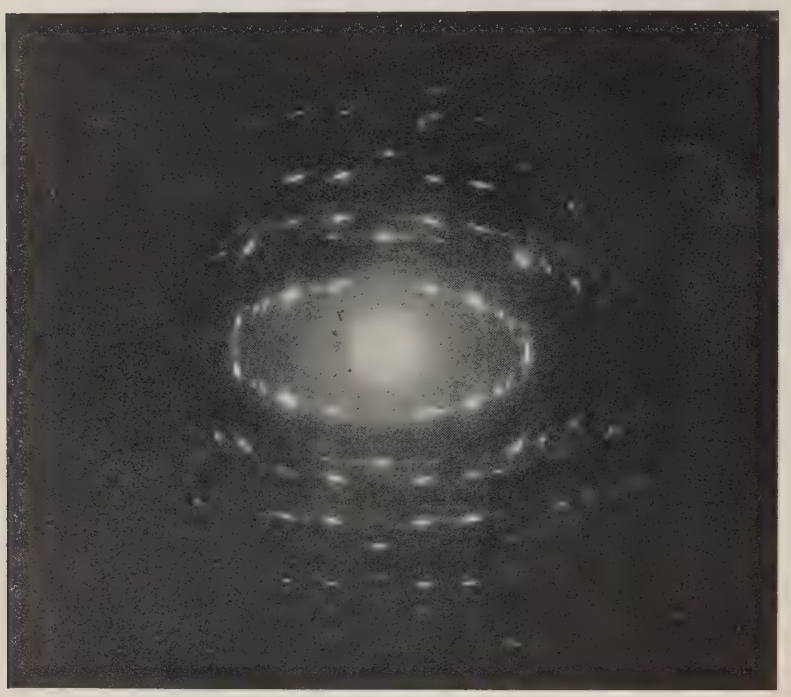

Fig. 3. – Electron diffraction pattern from a texture of Bi_2Se_3 (angle of tilt 65°). Specimen produced by sublimation in vacuum.

of the corresponding planes of the reciprocal lattice, or three patterns having no common row of points. Spot electron diffraction patterns from different zones can be in some cases produced by a few natural orientations of the crystals of a given substance on a support. Another, more general method of producing spot patterns is the rotation method. It consists of successively placing in a reflecting position the different planes of the reciprocal lattice by tilting the specimen. The mutual arrangement of these planes is determined by the structure of the plane perpendicular to all of these sections, which is not directly revealed on the photographs.

To calculate the periods and angles of this plane the following formula is used:

$$(1) \qquad c^{*2} = (H^2_{hk(l+l_1)} + H^2_{hk(l-l_1)} - 2H^2_{hkl})/2l^2; \qquad \cos\beta^* = (H^2_{h0l} - H^2_{h0l})/4a^*c^*,$$

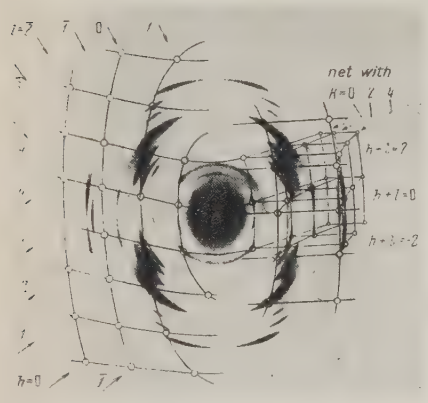

Fig. 4. – Oblique texture pattern from $NiCl_2 \cdot 2H_2O$ (angle of tilt 60°). Different types of interference lines are distinguished. On the left, net of $h0l$-reflections; on the right, representation of the entire reciprocal lattice on the electron diffraction pattern as a perspective curvilinear image (weak reflexion, situated in the peripheral portion of the photograph, not reproduced). Specimen obtained from aqueous solution by crystallization at a drying temperature of 70 °C.

previously proposed by the author for patterns from textures [30], where $H_{hk(l+l_1)}$, $H_{hk(l-l_1)}$, H_{hkl} are the vectors of the reciprocal lattice measured on several electron diffraction patterns. The rotation method is convenient also for a subsequent determination of reflexion intensities.

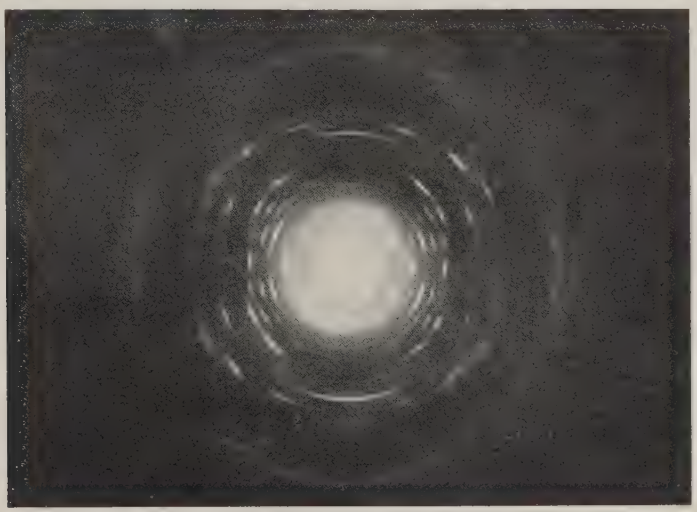

Fig. 5. – Electron diffraction pattern from a texture of diketopiperazine. Angle of tilt 60°. Specimen produced by crystallization from aqueous solution.

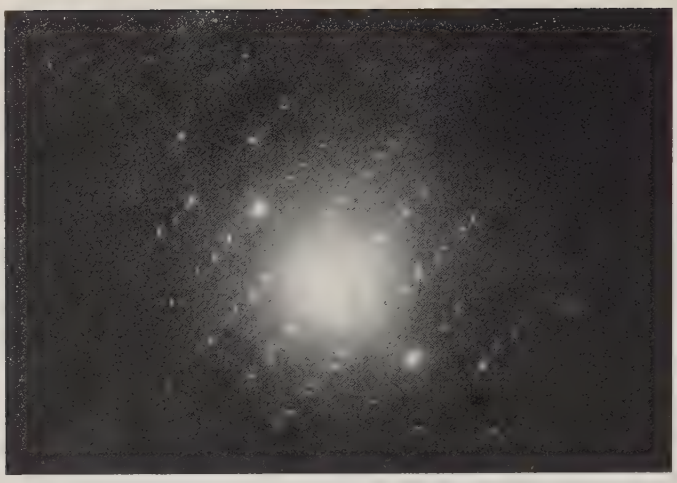

Fig. 6. – Electron diffraction pattern from an acicular texture of urea.

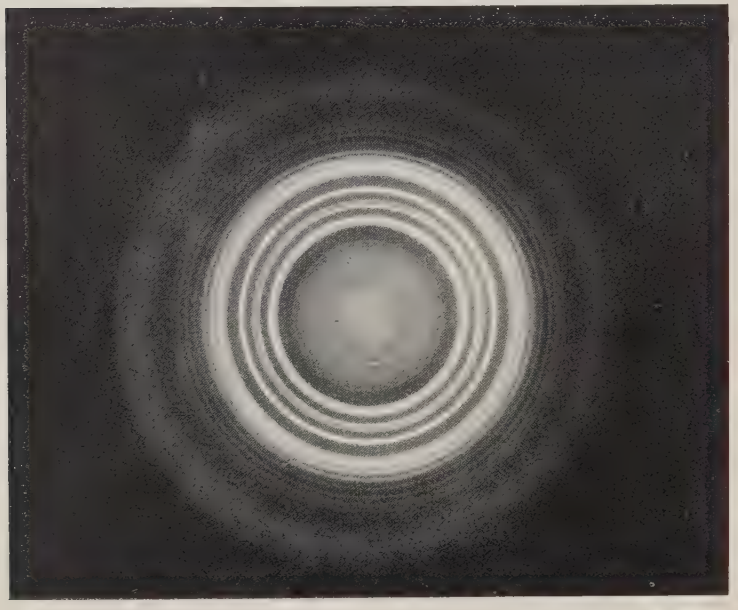

Fig. 7. – Electron diffraction pattern of a polycrystal of $CoCl \cdot 2H_2O$.

The structure analysis is considerably facilitated if a particular substance, being crystallized on the support, forms textures [6]. If all the crystallites are oriented with one principal face against the support but are distributed at random over the azimuth, this is a case of lamellar texture. The reciprocal lattice of the texture is a system of rings, since a continuous set of azimuth orientations is equivalent to a spot reciprocal lattice rotating about the axis of the texture. If the specimen is perpendicular to the beam, the photograph represents a system of rings; when the specimen is tilted, photographs of the so-called oblique texture type are produced, the reflexions of which have the appearance of small arcs and are arranged according to definite rules.

In order to find the cell and to index the electron diffraction patterns from textures, it is essential to distinguish interference lines in which the straight lines of the reciprocal lattice are represented. Z. G. PINSKER, who has proposed methods for calculating electron diffraction patterns from textures of orthogonal crystals [31], has suggested an explanation of the presence of ellipses and layer lines (Fig. 3). The geometric scheme in the general case is as follows [32]. In a reciprocal lattice of a texture the straight lines are converted into rotation surfaces, which when being intersected by a plane yield curves of the second order. The most characteristic interference curves are ellipses and, for non-rectangular lattices, hyperbolae too, the appearance of parabolae being also possible (Fig. 4). An important particular case is that of straight interference lines. If the axis of the texture is selected as the c^* axis, the reflexions of a given ellipse have constant indices h and k, and the reflexions with a constant l are situated in the general case on the curvilinear net of hyperbolae. If the crystals are orthogonal and are arranged with their coordinate face parallel to the support, such nets degenerate into layer lines which are possible also for monoclinic crystals, if the b^* axis is the axis of the texture (Fig. 5). If the crystal has a low symmetry, its reciprocal lattice as a whole is represented on an electron diffraction pattern from texture by a two-dimensional perspective image (see Fig. 4).

The relation of the coordinates of points of the reciprocal lattice with the axes a^*, b^* and c^* and the $\alpha^*, \beta^*, \gamma^*$ angles, and of the Cartesian coordinates of the reflexion of electron diffraction patterns (ξ and η) is given by the relations:

$$(2a,b) \qquad \xi^2 = R^2 - (z \operatorname{cotg} \varphi)^2 ; \qquad \eta = z/\sin\varphi$$

$$(2c) \qquad z = ha^* \cos\beta^* + kb^* \cos\alpha^* + lc^*$$

$$(2d) \qquad R^2 = h^2A^2 + k^2B^2 + 2hkAB\cos\gamma' ; \qquad A = a^* \sin\beta^* ; \qquad B = b^* \sin\alpha^* .$$

Here φ is the angle of tilt of the specimen to the beam [32]. These relations enable us to find an analytical equation of the interference lines of electron

diffraction patterns, in which the straight lines of the reciprocal lattice are represented. In the case of orthogonal textures, the period c^* is determined by the formula [31]:

$$c^* = \sqrt{H^2_{hkl} - H^2_{hk0}}/l \,. \tag{3}$$

If the crystals have non-rectangular cells, the periods and angles are determined by formulae (1) [30, 32].

In the case when clay minerals are investigated, if the periods a and b of their cells are known in advance, the period or the angles of the cell can be determined by measuring the heights η of reflexions and by making use of the relations (2*b*, *c*) in the form: $\eta = (hp + kq + lr)/\sin\varphi$ [33]. The electron diffraction patterns of oblique textures are suitable for intensity measurements, since they at once reveal nearly all of the points of the reciprocal lattice.

Along with lamellar textures, acicular textures are also used in electron diffraction analysis; in these latter textures the crystals are oriented with their edge parallel to a certain direction (Fig. 6).

In structure determinations use may be made also of patterns from a polycrystal (Fig. 7). In the case of low symmetry of the crystals it is difficult to make a determination of cells by means of such photographs, but in some cases it is possible [34]; they are sometimes found to be useful for measuring intensities, as well as interplanar distances [35].

4. – Reflexion Intensities of Electron Diffraction Patterns.

The practice of structure analysis, an experimental study of atomic scattering and a theoretical consideration of the question of reflexion intensities of patterns show that in the majority of cases a satisfactory agreement with experimental data is secured by formulae of kinematic scattering, which are valid for small crystals with linear dimensions of 10^{-6} to 10^{-5} cm [6]. When electrons pass through thicker specimens, an increasingly important part is played by dynamic effects [36].

The atomic factor of electron scattering in Born's approximation [37], for a spherically symmetric atom has the form:

$$f_e = \frac{8\pi^2 me}{h^2} \int \varphi(r) r^2 \frac{\sin sr}{sr} \mathrm{d}r \,, \tag{4}$$

i.e., it is calculated from the distribution of the potential $\varphi(r)$ within the atom, just as the X-ray atomic factor f_x is calculated from the distribution of the electronic density $\varrho(r)$. The validity of the Born approximation has been repeatedly verified [6, 38]. A careful experimental verification of the atomic scat-

tering formula has been carried out by JAMZIN and PINSKER [39]. Using (4), as well as the well known relation

$$f_e = \frac{8\pi^2 me^2}{h^2} \cdot \frac{(Z - f_x)}{s^2}, \tag{5}$$

the author [40] has prepared tables of f_e-curves for all Z's, in the region of small angles for light atoms the phenomenon of their intersection (« reverse course ») having been detected [41], which is not observed for X-ray f_x-curves (see Fig. 8*a*).

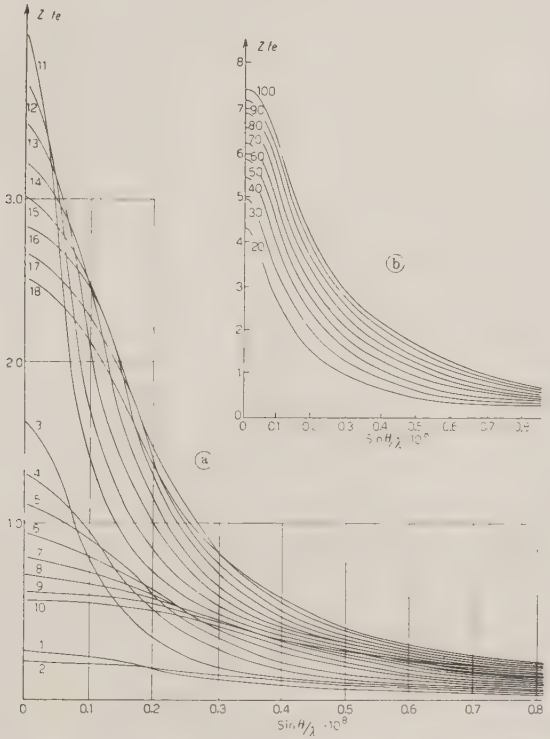

Fig. 8. - f_e-curves for light (*a*) and medium and heavy (*b*) atoms. The coefficient of transition to absolute values of f_e is equal to $2.393 \cdot 10^{-8}$ cm.

The amplitude of scattering by the unit cell of a crystal is determined by the Fourier integral from the potential of the cell:

$$\Phi_{hkl} = \int \varphi(\boldsymbol{r}) \exp\left[2\pi i(\boldsymbol{rH})\right] \mathrm{d}v_r . \tag{6}$$

Representing the cell potential as a superposition of the potentials of all atoms entering into the cell: $\varphi(\boldsymbol{r}) = \sum_i \varphi_i(\boldsymbol{r} - \boldsymbol{r}_i)$, an expression is obtained for the structure amplitude, analogous to that in the theory of X-ray scattering:

$$\Phi_{hkl} = \sum_i f_{e_i} \exp\,[2\pi i(\boldsymbol{r}_i \boldsymbol{H})]\,. \tag{7}$$

In electron diffraction work the temperature factor may be usually neglected; in certain cases, however, particularly in that of organic crystals, its influence is rather marked.

Let us consider the intensity of scattering from an ideal single crystal which in a kinematic approximation is determined by the formula:

$$J = \frac{J_0}{r^2} |\Phi_{hkl}|^2 |g|^2; \qquad |g|^2 = \prod_{i=1,2,3} \frac{\sin^2 \pi A_i h_i}{\sin^2 \pi a_i h_i}\,. \tag{8}$$

Here g is the Laue interference function, taking into consideration the shape and size of the crystal; A_i the dimension of the crystal in the i-direction; a_i the edge of the unit cell; h_i the distance in the reciprocal space. To calculate the integral intensity I_{hkl} of scattering from the crystal placed in a reflecting position, the integral from $|g|^2$ must be taken along the directions h_1 and h_2 (Fig. 9); it is equal to $(A_1/a_1^2)\cdot(A_2/a_2^2)$. For the third direction, h_3, the value of g^2 in a maximum should be used, which is equal to A_3^2/a_3^2. Since the reciprocal space is represented on the screen on a scale of $L\lambda$, when integrating, the multiplier $(L\lambda)^2$ will enter into (8). Considering too that r is the distance of the crystal to the screen L, we shall obtain as a result:

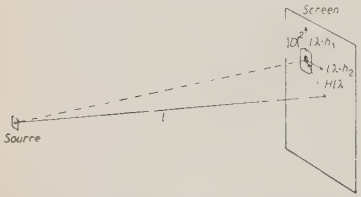

Fig. 9. – Scheme for calculating integral intensity in diffraction from a single crystal.

$$I_{hkl} = \lambda^2 J_0 \left|\frac{\Phi}{\Omega}\right|^2 V A_3 = W A_3\,, \tag{9}$$

where $V = A_1 A_2 A_3$ is the volume of the crystal, and $\Omega = a_1 a_2 a_3$ is the volume of the unit cell. Considering that $V = S A_3$, where S is the area of the crystal, we shall see that the ratio of the scattered intensity to the initial one, referred to the area of the crystal, is:

$$\frac{I_{hkl}}{J_0 S} = \lambda^2 \left|\frac{\Phi}{\Omega}\right|^2 A_3^2\,. \tag{10}$$

It is evident that if the scattered intensity becomes comparable in order to the initial one, i.e. if $I_{hkl} \approx J_0 S$, the basic condition of the kinematic theory —the weakness of secondary beams—is not satisfied. Consequently, an evaluation of the limit of its applicability may be obtained from the condition:

$$\lambda \left| \frac{\Phi}{\Omega} \right| A_3 \approx 1 , \tag{11}$$

where Φ must be calculated in absolute units. For simple structures (e.g. cubic lattices of metals) giving strong reflections with unitary structure amplitudes $\hat{\Phi} = 1$, the transition to dynamic scattering corresponds to a thickness of blocks about 100 Å, which is in accordance with the figures of Blackman [42]. However, bearing in mind that for complex structures $\hat{\Phi}$ is never equal to unity but on the average is equal to a value of 0.2 or less, we shall have that for most crystals the critical thickness of blocks is about 500 Å, and for crystals from light atoms (organic), 1500 Å.

The real specimens, yielding spot electron diffraction patterns, are not ideal single crystals but form a mosaic. The mosaic structure may be described by the function of crystal distribution among the angles $f(\alpha)$. Then g^2 should be integrated also along the third direction h_3, considering, in doing so, what a quantity of crystals is placed into the reflecting position. This is determined by the form of $f(\alpha)$. Making some assumptions as to the form of $f(\alpha)$, the following formula may be obtained:

$$I_{hkl} = W d_{hkl}/\alpha; \qquad |\Phi_{hkl}|^2 \sim I_{hkl}/d_{hkl} , \tag{12}$$

where α is the effective angular distribution of the small crystals in the mosaic, which is usually $2^\circ \div 3^\circ$, i.e. is about 1/20 of the radian. The conditions of applicability of this formula, which is in most cases suited to a calculation of $|\Phi|^2$ from the integral intensities I_{hkl} of the reflexions of spot patterns, are not satisfied, if the distribution function is very sharp ($\alpha < 0.5^\circ$).

To calculate the intensities of electron diffraction patterns from textures, one should take into consideration, first, the uniform azimuth distribution of crystals about the axis of the texture in an angular range of 2π, and second, the angular distribution α' of the texture axis itself, which leads to a certain extension of the small arcs of the electron diffraction pattern. The integral intensity of a small arc is determined by the formula:

$$I_{hkl} = W \frac{L\lambda \cdot p}{2\pi R' \sin \varphi}; \qquad |\Phi_{hkl}|^2 \sim (I_{hkl}/p) \cdot R' , \tag{13}$$

where R' is the horizontal coordinate of a given reflexion on the oblique texture

pattern, φ the angle of tilt, p a multiplicity factor for patterns from textures. In the majority of cases it is more convenient to measure the local intensity, I'_{hkl}, in the centre of the small arc, for which

$$I'_{hkl} = W \frac{d_{hkl} d_{hk0} \cdot \Delta}{\alpha' \cdot 2\pi L\lambda} \cdot p; \qquad |\Phi_{hkl}|^2 \sim I'_{hkl}/d_{hkl} \cdot d_{hk0} \cdot p\,, \tag{14}$$

where Δ is the length of the small intercept to be measured in the centre of the small arc, d_{hkl} the interplanar distance of a given reflexion, d_{hk0} that of the corresponding reflexion from the zero layer line. The latter multiplier is the same for all the reflexions of a given ellipse, since h and k for them are constant.

The local intensity of the portion of the ring having a length Δ on an electron diffraction pattern from a polycrystal is:

$$I''_{hkl} = W \frac{d^2_{hkl} \cdot \Delta}{4\pi L\lambda} \cdot p; \qquad |\Phi_{hkl}|^2 \sim I''_{hkl}/d^2_{hkl} \cdot p\,. \tag{15}$$

Let us briefly consider the question of the measurement of the reflexion intensities of the electron diffraction patterns. At the first stage of structure analysis satisfactory results are given by a visual evaluation on a scale of 100 [6]; subsequently use may be made either of microphotometry or of the method of multiple expositions. This method is as follows [44]. Let the darkening be $D = \log(It)$; finding such pairs of reflexions taken on electron diffraction patterns with multiple expositions, for which $D_1(h_1k_1l_1) = D_2(h_2k_2l_2)$, a relation between their intensities will be obtained: $I_{h_1k_1l_1}/I_{h_2k_2l_2} = t_2/t_1$ and the relation between t_2 and t_1 is known. The transition from the intensities to $|\Phi|^2$ is made in accordance with the type of patterns by means of formulae (12)-(15).

5. The Fourier Method in Electron Diffraction Analysis.

Since the formal mathematical apparatus of the theory of scattering of electrons in crystals is similar to that for X-rays, in the electron diffraction analysis, in principle, all the methods of the modern structure analysis are applicable. However, the physical distinction in the nature of scattering, i.e. differences in the potential distribution of the lattice $\varphi(\boldsymbol{r})$ when compared to the well known function of the electron density $\varrho(\boldsymbol{r})$, lead to several peculiarities. Reversing the Fourier integral (6) we find that the potential of the crystal

$$\varphi(\boldsymbol{r}) = \frac{1}{\Omega} \sum_{hkl} \Phi_{hkl} \exp[-2\pi i(\boldsymbol{r}\boldsymbol{H})] \tag{16}$$

can be obtained by summing up the Fourier series, the Φ_{hkl} values being

obtained directly from experimental data. The peaks of the series correspond to atoms. The potential of the atom is composed of the potential of the positive charge of the nucleus $\varphi_+ = Ze/r$, and the negative potential of electron shells $\varphi_{-\varrho(r)}$

$$\varphi = \varphi_+ - \varphi_- . \tag{17}$$

Owing to the fact that the positive charge is concentrated in the nuclei, and the negative charge is diffuse, $\varphi_+ > \varphi_-$, i.e. φ is everywhere positive.

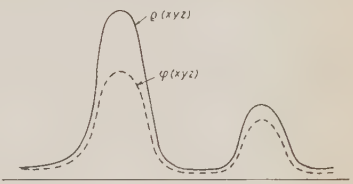

Fig. 10. – Comparison of the distribution of the electron density $\varrho(xyz)$ and the potential $\varphi(xyz)$. Peaks of electron density are sharper, but the ratio of peak heights of φ is less than for ϱ-peaks.

From the Thomas-Fermi statistical theory it follows that the potential φ represents a less sharp function than the electron density ϱ: ($\varphi \sim \varrho^{\frac{2}{3}}$, see Fig. 10). As a result of this a more rapid decrease of scattering of electrons with increasing $\sin\theta/\lambda$ is obtained as compared to X-ray scattering (Fig. 11), and the number of terms in the Fourier series of the potential is generally found to be two to four times less than in the electron density series. The convergence of the Fourier series of the potential is better, but the function obtained is less sharp. An essential advantage, however, is presented by its lesser sensitivity—as compared to the function giving the electron density—towards the difference in atomic numbers Z (see Fig. 10). The fraction of scattering by light atoms is relatively greater in the reflexion intensities of electron diffraction patterns than in the reflexions of X-ray diagrams. The fact that light atoms are better detected in electron diffraction work is particularly striking when the relative heights of atom peaks with different Z's are compared on Fourier syntheses of the potential and of electron density. The height of the peak, i.e. the value of $\varphi(0)$ (or $\varrho(0)$) in the centre of an atom can be calculated through the atomic-temperature factor

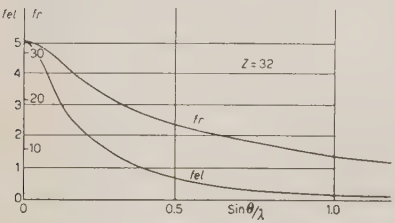

Fig. 11. – f_e- and f_X-curves for $Z = 32$.

$$\varphi(0) = \frac{1}{2\pi^2}\int f_{eT}(s)s^2\,\mathrm{d}s\,, \tag{18}$$

where $f_{eT} = f_e \cdot \exp[-B(\sin\theta/\lambda)^2]$ (to calculate $\varrho(0)$ one should substitute f_{xT} into the integral). The calculations made by the author [45] have shown that

the values of $\varphi(0)$ and $\varrho(0)$ are well approximated by a formula of the kZ^{α} type. Thus, for $B=2$, $\varrho(0) = 2.15 \cdot Z^{1.27}/\text{Å}^3$; $\varphi(0) = 57 \cdot Z^{0.79}$ V. The differences in the height of peaks in X-ray and electron diffraction work are particularly striking in the case of a strong difference in atomic numbers. For instance, the peak of the atom of lead ($Z=82$) is higher than that of the oxygen atom ($Z=8$) on the Fourier synthesis of the electron density nearly 20 times, and on the Fourier synthesis of the potential, only 6 times (with $Z_{\text{Pb}}/Z_{\text{O}} \approx 10$). The current simplified conception that the values of $\varrho(0)$ in X-ray analysis are proportional to Z, is far from being exact. It should be noted too that in the case of projections the values of α in X-ray analysis are nearer to 1 ($\alpha \approx 1.2$), and in electron diffraction analysis for projections, $\alpha \approx 0.7$. In both cases an increase of B markedly reduces k, and less strongly, α. Thus, for $B=4$, $\varphi(0) = 36 \cdot Z^{0.75}$ V. The slight dependence of the heights of peaks on the atomic number enables a good determination of hydrogen atoms to be made by means of electron scattering analysis. In X-ray work, for a carbon atom $\varrho(0)_{\text{C}} = 7 \div 10/\text{Å}^3$, and for a hydrogen atom $\varrho(0)_{\text{H}} = 0.6 \div 0.8/\text{Å}^3$; i.e. $\varrho_{\text{H}}/\varrho_{\text{C}} \approx \approx 1/13$, which gives the possibility to determine hydrogen only with a rather low precision in the most careful studies. In the electron diffraction work, $\varphi(0)_{\text{C}} = 140 \div 160$ V, $\varphi(0)_{\text{H}} = 30 \div 35$ V, i.e. $\varphi_{\text{H}}/\varphi_{\text{C}} \approx 1/4.5$, which reliably reveals the hydrogen atom.

We shall dwell now on the accuracy of determination of the atom coordinates in the electron diffraction analysis. The general formula

$$\Delta x_j = \frac{\partial \Delta\varphi}{\partial x} \Big/ \frac{\partial^2 \varphi_j}{\partial x^2}_{r=0}, \tag{19}$$

in which $\Delta\varphi$ arises as a consequence of the approximation used and of the errors in the determination of the experimental amplitude $|\Phi_{\text{obs}}|$, might be conveniently transformed by introducing formulae of the kZ^{α} type for the numerator and denominator, just as it has been done for the peak heights $\varphi(0)$. Then, for instance, for the case where $B=4$, the error of the three-dimensional series may be calculated by the formula

$$\Delta x_j = 0.093(b/\sqrt{\bar{\Omega}}) \sqrt{\sum_i Z_i^{1.48}} / Z_j^{0.80} \text{ (in Å)}. \tag{20}$$

The sum under the radical is taken over all the atoms of the unit cell, b is the average error in determining the amplitudes, which can be found by calculating the reliability factor

$$R = \frac{\sum \| \Phi_{\text{obs}}| - |\Phi_{\text{calc}} \|}{\sum |\Phi_{\text{obs}}|} \approx b .$$

The position of the heaviest atoms with an average accuracy of the experiment

($b \approx 0.2$) is determined by three-dimensional series with a precision of $0.01 \div 0.02$ Å. A comparison with X-ray analysis shows that, e.g. in a structure composed of three kinds of atoms, the heavy ones are determined by electron diffraction analysis less precisely, the medium atoms about as accurately, and the light ones, more precisely than by X-ray analysis.

In electron diffraction analysis various methods are used for reducing to the absolute scale the relative values of amplitudes obtained from experiment, these methods being analogous to those used in X-ray work [46-48]. The three-dimensional Fourier series of potential can be calculated in volts (see Fig. 17), the two-dimensional ones (projections), in volt·Å [49].

During the first stage of the analysis of structures by the electron-diffraction method, the Φ^2-Patterson series are widely used [50]. Direct methods for determining the structure from vector maps [51-54] have been also successfully used in electron diffraction work [55, 56]. In simple cases a preliminary analysis of the structure is carried out on the basis of geometrical and crystal-chemical considerations and by the trial-and-error method. The Fourier method is subsequently used; it permits not only to establish the atomic coordinates but sometimes also to make conclusions as to their thermal movement, ionization, etc., on the basis of an analysis of the height and shape of peaks.

6. – Experimental Structure Studies.

The general course of structure studies in electron diffraction analysis is about the same as in X-ray analysis, its principal stages being: determination of cell and indexing of electron diffraction patterns, measurement of intensities, finding of a preliminary model of the structure and further on, a more precise determination of atom coordinates.

In the Soviet Union, electron diffraction has been used to solve structural problems since the early '30ies by V. E. Laškarev and I. D. Usyskin [4]. In the early '40ies Z. G. Pinsker, using the trial-and-error method, found new polymorph modifications of cadmium halides and investigated the variable structure in these compounds [6, 57]. Since that time the number of works on electron diffraction analysis in the USSR has been rapidly increasing. The application of the Fourier synthesis in electron diffraction work [58] has increased the possibilities of the method and made possible a study of complex structures.

The first cases of using the Fourier method were investigations of barium halides and their crystal hydrates [25, 29]. A number of inferences concerning the part played by the water molecule in crystal hydrates have been made on the basis of a study of monoclinic structures of the hydrates of chlo-

rides of transition metals: $MeCl_2 \cdot 2H_2O$ (Me: Mn, Co, Fe, Ni) [60], the crystal chemical peculiarities of which have been found to depend largely on the nature of the metallic atom. From the substances listed, electron diffraction patterns of different types have been produced (see, e.g., Figs. 4, 7); cells and Fedorov (space) groups determined; and coordinates of all the atoms, determined by constructing Fourier syntheses. A common feature of all of these structures is the presence of chains of octahedra of $MeCl_2 \cdot 2H_2O$ (see Fig. 12), having common edges (Cl). The Cl atoms form around Me a regular square, while in the two other apices of the octahedron H_2O molecules are located. Fig. 13 represents a one-dimensional section of a three-dimensional potential series in the structure $MnCl_2 \cdot 2H_2O$, determining the position of water molecules. Fig. 14 shows a projection of the structure of $NiCl_2 \cdot 2H_2O$ along chains of octahedra, which here are arranged in zig-zag fashion. This projection has been constructed according to reflections shown on the left-hand side of the net of the pattern shown in Fig. 4. The monoclinic symmetry of the isomorphic structures of Mn, Fe, Co (Fig. 12*a*) is due to the formation of hydrogen bonds between H_2O and Cl of neighbouring chains. A structure, known from X-ray analysis data and related to these compounds, namely the $CdCl_2 \cdot 2NH_3$ structure, is orthorhombic, which fact is accounted for by the presence of a symmetrical rotating NH_3 group instead of the polar H_2O molecule. The complex nature of the $NiCl_2 \cdot 2H_2O$ structure as compared to that of $CoCl_2 \cdot 2H_2O$ is explained by the more covalent nature of the bond in the octahedron. In $CoCl_2 \cdot 2H_2O$ the distance Co – Cl = 2.54 Å is equal to the sum of ionic radii, while in $NiCl_2 \cdot 2H_2O$ the Ni – Cl distance, = 2.43 Å, is less than the sum of ionic radii. The position of atoms in the $NiCl_2 \cdot 2H_2O$ structure is described by seven parameters. The accuracy of determination of the coordinates of Cl in these structures is 0.02 Å; that of H_2O, 0.04 Å. Electron diffraction studies have been made also of other complex compounds of Co and Ni, as well as of Pt [56, 61].

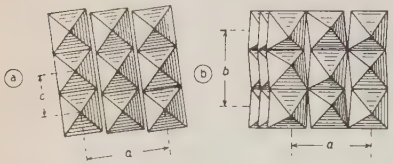

Fig. 12. (a) Structures of $CoCl_2 \cdot 2H_2O$ (also of $MnCl_2 \cdot 2H_2O$; $FeCl_2 \cdot 2H_2O$); and (b) of $NiCl_2 \cdot 2H_2O$.

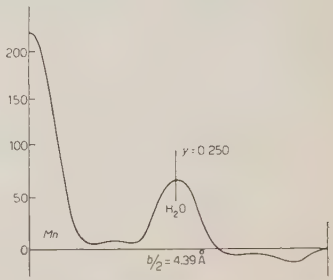

Fig. 13. $\varphi(0y0)$ section of a three-dimensional series in the structure of $MnCl_2 \cdot 2H_2O$ (in arbitrary units).

A number of new data have been obtained in the field of metal and alloy studies, in particular of Bi, Sb, Se, Te compounds, which are of interest to

the crystal-chemistry. In studying the binary systems Bi – Se and Bi – Te S. I. Semiletov [62, 63] has established in them the existence of new phases, previously unknown. An analysis of the electron diffraction patterns produced from specimens sublimated in vacuum, has revealed the region of homogeneity of the compounds Bi_2Se_3, Bi_3Se_4 and BiSe. For each of these, the cell dimensions may slightly vary in accordance with the excess of some component or other. The application of the close packing method, developed by Academician N. V. Belov [63], along with the construction of the Φ^2- and Φ-series, enabled the coordinates of all atoms to be determined. It is interesting to note that in the Bi – Se system a previously unknown compound Bi_3Se_4, with a hexagonal cell ($a = 4.20 \div 4.27$ Å, $c = 40.2 \div 41.0$ Å) has been established by means of only electron diffraction data. Lying at its base is a twelve-layer rhombohedral packing of Se, in which three quarters of the octahedral holes are filled with Bi atoms. Fig. 15 presents a section of the threedimensional Φ-series of Bi_3Se_4 along the c-axis.

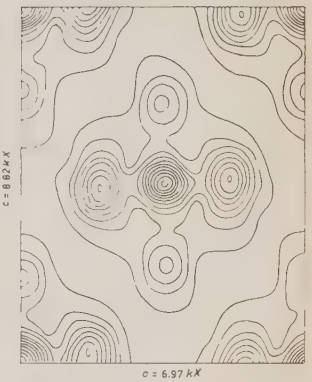

Fig. 14. Fourier projection of potential of the structure of $NiCl_2$ onto the (101) plane (in arbitrary units). The coordination octahedron about Ni is distinctly revealed. Cl ions are not precisely located one above the other, hence the maximum from them is somewhat stretched.

Fig. 16 represents the structure of a ternary compound, $Tl_2Sb_2Se_4$, established by Z. G. Pinsker with the aid of the Φ^2- and Φ-series. The packing of layers, consisting of Tl and Sb, alternates with chains of Se atoms, similar to those in the structure of elementary selenium but somewhat more straightened, which is naturally accounted for by an interaction with the neighbouring layers.

The peculiar feature of electron diffraction as a method giving the possibility to establish reliably the position of light atoms in the presence of heavy ones, has been successfully used in the study of iron carbides and nitrides [65, 66].

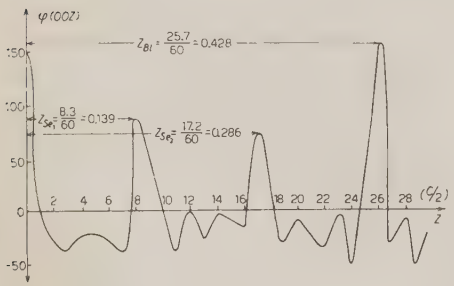

Fig. 15. – One-dimensional $\varphi(00z)$ section in the structure of Bi_3Se_3 (in arbitrary units).

The specimens were prepared by nitration or cementation in the gaseous phase of single-crystal films of α-Fe, produced by sublimation in vacuum onto orienting crystals of NaCl. In the study of iron nitrides several phases are obtained: a cubic γ'-phase of Fe_4N, two hexagonal ε-phases of Fe_3N, and two hexagonal phases of a Fe_2N composition with an ordered and disordered distribution of nitrogen atoms in the octahedral holes. The position of nitrogen atoms in these structures has been found by an analysis of the reflexion intensities. The mechanism of the phase transition $\gamma' \rightarrow \varepsilon$ has been studied. Both phases are based on a close packing of iron atoms, in which the Fe – Fe distance is equal to 2.76 Å, $a_{\gamma'}$ being equal to $2.76 \cdot \sqrt{2} = 3.90$ Å; $a_\varepsilon = 2.76 \cdot \sqrt{3} = 4.78$ Å; $c_\varepsilon = 4.41$ Å. In the initial stages of increase in nitrogen saturation the transition $\gamma \rightarrow \varepsilon'$ proceeds by small shifts of atoms over distances of the order of interatomic distances, i.e. this transition is a non-diffusional one. The mutual arrangement of cubic axes and of the related hexagonal axes remains unchanged. Further on, the orientation of the ε-phase with respect to the NaCl support is changing regularly, which fact is directly revealed by the arrangement of reflexions on spot diffraction patterns. The attention of workers using the diffraction electron method has been repeatedly attracted by iron carbides [67]. In cementing iron films Z. G. Pinsker and S. V. Kaverin discovered, in addition to the carbide Fe_3C, a new cubic carbide, previously unknown, namely Fe_4C, with $a = -3.875$ Å, in which one carbon atom is surrounded by a tetrahedron of Fe atoms.

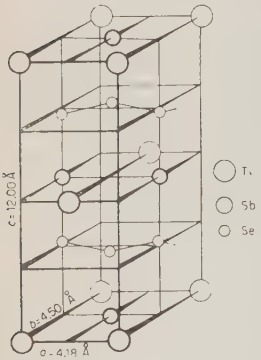

Fig. 16. – Structure of $Tl_2Sb_2Se_4$.

New information has been gained in the course of electron diffraction studies of the processes of oxidation of iron, copper, aluminium, and some other metals [7-10].

One of the most interesting uses of the electron diffraction method is the location of hydrogen atoms in crystals. The possibilities of a more reliable and precise location of hydrogen atoms than that attainable in X-ray work, are in general due to the fact that light atoms are better revealed in electron diffraction works, as already pointed out above. The ionization of hydrogen atoms possible in a number of cases, i.e. the decrease in their electron density, still further impairs the possibilities of X-ray analysis in this field. Ionization is, however, favourable for electron diffraction work, since the screening effect of the electron shell diminishes, and the potential, and hence the scattering power increases. The accuracy of determination of the hydrogen atomic coordinates in X-ray work is about 0.1 Å; in electron diffraction work, 0.03 Å; in neutron diffraction work, 0.02 Å.

In the early works on electron diffraction for determining the position of hydrogen atoms the trial-and-error method was used [68, 69]. The first example of the use of the Fourier synthesis to this purpose was the study of paraffin [70] carried out at the Institute of Crystallography of the Academy of Sciences of the USSR, followed by studies of hexamethylene-tetramine (urotropine) [71], diketopiperasine [72] and some other crystals. Later on, works in the same field have been done by Australian authors [73, 74].

The structure of diketopiperazine, 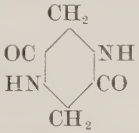 is interesting in that it includes hydrogen atoms, both forming hydrogen bonds and not forming any. The arrangement of heavy atoms of C, N, O is known from X-ray data [75]. From electron diffraction patterns produced from textures, the following cell dimensions have been found (in kX; in parentheses the data of Corey [75] are given): $a = 5.230 \pm 0.004$ (5.19_2); $b = 11.43 \pm 0.03$ (11.50); $c = 3.963 \pm 0.003$ (3.96_4); $\beta = 81°55'$ $(83 \pm 1)°$. The space group is $C_{2h}^5 - P2_1/a$.

In structure analysis work various modifications of the Fourier method have been used; ordinary, generalized, and partial projections, as well as three-dimensional syntheses were calculated. In all cases hydrogen atoms were well revealed, both those belonging to the CH_2 group, and this referring to the NH group. The most distinct results were furnished by the three-dimensional synthesis of the potential, carried out as a set of flat sections parallel to the *ab* face (Fig. 17).

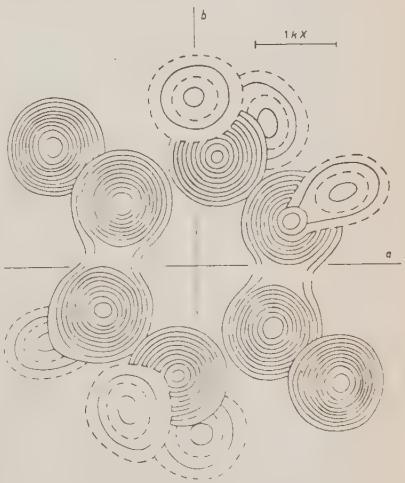

Fig. 17. – Three-dimensional Fourier synthesis of potential of a diketopiperazine molecule. Continuous lines drawn at intervals of 15 V; dashed lines, 7.5 V; the first continuous line, 15 V.

The distances between atoms in a diketopiperazine ring, all the angles of which differ little from 120°, are as follows (in kX): $C-N = 1.38_3$; $N-C_{H_2} = 1.40_0$; $C-C_{H_2} = 1.44_1$; the C – O distance is 1.22_1. In the CH_2 group the C – H distances are 1.09 and 1.11; the angle of bonding is near to a tetrahedral one of 107°. The H_{III} atom, realizing the hydrogen bond between the N and O of neighbouring molecules, is covalently bound with nitrogen and

is 0.98 kX distant from it. The hydrogen bond N – H ... O slightly deviates from rectilinearity; its length is 2.84 kX. The error of determination of the coordinates is $\Delta x_{C,N,O} = 0.008$ kX and $\Delta x_H = 0.03$ kX. The coefficient $R = \sum \| \Phi_{obs} | - | \Phi_{calc} \| / \sum | \Phi_{obs} |$ has a value of 20 per cent.

The elongated shape of the atomic peaks of H on the syntheses (see Fig. 17) suggests a different character of their thermal movement in the CH_2 group (oscillations of H about C as a centre) and in the NH group (oscillations along the bond). The potential values in the peaks for atoms of C, N, O are 150÷160 V; for H_I 33 V; H_{II} 32 V; H_{III} 36 V. An increase of the H_{III} potential corresponds to the ionization of this atom, which, probably, is in general characteristic of the hydrogen bond and explains some of its properties.

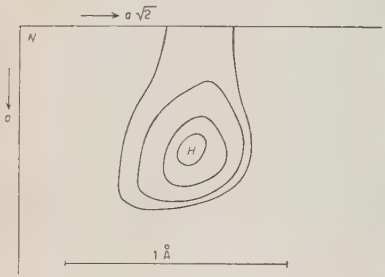

Fig. 18. – Portion of a two-dimensional $\varphi(xxz)$ section (along the (110) plane) of a three-dimensional series of the NH_4Cl structure, showing the shape of the peak of the H atom potential (the removed peak of the N atom was located at the origin of coordinates).

The oscillation of hydrogen atoms about a central atom, previously noted in the structure of paraffin [70], has been observed also for the NH_4 group in the structure of NH_4Cl studied by the Fourier method by the author and M. M. Stasova. Fig. 18 represents a portion of the flat section of a differentiated three-dimensional synthesis, from which the N atom, which had been at the 000 point, was removed. The shape of the remaining H atom suggests that the oscillations perpendicular to the bond have a greater amplitude than the oscillations along the bond. (An analogous deduction has been made from a neutron diffraction study of NH_4Cl [76]). The N – H distance is equal to (0.98 ± 0.04) kX.

The examples cited, as well as a number of electron diffraction works, which will not be dwelt upon here, for instance such as the studies of clay minerals [77-80], amorphous substances [81, 82] and many others, illustrate the contributions of Soviet scientists in this field. At present it is quite feasible to undertake electron diffraction studies of complex structures with a large number of atoms in the cell.

The versatility of problems that may be solved with the aid of electron diffraction structure analysis opens further possibilities for the development of this important method for studying the structure of matter.

REFERENCES

In the list of the literature chiefly the works of Soviet authors published after 1949 are cited. For references to works prior to 1949 the reader is referred to [6].

[1] P. S. Tartakovskij: *Eksperimentalnye osnovanija volnovoj teorii materii* (*Experimental Foundations of the Wave Theory of Matter*) (Moscow-Leningrad, 1932).

[2] A. A. Lebedev: *Nature*, **128**, 491 (1931).

[3] A. A. Lebedev: *Diffraktsija bystryh elektronov* (*The Diffraction of Fast Electrons*). Editor's notes to the Russian translation of H. Mark and R. Wierl: *Electron diffraction* (Moscow-Leningrad, 1933).

[4] V. E. Laškarev: *Diffraktsija elektronov* (*Electron Diffraction*) (Moscow-Leningrad, 1933).

[5] Z. G. Pinsker: *Trudy Vsesojuzn. Inst. Miner. Syr'ja*, no. 109 (1936).

[6] Z. G. Pinsker: *Diffraktsija elektronov* (*Electron Diffraction*). (Russ. edition, Moscow, 1949. Engl. edition, London, 1953).

[7] P. D. Dankov, N. A. Šišakov and D. V. Ignatov: *Elektronografičeskie issledovanija okisnyh i gidrookisnyh plenok na metallah* (*Electron Diffraction Investigations of Oxyde and Hydrooxide Films on Metals*), (Moscow, 1933).

[8] P. D. Dankov, N. A. Šišakov: *Žu. Fiz. Him.*, **23**, 1031 (1949).

[9] N. A. Šišakov: *Žu. Fiz. Him.*, **26**, 106 (1952).

[10] Z. G. Pinsker: *Izv. Akad. Nauk SSSR, Ser. Fiz.*, **13**, 473 (1949).

[11] A. V. Frost: *Vestnik Moskovskogo Gosudarstvennogo Universiteta*, **12**, 85 (1953).

[12] P. A. Akišin and L. V. Gurvič: *Učenye Zapiski Moskov. Gosud. Univ.*, **164**, 153 (1953).

[13] P. A. Akišin, L. V. Vilkov and V. P. Spiridonov: *Dokl. Akad. Nauk SSSR*, **101**, 77 (1955).

[14] Z. G. Pinsker and G. I. Distler: *Dokl. Akad. Nauk SSSR*, **72**, 315 (1950); *Žu. Fiz. Him.*, **23**, 1281 (1949); **24**, 1152 (1950).

[15] G. A. Korezkaja and. V. A. Kargin: *Kolloid Žu.*, **13**, 323 (1951).

[16] V. A. Kargin and G. S. Markova: *Žu. Fiz. Him.*, **27**, 1236 (1953); **27**, 1525 (1953).

[17] E. E. Rylov and V. L. Harpov: *Žu. Fiz. Him.*, **27**, 572 (1953); **27**, 579 (1953).

[18] A. L. Zaides and I. G. Sinizkaja: *Dokl. Akad. Nauk SSSR*, **80**, 213 (1951); **92**, 601 (1953).

[19] A. I. Bublik and B. Y. Pines: *Trudy Fiz. Otd. Fiziko-Matemat. Fakult. Harkov. Univ.*, **4**, 139 (1953).

[20] A. I. Bublik: *Dokl. Akad. Nauk SSSR*, **95**, 521 (1954).

[21] K. K. Gorbunova and N. A. Šišakov: *Izv. Akad. Nauk SSSR, Ser. Fiz.*, **17**, 242 (1953).

[22] N. A. Šišakov: *Žu. Èksper. Teor. Fiz.*, **22**, 241 (1952).

[23] A. I. Frimer: *Dokl. Akad. Nauk SSSR*, **63**, 255 (1948).

[24] G. O. Bagdykijanz: *Izv. Akad. Nauk SSSR, Ser. Fiz.*, **17**, 255 (1953).

[25] B. K. Vajnštejn and Z. G. Pinsker: *Žu. Fiz. Him.*, **23**, 1058 (1949).

[26] N. G. Sučkin: *Izv. Akad. Nauk SSSR, Ser. Fiz.*, **15**, 283 (1951).

[27] B. Y. Pines and A. I. Bublik: *Žu. Tehn. Fiz.*, **24**, 1139 (1594).

[28] *Primenenie rentgenovyh lučei k issledovaniju materialov* (*The Application of X-rays to Investigations of Materials*), (Moscow-Leningrad, 1949).

[29] B. K. Vajnštejn: *Trudy Inst. Kristall. Akad. Nauk SSSR*, **5**, 7 (1949).
[30] B. K. Vajnštejn: *Dokl. Akad. Nauk SSSR*, **73**, 103 (1950).
[31] Z. G. Pinsker: *Dokl. Akad. Nauk SSSR*, **30**, 795 (1941).
[32] B. K. Vajnštejn: *Trudy Inst. Kristall. Akad. Nauk SSSR*, **6**, 173 (1951).
[33] B. B. Zvjagin and Z. G. Pinsker: *Dokl. Akad. Nauk SSSR*, **68**, 65 (1949).
[34] B. K. Vajnštejn: *Dokl. Akad. Nauk SSSR*, **90**, 777 (1953).
[35] Z. G. Pinsker and B. K. Vajnštejn: *Trudy Inst. Kristall. Akad. Nauk SSSR*, **9**, 291 (1954).
[36] Z. G. Pinsker and B. K. Vajnštejn: *Izv. Akad. Nauk SSSR, Ser. Fiz.*, **14**, 295 (1950).
[37] H. F. Mott and H. S. W. Massey: *Theory of Atomic Collisions* (Oxford, 1949).
[38] S. Lennander: *Arkiv för Fysik*, **8**, N. 54 (1954).
[39] I. I. Jamzin and Z. G. Pinsker: *Dokl. Akad. Nauk SSSR*, **65**, 645 (1949); *Trudy Inst. Kristall. Akad. Nauk SSSR*, **5**, 69 (1949).
[40] B. K. Vajnštejn: *Žu. Éksper. Teor. Fiz.*, **25**, 157 (1953).
[41] B. K. Vajnštejn: *Dokl. Nauk Akad. SSSR*, **85**, 1239 (1952).
[42] M. Blackman: *Proc. Roy. Soc.*, A **173**, 68 (1939).
[43] B. K. Vajnštejn: *Trudy Inst. Kristall. Akad. Nauk SSSR*, **6**, 193 (1951).
[44] B. K. Vajnštejn and Z. G. Pinsker: *Dokl. Akad. Nauk SSSR*, **72**, 53 (1950).
[45] B. K. Vajnštejn: *Žu. Éksper. Teor. Fiz.*, **27**, 44 (1954).
[46] A. I. G. Wilson: *Acta Cryst.*, **2**, 318 (1949).
[47] B. K. Vajnštejn: *Dokl. Akad. Nauk SSSR*, **93**, 821 (1953).
[48] A. I. Kitajgorodskij, Ju. T. Stručkov and T. L. Hotsjanova: *Žu. Fiz. Him.*, **27**, 1490 (1953).
[49] B. K. Vajnštejn: *Trudy Inst. Kristall. Akad. Nauk SSSR*, **9**, 254 (1954).
[50] A. L. Patterson: *Zeits. f. Krist.*, **90**, 517 (1935).
[51] M. I. Buerger: *Acta Cryst.*, **3**, 87 (1950); **4**, 531 (1951).
[52] A. I. Kitajgorodskij: *Žu. Tehn. Fiz.*, **21**, 717 (1951).
[53] G. S. Ždanov and V. V. Sanadze: *Dokl. Akad. Nauk SSSR*, **73**, 111 (1950).
[54] B. K. Vajnštejn: *Dokl. Akad. Nauk SSSR*, **78**, 1137 (1951).
[55] B. K. Vajnštejn: *Trudy Inst. Kristall. Akad. Nauk SSSR*, **9**, 87 (1954).
[56] G. N. Tiščenko and Z. G. Pinsker: *Dokl. Akad. Nauk SSSR*, **100**, 913 (1955).
[57] See [6] Chapter X, and also Z. G. Pinsker: *Trudy Inst. Kristall. Akad. Nauk SSSR*, **7**, 35 (1952).
[58] B. K. Vajnštejn and Z. G. Pinsker: *Dokl. Akad. Nauk SSSR*, **64**, 49 (1949).
[59] B. K. Vajnštejn and Z. G. Pinsker: *Žu. Fiz. Him.*, **24**, 432 (1950).
[60] B. K. Vajnštejn: *Dokl. Akad. Nauk SSSR*, **68**, 301 (1949); **83**, 227 (1952); *Žu. Fiz. Him.*, **26**, 1774 (1952).
[61] G. B. Bokij, B. K. Vajnštejn and A. A. Babareko: *Izv. Akad. Nauk SSSR, Otd. Him. Nauk*, **6**, 667 (1951).
[62] S. A. Semiletov: *Trudy Inst. Kristall. Akad. Nauk SSSR*, **10**, 181 (1954).
[63] S. A. Semiletov, and Z. G. Pinsker: *Dokl. Akad. Nauk SSSR*, **100**, 1079 (1955).
[64] N. V. Belov: *Struktura ionnyh kristallov i metalličeskih faz* (*The Structure of the Ionic Crystals and Metal Phases*), (Moscow, 1947).
[65] Z. G. Pinsker and S. V. Kaverin: *Dokl. Akad. Nauk SSSR*, **95**, 797 (1954); **96**, 519 (1954).
[66] Z. G. Pinsker: *Trudy Inst. Kristall. Akad. Nauk SSSR*, **10**, 91 (1954).
[67] I. I. Trillat and S. Oketani: *Acta Cryst.*, **5**, 469 (1952).
[68] V. E. Laškarev and I. D. Usyskin: *Žu. Éksper. Teor. Fiz.*, **3**, 510 (1933).
[69] R. Rigamonti: *Gazz. Chim. Ital.*, **66**, 174 (1936).

[70] B. K. Vajnštejn and Z. G. Pinsker: *Trudy Inst. Kristall. Akad. Nauk SSSR,* **6**, 163 (1951); **10**, 145 (1954).
[71] A. N. Lobačev: *Trudy Inst. Kristall. Akad. Nauk SSSR,* **10**, 167 (1954).
[72] B. K. Vajnštejn: *Dokl. Akad. Nauk SSSR,* **99**, 81 (1954); *Trudy Inst. Kristall. Akad. Nauk SSSR,* **10**, 115 (1954); *Žu. Fiz. Him.,* **29**, 327 (1955).
[73] Y. M. Cowley, A. L. G. Rees and I. A. Spink: *Proc. Phys. Soc.,* A **64**, 609 (1951).
[74] Y. M. Cowley: *Acta Cryst.,* **6**, 516, 522, 846 (1953).
[75] R. B. Corey: *Jurn., Am. Chem. Soc.,* **60**, 1598 (1938).
[76] H. Levy and L. Peterson: *Phys. Rev.,* **86**, 766 (1952).
[77] Z. G. Pinsker: *Dokl. Akad. Nauk SSSR,* **73**, 107 (1950).
[78] B. B. Zvjagin and Z. G. Pinsker: *Dokl. Akad. Nauk SSSR,* **68**, 505 (1949).
[79] B. B. Zvjagin, E. L. Lapidus and V. P. Petrov: *Dokl. Akad. Nauk SSSR,* **68**, 377 (1949).
[80] B. B. Zvjagin: *Dokl. Akad. Nauk SSSR,* **86**, 149 (1952); **95**, 1305 (1954); **96**, 809 (1954); **97**, 251 (1954).
[81] V. I Kasatočkin: *Izv. Akad. Nauk SSSR, Ser. Fiz.,* **17**, 246 (1953).
[82] L. I Tatarinova and Z. G. Pinsker: *Dokl, Akad. Nauk SSSR,* **95**, 265 (1954).

INDICE DEL SUPPLEMENTO

AL VOLUME III, SERIE X, DEL
NUOVO CIMENTO
Anno 1956

Articoli scritti da fisici russi (I) . . . . . pag. I

E. Cambi – Possibility of Free Oscillations in a Variable-Parameter Resonant System . . . . . » 137

J. Combe – Étude d'interactions de haute énergie produites dans l'émulsion photographique . . . . . » 182

B. Gross – Lineare Systeme . . . . . » 235

P. Caldirola – A New Model of Classical Electron . . . . . » 297

K. Simonyi – Einige Probleme der Konstruktion und des Baues von kernphysikalischen Beschleunigungsanlagen für einige MeV Teilchenenergie » 345

C. P. Enz – Wechselwirkungskräfte und Renormalisation in der Photonpaar-Theorie . . . . . » 363

F. Čap – On the Casual Interpretation of Quantum Theories . . . . . » 418

J. L. Destouches – Quantization in the Functional Theory of Particles . » 433

F. Bopp – Note on a Surprising Result in Field-Mechanics . . . . . » 469

E. Clementel and C. Villi – Phaseshift Analysis of Pion-Nucleon Scattering Experiments. – I. General Outline . . . . . » 474

K. G. Emeleus – Oscillations and Fluctuations in Gas Discharges . . . . » 490

I. Gabrielli, G. Iernetti, E. Clementel and C. Villi – Phaseshift Analysis of Pion-Nucleon Scattering Experiments. – II. Operational Procedure . . . . . » 496

H. Enatsu – Relativistic Quantum Mechanics and Mass-Quantization . . » 526

Articoli scritti da fisici russi (II) . . . . . » 589

Fine del *Supplemento* al Volume III, Serie X,
del *Nuovo Cimento*, 1956

PROPRIETÀ LETTERARIA RISERVATA

Direttore responsabile: G. POLVANI Tipografia Compositori - Bologna

Questo fascicolo del *Supplemento* è stato licenziato dai torchi il 7-8-1956